2007

Design Synthesis and Evaluation Of Diterpenones As Potent Chemopreventive Agents For Aflatoxin B1 Induced Carcinogenesis In Human Liver Cells

Miguel Angel Zuniga
Virginia Commonwealth University

DESIGN, SYNTHESIS, AND EVALUATION OF DITERPENONES AS POTENT CHEMOPREVENTIVE AGENTS FOR AFLATOXIN B1 INDUCED CARCINOGENESIS IN HUMAN LIVER CELLS

A Dissertation submitted in partial fulfillment of the requirements for the degree of Doctor of Philosophy at Virginia Commonwealth University.

by

MIGUEL A ZUNIGA
Bachelor of Chemistry, Southwest Texas State University, 2002

Director: QIBING ZHOU, Ph.D
ASSISTANT PROFESSOR, DEPARTMENT OF CHEMISTRY

Virginia Commonwealth University
Richmond, Virginia
Sept 2007

Acknowledgement

First of all, I would like to acknowledge Dr. Qibing Zhou for his vital guidance during my graduate studies at VCU. His mentorship throughout the years has made my experience as a graduate student challenging, stimulating, and ultimately worthwhile. I have been very inspired by his example of dedication and professionalism with regard to his work. I am sincerely grateful for all the training and all he has done for me.

I would also like to acknowledge my committee members-Dr. Nicholas P. Farrell, Dr. Jennifer Stewart, Dr. Suzanne M. Ruder, and Dr. Vladimir Sidorov, who have also provided much needed support and direction not only at a professional level, but on a personal level as well. Also, a special thank you to Dr. Jennifer Stewart for her guidance and support. I would also like to thank everyone else in Dr. Zhou's research group: Dr. Dai, Ting Xu, Ling Zhang, and Mark Wehunt.

Most importantly, I would like to thank my wife Roxanne for her outstanding love, support, and encouragement when I decided to pursue my graduate studies to accomplish what I set out to achieve, since my first chemistry intern position at Dow Chemical. I also would like to thank my family in Texas- my mother, Elva, my father, Miguel Sr., my brother Alfonso, and sisters, Elsa, Alma, and Griselda for their love and support which helped me withstand the hardships of life in a different environment. I would also like to thank my in-laws, Eddie and Linda Acosta for their love and support. My friends and extended family, too numerous to mention, were always there to offer words of encouragement, thanks!! Without their encouragement none of this would have been possible. I am also grateful to the Department of Chemistry for providing me with a teaching assistantship to support my living and studies throughout the past five years.

Table of Contents

Page

List of Figures

Page

List of Schemes

Page

List of Abbreviations

^{2}H	Deuterium
AFB1	Aflatoxin B1
COSY	Correlated spectroscopy
DCC	N,N-Dicyclohexylcarbodiimide
DMAP	4-dimethylaminopyridine
DMF	N, N'-Dimethylformamide
EDCI	1-(3-dimethylaminopropyl)-3-ethylcarbodiimide hydrochloride
ESI-MS	Electrospray ionization mass spectrometry
HCC	Human hepatocellular carcinoma
Hep G2	Human hepatocellular carcinoma cells
mCPBA	meta-chloroperoxybenzoic acid
nBuLi	nButyllithium
NER	Nucleotide excision repair
NMO	N-Methylmorpholine-N-Oxide
NMP	N-Methylpyrrolidone
NOESY	Nuclear overhauser and exchange spectroscopy
PAGE	Polyacrylamide gel electrophoresis
Pd/C	Palladium on carbon
QM	Quinone methide

ROESY	Rotating frame Overhauser enhancement spectroscopy
ROS	Reactive oxygen species
SAR	Structure activity relationship
THF	Tetrahydrofuran
TPQM	Triterpene quinone methides
TsOH	*p*-Toluenesulfonic acid

Abstract

DESIGN, SYNTHESIS, AND EVALUATION OF DITERPENONES AS POTENT CHEMOPREVENTIVE AGENTS FOR AFB1 INDUCED CARCINOGENISIS IN HUMAN LIVER CELLS

By Miguel A. Zuniga, Ph.D.

A dissertation submitted in partial fulfillment of the requirements for the degree of Doctor of Philosophy at Virginia Commonwealth University.

Virginia Commonwealth University, 2007

Major Director: Qibing Zhou, Ph.D
Assistant Professor Department of Chemistry

Terpene quinone methides (TPQMs) have been isolated from a variety of plants and show broad activities against bacteria, fungi, and cancerous cell lines. The biological activity has been attributed to the reactive electrophilic QM moiety, this structural feature has long been recognized as an intermediate in organic synthesis and in certain biosynthetic processes. It has been shown that quinone methide structures play a key role in the chemistry of several classes of antibiotic drugs and antitumor compounds such as mitomycin C and anthracyclines. The goal of this study was to understand the basis of QM

bioactivity so that terpene catechols as analogs of natural TPQMs precursors can be designed as effective chemopreventive agents.

In order to investigate the oxidation pathway of terpene QM precursors, a homoconjugated diterpene catechol was synthesized. A review of the literature revealed that Cu^{2+} -induced oxidation of simple catechols proceeds through a two-step one electron transfer process, and *o*-quinone is the sole oxidation product. In contrast, our studies showed direct *p*-QM formation from a diterpene catechol and no *o*-quinone oxidation products were observed. Furthermore, the Cu^{2+}-induced oxidation pathway of our homoconjugated diterpene catechol revealed multiple *p*-QM formations under aqueous conditions. The implications of these findings suggest that terpene QM precursors can cause extensive DNA damage through in situ generated hydroxyl radicals or by DNA alkylations with *p*-QMs.

To elucidate the Cu^{2+}-induced DNA damage mechanism, a series of catechol analogues of natural terpene QM precursors were designed to investigate potential effects of stereochemistry, substitutiional, and functional groups on nucleobase alkylation and production of reactive oxygen species. The results of these tests suggested that production of ROS was the dominant mechanism for the observed DNA damage in the Cu^{2+}-induced oxidation regardless of stereo and structural differences of catechols or subsequent oxidation products as QM or quinone. From the DNA damage study we found that the presence of NADH significantly enhanced the extent of DNA damage by oxidation of these catechols. More specifically, in the case of alkene catechols, our results showed that DNA damage was independent of the concentration of catechols, thus providing ample

evidence for production of ROS through the redox cycle of catechols/quinones. Additional support for the formation of hydroxyl radical and futile redox cycling was clearly demonstrated by comparison of the fragmentation pattern with that of a Fenton reaction. The identify of the ROS was also shown to be in the form of a Cu(I)OOH complex by radical scavenging and metal chelation experiments.

Cis-terpenones were first shown to have chemoprotective activity by Dr. Zhou and colleagues. In collaboration with their efforts to identify the mode of action of cis-terpenones, another project to achieve an isotope labeled cis-terpenone was undertaken. The isotope study was employed to obtain and experimentally demonstrate the feasibility of incorporating a radioactive label in cis-terpenone for the future studies of cis-terpenone metabolism. An analysis of the deuterium labeled cis-terpenone from the isotope exchange reaction showed that the isotope was being incorporated into multiple positions through scattering processes. This non-radioactive isotope study made it possible to optimize the conditions prior to using a radioactive tritium label, which will be a requisite for future metabolic studies.

As an extension of this work, a structure activity relationship (SARs) study was undertaken with a focus on improving the physiochemical properties and chemical stability of cis-terpenones. The primary purpose of this study was to attempt to explain the reason for the observed protective effects of cis-terpenones against AFB1. Considerable efforts were made to introduce an unsaturated double bond in the structure of cis-terpenone by an intramolecular Pd (II) catalyzed Heck reaction. Unfortunately, this method was unsuccessful and which was attributed to the disconnection of our starting material during

the formation of an enolate intermediate. A second model study to generate desired coumarin and ditepene related structures was investigated with a Diels Alder [4+2] cycloaddition reaction. After numerous attempts, we found that the successfull synthesis of these compounds was highly dependent on the temperature, solvent, and the use of stabilizers in the reaction.

Finally, the targeted diterpene analogs were screened for protective effects against AFB1 by the MTT cell viability assay. However, these preliminary data showed that additional structural features and key modifications are still required to better correlate the structure with the mechanism of chemoprotection.

Chapter 1

Cancer chemoprevention

1.1 Background and significance.

The term of "cancer chemoprevention" was first coined by Sporn *et al*, in 1976, which he defined as a strategy for cancer control through administration of synthetic or natural compounds capable of halting or inhibiting the onset of carcinogenesis.[1,2] Sporn contended that the process of carcinogenesis had the potential to be controlled physiologically and pharmacologically during its preneoplastic stages, in which he suggested that the promotion phase could be stabilized, arrested, and reversed.[2,3] To date, most cancer chemoprevention research is based on the concept of multistage carcinogenesis, which includes cancer initiation, promotion, and progression stages. The promotion stage has been determined from animal studies to require a longer time to develop than both initiation and progression. This prolonged time is due to complex cellular mechanisms and protein synthesis that are necessary from the onset of cancer initiation to reach the point of tumor proliferation and progression.[4-6] It is generally agreed that unlike initiation and progression which are irreversible stages, cancer promotion can be a reversible stage, and thus is likely to be a valid target for cancer chemoprevention.[6-7]

Most chemopreventive agents act in two ways: they can prevent genetic mutations that lead to cancer and/or they can prevent and stop excessive replication of mutated cells. A variety of approaches have been considered in the prevention of carcinogenesis. These approaches include the inhibition of pro-carcinogen activation, the enhancement of cellular detoxification pathways, the interception of carcinogenic reactive products, and the

alteration of cellular signaling pathways.[7,8] Natural products have attracted considerable scientific interest in chemoprevention. This interest stems from the fact that many natural products possess biological activity with high selectivity and specificity, making them less prone to cause serious toxicity.[9-11] Results from animal studies have demonstrated that certain chemopreventive agents can induce apoptosis in tumor cells in vivo. For example, treatment with oral infusions of polyphenolic extracts in a mouse model for prostate cancer was found to promote a significant inhibition of prostate cancer development and increased overall survival.[12,13] In addition, the understanding of the carcinogenic process will lead to more effective chemopreventive agents.

In this chapter, a review of Aflatoxin B1 (AFB1) and the mechanisms by which it exerts its carcinogenic effect will be presented, and experimental studies with natural and semi-synthetic compounds having protective properties against AFB1 will be discussed. This is followed by a generalized intervention strategy against AFB1 by utilizing quinone methide (QM) analog as a model for rational development of novel chemopreventive agents.

1.2 Aflatoxin B1 as a potent procarcinogen

Aflatoxin B1 (AFB1) is a fungal metabolite that is produced by *Aspergillus flavus* and contaminates food such as corn, nuts, and cereals in many areas of the world. Because AFB1 has been detected in a variety of crops, it has been reported as a major procarcinogen for human health risk.[14,15] In 2002, it was classified by the World Health Organization (WHO) as a class one carcinogen, because the potency and epidemiological

evidence suggested that it is an important factor in the etiology of human liver cancers.[16,17] Bioactivation of AFB1 occurs through metabolic activation by phase one cytochrome P450 (CYP) enzymes to two metabolites AFB1 exo- 8,9-epoxide and endo-8,9-epoxide. The AFB1 exo-8,9-epoxide is highly reactive and subsequently alkylates DNA nucleobases such as N^7 of guanine and thus exerting its carcinogenic effect (Scheme 1.1).[17-20] In contrast, the AFB1 endo-8,9-epoxide only forms low levels of adducts upon reaction with DNA because nucleophilic attack by guanine N^7 is blocked by the oxirane ring upon its intercalation into DNA.[20-22]

Scheme 1.1 Biotransformation of AFB1 by CYP450

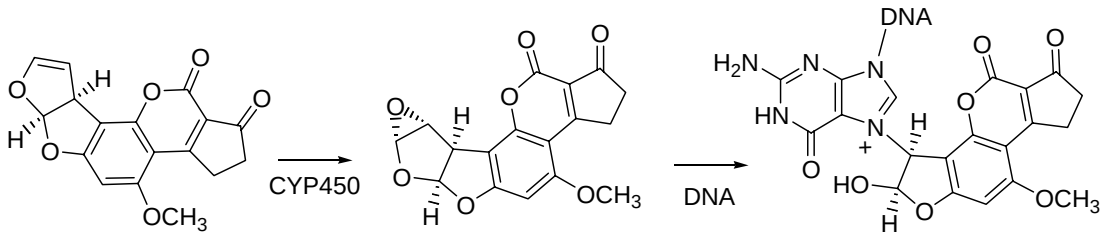

In the study by Corriea *et.al*,[23] the structure function relationships of CYP 450 and AFB1 were investigated. Their studies used P450 3A4 and 3A5 which are identical at 84% of their primary sequence to compare the active site differences and determine whether these differences could influence substrate binding and regioselectivity in AFB1 metabolism. Based on their computer modeling studies, it was suggested that P450 3A4

cannot accommodate AFB1 in an orientation conducive for its endo 8-9 oxidation while exo-8,9 oxidation can occur due to AFB1 bound in an orientation leading to its oxidation and stabilization with protein residues.[23] In contrast, the AFB1 furan moiety was found to bound through interaction with several regions of the somewhat more flexible P450 3A5 active site thereby favoring the exo-8-9 oxidation.[23]

Model studies performed by Essigmann *et.al*[24] suggested that exo-8,9-epoxide intercalates between DNA bases more efficiently than endo isomer, and that exo-8,9-epoxide is in a favorable position for SN2 attack by the N^7 guanine of DNA nucleobases (Figure 1.1).

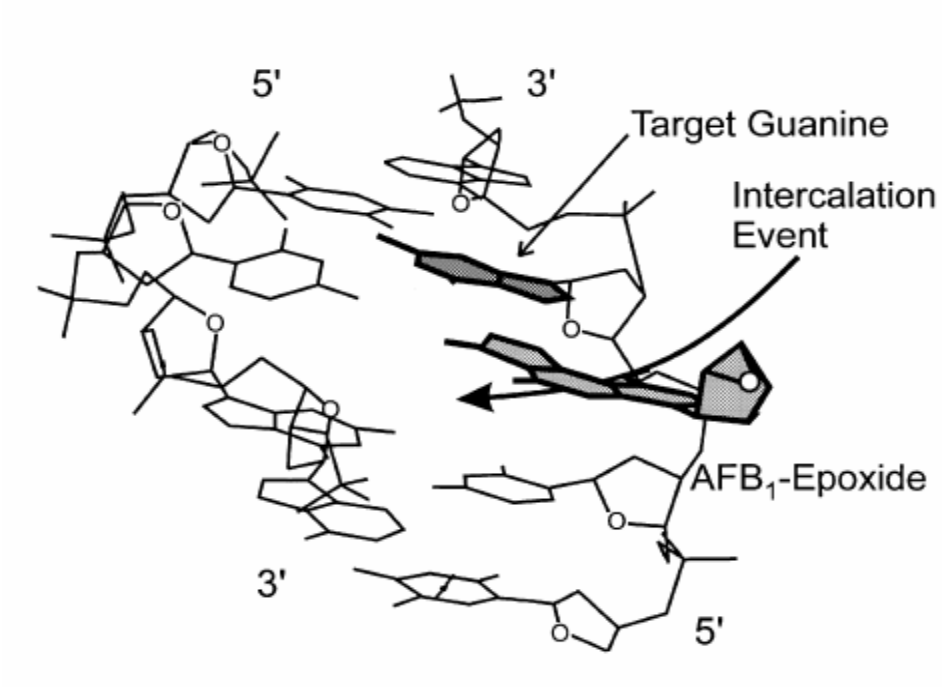

Figure 1.1. Intercalation of exo-8,9-epoxide and position for S_n^2 attack by N^7 guanine of DNA (*Essigman et. al., 2001*).

Harris and coworkers[25] have examined the reactivity of both exo and endo aflatoxin B1 epoxide toward hydrolysis in a phosphate buffer (pH 7.0) at 23 ºC. They found have that endo 8,9-epoxide is at least 40-fold more stable than the exo-8,9-epoxide toward hydrolysis.[25] However, the reactivity of the exo-8,9-epoxide is at least 10^3 times greater with DNA than the isomeric endo-8,9-epoxide.[26,27] This finding was attributed to a tight association between the aflatoxin molecule and the nucleobases, of which covalent bonds subsequently formed.[28-30] In contrast, the endo conformation precludes the insertion of the endo isomer within the DNA duplex. Of interest is that DNA intercalating molecules prefer to interact with double stranded DNA, due to the favorable thermodynamic gains through π-π base pair stacking and hydrophobic interactions.[30]

Raney and coworkers[31] suggested that exo-8,9-epoxide adduct formation was promoted through the specific orientation of bound epoxide, which intercalates on the 5' face of the guanine residue in double stranded DNA. They studied AFB1 analogs with modified ring systems and found that a decrease in planarity resulted in reduced intercalation ability.[31] For instance, a change from the planar comarin moiety and cyclopentenone ring system to the more puckered δ-lactone ring reduced the binding of aflatoxins to DNA.[31] This situation is known to exist with aflatoxin G1, which has a decreased planarity and affinity for DNA, resulting in lower cytotoxicity. Furthermore, addition of the intercalating agent ethidium bromide to target DNA prior to the treatment with AFB1 epoxide greatly reduced guanine alkylation by AFB1 epoxide.[32]

The reactivity of AFB1 exo-8,9 epoxide is also influenced directly by the proton concentration and plays a major role in the hydrolysis mechanism. Guengrich and

coworkers[33] investigated the rate of AFB1 exo-8,9 epoxide hydrolysis at various pH ranges. The half life of AFB1 exo-8,9 epoxide hydrolysis in aqueous buffer (pH 7.1) at 25ºC was found to be only ~1 s making it one of the most biologically relevant epoxides.[33,34] They found that the reaction rate of 2.3×10^3 M^{-1} s^{-1} increases linearly below (pH 5), indicating the predominance of an acid-catalyzed mechanism for hydrolysis in this range.[33] At the higher pH values (7-9), the hemiacetal ring opens at the furan rings, resulting in phenoxy anions and aldehydes in equilibrium with diols.[33] On the basis of stop flow kinetic studies, Guengerich *et. al*[35] demonstrated that covalent binding of the AFB1 *exo*-8,9-epoxide forming the DNA-intercalated adduct occurred at a rate of $k \approx 0.2$ s^{-1} due to the acid catalysis.[35] From these studies, it was also implied that an acidic microenvironment around the surface of DNA molecules[36,37] is also involved in acid catalysis of the AFB1-N^7 guanine alkylation. All of these results clearly indicate that AFB1 reactivity is highly sensitive to a large pH range and is also influenced by both electronic and structural conformations of the coumarin ring systems.

Evidence for the mutational spectrum of AFB1 has shown a prevalence of one genetic change: GC→TA transversion, even though there is a varied distribution of DNA adducts formed in cells when treated with this toxin. This mutation has been studied in several experimental systems including the endogenous *lacI* gene in an SOS-induced *Escherichia coli* strain, which contains the mucAB mutagenesis enhancing operon.[38,39]

Cerutti and coworkers[40,41] used restriction fragment PCR to investigate mutagenic effects of microsome activated AFB1 at codons 247-250 of the p53 gene in HepG2 cells. Their results suggested that AFB1 preferentially induced the transversion of G→T in the

third position of codon 249, resulting in replacement of arginine by serine. In addition, other G→T and C→A transversions into adjacent codons were observed, albeit at lower frequencies.[40] The G→T transversion was found to be in agreement with the mutational specificity of AFB1 and other carcinogenis that form bulky DNA adducts.[42]

The nucleotide excision repair enzymes (NER) in mammalian systems have been shown to play an important role in the repair of AFB1-induced DNA damage. For example, studies by Essigman *et,al*[43] showed that fibroblasts deficient in the xerodoma pigmentosum group A gene (XPA) responsible for NER showed a slower loss of AFB1-N7-Gua and accumulation of formamidopyridine adducts (AFB1-FAPY) compared to normal liver cells, suggesting that NER is an important mechanism for enzymatic repair of AFB1-DNA adducts.[43] While repair of AFB1-DNA adducts in bacteria is relatively well understood, further research is needed to fully characterize mammalian repair of these adducts.

Over the past 20 years, accumulated work carried out in several laboratories has provided useful insights into the mechanism of AFB1 biotransformation and have encouraged others to explore new chemoprevention strategies aimed at blocking AFB_1 biotransformation or inhibiting the enzymes that activate this procarcinogen in vivo. In the following discussion, examples of two chemopreventive agents used in clinical studies will be discussed. This is followed by several examples of natural compounds which are currently being evaluated as alternative chemopreventive agents.

1.3 Oltipraz and chlorophyllins as chemopreventive agents against AFB1

Oltipraz was investigated as a chemopreventive agent during the 1970-1980s on the basis that it is a facile synthesized natural product analog, and that it was already undergoing clinical trials as an antischistosomal agent.[44] Detoxification of AFB1 has been found to involve phase two enzymes such as glutathione S-transferases (GSTs) which promote the conjugation of gluthathione to the carcinogenic species, aflatoxin-8,9-epoxide, thereby diminishing DNA adduct formation by a mercapturic acid adduct (AFB-NAC) (Scheme 1.2)[45,46] Studies by Langouet *et.al*[46]reported twofold to fourfold elevations in the levels of μ and α glutathione S-transferases (GSTs) proteins in primary cultures of human hepatocytes when treated with a single dose of 500 mg /m^2 oltipaz at a concentration comparable to that in plasma of humans.[47]

In a chemoprevention study conducted by Groopman and coworkers[48] nucleic acid adduct AFB- N^7-Gua and albumin adducts were used as biomarkers, which were detected and quantified with immunoaffinity chromatography and liquid chromatography-electrospray mass spectrometry.[48,49] They suggested that because the primary aflatoxin nucleic acid adduct AFB-N^7-Gua was exclusively excreted in urine after its removal from DNA and has a short biological half life, its measurement thus reflect recent exposure to aflatoxins. While albumin adducts found in serum are also derived from the AFB1-8,9-epoxide, but are thought to reflect exposures over longer periods of time, which was based on a half life of three weeks for albumin circulated in humans.[50]

Scheme 1.2 General Metabolic Pathway of Aflotoxin B1 with Oltipraz treatment

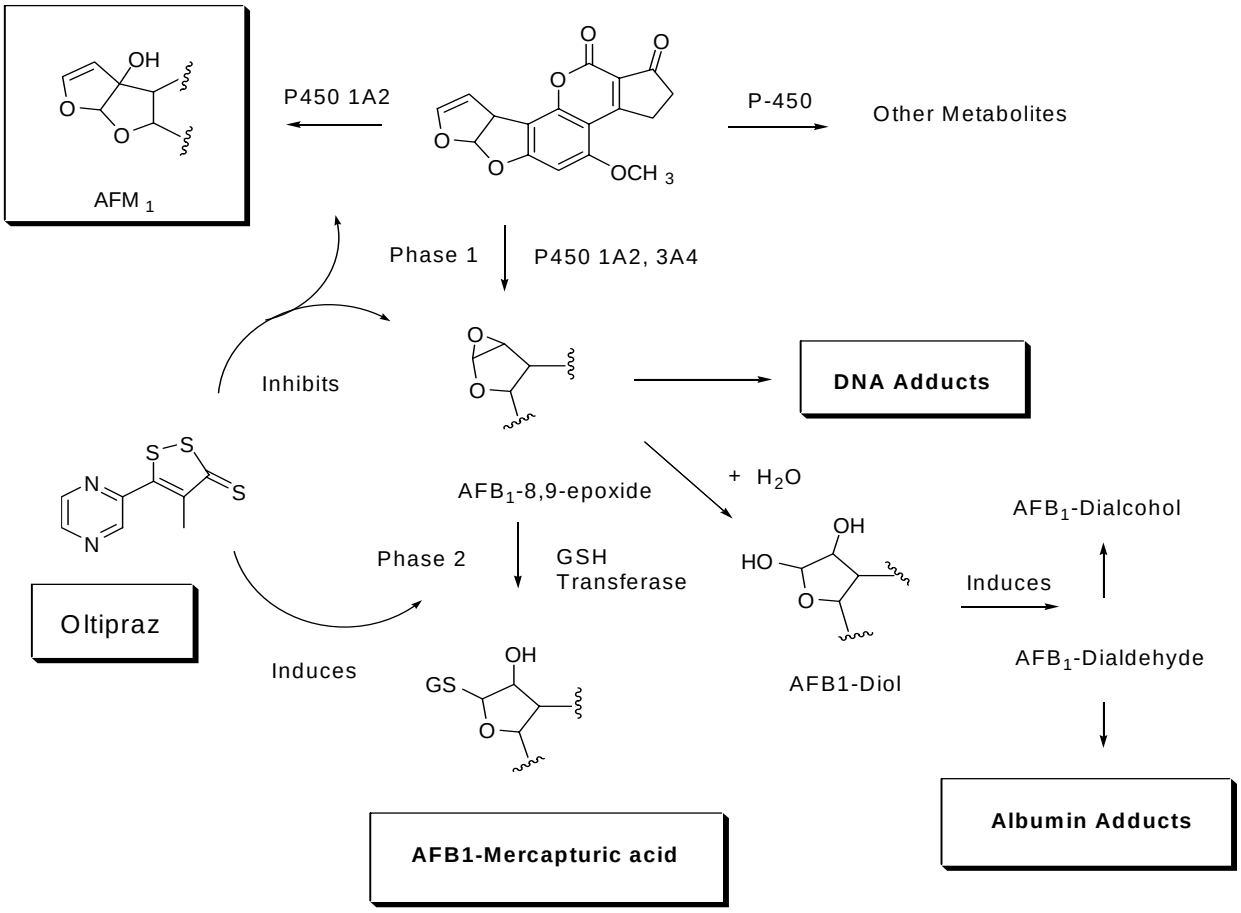

Metabolism of AFB1 and several adducts of AFB1 currently used as intermediate biomarkers of carcinogenesis (*Kensler et. al., 1999*).

Enzyme kinetic studies on heterologously expressed human CYP1A2 indicate that oltipaz is a competitive inhibitor of cytochrome P450 with an apparent inhibition constant (K_i) of 10 μM, a pharmacologically achievable concentration in rats and humans.[51] Inhibition of CYP1A2 by oltipraz results in diminished metabolism of aflatoxin to the genotoxic 8-9-epoxide and the hydroxylated aflatoxin metabolite M1.[51-54] As illustrated in Scheme 1.2, oltipraz exerts multiple effects on the metabolism of AFB1 in people

exposed to this potent hepatocarcinogen. Dose and schedule dependent inhibition of cytochrome P450-dependent activation and induction of GST-mediated detoxification of AFB1 has been observed in clinical trials. Induction of phase two enzymes has long been supported as an important mechanism for achieving chemoprevention.[55,56]

Although these studies suggest that chemopreventive agents can work by changing the metabolism of environmental carcinogens, important questions still need to be addressed, such as whether all phase two enzymes are inducible, or whether the genes are inducible in humans and how they contribute to chemoprevention.[57] While oltipraz has demonstrated chemopreventive effects against AFB1, it is still unclear whether it will actually inhibit hepatocellular cancer or acts by simply delaying cancer progression. Problems associated with oltipraz are that it causes acute gastrointestinal toxicity and can induce estrogen responsive genes.[58,59] Due to unknown and long term side affects of oltipraz, there is a need for alternative agents that can interfere and prevent the process of carcinogenesis and demonstrate still better activity and or less toxicity than oltipraz.

Another chemoprevention agent which has been tested as a treatment for AFB1 induced carcinogenesis is chlorophyllin (Scheme 1.3). Mechanistic studies suggest that chlorophyllin acts as an interceptor molecule, forming tight molecular complexes with AFB1 and thus impedes aflatoxin absorption in the liver. Kensler and Breinholt,[60-62] studied the effects of the uptake of AFB1 chlorophyllin to determine whether it could alter the uptake or block the bioavailabilty of AFB1. During their studies, levels of aflatoxin-N^7 –guanine adducts in urine samples were used as biomarkers and collected, which was spiked with 1.5 ng of aflatoxin B2 (AFB2) as an internal standard. Afterward the

aflatoxins were eluted with methanol and then loaded onto prepartive aflatoxin specific mAb immunoaffinity column. Aflatoxin-N^7-guanine and AFB2 were quantified by measuring the mass area of specific MS/MS daughter fragments MH^+ 152.1 and 259.1 derived from the parent ions of m/z 480.1 and 315.1, respectively. The final results of these studies suggested that chlorophyllin achieved an overall 55% reduction in urinary levels of AFB1 metabolites compared to subjects taking a placebo.[62]

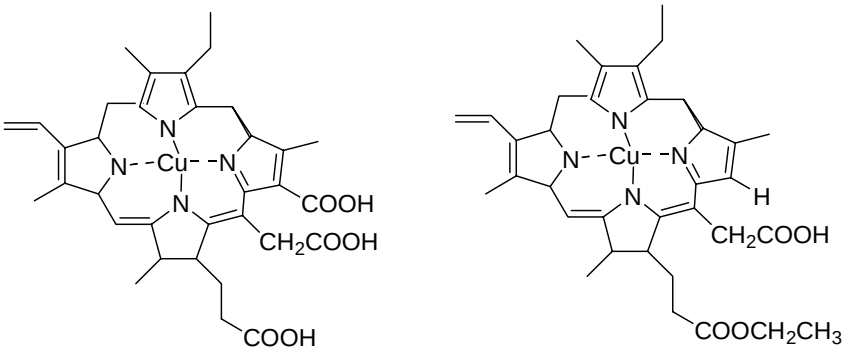

Scheme 1.3 Chlorophyllin structures used in the intervention

These studies suggest that chlorophyllin is an effective intervention agent and that it may favorably reduce the bioavailability of aflatoxins and other classes of environmental carcinogens. Unfortunately, although chlorophyllin is marketed as an over the counter drug (Derifil), primarily used to control body odor and to accelerate wound healing, its main disadvantage as an AFB1 chemoprevention agent is that it has low complexing constant, which required an excessive oral dose per day.[62] Another problem associated with chlorophyllin is due to its high water solubility; this reduces its effectiveness and ability to distribute in critical target organs and diseased human liver cells.

1.4 Alternative chemopreventive agents from natural products

Several dietary products have shown promise as alternative AFB1 chemopreventive agents. One particular interesting finding is rosmarinic acid which has shown anti-oxidant, anti-inflammatory, and antiviral activity (Scheme 1.4). This compound was investigated by Renzulli and coworkers[63] for chemopreventive activity against AFB1 induced cytotoxicity in a human hepatoma derived cell line (Hep G2). They found that the cell mortality upon AFB1 exposure was reduced when the cells were preincubated with 25-50 μM (Ros A) for a duration of 24 h.[63]

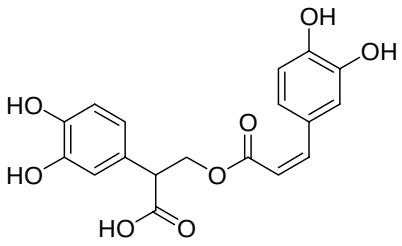

Scheme 1.4 Rosmarinic Acid

Besides DNA base alkylation, oxidative stress has been implicated by Galvano *et. al* [64] as potential mechanisms of AFB1 toxicity. Rosmarinic acid was found to significantly reduce the amount of reactive oxygen species (ROS) in HepG2 cells (Figure 1.2), suggesting it acts as an antioxidant and possibly can scavenge for reactive oxygen species (ROS).[63] However, the mechanism is not entirely known.

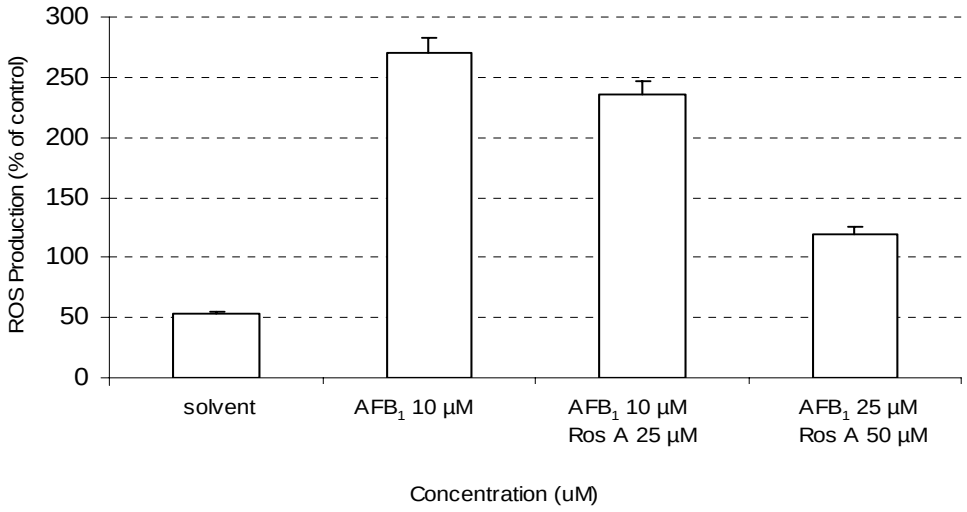

Figure 1.2. Reactive oxygen species production in HepG2 cells treated with AFB1, and cells treated with AFB1 and Rosmarinic acid (*Renzuli et.al., 2004).*

Diterpenes cafestol and kahweol (Scheme 1.5) were investigated by Calvin *et.al*[65] for chemoprotective effects against AFB1 induced genotoxicity in rat primary hepatocytes.[65] Results of western blot analysis showed that CYP2C11 and CYP3A2 expression was reduced as cafestol and kahweol were increased from 0-4 µg/mL. Subsequent studies by the Calvin group were aimed to determine whether cafestol and kahweol would have any significant inhibitory effect on the formation of AFB1-adducts. Results from DNA binding studies showed a dose dependent effect on the formation of AFB1-DNA adducts, with an increase in cafestol and kahweol concentration (0-4 µg/mL). Furthermore, highest inhibition of AFB1-DNA binding occurred after the cells were incubated for 48 hrs and then treated with 4 µg/mL of cafestol and kahweol[65] (Figure 1.3). The studies performed by Cavin *et.al* provide preliminary evidence for the protective effect

of natural diterpenes cafestol and kahweol and their use as potential therapeutic agents for AFB1 carcinogenesis.

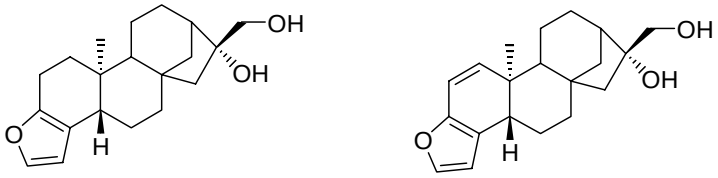

Cafestol Kahweol

Scheme 1.5 Structures of Diterpenes isolated from coffee extracts

These studies indicate that natural products and synthetic analogs derived from plants have useful properties for the prevention of AFB1 induced cytotoxicty. The activities of these natural products highly depend on their chemical structure as demonstrated by the various biological properties of compounds in carcinogenic and tumor bioassays and by their different mechanisms of action. However, the screening strategy for selection of more efficient chemopreventive agents has produced limited candidates. Thus, more efficient strategies such as a "mechanistic based" approach is needed to optimize promising drug candidates earlier in drug discovery processes.[66,67]

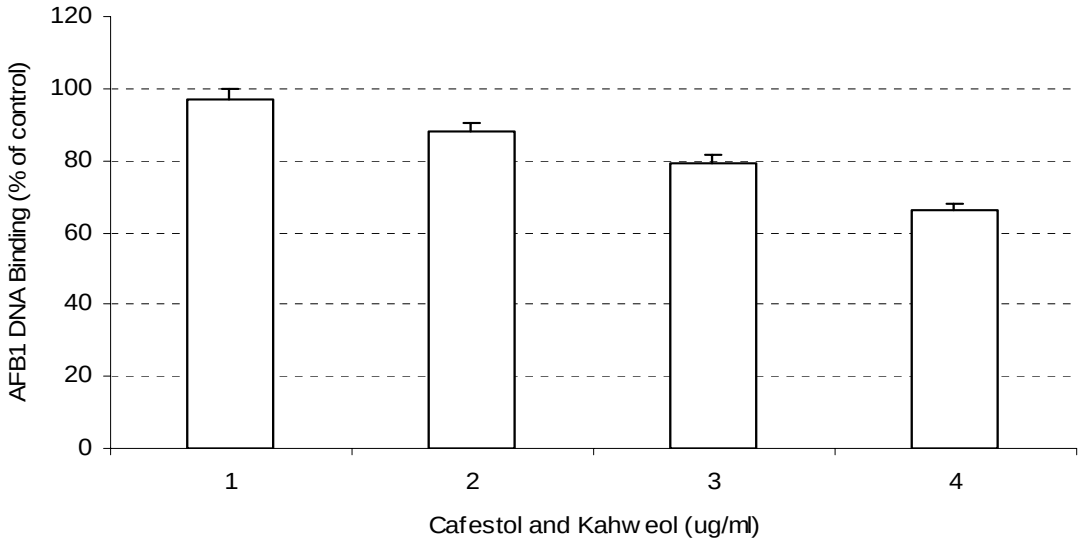

Figure 1.3. Cafestol and Kahweol treatment resulted in a decrease in AFB1/DNA adducts (*Calvin et. al., 2004*).

1.5 Biological activities of natural TPQMs and related QM structures.

One important category of natural products that have interested us as promising chemoprevention agents against AFB1 are natural triterpene quinone methides (TPQMs). These compounds have shown a broad spectrum of biological activities attributed to their reactive quinone methide (QM) moiety. The QM structural element is electrophilic and stabilized through both conjugation and electron donating functional groups.[68-69] Because the QM is polarized, nucleophilies can add readily under mild conditions at the methylene carbon (CH_2), and thus result in aromatic phenols, which is the basis for their reactivity (Scheme 1.6).[70,71] The origins of QM reactivity and selectivity are still being investigated, but it has been shown that steric and electronic environments play a major role in their alkylation products. This has prompted many studies pertaining to quinone methides in

alkylation and biomolecular alkylation processes. Most recently, the reversibility of simple ortho quinone methide (QM) generation has been investigated by Rokita's group toward efficient cross linking and taget-promoted alkylation.[72,73]

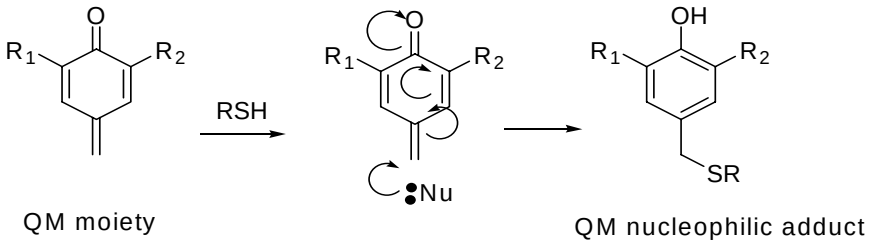

Scheme 1.6 Electrophilic QM moiety and subsequent nucleophilic addition

As previously mentioned, our interest in natural TPQMs is due to their broad spectrum of biological activities. One example of a bisnortriterpene quinone methide is isoguesterin, isolated from the root bark of *Salacia madagascariensis*. This compound was shown to have potent anti-leshminal activity 94.0 ng/mL against *L. donovani* and *L. mexicana* (Scheme 1.7).[74] Unfortunately, this compound is a skin irritant and is currently still under further investigation. Another example, leguminase a diterpene quinone methide has been shown to have potent activity 0.19 μg/mL against yeast *Candida albicians*.[75] These studies clearly demonstrate how the biological activites of QMs are affected by specific structural features. In particular, a well studied QM is that of 2,6-di-tert-butyl-4-methyl phenol (BHT). This compound is converted to BHT-QM through an enzymatic process and is toxic to liver and lung cells.[76] Again, the structural features of

this compound have been shown to be important in influencing QM reactivity and cytotoxicity in vitro.

Although these studies demonstrate the unique biological activities of natural TPQMs and QM compounds, it remains unclear whether analogs of natural TPQMs can be utilized as potential therapeutic or chemopreventive agents. Thus, the long term aim of these studies is to investigate the scope and utility of analog TPQMs as novel mechanism based chemoprotection agents.

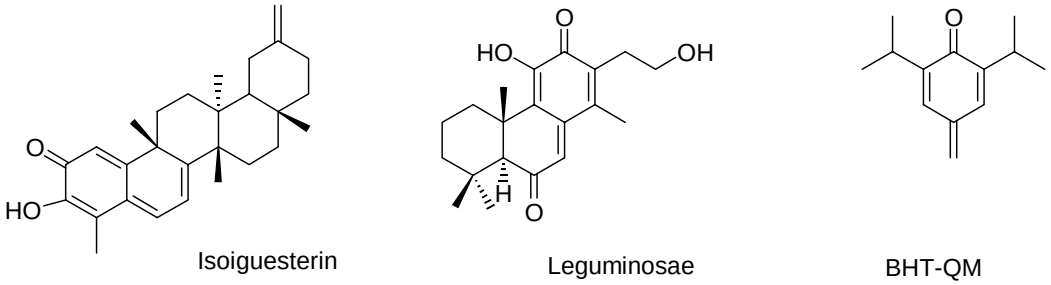

Scheme 1.7 Polyterpene and diterpene quinone methide derivatives. BHT is a quinone methide formed during a P450 catalyzed oxidation process.

1.6 General intervention strategy based on TPQM analogs

The risk of AFB1 cytotoxicity is attributed to the covalent DNA modification by the exo-epoxide metabolite, resulting in liver damage and possibly hepatocellular carcinomas. Hence, the purpose of these studies was to develop a general approach utilizing synthetic cis-terpenone as a potent chemopreventive agent for AFB1 in human liver cells. These compounds were investigated because experimental studies have been reported with other compounds and have shown induction and or inhibition of important enzymes involved in the biotransformation of AFB1. To determine whether cis-terpenone

has any chemoprotective effect against AFB1 induced cytotoxicity, the cis-terpenone compound was designed and has been investigated (Scheme 1.8).

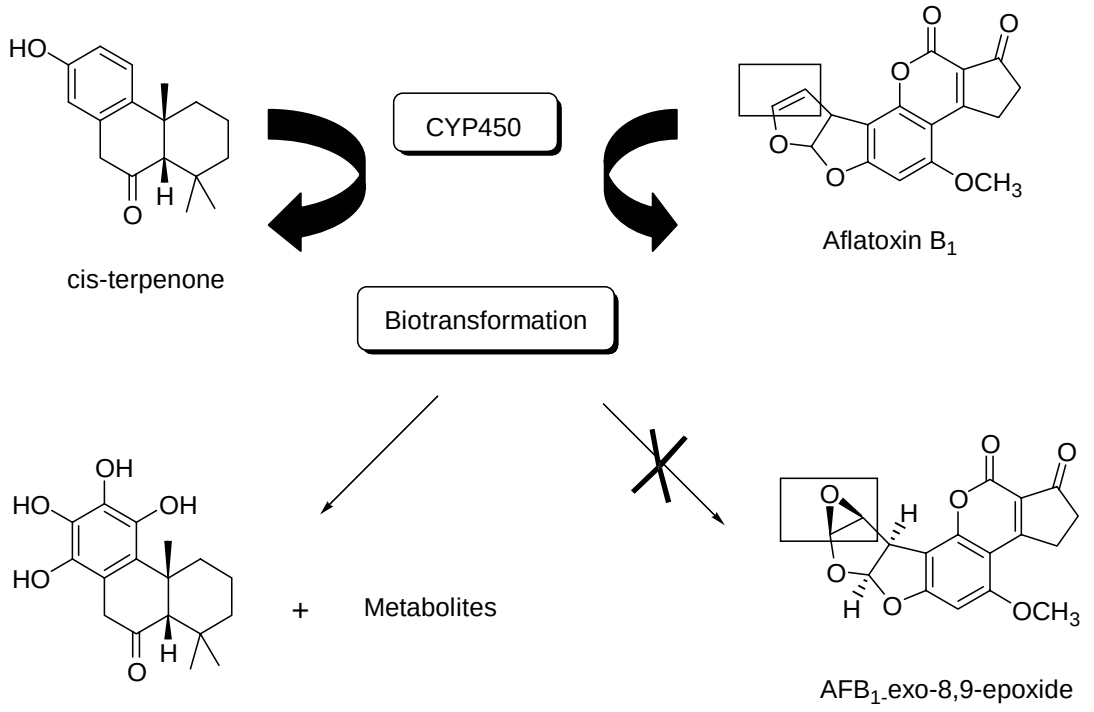

Scheme 1.8. General strategy of chemoprevention of AFB1 carcinogenesis based on model cis-terpenone or cis-terpenone metabolites. Terpenones are designed to block biotransformation of AFB1 by inhibiting or reducing the expression levels of CYP450s.

Our working hypothesis is that administration of cis-terpenone will influence and have an impact on blockage of CYP450 dependent AFB1 activation. Furthermore, the variation in AFB1 bioactivation will play a critical role toward the response of protective mechanisms in human liver cells. Because reducing the induction of P450s is a major challenge for chemopreventive drugs, the potential advantage of this strategy is that CYP450 oxidative metabolism of cis-terpenone may occur specifically within AFB1

induced carcinogenic cells. Another important advantage is that in contrast to other chemopreventive agents such as oltipraz, which is shown to elicit a wide range of AFB1 detoxification processes, metabolism of cis-terpenone may result in an essential intermediate that selectively targets and blocks CYP450 active sites. Most important, this may result in an increase in chemoprevention by enhancing the duration of cis-terpenone thereby maximizing protection against carcinogenic AFB1 exo- 8,9 epoxide formation.

The development of novel chemopreventive agents against AFB1 has been systematically approached by screening of natural or semi-synthetic compounds of natural origin. The research presented here has focused on several of these aspects. All of these results have been used in the ongoing systematic development of chemopreventive agents. However, to our knowledge there are no studies of cis-terpenones and related catechols as chemopreventive agents. This is likely due to the possible formation of quinone methide intermediates during the oxidative and metabolic transformation in biological systems and the known toxicity of quinone methide alkylation. In developing a model for chemoprevention against AFB1 based on cis-terpenone compounds, we have investigated the reactivity of diterpenone catechols and related derivatives under an induced oxidation process to assess their potential role and biological impact in human liver cells.

In the following chapter, direct QM formation through Cu^{2+} -induced oxidation of a precursor terpene catechol was investigated. These studies aimed to elucidate the oxidation pathway of terpene catechol, and to provide a method for generation of stable QM for future biological studies. This is followed by studies in chapter three that will attempt to elucidate the Cu^{2+} -induced DNA damage mechanism and to evaluate the

potential impacts of diterpenone catechols on duplex DNA. In that chapter, the relationship between the structures of catechol precursors of natural terpene QMs and their conversion into QM or quoinone oxidative products was investigated with a series of terpene catechols.

In chapter four, a novel method for the synthesis and characterization of isotope labeled cis-terpenone precursor will be presented. The goal of the labeling approach was to demonstrate the labeling position and secondly to prove the feasibility of incorporating a tritium label for future metabolite studies. In chapter five, analogs of the promising cis-terpenone chemopreventive agent were designed, synthesized, and investigated to maximize against AFB1 toxicity. With a diverse set of cis-terpenone and diterpene derivatives in hand, it was anticipated that structural modification and refinement of original cis-terpenone would provide clues to the mode of action of cis-terpenone.

Finally, chapter six consists of the different analogs that were successfully completed and a general classification of these compounds based on their partial structural similarities. The long term aim of these studies is to develop a rational and viable research program around the application of cis-terpenones as novel and effective chemopreventive agents.

Chapter 2

Synthesis of diterpene catechol and quinone methide formation by Cu^{2+} induced oxidation

2.1 Introduction

Numerous studies have shown broad biological activities of natural TPQMs through the reactive QM moiety as discussed in Chapter 1.[73-76] However, evaluation of natural TPQMs as effective therapeutics has remained a challenge due to isolation of these compounds in pure form and at room temperature, simple unsubstituted QMs can undergo dimerization in solutions at concentrations more than 10^{-5} M.[77,78] Because of these major difficulties, the studies presented in this chapter were focused on designing catechol precursors of natural TPQMs so that we could investigate their oxidative potential and oxidation pathway under aqueous conditions. The goal was to demonstrate direct QM formation through Cu^{2+} -induced oxidation of precursor terpene catechols, and to provide a method for generation of stable QM for future biological studies.

One objective of these studies was to elucidate the oxidation pathway of terpene catechols as different from simple catechols such as 2-hydroxyphenol. The oxidation pathway for this simple catechol is known to proceed through a two step one electron transfer process, producing o-quinone as the sole oxidation product.[79] In contrast, the homoconjugated terpene catechol **1** designed in our laboratory can undergo oxidation by three different pathways. For example, either o-quinone **2** or terpene QM **3** is directly formed in the oxidation process, or terpene QM **3** is formed through fast isomerization of terpene o-quinone **2** (Scheme 2.1).[80] In fact, the rate of isomerization of o-quinones to

QMs has been measured with 4-allyl catechols and found to be highly dependent on p-alkyl substituents.[81]

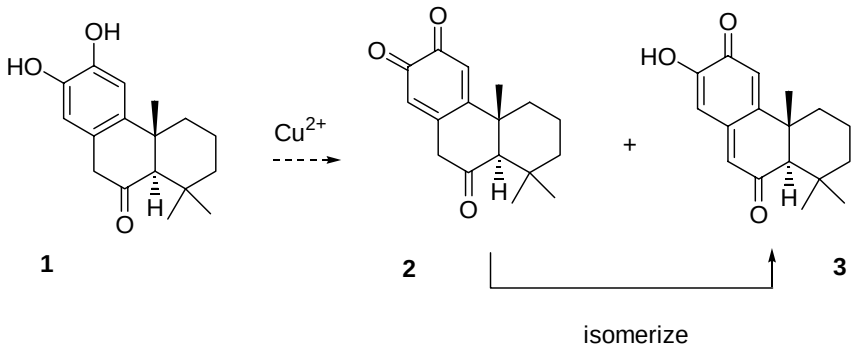

Scheme 2.1 Formation of different QM species through a homoconjugated catechol (Zhou et. al 2005)

The multiple oxidation pathways of our simple model terpene catechol **1** and the fact that catechols are readily oxidized suggested that oxidation within cells will be very likely. In this chapter, studies to determine the identity and structure of QM formation from our unique terpene catechol precursor were undertaken. And most important, these studies aimed to clarify the oxidation pathway of terpene QM precursors so their impact in biological systems could be addressed.

2.2 Modeling of terpenone QM analogs

One approach is to examine the molecular structure of terpene QM analogs by molecular modeling. Thus, models of natural terpene QMs **4** and QM analog **3** were

achieved with AM1 (Spartan, Wavefunction, Inc., Irvine, CA) molecular modeling by Dr. Zhou.

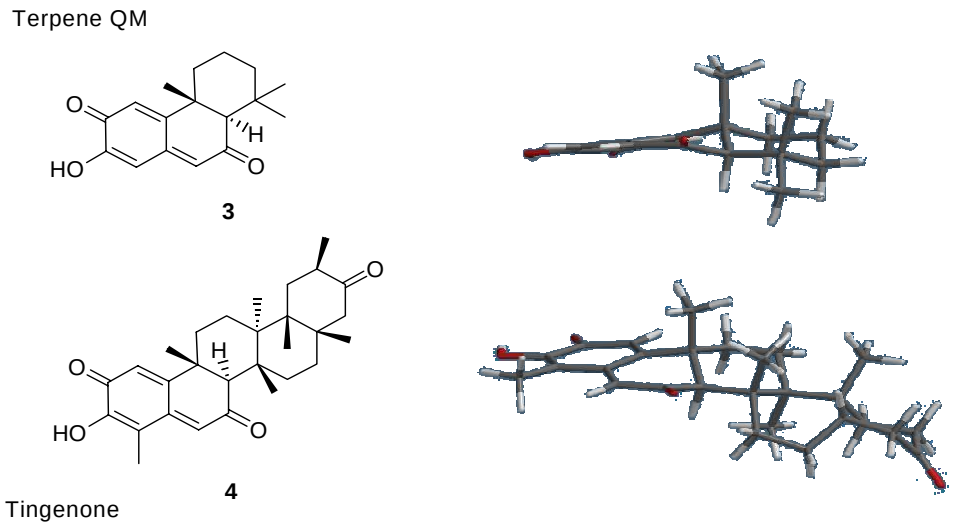

Figure 2.1. Comparison of molecular structures of tingenone a natural TPQM **4** and a synthetic terpene QM analog **3** using AM1 Semiempircal molecular modeling.

As can be seen in Figure 2.1, the presence of extended π conjugation results in flattening of the rings, which is often an important feature in natural products. In addition, the trans-fused ring systems show extended or open structure that relieves steric interactions between angular methyl groups and ring hydrogens. Both six membered rings in compound **3** exist in chair conformation and are in their lowest energy form. A notable difference between synthetic analog **3** and natural TPQM **4** is that this analog is smaller and has fewer asymmetric centers than natural TPQM.[82,83] As a result, these features simplify the synthetic process and will permit chemical modification at later stages of the synthesis. An important observation of this analog is its structural conformation, which is

similar to tingenone **4,** a natural TPQM. This finding suggests that this analog may have a similar mechanism of action and activity towards biomolecules.

2.3 Synthesis of first generation of diterpene analogs

Scheme 2.2. A general synthesis strategy for diterpenone catechols

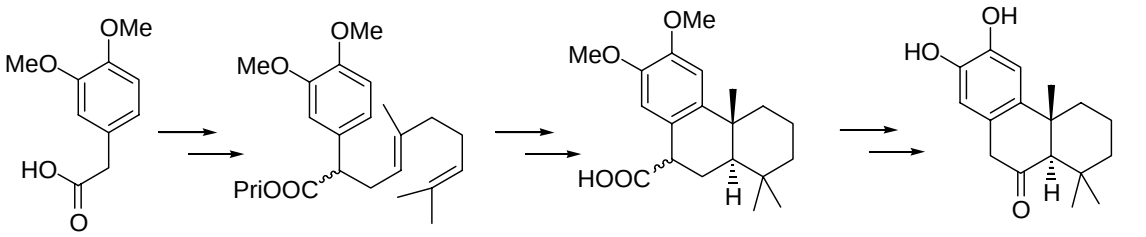

trans-diterpenone

The general strategy for synthesizing the desired trans diterpene catechol is illustrated in Scheme 2.2. The synthesis began with 3,4-dimethoxyphenyl acetic acid **5** (Scheme 2.3), which undergoes a coupling reaction with geranyl chloride at -78˚C to afford the desired compound **6** in 89% yield. This intermediate compound contained the desired carbon framework for the construction of the diterpene skeleton. Compound **6** then underwent an esterification reaction with EDCI and DMAP to produce **7** with the desired isopropyl ester functionality in 76% yield.[84] The importance of the isopropyl group is that it facilitated the desired trans stereochemistry during intramolecular cyclization of **7** into compound **8** in 61% yield (Scheme 2.3).[85] The cyclization of **7** into **8** was accomplished with BF_3OEt_2 in nitromethane to afford diastereoisomers. These diastereoisomers were not separated due to the later decarboxylation step, which removed one of the asymmetric centers. After chromatographic purification of compound **8,** this

compound was hydrolyzed under reflux conditions, to furnish the free acid **9** in 96% yield (Scheme 2.3). The cyclized free acid **9** was then decarboxylated with $Pb(OAc)_4$ and $Cu(OAc)_2$, which afforded the desired cyclic alkene **10** in 51% yield. The *trans* isomeric compound **10** was confirmed by 2D COSY and NOESY experiments described in the following (Figure 2.2).

Scheme 2.3. Synthesis of trans diterpenone

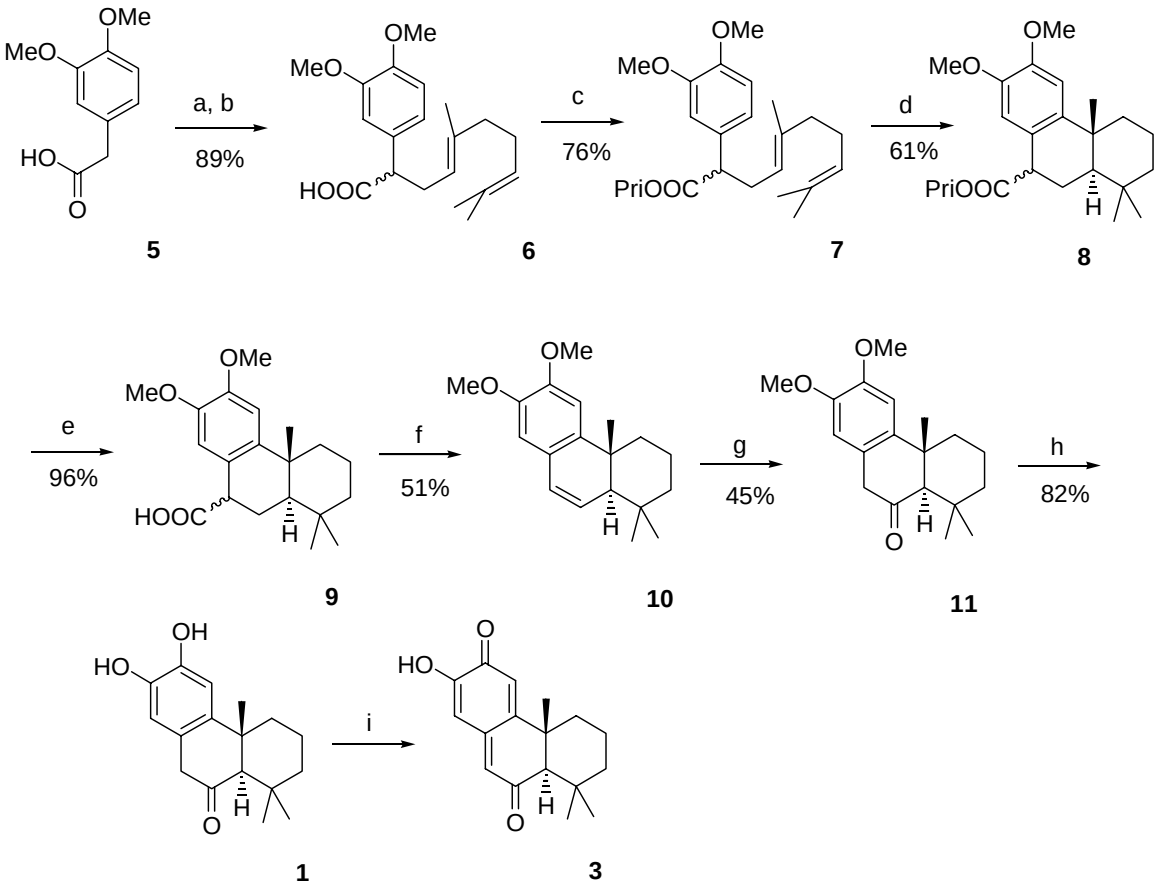

Reagents and conditions: (a) nBuLi, -78 °C in THF. (b) geranyl chloride, -78 °C in THF. (c) EDCI, DMAP, i-PrOH, room temp. in CH_2Cl_2. (d) BF_3OEt_2, room temp. in CH_3NO_2. (e) NaOH, reflux EtOH. (f) $Pb(OAc)_4$, $Cu(OAc)_2$, 140°C in quinoline. (g) mCPBA, TsOH room temp. in CH_2Cl_2. (h) BBr_3, room temp. in CH_2Cl_2. (i) Ag_2O, room temp. in CH_3CN.

Spectroscopic Analysis

COSY NMR is used to identify protons that are correlated through two and three bonds apart. Bond correlations appear as off diagonal cross peaks and are used to identify protons, which are connected throughout the molecule (Figure 2.2). We began the analysis by determining the location of proton Hc, which is expected to have a correlation with the alkene protons. The alkene protons are easy to identify because they are located at 5.91 and 6.45 ppm and appear as doublets due to spin spin coupling (Spectrum A). After expanding spectrum (A), it is then possible to identify proton H_c at 2.11 ppm because this proton is correlated with both alkene protons at 5.91 and 6.45 ppm. After identifying the location of proton H_c at 2.11 ppm, we acquired a NOESY spectrum to identify the relative stereochemistry at the ring junction of compound **10**. The NOESY spectrum is demonstrated in (Figure 2.3) and is used to identify protons which are normally no more than four angstrom apart and correlated through space rather than through bonds. Analysis of the cross peaks off the diagonal revealed that proton H_c is correlated through space with the region containing the methyl groups at 0.96, 1.21, and 1.62 ppm. Expanding this region and analysis revealed that proton H_c is only correlated through space with the methyl group located at 0.96 ppm. Additional analysis of cross peaks correlating with proton H_c revealed the absence of a through space correlation with the methyl group at ring junction as H_f located at 1.21 ppm. These results are now sufficient to confirm that the relative stereochemistry at the ring junction of compound **10** is a *trans* stereoisomer.

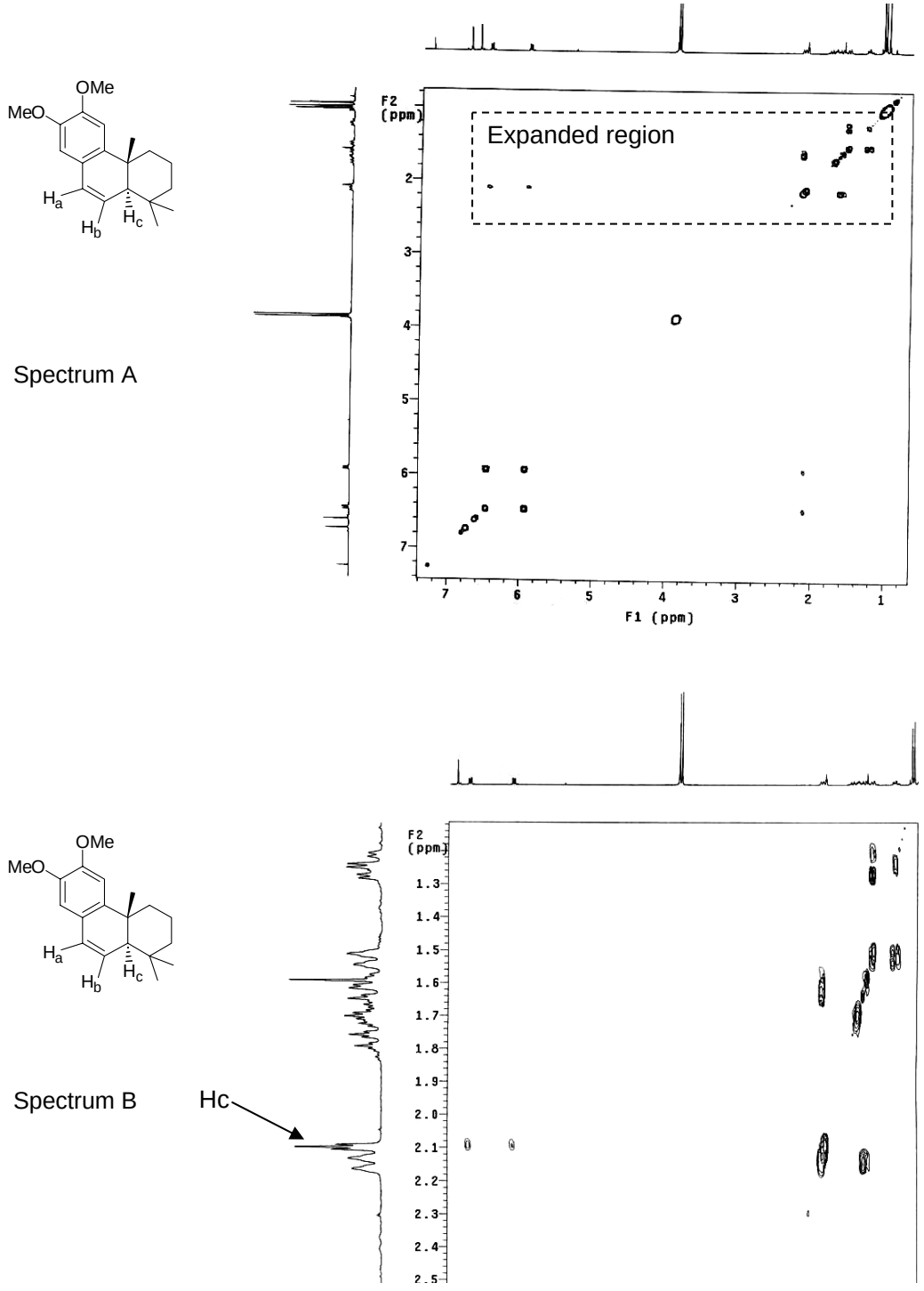

Figure 2.2. COSY spectrum of compound **10** (*Zhou et. al., 2005*)

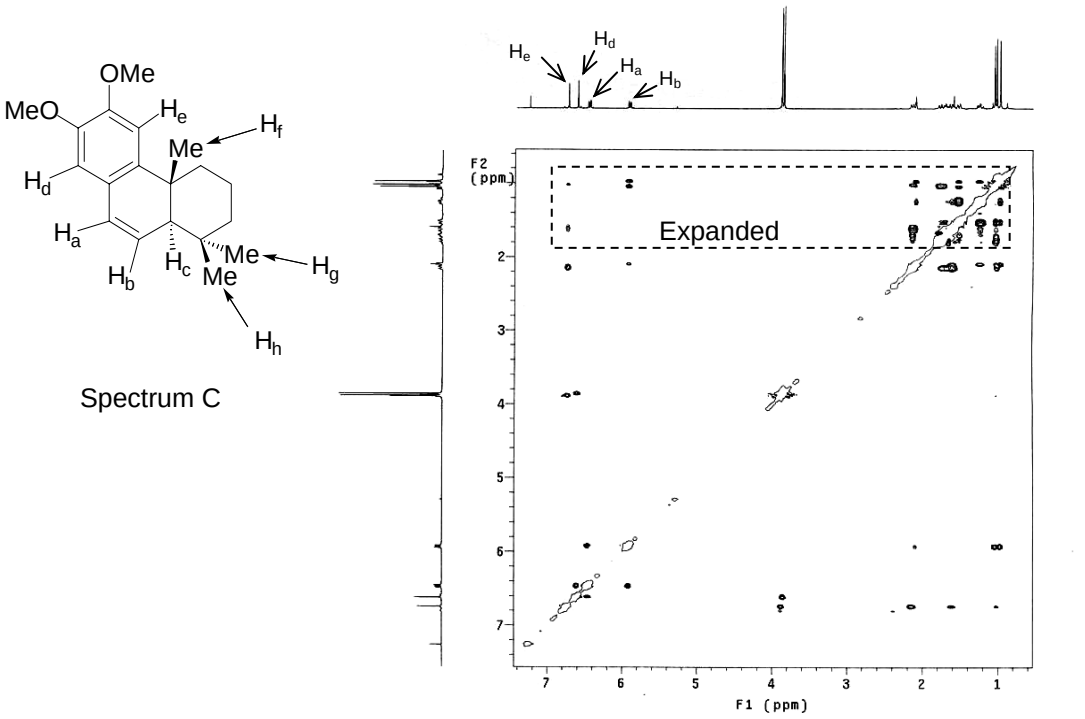

Expanded NOESY (400 MHz) in

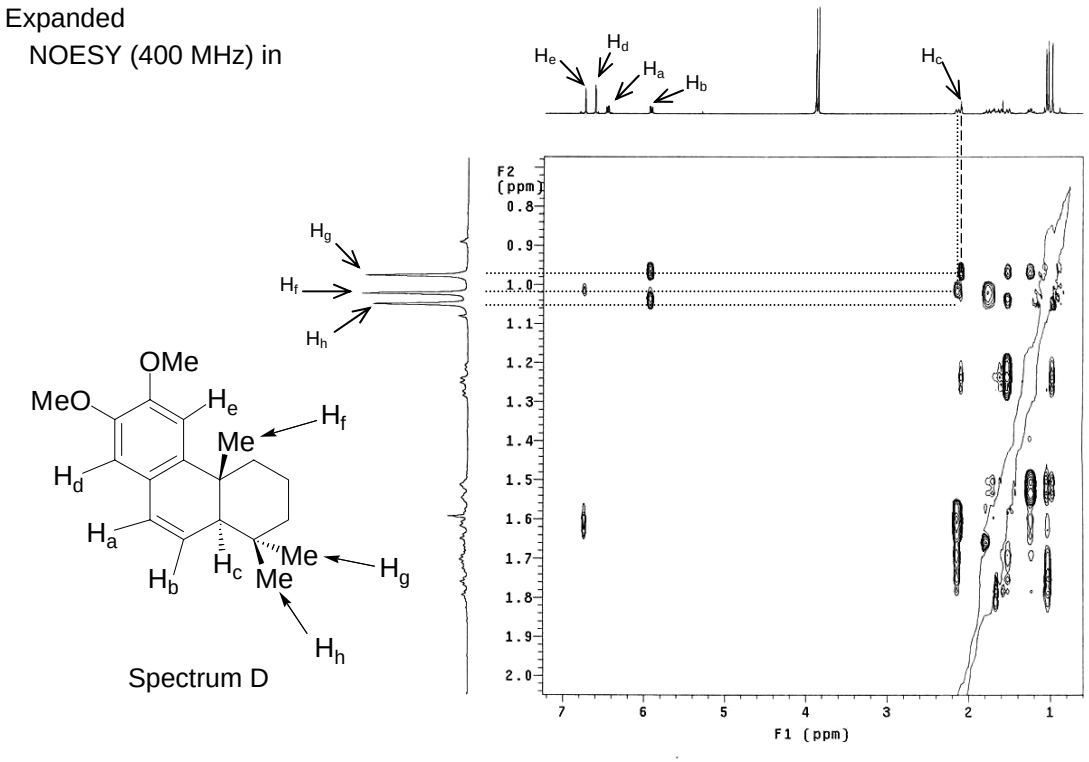

Figure 2.3. NOESY spectrum of compound **10** (*Zhou et. al., 2005*)

Compound **10** was subjected to electrophilic addition with mCPBA to form the intermediate epoxide, which underwent rearrangement under acidic conditions to produce the desired ketone **11** in 45% yield (Scheme 2.3). To form the desired catechol **1**, we used 0.5 mL of BBr_3 in CH_2Cl_2 as the ether cleavage reagent because of its high reactivity and ease of removal during the workup.[86] After treatment of **11** with BBr_3, the product **1** was formed in 82% yield. One problem we encountered when purifying **1** was that it was necessary to exclude air during the workup so that pure racemic diterpenone compound could be isolated.

The final diterpene quinone methide **3** was obtained by stirring a solution of **1** in CD_3CN with 5 mg silver (I) oxide at room temperature for 10 min. The suspension was then filtered through a 0.2 μm filter (Acrodisc, 13 CR, PTFE). The ^1H NMR analysis of **3** showed that aromatic and benzylic proton signals had disappeared while three new signals were observed at 6.30, 6.40 and 6.51 ppm. These observed signals were fully consistent with *p*-QM formation and indicated that o-quinone was not the oxidized product. Moreover, it is noteworthy that QMs can be distinguished from precursor catechols due to their very bright colors, a characteristic of conjugated quinone methides.[87]

2.4 Analysis of TPQM alkylation

To assess the QM **3** mode of action as a DNA alkylating agent, studies with compound **3** and deoxyguanosine (dG) under general acid conditions were undertaken. In these reactions, a solution of QM **3** (1.5 mM) in DMSO was added to 10 mM dG and 10 mM TsOH then analyzed at 260 nm with a gradient of 10-20% acetonitrile/water in

triethylammonium acetate buffer pH 4.2 by HPLC. The use of TsOH (pKa -7) was based on the fact that activation of QM through protonation has been shown to be a requirement in some cases of QM alkylation.[88] An HPLC trace of the reaction after 2 hours is shown in Figure 2.4c. As a comparison, the control incubations of QM **3** with and without dG are shown in Figure 2.4a and b, respectively. The broad unresolved peaks in Figure 2.4a indicate that QM **3** readily dimerized or polymerized. The polymerization of QM **3** is consistent with reported studies in which unsubstituted QMs readily polymerize due to the lack of a steric contribution by hydrophobic substituents.[89,90] The three peaks detected eluting at a position different from that of QM **3** are marked by a cross in Figure 2.4c. These peaks were collected for ^{1}H NMR analysis but unfortunately they revealed no structural information about the products in the reaction. Since the reactions of QMs are greatly influenced by the medium and reaction conditions,[91,92] it was felt that perhaps a weaker Bronstead acid would polarize and stabilize QM **3**, thereby reducing its tendancy to polymerize. Thus, studies with triflouroacetic acid (pKa 0.23) or acetic acid (pKa 4.75) were also explored, however, no adducts were found under these conditions.

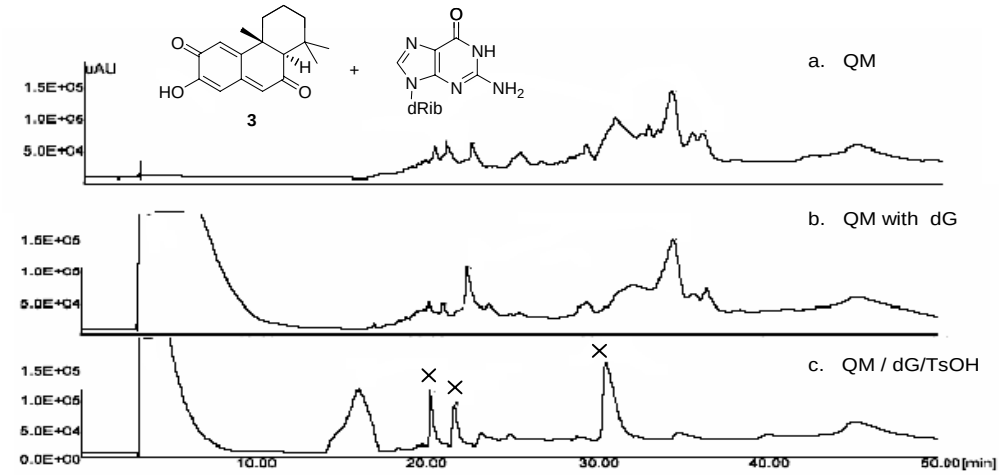

Figure 2.4 HPLC chromatogram of 1.5 mM QM **3** in DMSO incubated with 10 mM dG followed by addition of 10 mM TsOH and incubated for 2 hours at ambient temperature detected at 260 nm. (a) Control run with QM **3** in DMSO, (b) 1.5 mM QM **3** and 10 mM dG. (c) 1.5 mM QM **3**,10 mM dG, and 10 mM TsOH. Peaks indicated by a cross were isolated and analyzed by ^{1}H NMR.

2.5 QM formation by Cu^{2+} induced oxidation of diterpenone catechol 1

The reaction of terpene QM **3** and dG failed to provide any detectable dG-QM adduct, possibly due to polymerization of the reactive QM. This led us to examine the formation of diterpene QM **3** by homoconjugated terpene catechol **1** through Cu^{2+} -induced oxidation under aqueous conditions. As previously stated, one major difference between the Cu^{2+} -induced oxidation of terpene catechol **1** and that of a simple catechol is that *p*-QM or *o*-quinone can form during the oxidation of terpene catechol **1**.[93] In order to determine the identity of the oxidized products and the oxidation pathways, a thiol trapping approach was needed. This approach is useful for aquiring indirect structural information of quinones and quinone methides, since their high reactivity precludes their direct identification.[94] This study was employed by Dr. Zhou to investigate the oxidation products of diterpenone catechol **1** in the presence of Cu^{2+} upon the addition of

mercaptoethanol. In this manner, if an *o*-quinone or *p*-QM were formed in the reaction, then two isomeric thiol adducts should be identified.[93,95] On the other hand, if the rate of isomerization of *o*-quinone to *p*-QM had occurred at a rate comparable to the thiol addition, then four possible thiol adducts should be formed (Scheme 2.4). The formation of o-quinone thiol adducts can be distinguished based on the site of attachment on the aromatic ring, while p-QM thiol adducts should give two aromatic proton signals.

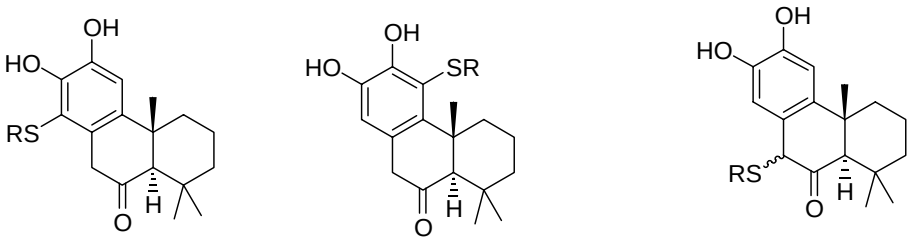

o-quinone thiol adducts p-QM thiol adduct

Scheme 2.4 Potential Thiol Adducts of Diterpenone o-Quinone and p-QM Zhou et. al. 2005

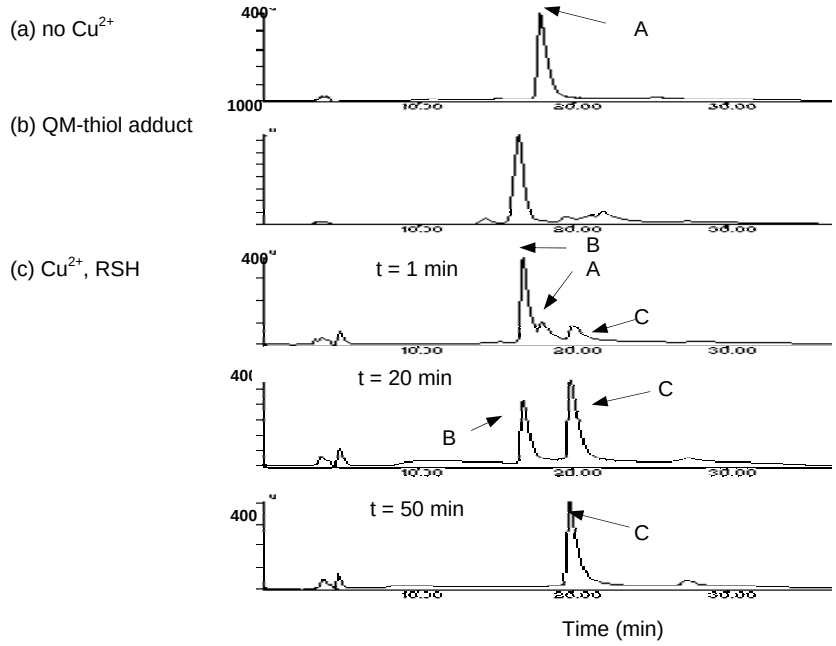

Figure 2.5. HPLC analysis of the thiol addition on diterpenone catechol **1** in the absence and presence of Cu^{2+} at room temperature. (a) compound **1** (0.25 μM) in phosphate buffer (5.0 mM, pH 7.0) without Cu^{2+}; (b) diterpenone QM-mercaptoethanol adduct under organic conditions; and (c) compound **1** (0.25 mM) in phosphate buffer (5.0 mM, pH 7.0) and mercaptoethanol (0.75 mM) in the presence of Cu^{2+} (1.0 mM). (Zhou. et. al. 2005).

Figure 2.5 demonstrates the progress of the thiol trapping experiment of catechol **1** as followed by HPLC analysis. The results in Figure 2.5a can be interpreted as follows, catechol **1** as shown by signal A in the absence of Cu^{2+} remains unchanged. For comparison, Figure 2.5b shows the reaction of thiol addition to a preformed p-QM of diterpenone catechol under organic conditions. Direct ESI-MS analysis of this fraction revealed four mass signals at 699, 349, 287, and 271 m/z, which were assigned as the noncovalently associated homodimer ($C_{38}H_{52}O_8S_2$-H^+), the molecular ion M^+ (349 for $C_{19}H_{26}O_4S$-H^+), M-62, and M^+ mercaptoethanol, respectively. Direct fragmentation of the dimeric mass ion signal by MS/MS confirmed the noncovalently associated homodimer.

The homodimer formation was also observed for the diterpenone catechol in the ESI-MS analysis, thus it was concluded that the signal in Figure 2.5b at 16 min was the direct mercaptoethanol adduct of the diterpenone p-QM. The reaction mixture in Figure 2.5c shows a gradual loss of catechol **1** as monitored by decrease in signal A in phosphate buffer (pH 7.0), mercaptoethanol (0.75 mM) and Cu^{2+} (1.0 mM). After 20 min the initial signal B is converted into a new signal C over a period of 50 min. From the analysis of signal C three mass signals at 695, 347 and 287m/z were identified. The molecular ion M^+ (calcd as 347 for $C_{19}H_{24}O_4S\text{-}H^+$), suggested that the initial p-QM thiol adduct B was further oxidized by Cu^{2+} under aqueous conditions and trapped intramolecularly. The structure of the thiol adduct obtained from signal C was confirmed by chemical shifts in both proton and carbon- 13 spectrum and illustrated in Scheme 2.5.

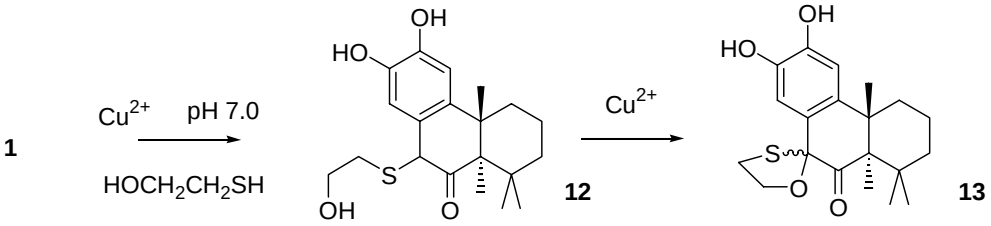

Scheme 2.5 Thiol adducts of diterpenone catechol **1** in the presence of Cu^{2+} (Zhou et. al. 2005)

2.6 Extent of DNA damage by diterpenone catechol 1 in the presence of Cu^{2+}

The direct mercaptoethanol thiol adduct **12** and **13** of the diterpenone catechol implied that the oxidation pathway of terpene catechol **1** proceeds solely through *p*-QM formation under aqueous conditions and may be unique for the diterpenone catechol **1** in

the Cu^{2+} induced oxidation process. Furthermore, the Cu^{2+} - mediated oxidation of diterpenone catechol was significant because of the implication that multiple DNA lesions could result from the oxidative DNA damage by the hydroxyl radicals and/or nucleobase alkylation by QMs.

To verify the extent of DNA damage with diterpenone catechol **1** in the presence of Cu^{2+} -induced oxidation, a polyacrylamide gel electrophoresis (PAGE) experiment was performed. This experiment was accomplished by Dr. Zhou using a 30-mer oligonucleotide as the target DNA and radiolabeled with ^{32}P-phosphate at the 5'-position with T4 polynucleotide kinase. In this study, the final reaction solutions contained 1.0 μM duplex DNA, 5.0 mM phosphate buffer (pH 7.0), $CuCl_2$ (0, 750, 0, 750, 250, 83, 150, 50, or 17 μM) and compound **1** (0, 0, 250, 250, 250, 250, 50, 50, or 50 μM, respectively) in 10% acetonitrile. After incubating these reactions at 37 ºC for 2 h, a portion of each reaction was then treated with formamide and separated by 20% denatured PAGE. The piperidine treatment was achieved by mixing the reaction solution with a 10% piperidine solution and subsequently heating at 90 ºC for 20 min. Afterward, each reaction solution was separated by 20% denatured PAGE and analyzed by gel image analysis software.

The results of these studies are summarized in (Figure 2.6). As expected, no DNA damage was detected with either Cu^{2+} or diterpenone catechol **1** alone. This indicates that catechol **1** does not undergo auto-oxidation and consistent with our previous study (refer to Figure 2.4a). However, in the presence of Cu^{2+} and compound **1**, the oxidative DNA damage was clearly non-sequence selective and in proportion to the concentration of compound **1**. Since no evidence for selectivity was detected in either single stranded

(ssDNA) or double stranded DNA (dsDNA), this suggested that the Cu(II)-diterpenone **1** system does not specifically target structural features of the DNA strand. When the DNA modification of ssDNA and dsDNA were compared, it was found that dsDNA is less susceptible to oxidative lesions than ssDNA.[96] These differences are most likely influenced by their different stacking conformation and most importantly, the greater stability of the duplex strand.

As shown in Figure 2.6 extensive DNA oxidation and base damage was observed with compound **1** 250 μM and $CuCl_2$, thus reflecting the high toxicity on DNA by terpene catechol **1**. Upon further analysis of these assays, the non-piperidine treated samples indicated that direct DNA cleavage was due to fragmentation of the DNA backbone by the hydroxyl radicals. In contrast, the samples treated with piperidine suggest that cleavage of the DNA was due to the considerable indirect nucleobase damage. However, no alkylation products were observed as evident by the lack of a higher molecular band in the conditions studied. Thus, it is inconclusive whether the indirect DNA nucleobase damage was due to either the oxidation or alkylation process or combination of both.

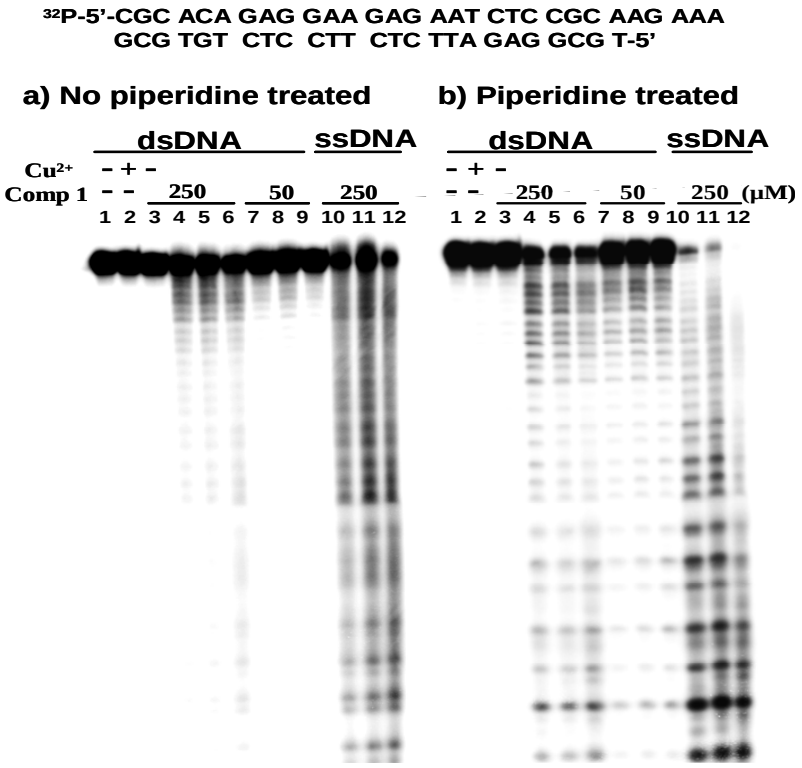

Figure 2.6 PAGE analysis of the oxidative damage on DNA by diterpenone catechol **1** in the presence of Cu^{2+}. Each reaction solution contained 1.0 μM oligonucleotide, phosphate buffer (5.0 mM, pH 7.0), and 10% CH_3CN. Reactions were initiated by adding a solution of **1** (250 or 50 μM), and the resulting solutions were incubated at 37 ºC for 2h. The piperdine treatment was achieved by adding a solution of 10% piperdine, and the resulting mixtures were subsequently heated at 90 ºC for 20min. The concentrations of Cu^{2+} in the lanes were as follows: 1, 0 μM; 2, 750 μM; 3, 0 μM; 4, 750 μM; 5, 250 μM; 6, 83.3 μM; 7, 150 μM; 8, 50 μM; 9, 16.7 μM; 10, 750 μM; 11, 250 μM; and 12, 83.3 μM (Zhou et. al. 2005).

2.7 Mechanism for oxidation of diterpenone catechol 1 in the presence of Cu^{2+}

The extensive DNA cleavage by compound **1** (250 μM) even at one-third the concentration of $CuCl_2$ (83 μM) was fully consistent with disproportionation of the Cu(II)/Cu(I) redox cycle. The similar DNA fragmentation pattern implied that a common

reactive oxygen species (possible hydroxyl radical), was produced during the oxidation process. Support for the presence of this reactive hydroxyl radical species was attributed to the cleavage of the DNA in a non-sequence specific manner.[97] To account for the production of this common reactive species, we proposed a mechanism for the Cu(II)-diterpenone **1** catechol system. In this process, we proposed that initial oxidation of diterpenone **1** produces *p*-QM through disproportionation of Cu^{2+}/Cu^{+} redox cycle with subsequent production of hydroxyl radical. This *p*-QM intermediate then undergoes nucleophilic addition to form a mono adduct diterpenone catechol which generate hydroxyl radicals and a second p-QM in the Cu^{2+}/Cu^{+} redox cycle. The second *p*-QM then reacted with another nucleophile to form a stable bis adduct diterpenone catechol as the final product (Scheme 2.6).

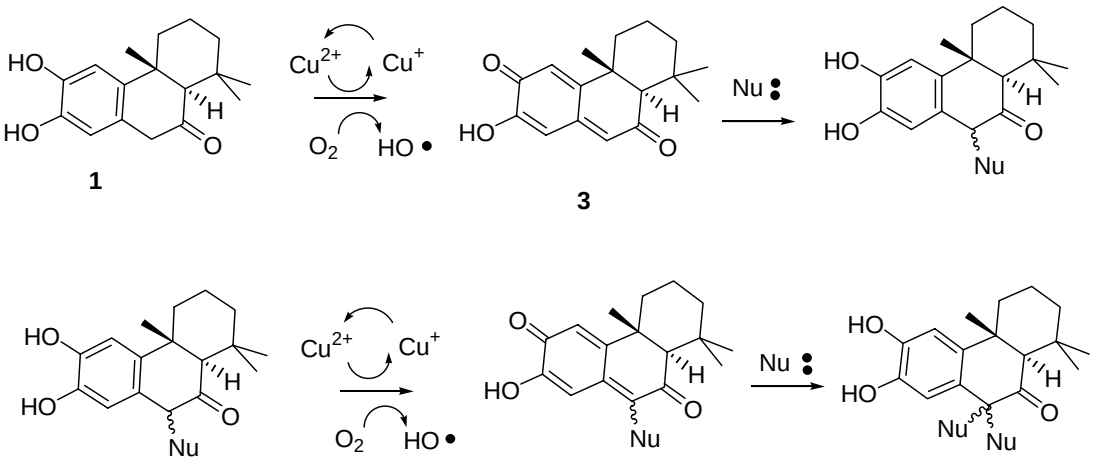

Scheme 2.6 Catechol oxidation and generation of hydroxyl radicals (Zhou et. al. 2005)

The significance of this process is that a terpene QM **3** as an analog of a triterpene QM was generated from the induced oxidation of a terpene catechol **1** under aqueous conditions. Most importantly, we found that a second oxidation of this thiol adduct resulted in formation of a bis-mercaptoTPQM **13** adduct. Support for the conversion of an initial QM adduct to another QM, is the oxidation of an ammonium adduct of a natural diterpene QM reported by Kupchan *et.al*.[98] The fundamental novelty in our studies is that our results suggest a unique Cu^{2+} induced oxidation pathway for a homoconjugated terpenone catechol **1**, which formed multiple QMs from this one compound. Furthermore, a *p*-QM is generated in preference over *o*-quinone formation under the conditions studied.

2.8 Conclusion

The reported biological activities of triterpene quinone methides (TPQMs) has led our investigation of the terpene catechol **1** as potential antitumor or anticancer agent. A synthetic analog of a natural TPQM **3** was synthesized and investigated for a possible QM-dG nucleoside adduct. Unfortunately, no adduct was observed under these experimental conditions, possibly due to the undesirable polymerization of terpene QM **3** as side reaction. The oxidation pathway of diterpene catechol **1** as a TPQM precursor was found to form a *p*-QM capable of undergoing consecutive nucleophilic additions and further oxidation to QMs. Our analysis of the DNA damage by terpene catechol **1** in the presence of Cu^{2+} induced oxidation showed extensive DNA oxidation and fragmentation of both single stranded and double stranded DNA. The similar cleavage pattern of DNA oxidative damage by diterpene catechol **1** in the presence of copper (II) suggests a common

reactive species. This reactive species could be hydroxyl radicals generated in situ and responsible for causing the non-sequence selective cleavage of the DNA. The studies in this chapter suggest that natural terpene QMs may exist as terpene catechol prior to their isolation or conversion by oxidative enzymes. If so, then catechol precursors may be useful intermediates in the design of QM based drugs.

Chapter 3

DNA modification by diterpene quinone methide analogs

3.1 Introduction

The results of our previous studies in chapter 2 demonstrated that multiple terpene QM's were formed from a homoconjugated catechol precursor **1** through the disproportionation of Cu(II)/Cu(I) redox cycle (Scheme 3.1). The high reactivity of QM **3** toward nucleophiles was confirmed, and extensive DNA damage was observed during the oxidation process.[99] Because cytotoxicity of catechols has been attributed to o-quinone formation and subsequent alkylation and/or redox cycles, the studies in this chapter are aimed at clarifying whether DNA damage in the presence of terpene catechol is due to the reactive QM intermediates and/or from reactive oxygen species generated from the disproportionation of Cu(II)/(Cu(I) redox cycle (Scheme 3.1).[99] Therefore, the objective of this study was to elucidate the Cu^{2+} induced DNA damage mechanism and to evaluate the potential impacts of diterpenone catechols on a short 30mer DNA oligonucleotide. To achieve this, a series of catechols were designed to study the potential effects of stereo-, substitutional, and functional groups on the QM formation and subsequent damage on DNA.

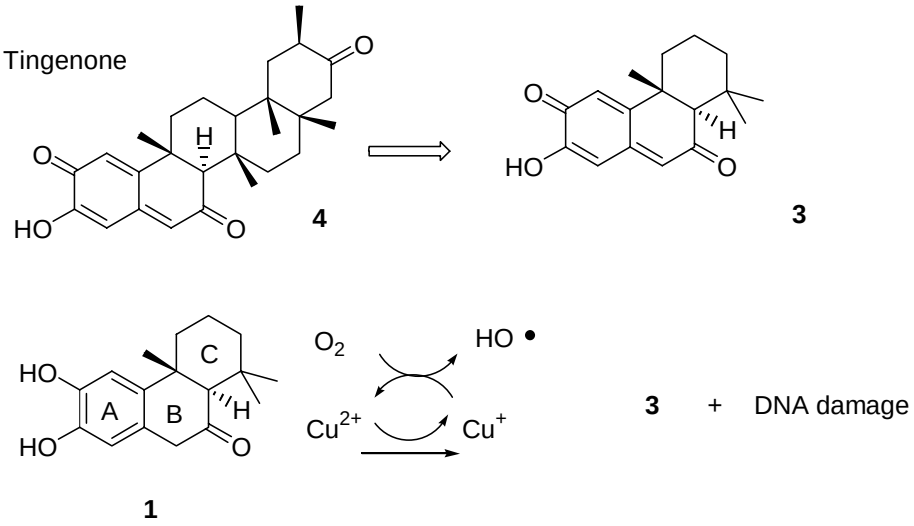

Scheme 3.1 Diterpenone Catechol **1** as a precursor for terpene QM **4** resulted in DNA damage in the presence of Cu^{2+} (Zuniga et. al. 2006)

3.2 Synthesis of methyl substituted diterpenone catechol

One disadvantage of our previously synthesized terpene QM **3** was that it was stable only in anhydrous acetonitrile at a diluted concentration, and red precipitation was observed upon concentration due to polymerization. To overcome this, we envisioned that a methyl substituent may contribute enough steric hindrance to prevent polymerization and this may contribute to additional selectivity of quinone methides toward certain nucleophiles.[100] It has been pointed out by Angle and coworkers that intrinsic structural features, such as the distortion of the quinoid ring and electronic delocalization play an important role in lowering the reactivity of 2, 6 –disubstituted and other QMs in comparison to unsubstituted QMs.[101] Most recently, Rokita's group demonstrated that electron donating substituents stabilize formation of QMs and adduct distribution toward DNA nucleosides.[100,102] Therefore, to investigate the effect of a methyl substitutent on the

QM formation, we synthesized this compound using our previously established methods.[103]

In this synthetic pathway, commercially available 2,3-dimethoxytoluene **14** was reacted with chloromethyl ethyl ether by a Friedel Craft alkylation to generate benzyl chloride **15** in 47**%** yield. Afterward, nucleophilic substitution of benzyl chloride **15** by cyanide furnished **16** in 92% yield. Subsequent hydrolysis of **16** was achieved by refluxing in sodium hydroxide solution to produce the free acid **17** in 63% yield. The coupling reaction of free acid **17** with geranyl chloride produced unconjugated free acid in 70% yield (structure not shown). The uncyclized free acid was converted into ester **18**, by standard esterification conditions and then cyclized to the desired methyl ester **19** in 60% yield (Scheme 3.2). This intermediate was different from isopropyl ester **7** in our synthesis of unmethylated diterpenone catechol **1** (refer to Scheme 2.3). For this synthetic route, we found that the methyl ester **19** resulted in higher cyclization yield, than that of isopropyl ester possibly due to steric effects around the aromatic ring.[104] Subsequent hydrolysis of **19** resulted in **20**, which was then decarboxylated to furnish the desired alkene **21** in 53% yield. This compound was then epoxidized with mCPBA followed by rearrangement in the presence of TFA to produce ketone **22F** in 41% yield. Cleavage of the methyl ether groups generated diterpenone catechol **23** in 54% yield (Scheme 3.2). Catechols **25** in 80% yield and **26** in 68% yield, were obtained directly from the deprotection of the alkene intermediates **21** and **10** from the synthesis of analogues **1** and **23**.

Scheme 3.2. Synthesis of methyl substituted trans diterpenone

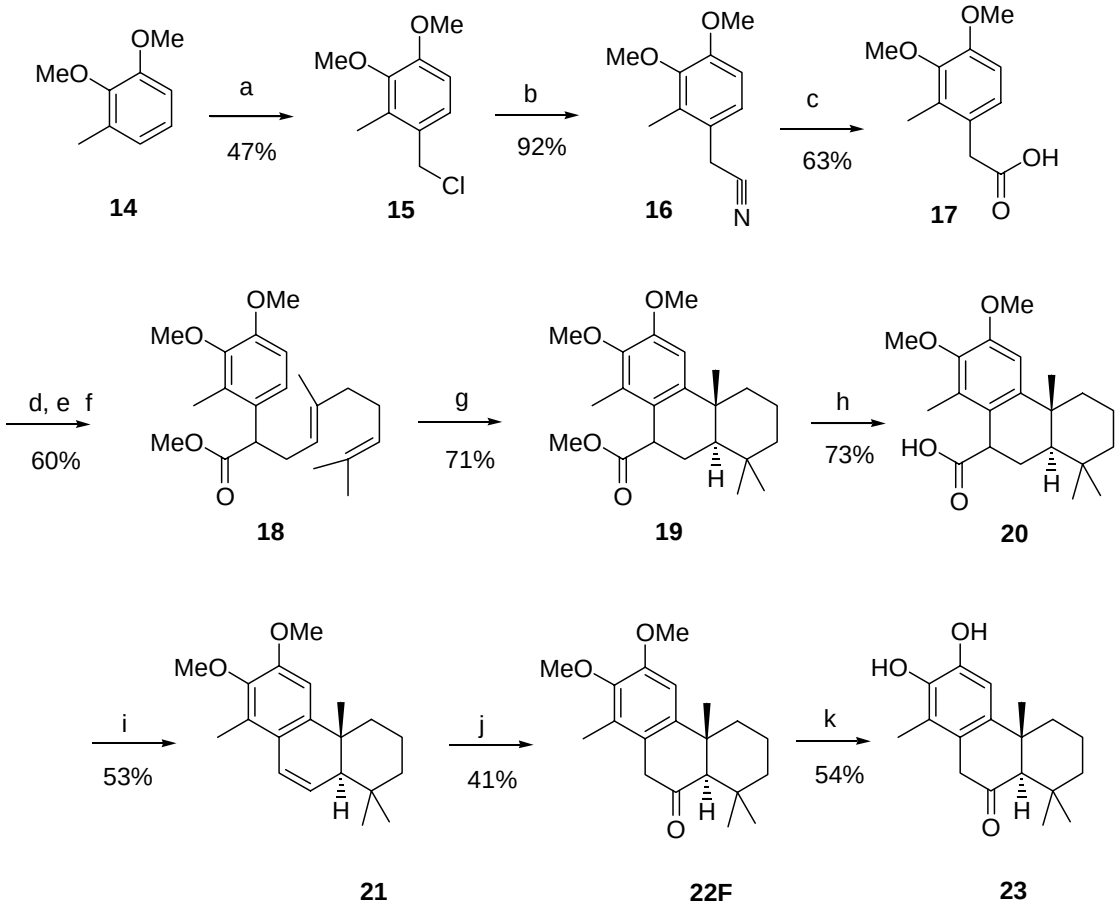

Reagents and conditions: (a) chloromethylethylether, in AcOH room temp (b) 18-crown-6 ether, KCN, in DMF at room temp (c) NaOH, reflux MeOH (d) nBuLi, -78 ºC in THF (e) geranyl chloride, in THF (f) DCC, DMAP, MeOH, room temp. in CH_2Cl_2 (g) BF_3OEt_2, room temp. in CH_3NO_2. (h) NaOH, reflux MeOH (i) $Pb(OAc)_4$, $Cu(OAc)_2$, 140 °C in quinoline (j) mCPBA, TFA, 0^oC in CH_2Cl_2. (k) BBr_3, room temp. in CH_2Cl_2.

3.3 Synthesis of *Cis* -Diterpenone

An interesting feature of natural TPQMs is that all of these compounds have *trans* fused ring systems, and no natural compounds with *cis* fused ring systems have been reported. Based on model studies, we found that *cis*-diterpenone adopts a bent conformation that shields the carbonyl group at the rigid fused ring junction. In contrast, *trans* diterpenone lies in a relatively flat conformation and exposes the carbonyl group at the fused ring junction (Figure 3.1). The unique structural conformation of the *cis*-fused system led us to synthesize *cis* diterpene catechols as precursor analogs of TPQMs and evaluate their potential QM formation and the corresponding properties.

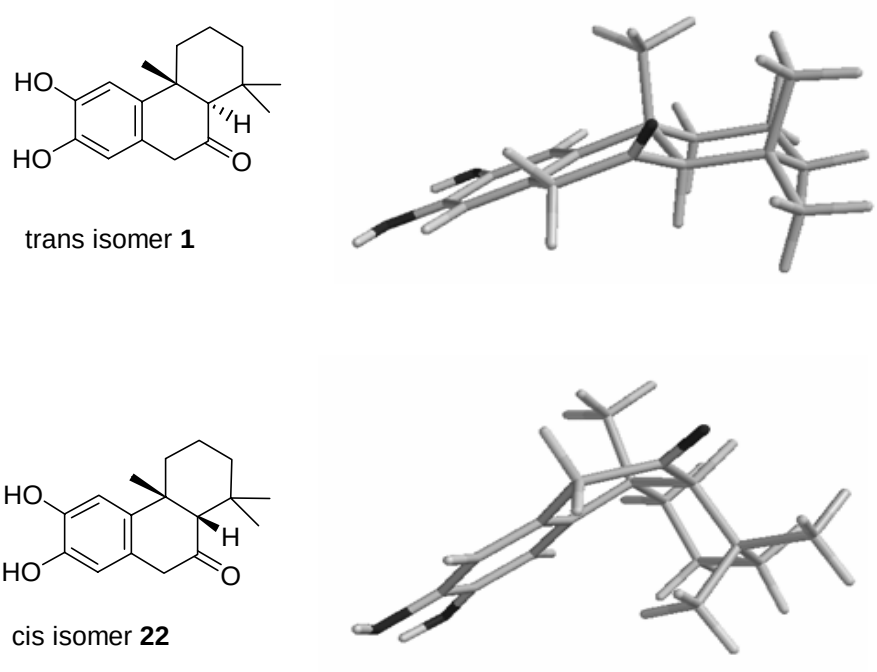

Figure 3.1. Conformational analysis of diterpenones based on AM1 molecular modeling. The cis-isomer **22** adopts a unique bend structure while trans-isomer **1** is in a flat conformation. (Zuniga et. al. 2006).

For the synthesis of cis-diterpene catechols, the carbonyl group of commercially available geranyl aldehyde **27** was protected with 1,3-propanedithiol to form **28** in 88% yield. Compound **28** and previously synthesized **15a, b** were then coupled with n-butylithium at -40 ºC with a dry ice and acetonitrile bath for 5 hours to form product **29a,b** and purified as a cis/trans diastereoisomeric mixture by a flash column separation (Scheme 3.3). Initial attempts to use bromide, rather than chloride of **15a**,**b** were unsuccessful due to the direct competition of the halogen metal exchange of the benzyl bromide. We also found that the temperature of this reaction was critical to facilitate the formation of lithiation of dithiol **28**.[105] For example, when the temperature was lowered to -78º C, the reaction gave unsatisfactory results and a mixture of undesired products.

To remove the thiol protecting group of **29a,b** we first investigated the use of carbonate salts and $HgCl_2$ in a mixture of methanol and water (9:1). The role of the carbonate salts is to neutralize the mixture which becomes acidic during the deprotection. We found that deprotection of **29a,b** to form **30a,b** was achieved in 50% yield with HgO and $HgCl_2$. Similar yields were obtained when $HgCl_2$ was used with K_2CO_3, $CaCO_3$ or $CsCO_3$ but the reaction was sluggish. After further investigating the reaction conditions, we found that a higher yield could be obtained with a shorter reaction time and when compound **29a,b** was completely dissolved in methanol before the addition of water. Cyclization of conjugated product **30a,b** furnished **31a,b** at room temperature with BF_3OEt_2 in nitromethane (Scheme 3.3). Similar to the cyclization step of the previous methyl ester, we observed that the yield of **31b** was much higher than **31a**, possibly due to the additional methyl group. Cleavage of the methyl ethers on compound **31a,b** with BBr_3

produced the desired compound **22** or **24** which were purified by a flash column separation.

Scheme 3.3 Synthesis of methyl cis diterpenone

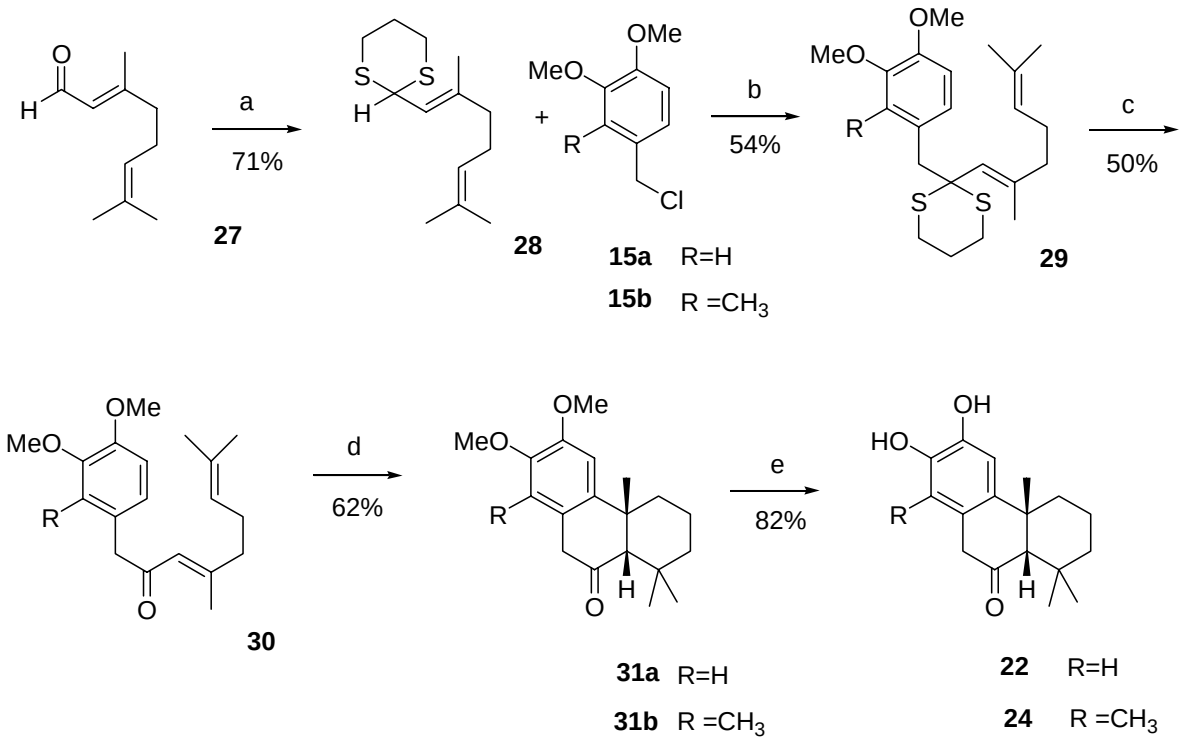

Reagents and conditions: (a) $HS(CH_2)_3SH$, BF_3OEt_2, -50 ˚C in THF (b) nBuLi, -40 ˚C in THF (c) $HgCl_2$ HgO, room temp. 9:1 MeOH/H_2O (d) BF_3OEt_2, in CH_3NO_2. (e) BBr_3, room temp in CH_2Cl_2. The yields are only representative of compound **24**.

Spectroscopic analysis

The proton and carbon chemical shift assignments for the cis isomer **31a** were confirmed by ^{1}H NMR, NOESY, and ^{13}C NMR techniques. The ^{1}H NMR spectrum of **31a**

showed the chemical shifts corresponding to the three methyl groups on the C-ring (refer to Scheme 3.1) at approximately 1.02, 0.94, and 0.36 ppm. By contrast, the methyl groups on the C-ring of *trans* isomers **11** and **22** occured between 1.32-0.97 ppm. The *cis* - isomer **31a** showed a large coupling constant of 23.0 Hz for the benzylic hydrogen atoms at 3.39 ppm. This coupling constant was not observed for the previously synthesized *trans* isomer **11**, which showed a singlet for the benzylic hydrogen atoms at 3.55 ppm.

The stereochemistry of cis isomer **31a** was confirmed by 2D NMR NOESY analysis. The NOESY spectrum (Figure 3.2) indicates that proton H_e located at the ring junction is at 2.09 ppm. Analysis of the diagonal crosspeaks indicated strong NOE signals to the methyl groups located at 1.05 and 0.94 ppm. This suggested that proton H_e is correlated through space with two angular methyl groups; this is in contrast to one correlation observed in Spectrum D in Figure 2.3. On the basis of these NOESY correlations, we confirm that the relative stereochemistry of compound **31a** is a *cis* stereoisomer.

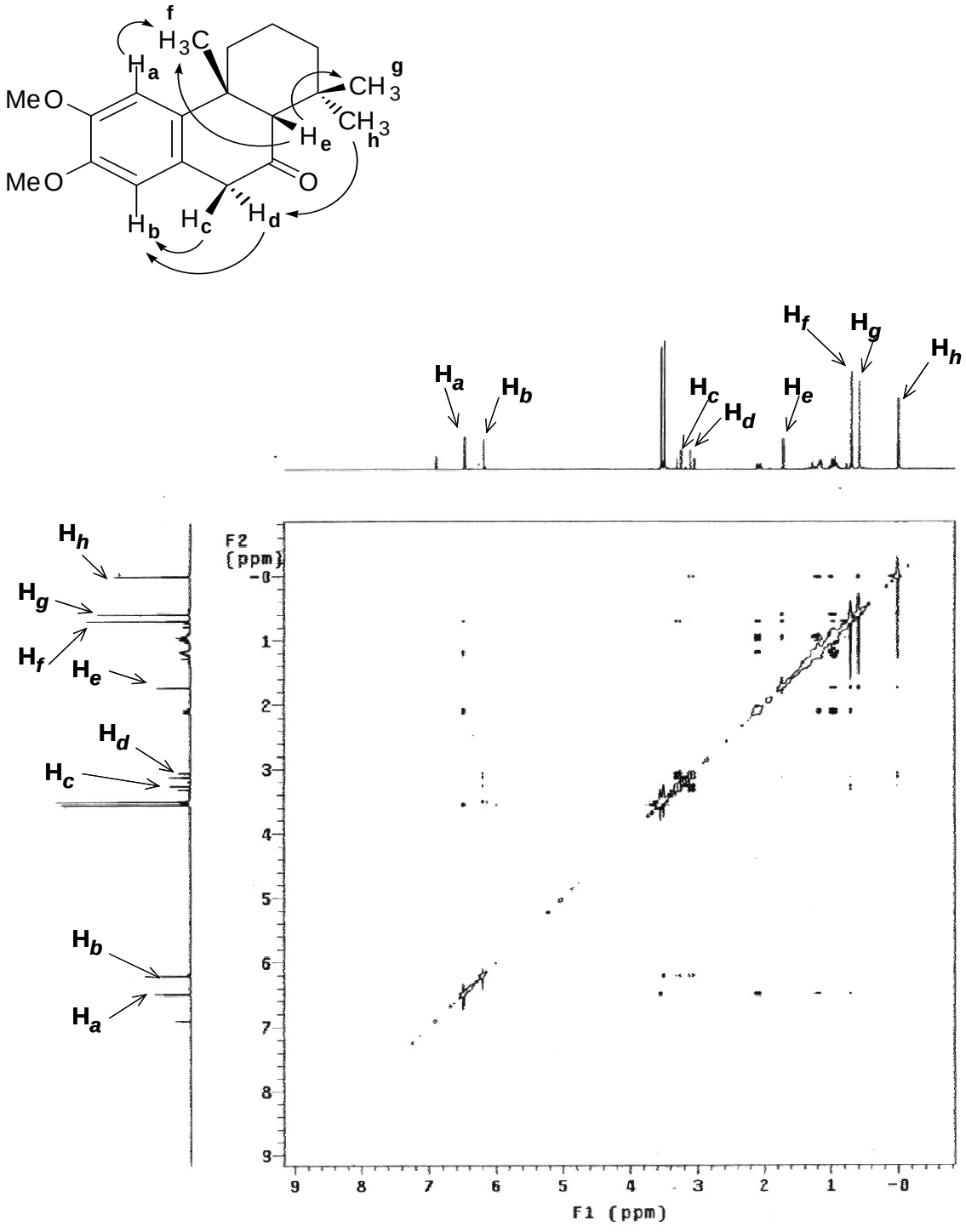

Figure 3.2 NOESY spectrum of analog compound **31a** (*Zhou et. al., 2006*).

The oxidation of *cis* catechol **22** with Ag_2O in $CDCl_3$ afforded analytically pure *p*-QM **32**, which was confirmed by both ^1H and ^{13}C NMR analysis (Figure 3.3). In the ^1H NMR spectrum, the signals of benzylic protons of **22** at 3.5 ppm disappeared completely upon oxidation, while four singlets were observed between 6.20 and 6.90 ppm (Figure 3.3). The ^{13}C NMR shown in Figure 3.3 also revealed eight carbon signals above 100 ppm as compared to seven of **22** which indicates formation of the conjugated QM. An important finding of this work was that in contrast to the high reactivity of our previous terpene QM **3**, we found that *p*-QM **33** of the cis catechol **31** remained unchanged upon concentration and storage over several weeks at -4 ºC. The remarkable stability of *p*-QM **33** was attributed to its unique bent conformation (refer to Figure 3.1), which may effectively prevent polymerization upon concentration.

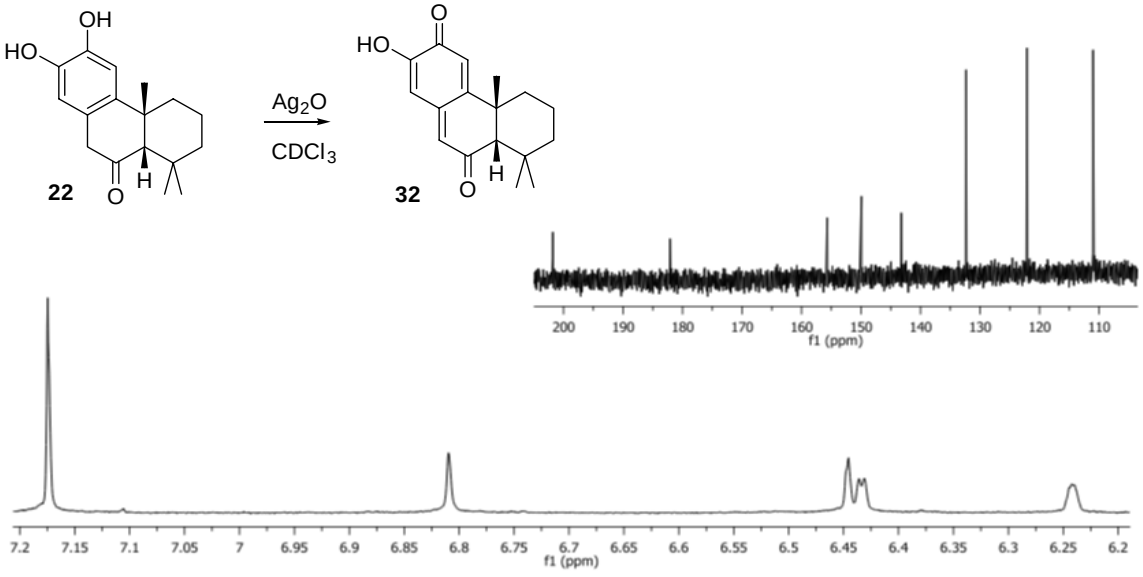

Figure 3.3. ^1H and ^{13}C NMR spectrum of **32** showing distinguishable proton resonances and carbon signals.

In a similar fashion, catechol **25** was oxidized and formed selectively o-quinone **33**, which was confirmed by both ^{1}H and ^{13}C NMR analysis**.** The ^{1}H NMR analysis showed four proton resonances from 6.0-6.5 ppm (Figure 3.4). The two proton resonances at 6.5 ppm have a small coupling constant of 2.2 Hz and are in the characteristic alkene region. The ^{13}C NMR shown in Figure 3.4 revealed eight carbon signals above 100 ppm, with two distinguishing signals at 181 and 180 ppm corresponding to the diketone. The significance of these investigations was that these studies suggested that *p*-QM formations are unique to homoconjugated catechols as the oxidation products, while o-quinones are formed preferably for simple catechols or conjugated catechols.

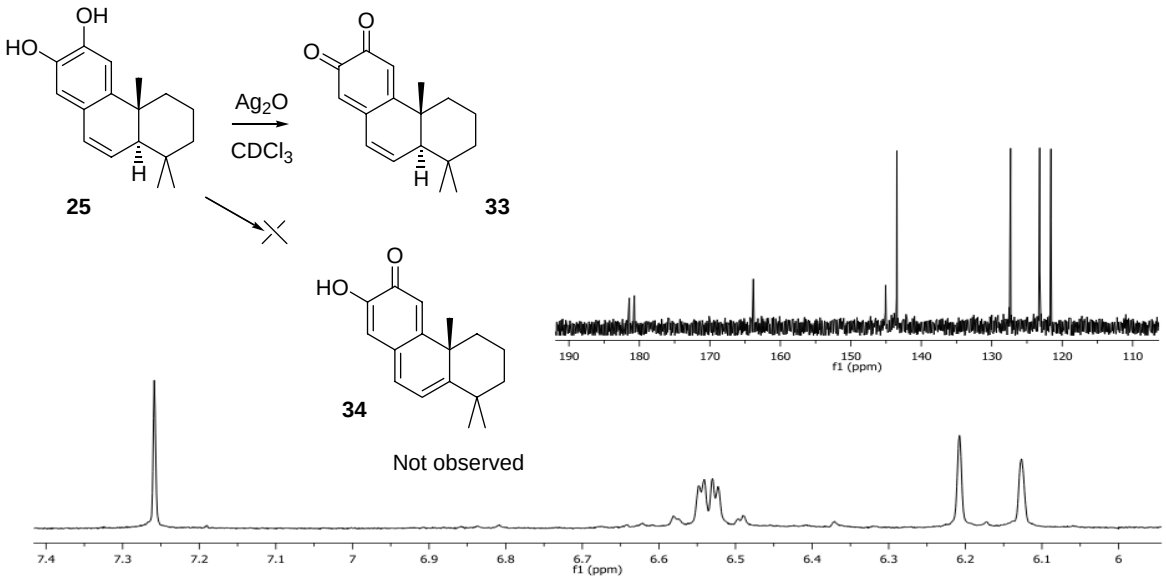

Figure 3.4. ^{1}H and ^{13}C NMR spectrum of **33** showing distinguishable proton resonances and carbon signals.

3.4 DNA oxidative damage by a series of terpene catechols

As previously stated, the Cu^{2+}- induced oxidation of diterpenone catechols was investigated with a wide range of compounds having stereo- , substitutional, and functional group differences as shown in Scheme 3.4. As demonstrated in earlier studies, the homo-conjugated compounds **1**, **22- 24** are capable of forming *p*-QM's, while conjugated compounds **25**, and **26** form exclusively *o*-quinones from catechol compounds.[106]

Scheme 3.4. Catechol analogs screened in DNA damage experiments

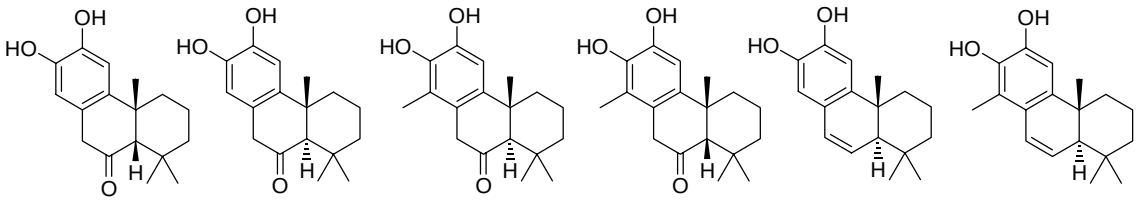

22 1 23 24 25 26

To examine the potential of DNA modification and the extent of DNA lesions by diterpenone catechols, a short 30/25 mer oligonucleotide was used as the target sequence. For the DNA damage study, reactions were initiated by mixing 0.25 μM duplex DNA, 40 μM copper (II) chloride, and catechols **1**, and **21-26** at concentrations of 10-40 μM in 10% acetonitrile and then incubated at 37°C for 12 hours. The samples were then treated with piperidine and separated through a 20% polyacrylamide gel electrophoresis (PAGE). The percentage of DNA damage was calculated based on the amount of the originally radiolabeled DNA band versus the total amount of radioactive DNA determined with the

Molecular Dynamics Typhoon 8600 Variable Mode Imager and Image Quant software (Molecular Dynamics).

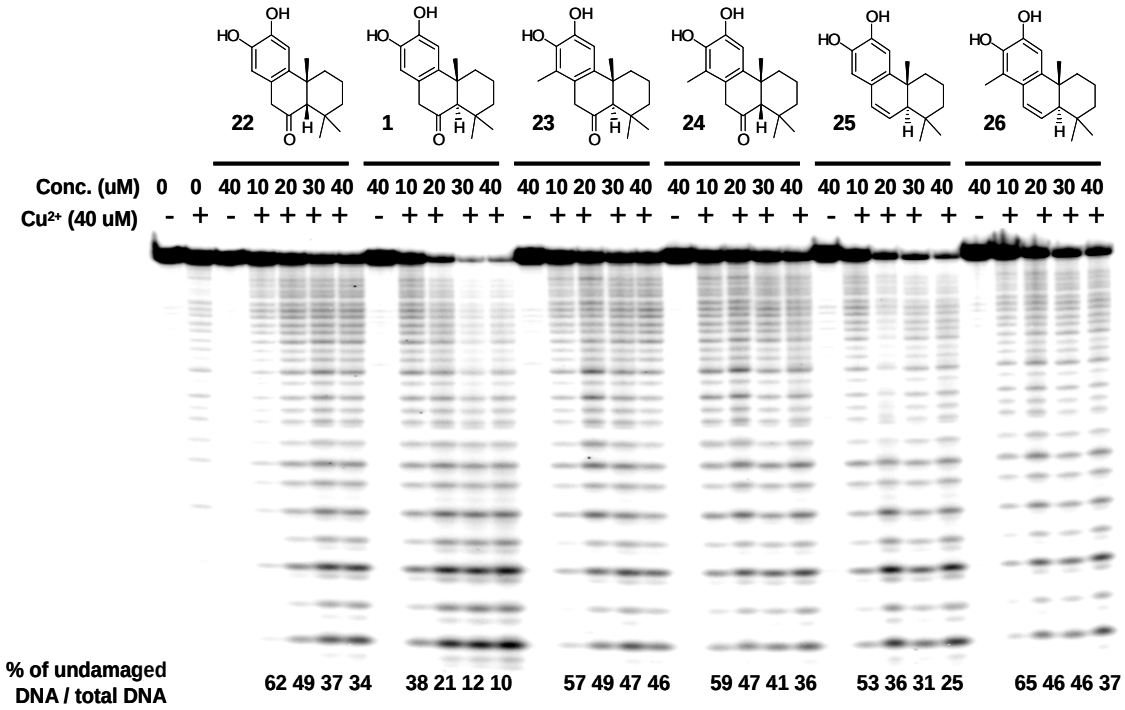

Figure 3.5. DNA damage experiment after piperidine treatment. 40 μM Cu^{2+}, 10-40 μM catechols **1**, and **22-26**, 0.25 μM DNA, 0.5 mM $MgCl_2$, 10 mM Phosphate buffer (pH 7.40) at 37 ºC for 12 hr treatment. The percentage was calculated as the average from three independent experiments using the amount of undamaged radiolabeled DNA versus the total amount of radioactive DNA. The average standard deviation was 5%. (Zuniga et. al. 2006).

The results after piperidine treatment are shown in Figure 3.5. As was expected, neither diterpene catechols **1**, and **22-26** alone nor Cu^{2+} at (40 μM) was able to induce detectable DNA damage. On the other hand, the gel analysis following piperidine treatment showed an increase in DNA fragmentation with all diterpene catechols **1**, and **22-26** suggesting that these compounds induced base damage (Figure 3.5). From the piperidine treated gel assay in Figure 3.5, the results showed an increase in the percentage

of damaged DNA with increase in concentration (10-40 μM) of all the diterpene catechols **1**, and **22-26**. It is clear from Figure 3.5 that the extent of DNA damage after piperidine treatment was concentration dependent within each compound yet varied from one another.[106] The percentage of undamaged DNA by each diterpene catechol **1**, and **22-26** is quantified in the bottom of Figure 3.5. On the basis of the percentage of undamaged DNA in (Figure 3.5), we found that *trans* diterpene catechols **1** and **25** caused more DNA damage than other analogs at the same concentration. When comparing DNA damage by alkene catechols **25** to **26**, we found that **25** causes slightly more damage than **26**. Comparison of catechol **1** to **23** showed that the additional methyl group on the A-ring decreased the amount of DNA damage significantly, and moderate decrease was observed in the case of **25** and **26**. However, this effect was not observed with *cis*-catechols **22** and **24**, suggesting that DNA damage cannot be directly correlated with methyl substituted diterpene catechols. Interestingly, we found that the amount of DNA damage by *cis* catechol **22** was much lower than by *trans* catechol **1**, probably due to its unique bent conformation.[106]

From the gel analysis of Figure 3.5, we found that despite the different levels of DNA damage, all the diterpene catechols **1**, and **22-26** induced a similar fragmentation pattern. For example, when compared with the same percentage of DNA damage at 30 μM of **22**, 10 μM of **1**, and 20 μM of **25**, almost identical patterns were observed. The similarity in the fragment pattern indicated that DNA damage was due to a common mechanism in the presence of Cu^{2+}.[106,107]

3.5 DNA oxidative damage in the presence of NADH and Cu^{2+}

The above DNA studies were aimed at examining the role of stereo, substitutional, and functional group effects on diterpene catechols in relation to their impact on DNA damage. In related studies, Penning *et al*, reported that redox cycling of polyaromatic hydrocarbon o-quinones caused three types of DNA damage in the presence of NADPH and $CuCl_2$.[107,108] Because NADH can participate in electron transport, and function as a one electron reductant, it has been proposed that the high redox potential of copper metal ion can catalyze NADH autooxidation to NAD• being further oxidized to NAD+ with generation of ROS to form active oxygen species cauing DNA damage.[109] Therefore, the purpose of this study was to clarify the role of NADH in Cu^{2+} induced oxidation of our catechols and to evalutate the effects on DNA damage. Thus, we continued to investigate the role of a reducing agent on the oxidation of our diterpene catechols with specific attention to conjugated catechols **25** and **26**.[106]

The DNA study was performed under similar conditions as previously described in the DNA damage study of Figure 3.5. A major difference in this experiment was that NADH to mimic NADPH was added and the concentration of each diterpene catechol and copper were reduced eight and four fold, respectively. The objective of using lower concentration of diterpene catechols is to determine whether the DNA damage is a result of the hydroxyl radical regenerated in redox cycle and/or due to diterpene catechol. For this study, a reaction solution with 100 μM NADH, compounds **1**, and **22-26** (0.5, 1, 2, and 5 μM respectively), 0.25 μM DNA, 5 μM Cu^{2+} in 10% acetonitrile was incubated at 37º C for 6 hours. The samples were then treated with piperidine and separated through a 20%

polyacrylamide gel electrophoresis. The percentage of DNA damage was calculated based on the amount of the originally radiolabeled DNA band versus the total amount of radioactive DNA determined with the Molecular Dynamics Typhoon 8600 Variable Mode Imager and Image Quant software (Molecular Dynamics).

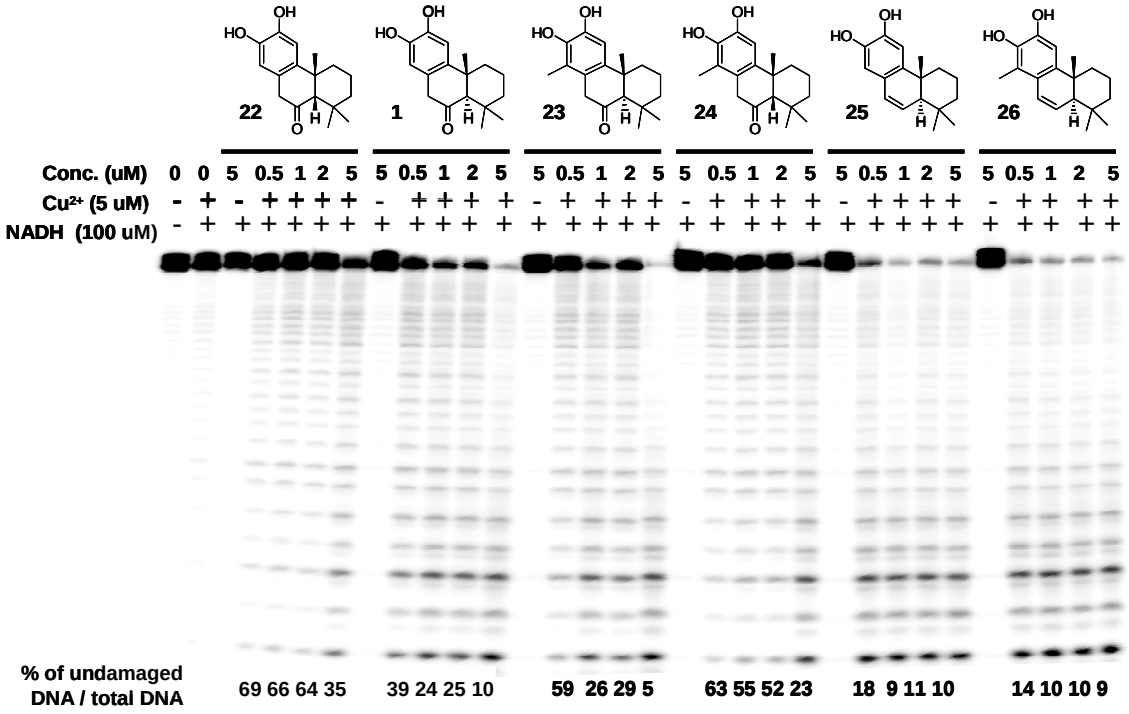

Figure 3.6. DNA damage experiment, with 100 μM NADH and 5 μM Cu^{2+} with compounds **1**, 22-26 at concentrations of 0.5-5 μM after piperdine treatment. The concentration of duplex DNA was 0.25 μM DNA in a 10 mM Phosphate buffer (pH 7.40) and 1 mM $MgCl_2$. The percentage was calculated using the amount of undamaged radiolabeled DNA versus the total amount of radioactive DNA, and the average standard deviation was 5%. All the reactions were repeated three independent times. (*Zuniga et. al. 2006).*

The results after piperdine treatment are shown in Figure 3.6. Comparison of the gel image in Figure 3.6 revealed a similar fragment pattern to that without NADH shown in Figure 3.5. However, a major difference in this study was that more than 80% of the

original DNA was damaged with diterpene catechols **25** and **26**. As shown in Figure 3.6, the extent of DNA damage is not concentration dependent with catechols **25** and **26**, this is demonstrated by comparing the percentage of undamaged DNA at 1 versus 5 μM of catechols **25** and **26**.[106] Furthermore, DNA damage was found to be higher with *trans*-diterpenone catechols **1** and **23** than with cis-catechols **22** and **24** in a concentration dependent manner, but the methyl effect was not apparent.

From the gel analysis of Figure 3.6, the enhanced DNA damage with NADH in the Cu^{2+} induced oxidation of diterpene catechols **1** and **22-26** was attributed to the reducing capability of NADH. For example, the concentration dependent DNA damage with catechols **1** and **22-24** implied that NADH might reduce the oxidation products only partially. However, the extent of DNA damage with alkene catechols **25** and **26** seemed not concentration dependent. This suggests that alkene catechols **25** and **26** undergo oxidation into their quinone forms and then fully reduced by NADH to the initial catechol **25** and **26**, forming a complete redox cycle of catechol/quinone with Cu^{2+} induced oxidation (Scheme 3.5).[106] Further support for the reducing capability of NADH can be seen in the increase in DNA damage by catechols **1** and **22-24** even at low 5 μM Cu^{2+} concentration, suggesting NADH may participate in the disproportionation of hydroxyl radical generated by Cu^{2+} induced oxidation of catechol.

Scheme 3.5 Redox cycle of terpene catechol/quinone through Cu^{2+} and NADH (Zuniga et. al. 2006)

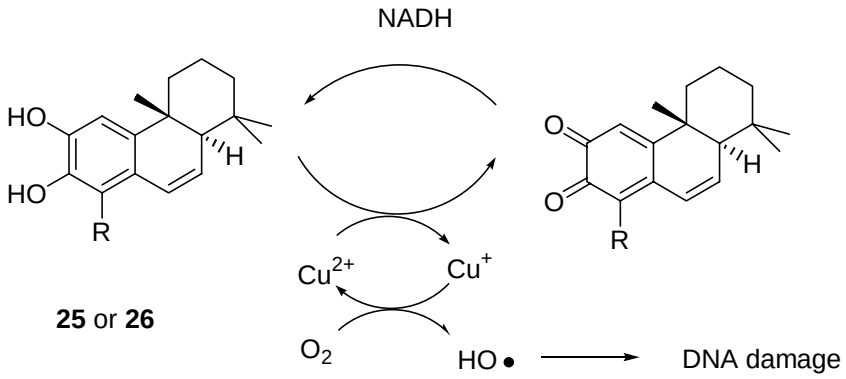

3.6. DNA oxidative damage vs QM alkylation damage

Our previous studies suggest that hydroxyl radicals generated during diterpenone Cu(II)/Cu(I) redox cycles may be responsible for the observed non sequence selective DNA damage. In order to further investigate this, we compared the cleavage of a 30-mer oligonucleotide by diterpenone catechol **1** to that by a known non selective DNA radical damaging system. We only selected compound **1** in this study to use as a representative example and for comparison to a Fe(III)-EDTA system which causes non selective damage by free hydroxyl radical, known as Fenton reaction.[110,111] The Fenton sequencing analysis involves Fe (II) salt mediated decomposition by dihydrogen peroxide, which produces highly reactive hydroxyl free radical (Refer to balanced disproportionation reaction 1). Furthermore, the oxidized Fe(III) is reduced back to Fe(II) in situ by ascorbic acid as the reducing agent and EDTA prevents iron from binding to a substrate, as a result, it accelerates hydroxyl radical formation at a low concentratrion.[110]

$$Fe^{2+} + H_2O_2 \dashrightarrow Fe^{3+} + \bullet OH + OH^- \quad (1)$$

$$Fe^{3+} + H_2O_2 \dashrightarrow Fe^{2+} + \bullet OOH + H^+$$

For the Fenton reaction, the reaction was inititated by freshly mixing mixing (1 mM) Fe(II)EDTA, 10 mM of ascorbic acid, 0.25 μM of DNA, with H_2O_2 0.1, 1, and 3 % and the reaction were then incubated for 10 and 20 minutes, respectively. DNA damage with (10-40 μM) of *trans*- diterpenone catechol **1** were performed with 40 μM Cu^{2+} for 12 hours. The samples were then treated with piperidine and separated through a 20% polyacrylamide gel electrophoresis. Both gel assays were compared with their fragmentation pattern by phosphoimage analysis with Image Quant Version 1.1 (Molecular Dynamics).

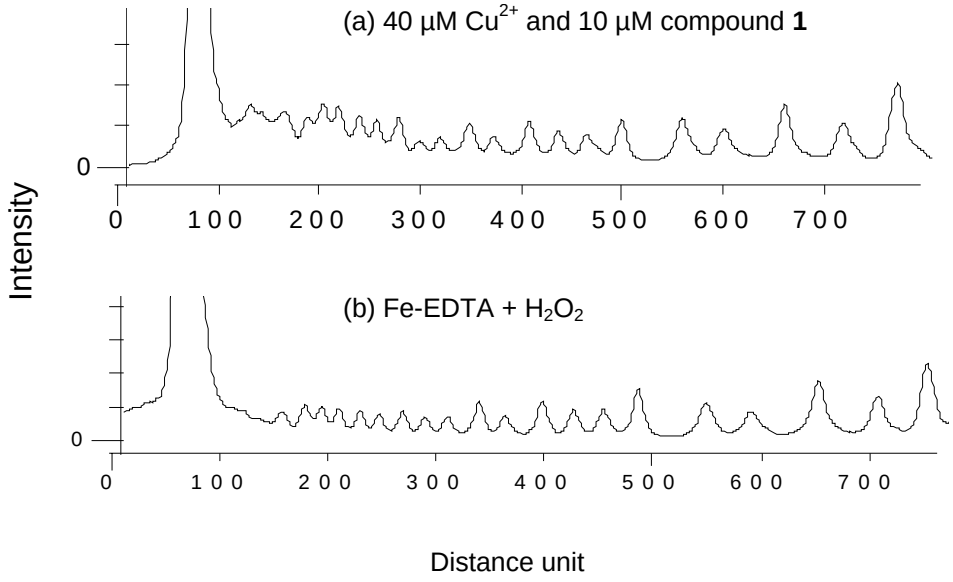

Figure 3.7. Relative DNA cleavage intensities by laser densitiometry analysis of electrophoresis gels. Similar fragment pattern was obtained in the DNA damage by Cu^{2+} induced oxidation of catechols versus that by hydroxyl radical, revealing ROS as the DNA damaging mechanism. DNA fragment patterns were obtained with (a) **1** at 10 µM; (b) Fe^{3+} -EDTA and H_2O_2. *(Zuniga et. al. 2006).*

As shown in Figure 3.7, a similar DNA cleavage pattern was observed between Cu^{2+} induced oxidation of diterpenone **1** and the Fe(II) EDTA Fenton reaction. The similar cleavage pattern supported our previous hypothesis that DNA damage is formed through in situ generated hydroxyl radicals as a non selective DNA damage.[112] This DNA fragmentation pattern is consistent with 4'-deoxyribose cleavage followed by fragmentation of DNA backbone.[113,114] These results imply that despite the initial structural differences of catechol compounds **1**, and **22-26** and their subsequent oxidation products as QM or quinone, the dominant mechanism for DNA damage was through production of reactive oxygen species.

DNA damage by hydroxyl radical has been fully studied and several mechanisms have been proposed. For example, Penning[114] and coworkers suggested that degradation of calf thymus DNA by aromatic hydrocarbon o-quinones in the presence of NADPH and $CuCl_2$ was attributed to DNA strand scission.[114] They proposed that the DNA strand scission is initiated by abstraction of the C-4' proton of 2'-deoxyribose by ·OH, which forms a peroxyl radical through the addition of molecular oxygen. In a second step, oxidative cleavage of the C-3'-C-4' bond yields a base propenal or 4'-keto-1'-aldehyde abasic site which is consistent with oxidation at the 4' position of deoxyribose (Scheme 3.5).[114] This mechanism is largely accepted for the 4' DNA strand scission by hydroxyl radicals. However, more recent studies have reported that ·OH can add to the double bond of the nucleic acid base followed by molecular oxygen to generate a peroxyl radical.

One common method used to identify which ROS is responsible for DNA damage is by using ROS scavenging agents. By using specific ROS scavengers and metal chelators, the identity and involvement of •OH can be inferred, which can then be used to help predict the DNA damaging mechanisms.[115] For example, radical scavengers such as mannitol, DMSO, EtOH, and sodium formate are known to inhibits free hydroxyl radical •OH.[115,116] However, superoxide dismutase is a superoxide anion $O_2^{\bullet-}$ scavenger, while catalase specifically quenches hydrogen peroxide H_2O_2. Copper (I) metal chelators are also frequently used to detect whether Cu^+ is involved in DNA damage, the typical metal chelators are bathacuproine and catalase.

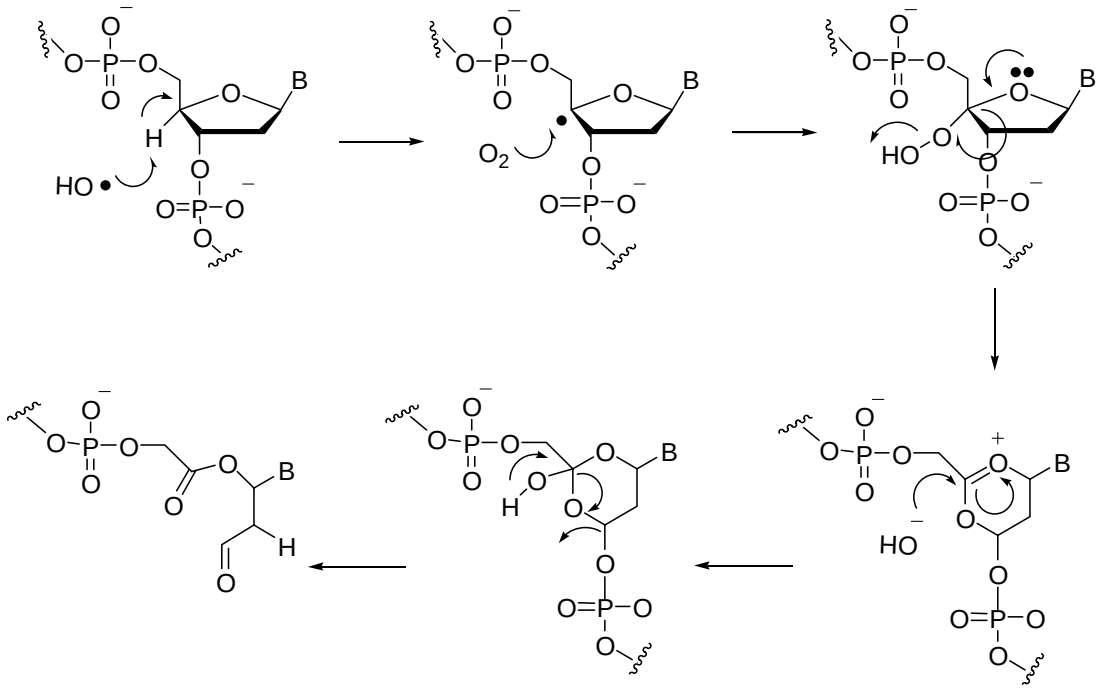

Scheme 3.6. Proposed reaction mechanism of DNA strand scission by hydroxyl radical produced during the reaction of PAH o-quinones, NADPH, and Cupric Chloride. Only hydroxyl attack at C4' is indicated. Although other mechanisms of strand scission are possible, aerobic DNA cleavage via a C-4' Criegee rearrangement is preferred. *(Penning et. al. 1997).*

To fully the reveal the identity of the HO• in our Cu^{2+} induced oxidation, we further conducted the experiements of hydroxyl radical scavengers and metal chelators on DNA damage by the Cu(II) diterpenone **1** system. The results of our studies are shown in Figure 3.8, which clearly demonstrated that all of the free hydroxyl radical scavengers had no effect on the extent of DNA damage.[117] This observation is in agreement with studies by Oikawa and coworkers which reported that DNA damage induced by 2-hydroxy catechol was not inhibited by the free hydroxyl radical scavengers.[118] However, further analysis of Figure 3.8 shows that Cu^{+} specific metal chelators catalase and bathocuproine

completely inhibited DNA damage. Also methional, a well known copper hydroperoxy complex (Cu(I)OOH) chelator, completely blocked Cu^{2+}-induced DNA damage. These results suggest that a Cu(I)-hydroperoxo complex is likely responsible for the observed DNA damage, and not the free hydroxyl radical in the Fenton reaction, although a similar DNA fragment pattern was observed.[117]

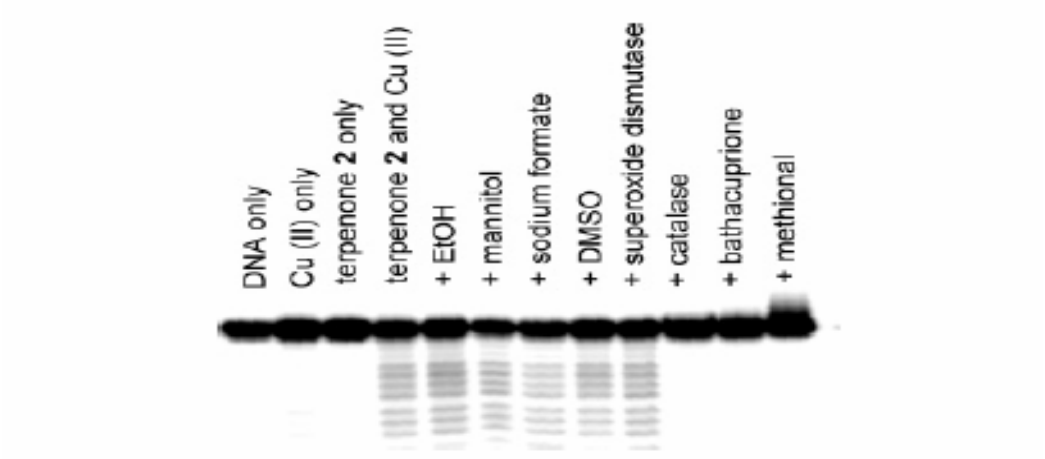

Figure 3.8. The effect of radical scavenger and copper chelators on DNA damage by diterpenone **1** (20 μM) and Cu^{2+} (20 μM) after piperdine treatment. Concentration duplex DNA was 0.25 μM in 10mM phosphate buffer (pH 7.40) and 1 mM $MgCl_2$. Radical scavengers and chelator concentrations were as follows: 5% for ethanol, 0.1 M for mannitiol, 0.1 M for sodium formate, 5% for DMSO, 1.5 unit/10 μL for superoxide dismutase, 1.5 unit/ 10 μL for catalase, 50 μM for bathocuproine, and 0.1 M for methional, respectively. (*Zuniga et. al. 2006*).

3.7 Conclusion

In this chapter, we investigated DNA damage with a series of terpene catechols **1**, **22-26** as analogoues of natural QM precursors and suggested that production of ROS was the dominant mechanism for the observed DNA damage in the Cu(II)-induced oxidation. We found that DNA damage by hydroxyl radical was non- sequence selective. Nucleobase

cleavage occurred with all the diterpene catechols **1**, and **22-26** regardless of stereo- and structural differences. In addition, the extent of DNA damage was greater in the presence of NADH than that without NADH, which was attributed to the reducing capability of NADH. In the case of conjugated catechols **25** and **26**, the extent of DNA damage was not concentration dependent, suggesting that NADH was able to reduce the formed quinones fully to the initial catechol thereby forming a complete redox cycle of catechol/quinone with Cu^{2+} induced oxidation. As a result, disproportionation of Cu(II)/Cu(I) with oxygen continuously produced ROS until all of NADH was fully depleted. These results provide a fundamental basis for future biological studies on oxidative metabolism of terpene catechols. This may further contribute to the understanding of natural catechols and their ability to act as complete carcinogens.

Chapter 4

Chemoprotection against AFB1 by cis-terpenone and isotope labeling

4.1 Introduction

The previous studies in chapter 3 demonstrated that cis-diterpene catechol **21** showed less DNA damage than alkene and trans diterpene catechols while no direct nucleobase alkylation products were observed.[119] On the other hand, the carcinogenic effect of estradiol has been shown to undergo a metabolic process through o-hydroxylation oxidation to quinone/QM and subsequent nucleobase alkylation.[120,121] Therefore, an analogous metabolic pathway is possible for the natural terpene QM, which can be produced from *p*-hydroxylation of cis terpenone **35** and subsequent oxidation to QM as shown in Scheme 4.1. The hypothesized hydroxylation of cis-terpenone **35** is based on reported aromatic hydroxylation of similar compounds such as estrogens by P450 mediated reaction.[120,121]

One important difference between estrogenic compounds and designed cis-terpenone **35** is the unique bent conformation. This unique bent distortion has been implicated in the interesting reactivity of cis-diterpene catechol **21** and exceptional stability of a synthesized cis-terpene QM **32**.[119] Furthermore, the hypothesized hydroxylated metabolite of **35** is identical to our chemically synthesized cis catechol **21** and partially resembles the structure of reservatol, a potent inhibitor of P4501A/B activity.[122,123] Since the carcinogenic and acute toxic responses of AFB1 are dependent on its metabolic activation, then one conceivable approach to reduce or block AFB1 biotransformation to its exo-8,9 epoxide, would be to prevent its activation by CYP450 enzymes.[124] As

previously dicussed, the general intervention strategy in Chapter 1 implies that cis-terpenone **35** may be a suitable substrate for CYP450 enzymes. Therefore cis-terpenones were selected as ideal candidates to investigate for protective effects against AFBl induced toxicity and to determine whether cis-terpenones have inhibitory potential on P4501A/B.

Scheme 4.1 Hypothesized hydroxylation of cis-terpenone based on reported estradiol metabolism

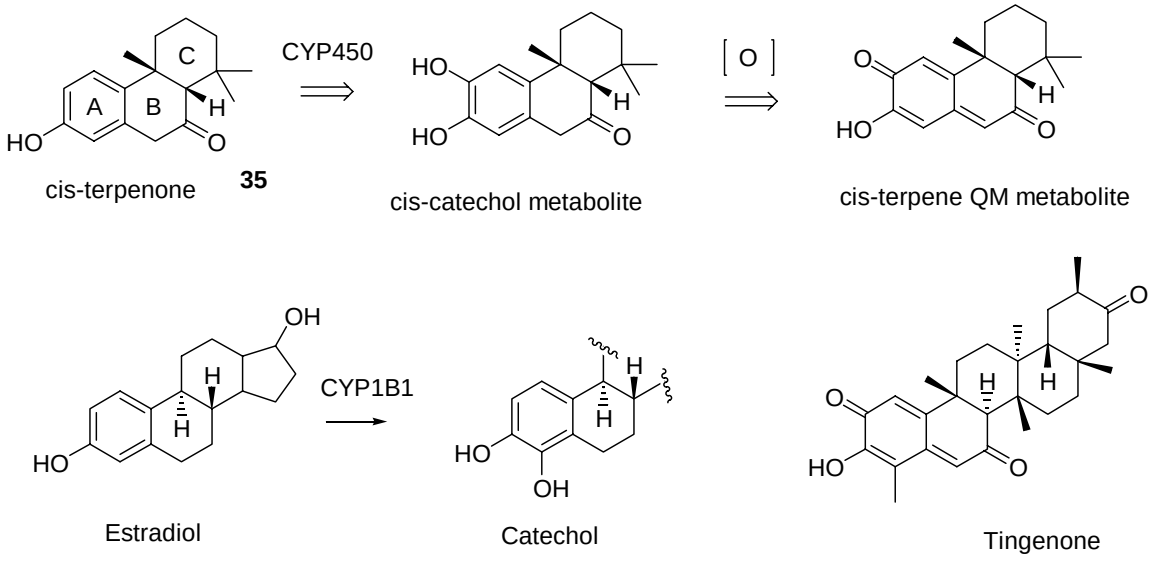

The chemoprotection effects associated with cis-terpenones **35-37** were first demonstrated by Dr. Zhou and colleagues using cell viability assay and other studies.[125] They also reported that **35** can block the activity of CYP 1A/B induced by the carcinogen 2,3,7,8- tetrachlorodibenzo-p-dioxin (TCDD).[125] In connection with their chemoprotection studies, they used the MTT tetrazolium assay to determine effects on cell viability of cis-terpenone derivatives **35-37** substituted at primarily one position of the A ring system.

The results of this study are shown in Figure 4.1 and show that co-treatment of 2 μM AFB1 and cis-terpenones **35-37** at various concentrations (10-40 μM) resulted in a gradual increase of cell survival with increasing concentrations of cis terpenones up to 80% at 40 μM. Furthermore, no cytotoxicity was observed by cis-terpenone alone. Also shown in Figure 4.1, is that there is no significant change in the activity of cis-terpenones by these various derivatives **35-37**. This is demonstrated by the similar chemoprotection and concentration-dependent effect with all three cis-terpenones **35-37** despite the difference in chemical functionality (phenol, methyl, and ester group). Based on these results, cis-terpenones are promising candidates for novel mechanism based preventive agents, but futher research to understand the protective effect of cis-terpenones is needed.

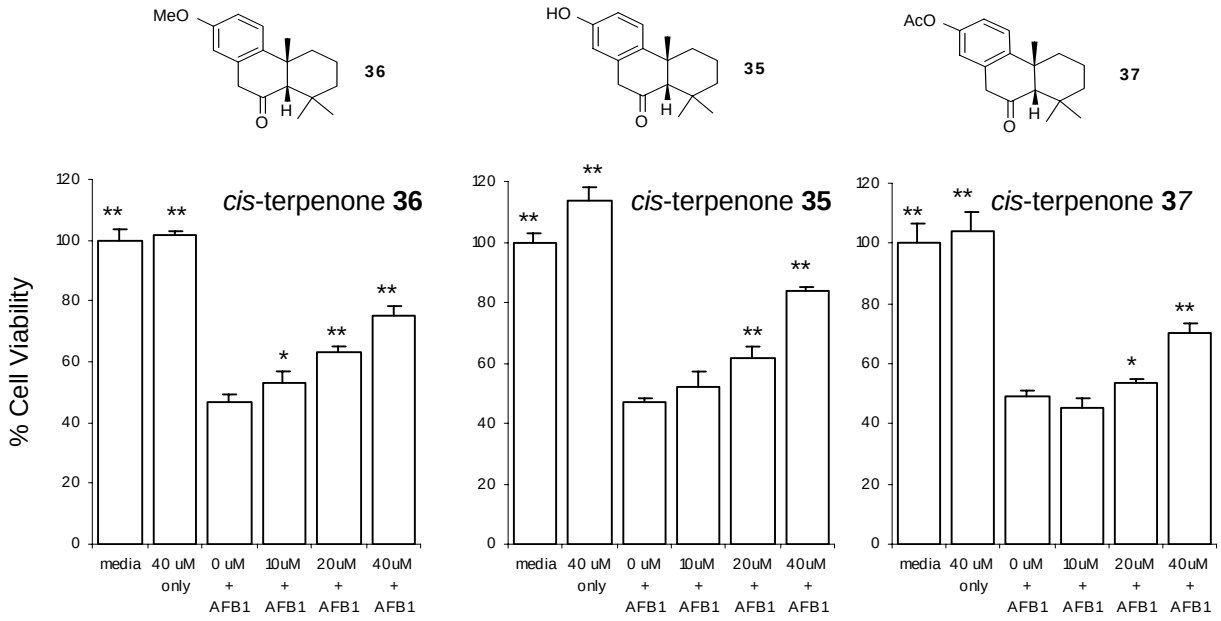

Figure 4.1 Chemoprotection with cis-terpenones against AFB1-induced cytotoxicity. HepG2 cells were co-treated with AFB1 (2 μM) and cis-terpenones **35-37** at various concentrations (10-40 μM) and incubated for 72 h. Cell viability was measured with the MTT assay. The percentage of viable cells was based on cells treated with medium only. Each bar represents the mean +/- SD of four replicates. The data are representative of three independent experiments. *P< 0.05 and **P < 0.001 compared to treatment with AFB1 by one way ANOVA and Dunnett's test. (Zhou et. al. 2006).

4.2 Design of isotope labeled terpenone precursor

To fully investigate the mechanistic action of the cis-terpenone **35** and evaluate how cells metabolize this compound a stable radiolabeled **35** is needed. One effective way of radiolabeling is to incorporate an isotopic label in the structure. The ideal radioactive tracer for the metabolic studies was tritium because it has similar chemical properties as ^{1}H and a high specific activity 29 Ci/mmol. A main advantage of high specific activity is that it allows for confirmation of the related metabolites.[126,127] In addition, radioactive tritium has a relatively long half life ($t_{1/2}$) of 12.5 years as compared to ^{32}Phosphorous ($t_{1/2}$ 2 weeks) and decays through weak β^- emission at 5 keV.[128] The relatively long half life and weak emission of tritium will minimize its handling and exposure. Based on the above consideration, protection of laboratory personnel can be achieved by proper shielding, wearing a lab coat, gloves, and keeping a routine wipe test. We started the synthesis of **41** containing a non-radioactive isotope to optimize the conditions for the tritium labeling of cis-terpenone. The purpose of this model study was to first demonstrate the labeling position and secondly to prove the feasibility of incorporating a tritium label in *cis*-terpenone. After demonstrating successful isotope incorporation, these studies can be extended with a radio-isotope to track the cis-terpenone metabolites and quantify the distribution of these metabolites.

4.3 Deuterium label model reaction

As previously stated, before preparing a tritium labeled compound, the reaction conditions with a non-radioactive deuterium were optimized to investigate the positions of isotopic incorporation and to minimize competing side reactions. Synthesis of deuterium labeled **41** began by using commercially available 3-methoxybenzyl chloride **38**. This compound was coupled with previously synthesized **28** with n-butylithium at -40 ºC in dry THF, to afford **39** in 51% yield. Deprotection of **39** with HgO and $HgCl_2$ resulted in formation of the conjugated ketone **40** in 54% yield (Scheme 4.2).

Scheme 4.2 Synthetic pathway of deuterium labeled terpenone

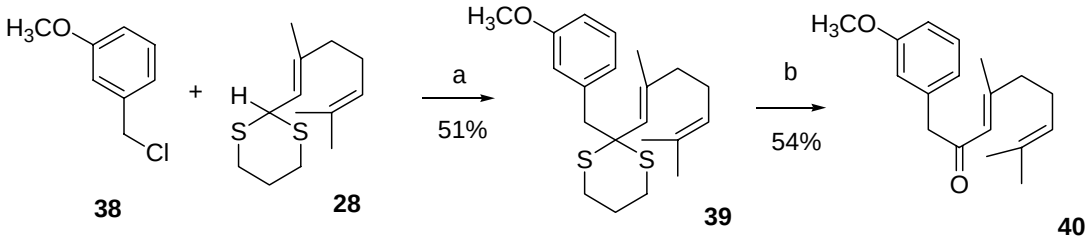

Reagents and conditions: a. nBuLi, -78 ^{o}C in THF b. HgO/$HgCl_2$ in MeOH/H_2O

Before the key next step, we proposed a plausible mechanism for the desired isotope exchange reaction as illustrated in Scheme 4.3. The first step is the initial formation of the enolate intermediate through electron donation by the methoxy group. This intermediate undergoes a subsequent intramolecular cyclization with the electron deficient polyene π electrons which is coordinated through an electronic interaction with

D_2O and BF_3OEt_2. Coordination of D_2O and BF_3OEt_2 promotes deuterium bond breakage, by stabilization of the positive charge and release of HOD and BF_3OEt_2. One of the later steps is the subsequent loss of hydrogen atom to reform the aromatic ring system and desired **41** (Scheme 4.3).

Scheme 4.3 Proposed mechanism of deuterium exchange

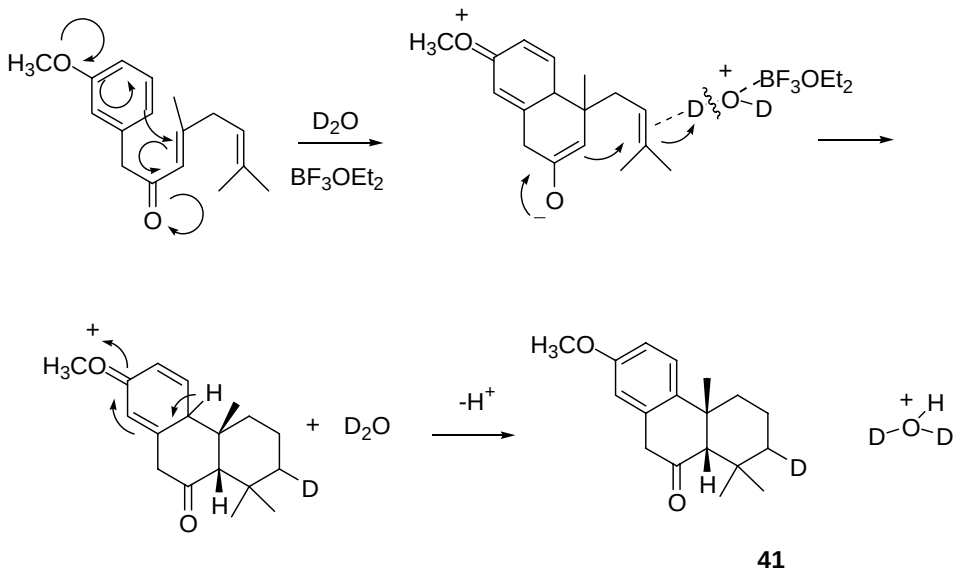

To test our hypothesis, we reacted **40** with 5eq DCl and 10 eq BF_3OEt_2. After purification, the product was identified as starting material and there was no cyclized product **41** formed by ^1H NMR. As a result of the failure of DCl to produce the desired cyclized product, an alternative isotopic reagent D_2O, was investigated. Deuterated oxide (D_2O) was chosen as the alternative since literature data indicated that it had been effectively used to introduce deuterium in conjugated polyene systems.[129] The deuterium incorporation was carried out with 10eq D_2O and 15eq BF_3OEt_2 which we believed formed our desired product **41**. Based on our standard workup, we initially thought **41** to to be of

high purity since only one major spot was observed by TLC and purification by flash chromatography was straightforward.

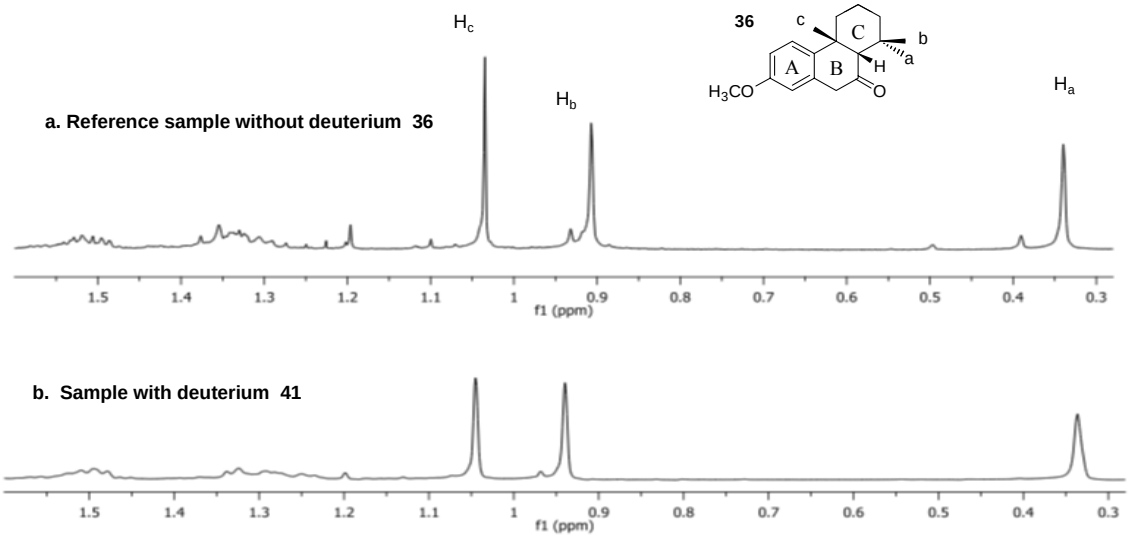

Figure 4.2a,b. ^{1}H NMR spectrum of sample containing deuterium **41** and sample without deuterium **36** dissolved in $CDCl_3$, the chemical shift region is expanded to show only the region of interest. Both spectra are referenced to $CDCl_3$ signal at 7.2ppm (not shown).

At first, we investigated the incorporation of isotopic deuterium in **41** with ^{1}H NMR and ^{13}C NMR analysis. The ^{1}H NMR spectra of labeled and unlabeled samples are shown in Figure 4.2a and b, which contain the expanded chemical shift region for the C-ring of **36** without D_2O and Figure 4.4b, the expected labeled product **41**. By comparison of ^{1}H NMR spectra data, we observed little difference in splitting patterns or resonance shift, while integration of the ^{1}H signals was inconclusive. In the case of our ^{13}C NMR analysis, a triplet splitting pattern of 1:1:1 was observed in the range of 18-22 ppm. This signal seemed to be consistent with one deuterium labeled methine (CH) in the methylene substituent (CH_2) a shown in Figure 4.3. The coupling constant was measured at 8 Hz, and the intensity of this triplet could be rationalized as the coupling by the deuterium, (spin

number *I*=1) as compared to the deuterated chloroform ($CDCl_3$) signal. If this were a true deuterium signal, then this indicates that around 50% deuterium was incorporated in the product **41**.

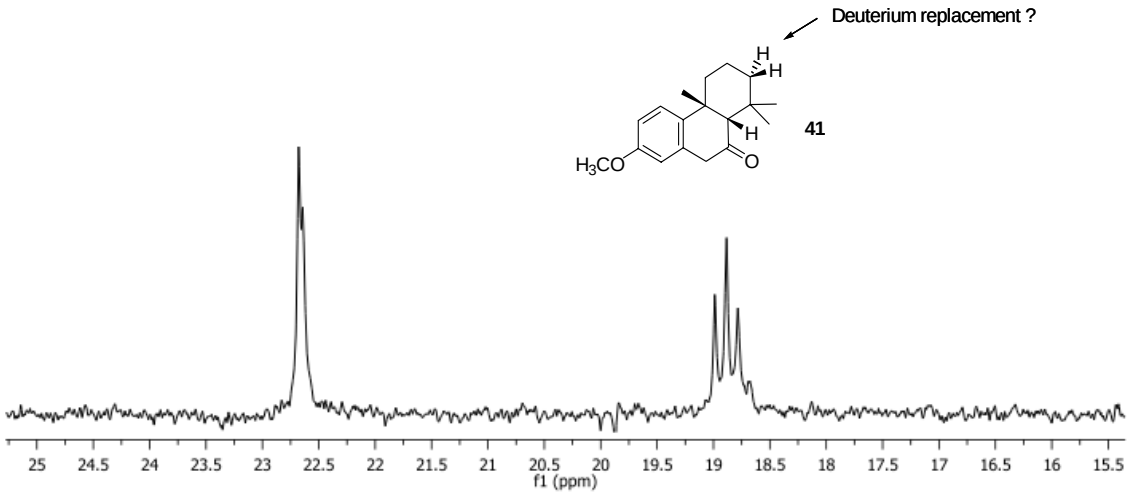

Figure 4.3. ^{13}C NMR spectrum of **41** dissolved in $CDCl_3$. The region of interest corresponds to the expected labeled position. The triplet resonance at 18.9 ppm is due to deuterium magnetic spin number *I*=1 and the coupling constant was measured at 8 Hz.

Electrospray ionization mass spectrometry was also used to investigate for the incorporation of deuterium. In the MS spectrum of expected deuterium labeled **41** and unlabeled **36**, the $[M + H]^+$ at 273.1776 for unlabeled **36** was not observed. Therefore, MS/MS of m/z 310 was investigated for ions near the target compound mass. In Figure 4.4a, molecular ion species were detected in labeled sample **41** which correspond to (M+1), (M+2), and (M+3) ion species greater than the expected mass of unlabeled **36**. Comparison of Figure 4.4a and b shows that molecular ions are of higher intensity in the expected labeled **41**, but greater sensitivity to locate the $[M+H]^+$ of unlabeled **36** with ESI-MS conditions is needed. Based on the observed mass shift units of the expected labeled

41 in Figure 4.4a, these studies suggest that deuterium atoms were possibly incorporated in **41** in the prescence of D_2O.

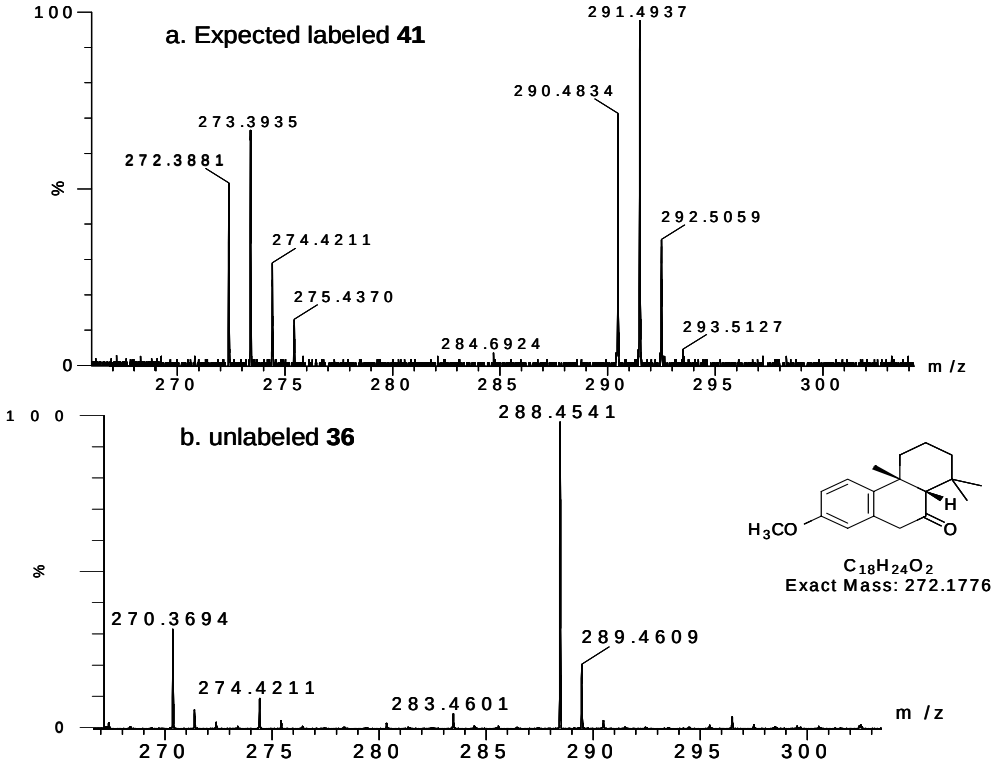

Figure 4.4. ESI-MS of both expected labeled **41** and unlabled **36** dissolved in CH_3OH and fragmented in positive ion mode. The mass unit shifts and the intensity pattern of expected labeled **41** correspond to the molecular ion related peaks m/z 272, 273, and 274 show one or two unit difference.

To further confirm the incorporation of deuterium, we conducted an additional ^{13}C DEPT experiment. This experiment can provide detailed analysis about the types of substituted carbons and therefore would allow us to differentiate CH, CH_2 and CH_3 signals. The merit of this study is that if deuterium were incorporated at the proposed CH_2 position, an additional CH carbon signal would be observed in the ^{13}C DEPT experiment (Figure 4.5). Based on the chemical structure of cis-terpenone structure **36**, we would expect 4

CH_2 signals if it were unlabeled and 3 CH_2 signals in the DEPT experiment if deuterium were in fact incorportated. Surprisingly, we found that the ^{13}C DEPT experiment indicated that the number of CH_2 carbons signals remained unchanged, while several weak signals were observed. In addition, the triplet 1:1:1 signal remained unchanged, indicating limited deuterium was incorporated.

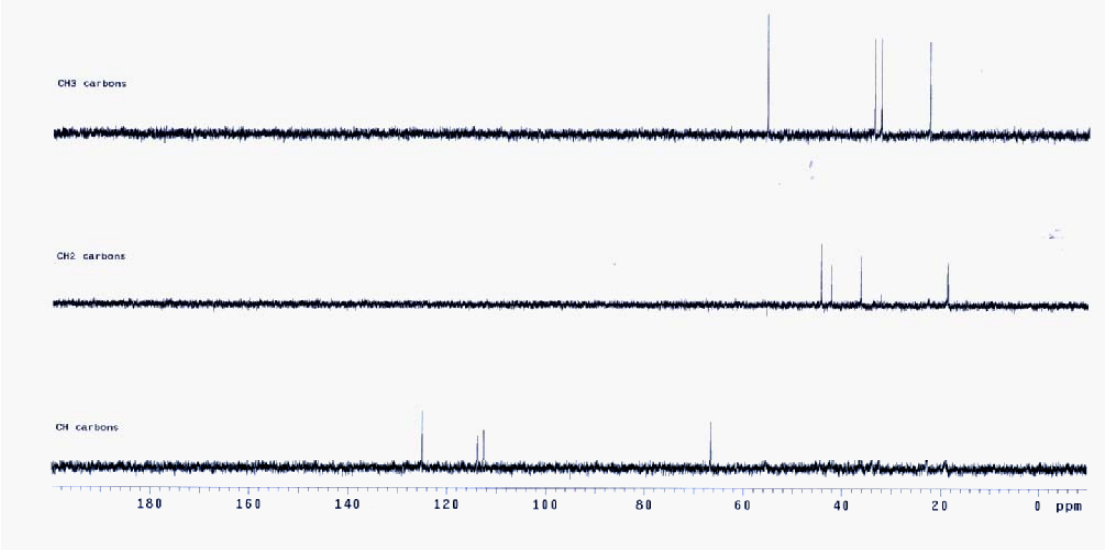

Figure 4.5. DEPT experiment indicating the different type of carbons containing hydrogens within expected labeled **41**. In this experiment there are 4 CH_3 signals, 4CH_2 signals, and 4CH signals indicating only partial deuterium incorporation. The triplet signal at 18.9 ppm remains unaffected.

Finally, the incorporation of isotopic deuterium was fully confirmed with a ^1D deuterium NMR experiment (Figure 4.6). In this experiment, the parameters were set up as follows: sample was dissolved in non-deuterated solvent, turned "lock off", "lock pwr" and "lock gain" were set at 0. A standard C13 parameter set was used but it was changed to "lk", in this case the lock channel was used for data collecting. The internal reference was $CDCl_3$ set at 7.27 ppm and any ^2H reference position was redeemed as ^1H position.

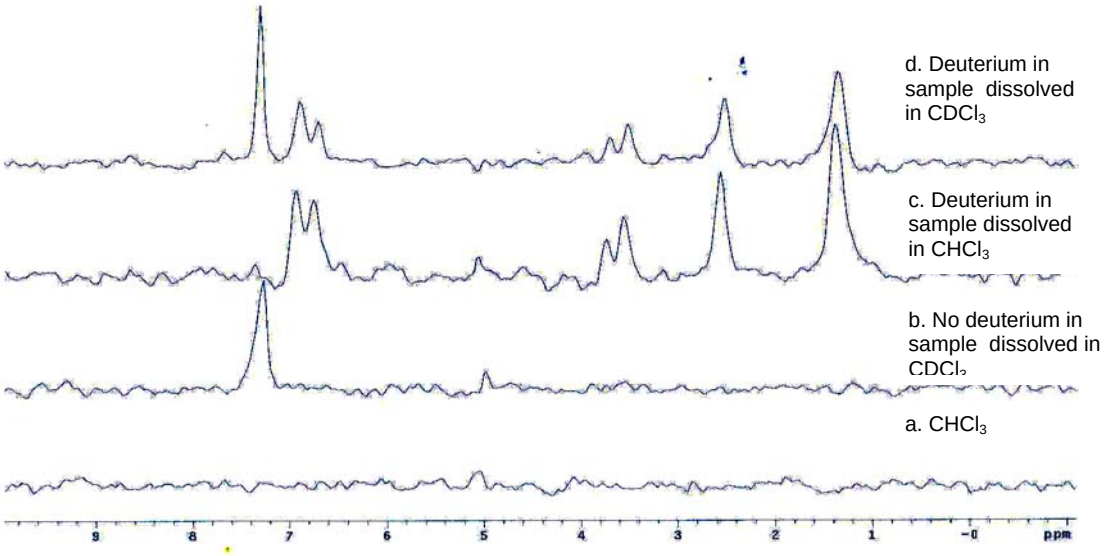

Figure 4.6 ^{1}D NMR spectrum indicating positions of isotope incorporation. Based on the observed resonances deuterium is incorporated in six positions of **41**. The largest signal is at 1.2 ppm which corresponds to the location of the CH_2 hydrogens.

In the ^{1}D deuterium NMR analysis, the peaks observed at 6.6-6.8 ppm indicate that deuterium is incorporated in the aromatic ring of **41**, while the signal observed at 1.2 ppm is attributed to incorporation at the desired position, and is consistent with our proposed mechanism. Figure 4.6 also shows that the signal at 1.2 ppm is more intense with respect to the other observed signals. This suggests that more incorporation of deuterium is observed at 1.2 ppm. A hypothetical structure with the isotope substitution at this position is illustrated in (Scheme 4.4).

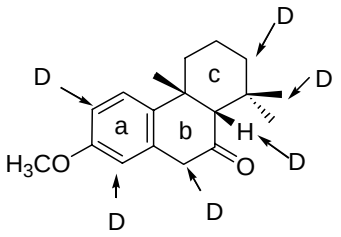

Scheme 4.4 Proposed isotope labeled **41**

The isotope scattering in the structure observed in this study, was consistent with scrambling of H-D exchange reported by Sajiki[130,131] and coworkers using compounds containing labile carbonyl functional groups.

4.4 Conclusion

This work established the feasibility and usefulness of incorporating an isotope label in our cis-terpenone molecule **41**. This isotope labeled compound was designed based on our previous synthetic route and characterized by MS analysis, ^{13}C NMR and subsequent deuterium NMR techniques. It was shown that deuterium can be incorporated using isotopic exchange reaction with D_2O and BF_3OEt_2 at several positions of the compound. As a result, these studies will allow us to use a radioisotope to monitor cis-terpenone metabolic transformation and the formation of potential reactive metabolites in human liver cells.

Chapter 5

Synthesis of diterpene analogs for structural activity relationship study

5.1 Introduction

Although cis-terpenone **35** showed chemoprotection against the procarcinogen AFB1 in liver cells and has low cyto-toxicity by itself, it was not clear at the current stage why this compound has such a unique effect. In this chapter, synthesis of diterpene analogs were undertaken to investigate the activity and clarify the chemo structures responsible for the protective effect of cis-terpenones.[132] The overall design of the analogs was summarized in Scheme 5.1. The diterpene analogs A were designed to block the aromatic positions on the A ring system, so that formation of potential QM/quinone intermediates could be prevented. It was anticipated that by preventing QM formation, competing side toxic reactions could be minimized and, as a result, only desired chemoprotective effects would be enhanced. For the diterpene analogs B, the idea was to incorporate substituents so that the metabolism of the parent compound could be altered. For example, the bromo group will block the positions for the hypothesized hydroxylation by CYP450 enzymes, which has been shown as a major toxic pathway.[132,133] Therefore, with diterpene analog B, we could examine whether certain aromatic position is required for the protective effect of diterpenes. For diterpene analogs C, a secondary hydroxyl group was introduced at the C ring system to increase the solubility in the medium and/or perhaps the cellular absorption of these compounds across lipid membranes. The fourth model was constructed based on a coumarin system so that we could evaluate whether the benzylic hydrogens play a role in the protective effects of diterpenes. It was also thought that the lactone ring might be a key structural

feature in the protection; furthermore, additional functional groups on the C ring will be evaluated (Scheme 5.1). The overall goal of these diterpene analogs was to attempt to characterize the chemical structural features that are involved in the protective effects of diterpenes.

Scheme 5.1 Analog Design of diterpene analogs of cis terpenone for SARs

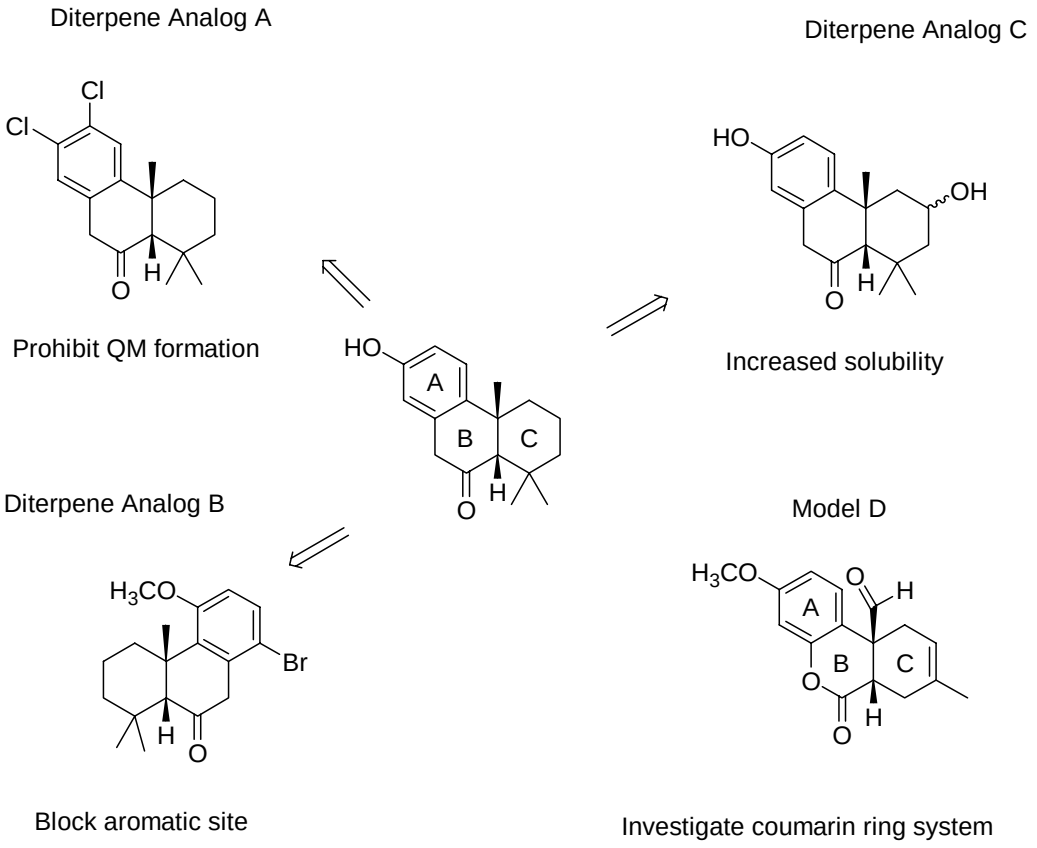

5.2 Synthesis of diterpene analogs for SARs

Model A

Our route for diterpene analog A began with the commercially available 3,4 dichlorobenzylic chloride **42**. This compound was coupled with previously synthesized

28 with nBuLi at -40°C to form **43** in 53% yield. Subsequent deprotection of **43** with HgO and $HgCl_2$ proceeded smoothly to furnish **44**. Cyclization of **44** by treatment with BF_3OEt_2 in nitromethane, generated a mixture of impurities and a partial cyclization product. In an effort to produce **46**, the reaction temperature was lowered and alternative Lewis acids such as $SnCl_4$ and/or TFA in nitromethane were used.[134] After monitoring the reaction by TLC, the structure of the major product of these reactions was determined by ^1H NMR analysis. The major product **45** was identified as an intermediate in the reaction. Based on these results, it was suspected that the chloride atoms are weak electron donors and therefore prohibit the formation of our desired product **46** as shown in Scheme 5.2.

Scheme 5.2 First diterpene analog study to prohibit QM formation

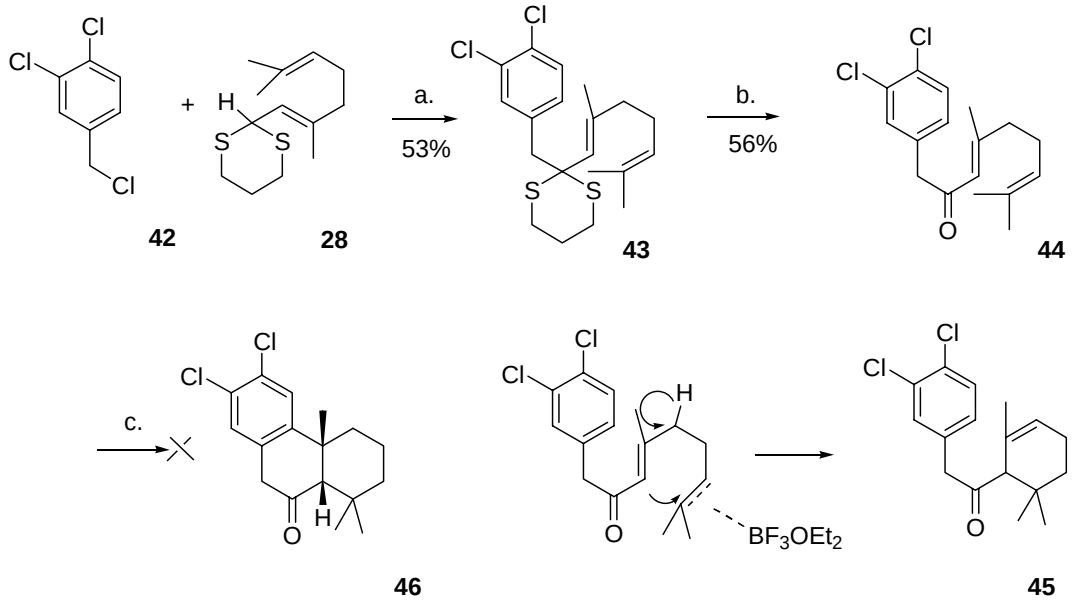

Reagents and conditions: a. nBuLi -78 ^oC THF, b. $HgO/HgCl_2$ $MeOH/H_2O$, c. BF_3OEt_2, CH_3NO_2

Model B

The synthesis of model B would serve two purposes: 1) it would allow us to determine whether all the aromatic positions are required for activity, and 2) whether the larger size of the bromide would affect the biological properties of terpenone structure. In this study, commercially available 3-methoxybenzyl chloride **47** was first brominated by standard conditions using 10% Br_2 solution in CH_2Cl_2 (Scheme 5.3). As indicated by ^1H NMR analysis, this procedure was fairly consistent and generated the desired **48** with few side products. The para position of the bromide with respect to the methoxy group was confirmed by ROESY spectra analysis (see appendix).

Scheme 5.3 Synthesis of bromine substituted diterpenone analogs

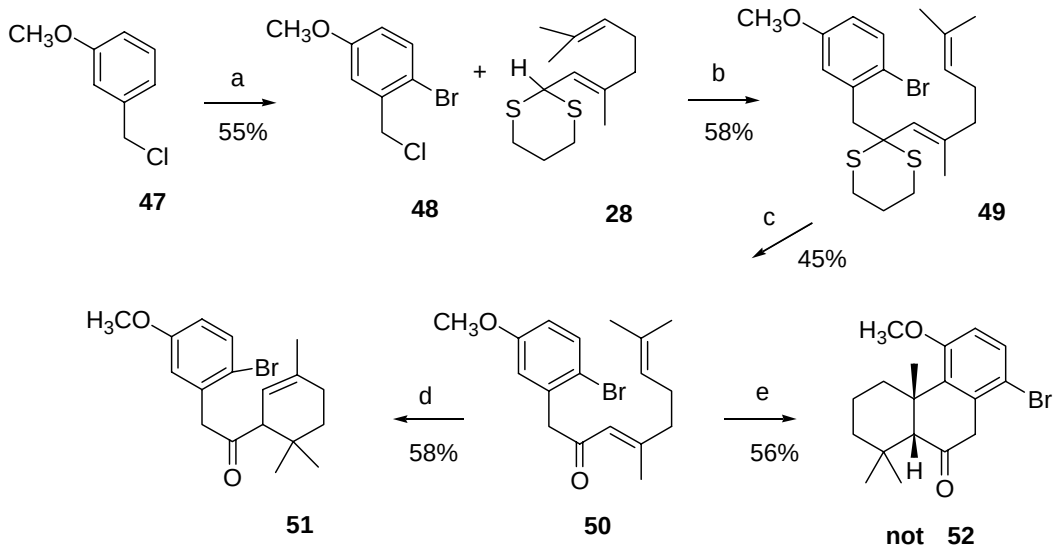

Reagents and conditions: (a) Br_2 in CH_2Cl_2, 0^oC. (b) nBuLi -78^oC in THF. (c) HgO, $HgCl_2$ in 9/1 MeOH:H_2O. (d) BF_3OEt_2 in CH_3NO_2 at room temp. (e) BF_3OEt_2 in CH_3NO_2, $50\ ^oC$

Coupling of **48** and **28** was achieved using n-butyllithium to form **49** in 58% yield. Removal of the thiol group with HgO and $HgCl_2$ in a mixture of methanol and water (9:1) generated **50** in 45% yield. The attempted cyclization of **50** by addition of BF_3OEt_2 at room temperature in nitromethane failed to generate the desired product **52**. After isolating the major side product in the reaction, analysis by ^1H NMR showed that a partial cyclization product was formed **51**. Based on the structure of this side product, it was believed that at room temperature, sterics prevent the molecule from complete cylization. The ^1H NMR of **51** is shown in Figure 5.1, and revealed three resonances in the aromatic region which suggest that the tricyclic ring was not completed. Furthermore, the resonance at 5.5 ppm confirmed the presence of an alkene hydrogen.

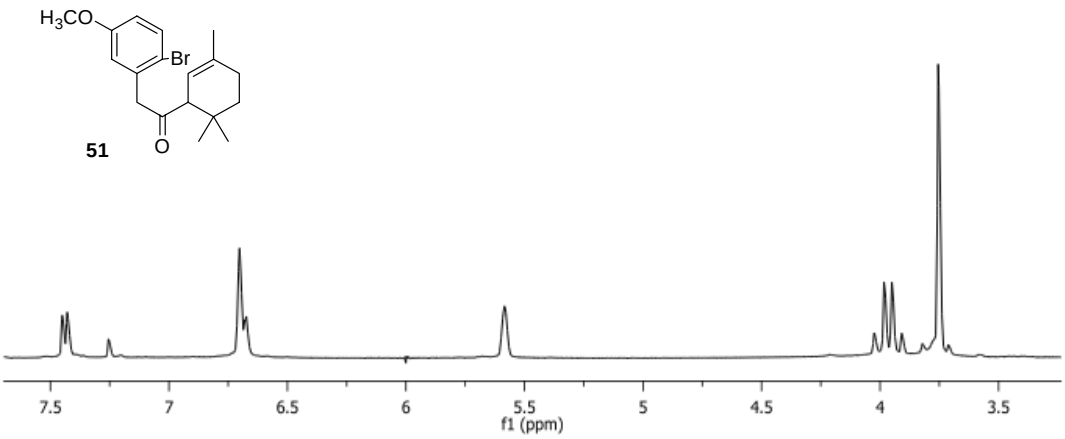

Figure 5.1. ^1H NMR spectrum of **51** showing distinguishable proton resonances

On the other hand, when the temperature was elevated to 50 °C, the cyclization of **50** proceeded smoothly to give a major product **52**, which we initially thought to be the cis-isomer. However, based on ^1H and ^{13}C NMR analysis shown in Figure 5.2 two doublets at 7.3 and 6.6 ppm with a coupling constant of 8.7 Hz corresponding to the

aromatic hydrogen resonances where observed, while three methyl signals at 1.00, 1.24, and 1.35 ppm confirmed **53** as a *trans* stereoisomer. From the ^{13}C NMR analysis in Figure 5.2, eight carbon signals where observed above 100 ppm with one distinctive signal at 198 ppm corresponding to the carbonyl carbon.

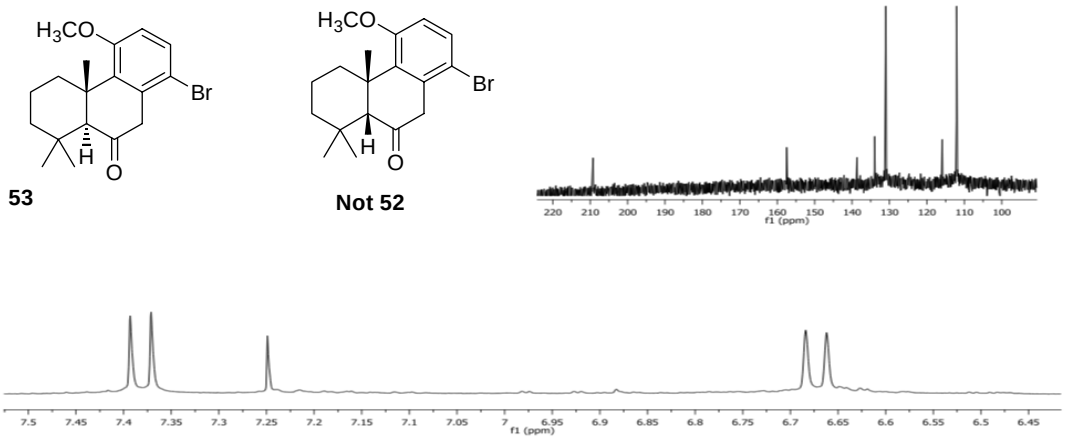

Figure 5.2. ^{1}H and ^{13}C NMR spectra of **53** showing distinguishable proton resonances and carbon signals.

Model C

The synthesis of diterpene analog C aimed to insert a secondary hydroxyl group into the C ring system of terpenone closely paralleled that of the previously discussed cis-terpenones. Conversion of unconjugated polyene **40** into **54** proceeded smoothly by way of treatment with mCPBA in 56% yield (Scheme 5.4).

Scheme 5.4 Attempted insertion of hydroxyl group by Analog C

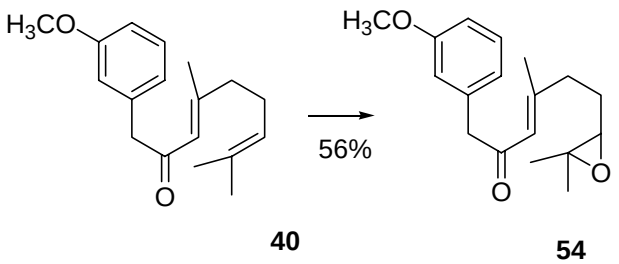

Before attempting the next key step, a possible mechanism to form the desired product **55** was proposed as shown in Scheme 5.5.

Scheme 5.5 Proposed pathway for formation of hydroxyl substituted diterpenone

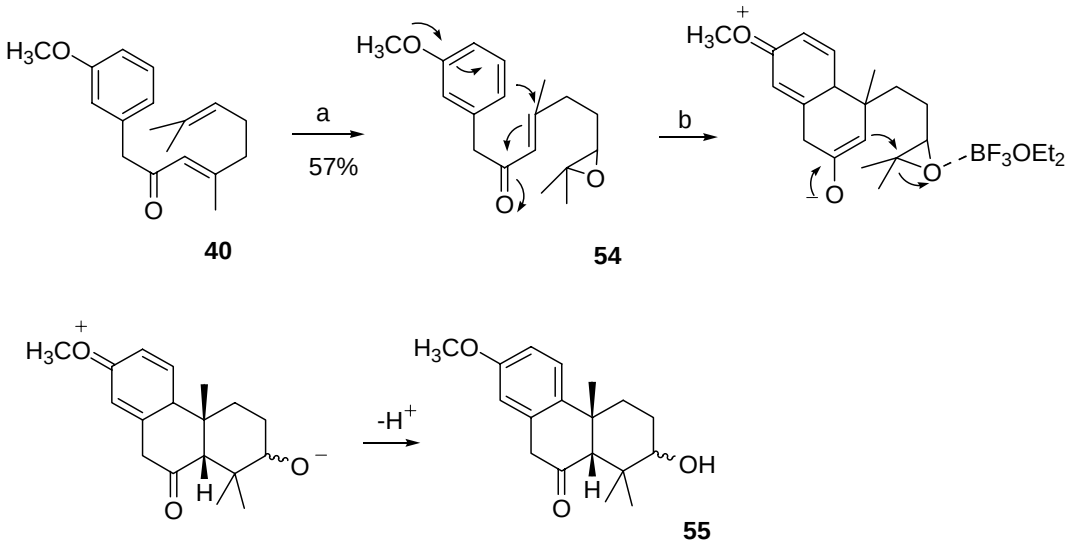

Reagants and conditons: a, mCPBA, in CH_2Cl_2 b. BF_3OEt_2 in nitromethane

In this mechanism, electron donation by the methoxy group will activate the initial enolate. This enolate is then expected to donate its electrons to reform a carbonyl and activate the alkene to attack the subsequent epoxide ring to form the diterpene skeleton. Once open, the epoxide will reprotonate to form a secondary alcohol and the aromatic system will be regenerated upon the release of hydrogen.

To test our hypothesis, compound **40** was treated with BF_3OEt_2 in nitromethane and reacted for 3 hours. Upon workup of the reaction, we found that the desired product **55** was not formed. Based on ^1H NMR analysis, the structure of one characterizable side product **56** was found as five member ring ether. A mechanism for the formation of this undesired product is illustrated in Scheme 5.6, which shows that the side product

proceeds by the faster five member ring formation to a stable cyclic product. Attempts to open the epoxide ring under slightly acidic conditions were unsuccessful and led us to try a different approach for introduction of a hydroxyl group.

Scheme 5.6 Proposed competitive side reaction

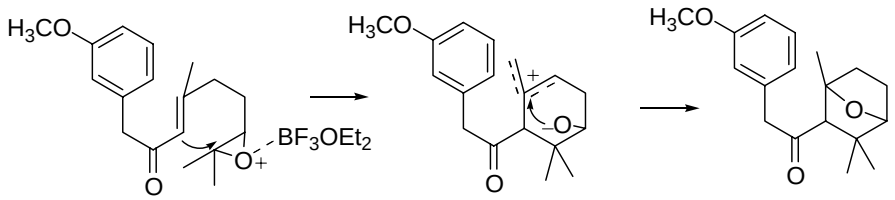

54 **56**

Thus, we decided to transform our previously synthesized **51** into **58** by conventional mCPBA reaction. Interest in **57** was due to the anticipated opening of the epoxide to form **58**, a tertiary alcohol by way of a Grignard reaction.[135] However, these experiments were unsuccessful due to the sluggish formation of the Grignard and therefore not further investigated (Scheme 5.7).

Scheme 5.7 Formation of Diterpene B model

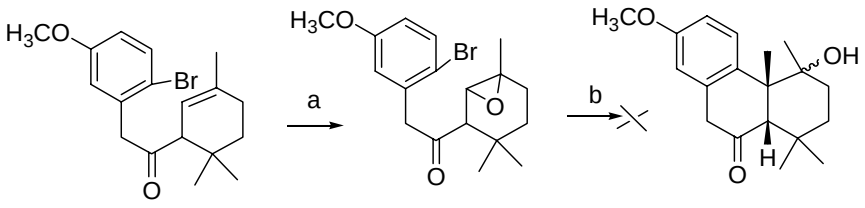

51 **57** **58**

Reagants and conditions a. mCPBA in CH_2Cl_2 b. Mg in THF

As an extension of this work, efforts to facilitate the introduction of a double bond in the terpenone structure were undertaken. The idea of introducing a double bond was twofold, first this would flatten the C ring system, and second this would increase the lipophilic character of diterpene analogs. In these studies, we selected the Heck reaction by which to perform the key cyclization of **50** due to its well known versatility in constructing complex ring systems.[136,137] The general mechanism for the Heck reaction proceeds with formation of a palladium species followed by the elimination of palladium to give an arylated alkene derivative. Thus the Heck reaction was considered to be an effective approach to form our desired target **59**.

Scheme 5.8 Studies on diterpenone formation using Heck Reaction

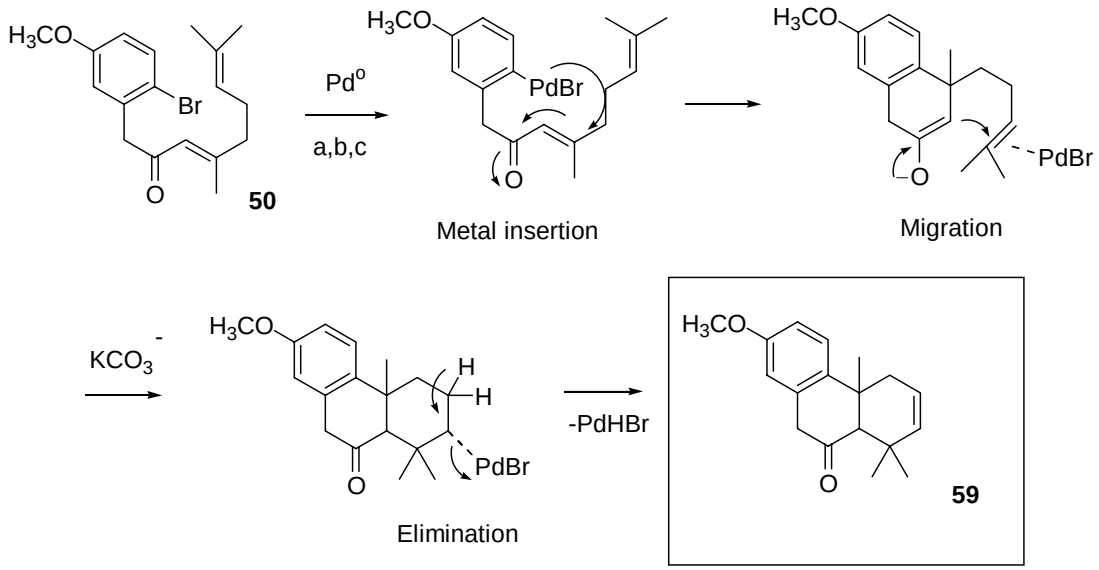

a) $Pd(OAc)_2/PPh_3$, K_2CO_3, DMF, 125 ^oC 12 hours

b) $Pd(Cl)_2/PPh_3$, Cs_2CO_3, NMO, 130 ^oC 24 hours

c) $Pd(OAc)_2/PPh_3$, NMP, 130 ^oC 12 hours

To form the target compound **59**, polyene **50** was reacted with $Pd(OAc_2)/PPh_3$ and K_2CO_3, in DMF and then heated at 125 ºC for 12 hours. After the reaction was complete, we found that none of the desired Heck products were formed. Attempts to modify the Heck reaction conditions by different procedures are shown in Scheme 5.8. In these experiments either the base or solvent, or both variables were modified, but this reaction resulted in a complex mixture of various degradation products. In addition, a significant quantity of **50** was recovered along with an undetermined amount of fragmentation products. To minimize observed fragmentation of **50**, different Pd(II) species and bases were employed, but these methods also failed to provide **59**. Several possible reasons for not generating **59** could be ascribed to the unsuccessful optimization of the palladium catalyst or the need for stoichiometric amounts of metal additives to form nucleophilic reagents *in situ*.[138] This led to the use of tetrabutylammonium fluoride to accelerate the reaction, but this also was found to be ineffective. Based on the general mechanism of the Heck reaction, it is highly possible that the initial oxidative insertion of palladium into the arylbromide bond may be too slow and furthermore not well tolerated due to the enolate intermediate formed by compound **50** during the Pd(O) migration step of the reaction.

Model D

A fouth model study to design coumarin derivatives was investigated. In these studies, an oxygen atom of a lactone ring was chosen to substitute for the benzylic hydrogens previously occuping this position. It was felt that these oxidizable benzylic hydrogens could possibly lead to unstable intermediates such as enols, and therefore limit

desirable properties of diterpene structure. Thus, modification at this labile position was expected to have a positive contribution to the activity of this new model compound. The synthesis of coumarin derivatives began with commercially available 1,3-catechol **60** which was treated with **61** to undergo a Pechmann condensation to furnish **62** in 67% yield (Scheme 5.9).[139] This important transformation established the required lactone ring structure without the need for additional steps. To this end, the phenol group of **62** was converted into the methyl ester **63** upon treatment with methyl iodine and K_2CO_3 in 54% yield as shown in Scheme 5.9.

Scheme 5.9 Formation of Diels Alder Adduct and Derivatives

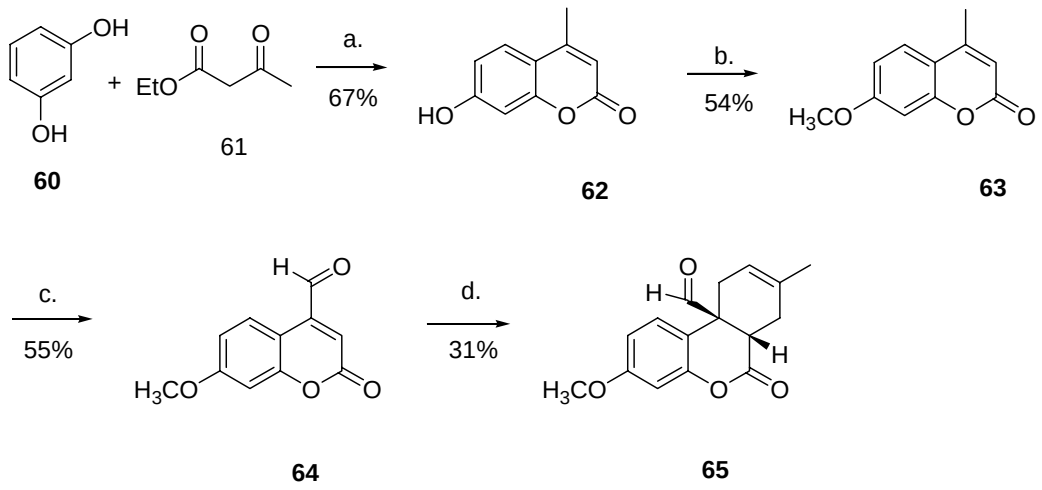

Reagents and conditions: a. H_2SO_4, room temp. b. K_2CO_3, CH_3I, CH_3CN c. SeO_2, xylene d. isoprene,1,4 hydroquinone in CH_3CN at 50 ^oC

As a means to construct the desired ring structure of **65**, a Diels Alder reaction was investigated. Following the work of Vaccaro *et.al*[140] the initial reaction conditons for the Diels alder employed treatment of **63** with isoprene in refluxing xylene. These

conditions, however, were unable to affect the desired [4+2] cyclization. After further reviewing the literature, we found that an electron withdrawing group is necessary to facilitate dienophilicity of the coumarin double bond. Therefore, selective conditions for the oxidation of the methyl group on the double bond of **63** with selenium dioxide were investigated.[140] From these investigations, we found that the optimal conditions for the oxidation of **63** was when **63** was treated with selenium dioxide in xylene and then heated at 50 ºC in a sealed vessel for a 24 hour period.

Structural confirmation of **64** was achieved by ^{1}H NMR analysis, which showed a single resonance near 10.2 ppm due to the aldehyde hydrogen (Figure 5.5). One problem encountered during the purification was that it was necessary to dissolve **63** in CH_2Cl_2 due to its low solubility in hexane.

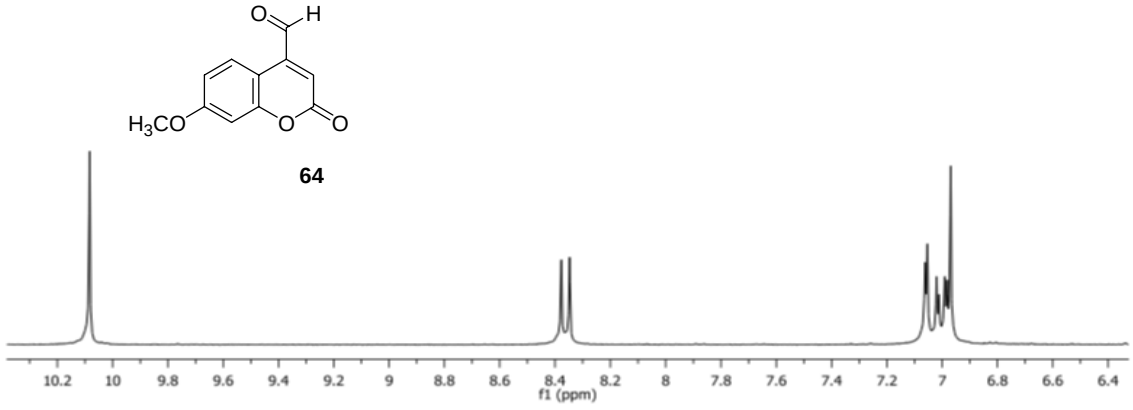

Figure 5.3. ^{1}H NMR spectrum of **63** showing distinguishable proton resonances

Serving as the key step for **65**, the cycloaddition of **64** with isoprene in xylene at 90 and 150 ºC, respectively, revealed only unreacted **64**. To overcome this problem, we first dissolved **64** in CH_3CN due to its low solubility in xylene. Secondly, we treated **64**

with an excess of isoprene and a few crystals of hydroquinone in a sealed tube at 50 ºC for 24 hrs. This reaction worked well and product **65** was confirmed by ^{1}H and ^{13}C NMR shown in Figure 5.4. Based on ^{1}H NMR, an unseperable mixture of cycloadduct and starting material were observed. The presence of two peaks at 9.2 ppm was characteristic of the aldehyde intact and the additional resonance at 6.1ppm indicated the proton of the alkene. Analyis of ^{13}C NMR showed a signal at 168 and 197 ppm corresponding to the carbonyl of the aldehyde and lactone, respectively. Furthermore, the presence of two carbon signals at 154 and 163 ppm are consistent with the presence of the alkene segment.

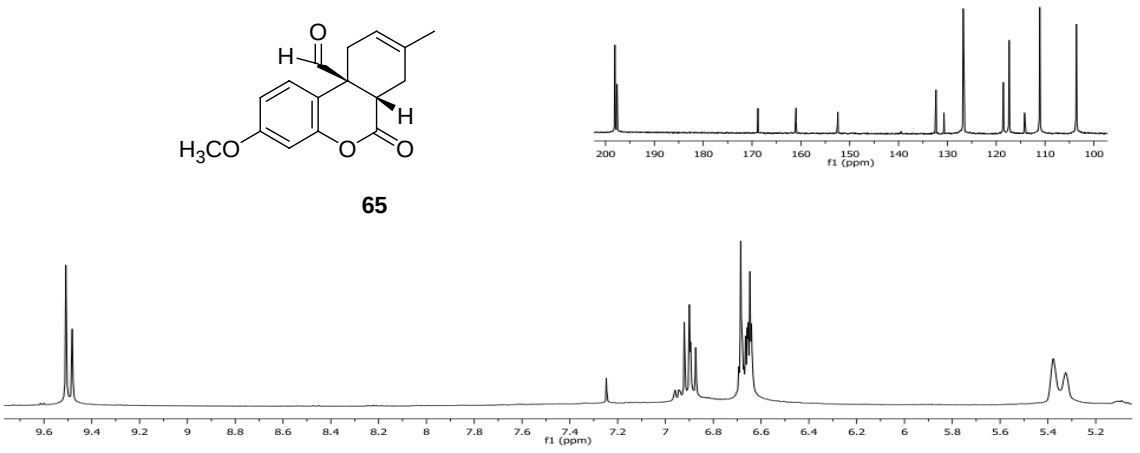

Figure 5.4. ^{1}H and ^{13}C NMR spectra of **65** showing distinguishable proton resonances and carbon signals.

The use of hydroquinone crystals turned out to be quite important experimentally. First this group allowed us to separate the mixture of starting material **64** from product **65** by filtration, and secondly, hydroquinone crystals prevented the polymerization of isoprene.[142,143] After the synthesis of **65**, we intended to elaborate these studies by

conversion of **65** into **66** via hydrogenation. Unfortunately, hydrogenation under a variety of conditions (Pd/C and various solvents) failed to produce characterizable products. Instead decomposition of the initial adduct **65** was observed. This straightforward reaction illustrates the challenges of derivatizing **65**, since it is highly sensitive to the reaction conditions, which could drive the reverse Diels-Alder reaction to the starting matierials (Scheme 5.10).

As stated above, coumarin derivatives were of prime importance for further biological evaluation and analogue synthesis. Treatment of **65** with $NaBH_4$ in ethanol resulted in fragmentation of the starting material and consistent under mild basic conditions due to the removal of the acidic hydrogen as exemplified by Scheme 5.10.

Scheme 5.10 Fourth model coumarin derivatives

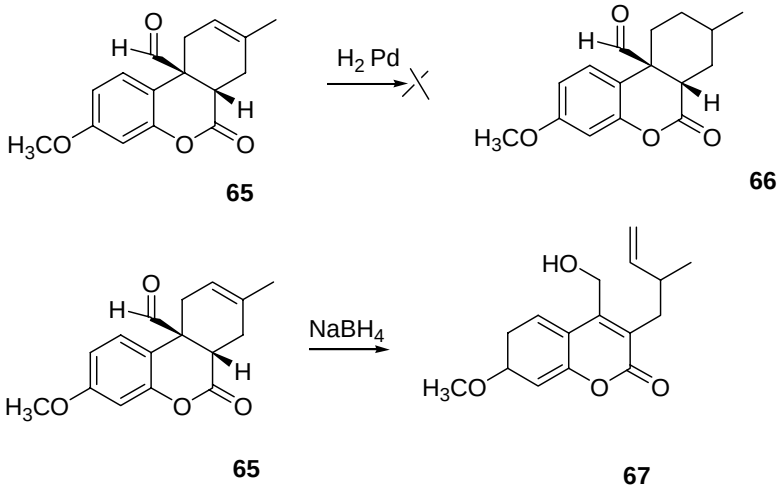

5.3 Conclusion

To investigate for the pertinent structural elements of diterpene structure, synthesis of analogs for structural activity relationship studies (SARs) were investigated.

The first diterpene analogs were designed to introduce chloride atoms in the A ring system of diterpene. The idea was that in contrast to a phenol ring, a less reactive aryl chloride could prevent the formation of QM. As a consequence of this work, the less reactive aryl chloride completely prevented the full cyclization of **46**. The investigation of our diterpene analogs B, were to generate a structure containing a bromine substituent on the aromatic system. The interest in **53** was due to its unique structure and particular functionality. Synthesis of this compound was performed by way of our previously reported polyene cyclization. These studies showed a temperature dependent effect on the reaction. At room temperature an intermediate side product **51** was observed, while at elevated temperature full cyclization proceeded to generate **53**.

Further studies to establish an unsaturated double bond into the C ring system of diterpene structure via the Heck reaction were unsuccessful. The corresponding products of this reaction were characterized and identified as a fragmented segment of the starting material **50**. The disconnected products of this reaction were attributed to the formation of an enolated during the migration of the PdBr in the reaction pathway. Continuing our synthesis of SARs, a Diels-Alder reaction for the generation of coumarin derivatives **65** was investigated. It was anticipated that the biological activity of structurally interesting diterpene analogs could be enhanced by the substitution of the benzylic hydrogens. To this end a lactone ring system was selected to replace the labile benzylic hydrogens with that of an oxygen group. Results of these studies showed that **65** could be formed conveniently by treatment with isoprene, xylene, and subsequent addition of hydroquinone and heated in a closed reaction vessel.

These diterpene analogs should provide a good fundamental basis for testing the chemo structural features involved in the biological properties of diterpene and cis-terpenone structure.

Chapter 6

Future studies on diterpenone as potent chemopreventive agents

6.1 Introduction

In the previous chapter 5, synthesis of diterpene analogs for structural activity relationship was investigated. Due to the synthetic challenges presented during the synthesis of our desired targets, this study is not fully completed. However with the compounds successfully synthesized, we were able to achieve a diverse set of structures. In this chapter, we have arranged diterpene analogs and related compounds into different classes so that we could more easily correlate their activity to our original cis-terpenone structure. The goal of these studies was to increase our understanding of the mechanistic action of cis-terpenones.

6.2 Initial studies and future efforts

Successful chemopreventive agents against AFB1 should demonstrate better physiochemical properties such as increased solubility and cellular absorption for maximum protective effects in biological systems. Therefore the structures in Scheme 6.1 represent chemical modifications of our unique diterpenes and interesting synthetic intermediates. These compounds will be screened to evaluate their chemical structural features and to investigate their effects in human liver cells against AFB1 toxicity.

Scheme 6.1 Comparison of chemical structure and derivatives of diterpenone

Group I

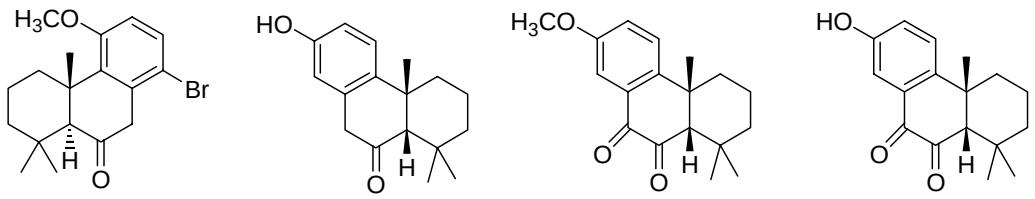

Group II

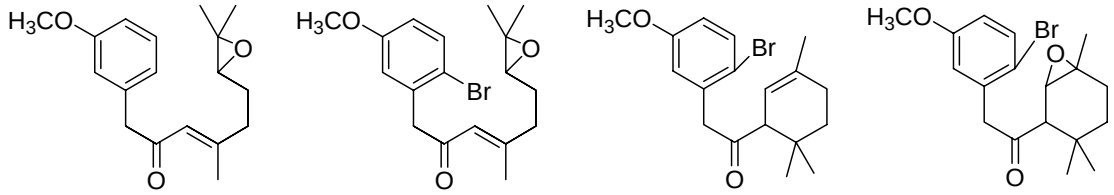

Group III

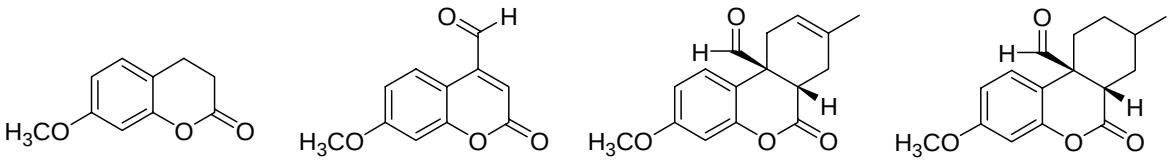

The first group of compounds were designed to examine the effects of substitution by a halogen group and to compare mon-versus diketone functional groups. The diketone structures were synthesized and characterized in collaboration with Dr. Zhou. Compounds in the second group were designed to evalutate the protective effects of compounds having a cyclic epoxide or alkene functional groups. This group will also be used to determine whether substitution of the uncyclized form of diterpene skeleton has potential biological activities. Finally, the elimination of the alpha hydrogens in all four compounds of group

three will allow us to investigate whether this position is necessary for chemoprotection. The biological investigations of these compounds using cell viability assay experiments are still in progress at this stage. This work provides the basis for a chemopreventive intervention strategy based on cis-terpenone and demonstrates the potential for developing cis-terpenones as effective chemopreventive agents.

Experimental Section

General methods. All solvents and chemicals were purchased from Fisher Scientific (Pittsburgh, PA) or Sigma-Aldrich (Milwaukee, WI) and used without further purification. The flash column chromatographic separations were performed with silica gel 60 (230-400 mesh). All ^{1}H NMR and ^{13}C NMR spectra were recorded on Varian 300 and 400 NMR spectrometers. All NMR chemical shifts (δ) were reported in parts per million (ppm) and were determined relative to the standard values for deuterated solvents. Electrospray ionization mass spectroscopy (ESI-MS) analysis was carried out using Q-TOF2 from Micromass (Manchester, U.K.). Some compounds were separated and quantified analytically by a Varian reversed-phase C18 column using a Jasco HPLC system.

Isopropyl (4E)-2-(3,4-Dimethoxyphenyl)-5,9-dimethyl-deca-4,8-dienoate (7). To a solution of fresh distilled diisopropylamine (3.1 mL, 22 mmol) in dry THF (10 mL) at -78 ºC under N_2 was added a solution of n-butyllithium (2.5 M, 8.8 mL). After 10 min at -78 ºC, a solution of 3,4-dimethoxyphenylacetic acid (2.0 g, 10 mmol) in dry THF (10 mL) was slowly added. The resulting solution was stirred for 1 h at -78 ºC , and then, geranyl chloride (2.0 mL, 11 mmol) was added. The reaction solution was stirred under N_2 for 18 h and allowed to slowly warm to room temperature. The reaction solution was then quenched with 1 N HCL (250 mL) and extracted with CH_2Cl_2. The organic layers were

collected, washed with brine, dried with $MgSO_4$, and concentrated. Flash chromatographic separation (0.5-7% MeOH in CH_2Cl_2) afforded the free acid **6** as a yellow oil (3.0 g) in 89% yield. ^{1}H NMR ($CDCl_3$, 300MHz): δ 6.87-6.79 (m, 3H), 5.06-4.99 (m, 2H), 3.87(s, 3H), 3.85 (s, 3H), 3.49 (t, *J*= 7.5Hz, 1H), 2.79-2.69 (m, 1H), 2.50-2.40 (m, 1H), 2.00-1.93 (m, 4H), 1.64 (s, 3H), 1.56 (s, 3H), 1.56 (s, 3H). ^{13}C NMR ($CDCl_3$, 75 MHz): δ 179.4, 149.1, 148.5, 138.0, 131.6, 130.9, 124.2, 120.7, 120.5, 111.2, 111.2, 56.0, 51.4, 39.9, 31.9, 26.7, 25.8, 17.8, 16.3. HRMS calcd for $C_{20}H_{28}O_4$, 332.1988; found, 332.2003.

To a solution of the resulting acid **6** (3.0 g, 9.0 mmol) in CH_2Cl_2 (25 mL) were added 4-(dimethylaminopropyl)-3-ethylcarbodiimide hydrochloride (EDCI) (1.7 g 1.1 mmol) and 2-propanol (0.76 ml, 9.9 mmol). Flash chromatographic separation (5-10%EtOAc in hexanes) afforded product **7** as a colorless oil (2.5 g) in 76% yield. ^{1}H NMR ($CDCl_3$, 300 MHz): δ 6.87-6.77 (m, 3H), 5.06-4.96 (m, 3H), 3.87 (s, 3H), 3.85 (s, 3H), 3.43 (t, *J*= 7.9 Hz, 1H), 2.77-2.67 (m, 1H), 2.45-2.35 (m, 1H), 2.00-1.93 (m, 4H), 1.66 (s, 3H), 1.57 (s, 6H), 1.21 (d, J = 6.3 Hz, 3H), 1.14 (d, J=6.3 Hz, 3H). 13C NMR (CDCl3, 75MHz): δ 173.7, 148.9, 148.2, 137.6, 132.0, 131.6, 124.3, 121.1, 120.0, 111.1, 111.0, 68.0, 56.0, 51.9, 39.9, 32.6, 26.8, 25.9, 22.0, 21.8, 17.8, 16.4. HRMS calcd for $C_{23}H_{34}O_4$, 374.2457; found, 374.2463.

1,2,3,4,4a,9,10,10a-Octahydro-6,7-dimethoxy-1,14a-trimethylphenanthrene-9-carboxylic acid (9). To a solution of **7** (2.5 g, 6.8 mmol) in dry CH_3NO_2 (20 ml) at -15ºC was added BF_3NO_2 (1.6 mL, 13 mmol), and the resulting reaction solution was stirred under N_2 at -15ºC for 2 h and then room temperature for 0.5 h. The reaction solution was diluted with a solution of saturated $NaHCO_3$ (150 mL) and extracted with CH_2Cl_2. The

organic layers were collected, washed with brine, dried with $MgSO_4$, and concentrated. Flash chromatographic separation (10-12% EtOAc in hexanes) afforded the diastereoisomeric mixture of isopropyl ester **8** as a colorless oil (2.1 g) in 61% yield. This diastereoisomers were not further separated since one of the chiral centers was removed during the decarboxylation step. ^{1}H NMR ($CDCl_3$, 300 MHz) for the major isomer: δ 6.76 (s, 1H), 6.63 (s, 1H), 5.12-5.00 (m, 1H), 3.84 (s, 3H), 3.80 (s, 3H), 3.80-3.79 (m, 1H), 2.26-1.99 (m, 3H), 1.77-1.41 (m, 6H), 1.29-1.16 (m, 10H), 0.97 (s, 3H). ^{13}C NMR ($CDCl_3$, 75 MHz) for the isomers: δ 175.2, 174.9, 148.0, 147.0, 142.9, 123.9, 112.1, 110.3, 107.6, 67.9, 55.8, 55.6, 48.9, 46.9, 41.5, 39.0, 37.3, 33.3, 33.1, 24.8, 23.1, 21.8, 21.7, 21.4, 19.1. HRMS calcd for $C_{23}H_{34}O_4$, 374.2457; found, 374.2446.

To a solution of the resulting ester **8** (2.0 g, 5.3 mmol) in ethanol (20 mL) was added crushed NaOH pellet (2.1 g), and the resulting mixture was refluxed for 3 h. The reaction solution was acidified with 2.5 N HCl (150 mL), and the aqueous solution was then extracted with CH_2Cl_2. The organic layers were collected, washed with brine, dried with $MgSO_4$, and concentrated to afford the diastereoisomeric mixture of **9** as viscous oil (1.7 g) in 96% yield. ^{1}H NMR ($CDCl_3$, 300 MHz) for the major isomer: δ 6.77 (s, 1H), 6.67 (s, 1H), 3.84 (s, 3H), 3.81 (s, 3H), 3.81 (m, 1H), 2.34-2.17 (m, 2H), 2.07-1.98 (m, 1H), 1.76-1.16 (m, 9H), 0.94 (s, 3H), 0.94 (s, 3H). ^{13}C NMR ($CDCl_3$, 75 MHz) for the major isomer: δ 182.0, 148.3, 147.1, 143.3, 122.9, 111.0, 107.8, 56.1, 56.0, 49.2, 46.5, 41.7, 39.2, 37.5, 33.6, 33.3, 24.9, 23.6, 21.6, 19.5. HRMS cacld for $C_{20}H_{28}O_4$, 332.1988; found, 332.1985.

1,2,3,4,4a,10a-Hexahydro-6,7-dimethoxy-1,1,4a-trimethylphenanthrene (10). To a mixture of **9** (1.6 g, 4.8 mmol), lead (IV) acetate (4.8 g, 11 mmol), and copper (II) acetate (0.98 g, 5.4 mmol) was added quinoline (30 mL). The resulting dark solution was degassed under vacuum and then heated under N_2 at 130 ºC for 3 h. After it was cooled to room temperature, the reaction solution was diluted with 1 N HCL and extracted with CH_2Cl_2. The organic layers were collected, washed with brine, dried with $MgSO_4$, and concentrated. Quinoline from the resulting residue was removed by vacuum distillation. Flash chromatographic separation (5-10% EtOAc in hexanes) afforded product **10** as a colorless oil (720 mg) in 51% yield. ^{1}H NMR ($CDCl_3$, 400 MHZ): δ 6.72 (s, 1H), 6.60 (s, 1H), 6.45 (d, *J*= 2.8 Hz, 1H), 5.91 (d, J=2.8Hz, 1H), 3.87 (s, 3H), 3.84 (s, 3H), 2.14-2.08 (m, 2H), 1.77-1.49 (m, 4H), 1.26-1.19 (m, 1H), 1.03 (s, 3H), 1.00 (s, 3H), 0.96 (s, 3H). 13CNMR (CDCl3, 75 MHz): δ148.3, 146.8, 141.4, 128.7, 127.1, 126.1, 110.1, 106.3, 56.2, 56.1, 51.5, 41.2, 37.9, 36.4, 33.0, 32.8, 22.7, 20.2, 19.2. HRMS calcd for C19H26O2, 286.1933; found, 286.1944.

4b, 5, 6, 7, 8, 8a-Hexahydro-2-3-dimethoxy-4b,8,8-trimethylphenanthren-9(10H)-one (11). To a solution of **10** (184 mg, 0.64 mmol) in CH_2Cl_2 (10 mL) at 0 ºC was added *m*-chloroperoxybenzoic acid (70-75%, 220 mg). The resulting reaction solution was stirred at 0 ºC under N_2 for 3 h. The reaction solution was quenched with a solution of 5% $Na_2S_2O_3$ and extracted with CH_2Cl_2. The organics were collected, washed with brine, dried with $MgSO_4$, and concentrated. The residue was dissolved with in $CHCl_3$ (10 mL), and trifluoroacetic acid (1 mL) was added. The resulting solution was stirred under N_2 for 18 h and then diluted in CH_2Cl_2 (100 mL). The organic solution was washed with

solutions of saturated $NaHCO_3$ and brine, dried with $MgSO_4$, and concentrated. Flash chromatography separation (10-15% EtOAc in hexanes) afforded product **11** as a colorless oil (88 mg) in 45% yield. ^{1}H NMR ($CDCl_3$, 400 MHz): δ 6.83 (s, 1H), 6.53 (s, 1H), 3.88 (s, 3H), 3.85 (s, 3H), 3.55 (s, 2H), 2.41 (s, 1H), 2.31-2.27 (m, 1H), 1.79-1.68 (m, 3H), 1.45-1.39 (m, 1H), 1.31 (s, 3H), 1.31-1.16 (m, 1H), 1.14 (s, 3H), 1.08 (s, 3H). ^{13}C NMR ($CDCl_3$, 75MHz): δ 209.8, 147.9, 147.7, 124.4, 111.0, 107.4, 63.0, 56.3, 56.1, 44.9, 42.9, 40.6, 39.0, 33.1, 32.7, 24.9, 21.7, 18.9. HRMS calcd for $C_{19}H_{26}O_3$, 302.1882; found, 302.1898.

4b, 5, 6, 7, 8, 8a-Hexahydro-2-3-dimethoxy-4b,8,8-trimethylphenanthren-9(10H)-one (1). To a mixture of **11** (50 mg, 0.17 mmol) in CH_2Cl_2 (3.0 mL) under N_2 was added BBr_3 (1.0 M in heptane, 0.5 mL, 0.5 mmol). The resulting dark solution was stirred at room temperature for 2 h. The reaction solution was quenched with a solution of brine and extracted with degassed EtOAc. The organic layers were collected, dried with $MgSO_4$, and concentrated. Flash chromatographic separation (25-35% EtOAc in hexanes) under N_2 afforded product **1** as a brown oil (38 mg) in 82% yield. ^{1}H NMR (CD_3CN, 400 MHz): δ 6.80 (s, 1H), 6.58 (br s, 1H), 6.51 (s, 2H), 3.52 (d, J = 21Hz, 1H), 3.38 (d, J= 21 Hz, 1H), 2.41 (s, 1H), 2.26-2.23 (m, 2H), 1.76-1.69 (m, 1H), 1.63-1.60 (m, 2H), 1.40-1.36 (m, 1H), 1.27 (s, 3H), 1.21-1.16 (m, 1H), 1.08 (s, 3H), 1.04 (s, 3H). ^{13}C NMR (CD_3CN, 75 MHz): δ 209.9, 143.3, 142.9, 141.3, 124.3, 114.7, 110.9, 62.4, 44.3, 42.5, 40.1, 38.7, 32.4, 32.3, 24.3, 21.2, 18.7. ESI-MS calcd for $C_{34}H_{44}O_6$-H^+ (dimer), 547, and for $C_{17}H_{22}O_3$-H^+, 273; found, 547 and 273.

Formation of Diterpene QM under Organic Conditions. The oxidation of catechols was achieved using Ag_2O as an oxidant. After vigorous stirring at ambient temperature for 20 min, the solids were removed by filtration with a 0.2μm filter (Acrodisc, 13 CR, PTFE).

Diterpene QM 3 (5 mg in 0.8 mL $CDCl_3$). ^{1}H NMR (CD_3CN, 400 MHz): δ 7.43 (br, 1H), 6.51 (s, 1H), 6.40 (s, 1H), 6.30 (s, 1H), 2.60 (s, 1H), 1.80-1.60 (m, 4H), 1.40-1.20 (m, 2H), 1.24 (s, 6H), 1.15 (s, 3H). Because of high reactivity ^{13}C NMR was unsuccessful.

1-(Chloromethyl)-3,4-dimethoxy-2-methylbenzene (15). To a solution of chloro methyl ethyl ether (6.05 g, 64.0 mmo) in acetic acid (5.5 mL) was added 2,3-dimethoxytoluene **14** (5.20 mL, 34.7 mmol), and the reaction was initiated by slightly heating. The reaction solution was stirred under N_2 at room temperature for 16 h and then cooled in ice to precipitate the product. The solid was collected by filtration and washed with water. Flash chromatographic separation (5-10% EtOAc in hexanes) afforded compound **15** as a white solid (3.21 g) in 47% yield. ^{1}H NMR ($CDCl_3$, 300 MHz): δ 7.04 (d, J = 8.3 Hz, 1H), 6.73 (d, J = 8.3 Hz, 1H), 4.58 (s, 2H), 3.85 (s, 3H), 3.79 (s, 3H), 2.35 (s, 3H). ^{13}C NMR ($CDCl_3$, 75 MHz): δ 153.4, 147.7, 131.9, 129.0, 125.9, 109.5, 60.5, 55.8, 45.6, 11.6. ESI-MS calcd for $C_{10}H_{13}ClO_2$ (M-Cl), 165.09; found, 165.05

3,4-Dimethoxy-2-methylphenylacetic acid (17). To a solution of **15** (3.21 g, 16.0 mmol) in dry DMF (35 mL) was added KCN (1.03 g, 1.05 equiv) and 18-crown-6 (5.04 g, 1.2 equiv). The reaction was stirred under N_2 for 16 h. The reaction solution was then extracted with ether (250 mL x 2). The organic layers were collected, dried with $MgSO_4$, and concentrated. Flash chromatographic separation (5-10% EtOAc in hexanes) afforded

the cyanide product **16** as an oil (2.81 g) in 92% yield. ^{1}H NMR ($CDCl_3$, 300MHz): δ 7.02 (d, *J* = 8.4 Hz, 1H), 6.74 (d, J = 8.4 Hz, 1H), 3.83 (s, 3H), 3.76 (s, 3H), 3.58 (s, 2H), 2.23 (s, 3H), ^{13}C NMR ($CDCl_3$, 75 MHz): δ 152.8, 147.8, 130.6, 124.3, 121.6, 118.1, 109.9, 60.6, 55.9, 21.8, 12.1. ESI-MS calcd for $C_{11}H_{15}NO_2$ (M + H+), 192.10; found, 192.07. The cyanide adduct (2.81 g, 14.7 mmol) was refluxed in a solution of NaOH (8.5 g) in ethanol (30 mL) for 18h. The reaction solution was then acidified with HCl to pH 2 and extracted with CH_2Cl_2. The organic layers were collected, dried with $MgSO_4$, and concentrated. Flash chromatography separation (2-7% MeOH in CH_2Cl_2) afforded compound **17** as white solid (1.95 g) in 63% yield. ^{1}H NMR ($CDCl_3$, 300MHz): δ6.91 (d, *J* = 8.3 Hz, 1H), 6.72 (d, J = 8.3 Hz, 1H), 3.83 (s, 3H), 3.77 (s, 3H), 3.60 (s, 2H), 2.21 (s, 3H). ^{13}C NMR ($CDCl_3$, 75 MHz): δ 178.4, 152.3, 147.5, 131.6, 126.0, 125.5, 109.7, 60.4, 55.8, 38.9, 12.4. ESI-MS calcd for $C_{11}H_{15}O_4$ ($M + H^+$), 211.10; found 211.10.

Methyl (4E)-2-(3,4-Dimethoxy-2-methylphenyl)-5,9-dimethyldeca-4,8-dienoate (18). To a solution of freshly distilled diisopropylamine (2.20 mL, 15.7 mmol) in dry THF (20 mL) at -78C under N_2 was added a solution of n-butyllithium (2.5 M, 6.28 mL). After 10 min at -78 ºC, a solution of 3,4-Dimethoxyphenylacetic acid (1.40 g, 7.13 mmol) in THF (10 mL) was slowly added. The resulting solution was stirred for 1 h at -78 ºC, and then geranyl chloride (1.45 mL, 7.85 mmol) was added. The reaction solution was stirred under N_2 for 18 h and then allowed to slowly warm to room temperature. The reaction solution was then quenched with 1 N HCl (250 mL) and extracted with CH_2Cl_2. The organic layers were collected, washed with brine, dried with $MgSO_4$ and concentrated. Flash chromatographic separation (0.5-7% MeOH in CH_2Cl_2) afforded the free acid (not

numbered) as a yellow oil (1.65 g) in 70% yield. ^{1}H NMR ($CDCl_3$, 300 MHz): δ7.06 (d, *J* = 8.6 Hz, 1H), 6.75 (d, J = 8.6 Hz, 1H), 5.04 (m, 2H), 3.83 (s, 3H), 3.76 (s, 3H), 3.76 (m, 1H), 2.77-2.70 (m, 1H), 2.41-2.34 (m, 1H), 2.29 (s, 3H), 2.00-1.94 (m, 4H), 1.65 (s, 3H) 1.57 (s, 6H). ^{13}C NMR ($CDCl_3$, 75 MHz): δ 180.5, 151.9, 147.2, 137.8, 131.6, 131.2, 130.3, 124.3, 122.8, 120.9, 109.8, 60.5, 55.8, 47.0, 39.9, 31.6, 26.7, 25.8, 17.8, 16.3, 12.1. ESI-MS calcd for $C_{21}H_{31}O_4$ ($M + H^+$), 347.22; found 347.22.

To a solution of the resulting free acid (1.57 g, 4.72 mmol) in CH_2Cl_2 (35 mL) were added 4-(dimethyamino)pyridine (6.81 mg, 1.2 eq), DCC (1.16 g, 1.2 eq) and methanol (210 μL, 1.1 eq). The resulting reaction mixture was stirred under N_2 for 18 h at room temperature. The reaction solution was then quenched with 1 N HCl (250 mL) and extracted with CH_2Cl_2. The organic layers were collected, washed with brine, dried with $MgSO_4$ and concentrated. Flash chromatographic separation (5-20%EtOAc in hexanes) afforded diastereoisomeric pure trans compound **18** as a yellow oil (1.03 g) in 60% yield. ^{1}H NMR ($CDCl_3$, 300MHz): δ 7.04 (d, *J* = 8.5 Hz, 1H), 6.74 (d, *J* = 8.5 Hz, 1H), 5.05-5.00 (m, 2H), 3.83 (s, 3H), 3.77 (s, 3H), 3.76 (m, 1H), 3.64 (s, 3H), 2.76-2.71 (m, 1H), 2.38-2.34 (m, 1H), 2.27 (s, 3H), 2.00-1.93 (m, 4H) 1.66 (s, 3H) 1.57 (s, 6H). ^{13}C NMR ($CDCl_3$, 75 MHz): δ 174.9, 151.7, 147.2, 137.6, 131.6, 130.9, 130.8, 124.3, 122.6, 121.2, 109.7, 60.4, 55.8, 52.0, 47.1, 39.9, 32.1, 26.8, 25.9, 17.8, 16.3, 12.0. ESI-MS calcd for $C_{22}H_{33}O_4$ ($M + H^+$), 361.24; found 361.24.

4b, 5, 6, 7, 8, 8a-trans-Hexahydro-2,3-dimethoxy-1,4b,8,8-tetramethylphenanthrenene (21) To a solution of **18** (992 mg, 2.73 mmol) in dry CH_3NO_2 (20 mL) at -15 ºC was added BF_3OEt_2 (2.40 mL, 7eq), and the resulting solution

was stirred under N_2 at -15 ºC for 4 h. The reaction solution was diluted with saturated $NaHCO_3$ (150 mL) and extracted with CH_2Cl_2 (150 mL x3). The organic layers were collected, washed with brine, dried with $MgSO_4$ and concentrated. Flash chromatographic separation (5-10% EtOAc in hexanes) afforded the diastereoisomeric mixture of isopropyl ester **19** as colorless oil (619 mg) in 71% yield. These diastereoisomers were not further separated since one of the chiral centers was removed during the decarboxylation step. ^{1}H NMR ($CDCl_3$, 300MHz): δ 6.73 (s, 1H), 3.83 (s, 3H), 3.73 (s, 3H), 3.69 (s, 3H), 3.66 (m, 1H), 2.33-2.23 (m, 1H), 2.02 (s, 3H), 1.79-1.17 (m, 11H), 0.94-0.88 (m, 6H) ^{13}C NMR ($CDCl_3$, 75 MHz): δ 177.1, 151.3, 147.1, 145.3, 131.03, 123.9, 106.6, 105.9, 60.4, 55.7, 52.3, 48.6, 46.6, 45.2, 44.2, 41.7, 41.3, 39.7, 39.0, 38.0, 33.6, 33.2, 33.0, 25.2, 25.1, 24.7, 24.0, 21.7, 19.5, 19.4, 12.3, 12.1. ESI-MS calcd for $C_{22}H_{33}O_4$ ($M + H^+$), 361.24; found 361.24.

To a solution of the resulting ester (617 mg, 1.70 mmol) in ethanol (20 mL) was added 3 g crushed NaOH pellets, and the resulting mixture was refluxed for 3 h. The reaction solution was acidified with 2.5 N HCl and extracted with CH_2Cl_2. The organic layers were collected, washed with brine, dried with $MgSO_4$, and concentrated to afford a diastereoisomeric mixture of **20** as a viscous oil (432 mg) in 73% yield. ^{1}H NMR ($CDCl_3$, 300MHz): δ 6.75 (s, 1H), 3.84 (s, 3H), 3.84 (m, 1H), 3.75 (s, 3H), 2.45-2.17 (m, 2H), 2.11 (s, 3H), 1.89-1.18 (m, 10H), 0.96-0.94 (m, 6H). ^{13}C NMR ($CDCl_3$, 75 MHz): δ 182.9, 181.9, 152.1, 151.5, 147.3, 146.9, 145.3, 140.3, 131.1, 125.2, 123.3, 107.2, 106.5, 106.0, 60.5, 60.4, 55.8, 50.3, 48.6, 46.6, 44.8, 44.0, 42.1, 41.8, 41.3, 39.7, 39.0, 38.9, 38.7, 37.9,

37.7, 34.9, 34.4, 33.7, 33.2, 33.0, 32.7, 25.2, 24.6, 24.0, 21.7, 21.7, 19.5, 12.4, 12.0. ESI-MS calcd for $C_{21}H_{31}O_4$ ($M + H^+$), 347.22; found, 347.22.

To the resulting mixture (398 mg, 1.25 mmol), lead (IV) acetate (1.20 g. 2.2 equiv) and copper (II) acetate (248 mg, 1.1 equiv), was added quinoline (15 mL). The resulting dark solution was degassed under vacuum and then heated under N_2 at 140 ºC for 3 h. After cooling to room temperature, quinoline from the resulting was removed by vacuum distillation. The reaction solution was diluted with 1 N HCl (200 mL) and extracted with CH_2Cl_2 (150 mL x 3). The organic layers were collected, washed with brine, dried with $MgSO_4$, and concentrated. Flash chromatographic separation (5-20% EtOAc in hexanes) afforded product **21** as a colorless (200 mg) in 53% yield. ^{1}H NMR ($CDCl_3$, 300MHz): δ 6.68 (d, J=2.8Hz, 1H), 6.64 (s, 1H), 5.95 (d, J=2.8Hz, 1H), 3.86 (s, 3H), 3.75 (s, 3H), 2.26 (s, 3H), 2.19-2.07 (m, 2H), 1.75-1.50 (m, 4H), 1.24-1.20 (m, 1H), 1.05 (s, 3H), 1.02 (s,3H), 0.97 (s,3H). ^{13}C NMR ($CDCl_3$, 75 MHz): δ 151.9, 145.2, 145.0, 128.4, 127.9, 125.2, 124.2, 104.4, 60.5, 55.9, 50.7, 41.2, 38.5, 36.6, 33.0, 32.7, 22.7, 20.1, 19.3, 11.8. ESI-MS calcd for $C_{20}H_{29}O_2$ ($M + H^+$), 300.21; found 300.09.

4b, 5, 6, 7, 8, 8a-trans-Hexahydro-2,3-dimethoxy-1,4b,8,8-tetramethylphenanthrenene-9(10H)-one (22F). To a solution of **21** (270 mg, 0.899 mmol) in CH_2Cl_2 (10 mL) at 0 ºC was added m-chloroperoxbenzoic acid (70-75%, 443 mg, 1.5 equiv). The resulting reaction was stirred at 0 ºC under N_2 for 3h. The reaction was quenched with a solution of 5% $NaHCO_3$ (150 mL) and extracted with CH_2Cl_2 (150 mL x 3). The organic layers were collected, washed with brine, dried with $MgSO_4$ and concentrated. Flash chromatographic separation (5-10% EtOAc in hexanes) afforded

product **22F** as a colorless oil (119 mg) in 41% yield. ^{1}H NMR ($CDCl_3$, 300 MHz): δ 6.76 (s, 1H), 3.85 (s, 3H), 3.76 (s, 3H), 3.46 (d, *J*= 21.4Hz, 1H), 3.37 (d, *J*= 21.4Hz, 1H), 2.44 (s, 1H), 2.30-2.28 (m, 1H), 2.10 (s, 3H), 1.72-1.64 (m, 4H), 1.43-1.38 (m, 1H), 1.32 (s, 3H), 1.18 (s, 3H), 1.06 (s, 3H). ^{13}C NMR ($CDCl_3$, 75MHz): δ 209.7, 151.4, 145.8, 144.7, 129.7, 124.0, 105.8, 62.4, 60.5, 56.0, 43.5, 42.8, 41.1, 39.1, 33.0, 32.7, 25.1, 21.8, 19.0, 12.1. ESI-MS calcd for $C_{20}H_{29}O_3$ ($M + H^+$), 317.21; found, 317.20.

4b, 5, 6, 7, 8, 8a-trans-Hexahydro-2,3-dihydroxy-1,4b,8,8-tetramethylphenanthrenene-9(10H)-one (23). To a mixture of **22F** (11 mg, 0.35 mmol) in CH_2Cl_2 (3.0 mL) under N_2 was added BBr_3 (1.0 M in heptane, 0.5 mL, 0.5 mmol). The resulting dark solution was stirred at room temperature for 2h. The reaction solution was quenched with a solution of brine and extracted with degassed EtOAc. The organic layers were collected, dried with $MgSO_4$, and concentrated. Flash chromatographic separation (25-35% EtOAc in hexanes) under N_2 afforded product **23** as a brown oil (5.4 mg) in 54% yield. ^{1}H NMR ($CDCl_3$/CD_3OD, 300 MHz): δ 6.64 (s, 1H), 3.53 (s, 2H), 3.43-3.18 (q, *J*= 21.4Hz, 2H), 2.39 (s, 1H) 2.17-2.14 (m, 1H), 2.01 (s, 3H), 1.63-1.53 (m, 4H), 1.35-1.30 (m, 1H), 1.24 (s, 3H), 1.02 (s, 3H), 0.97 (s, 3H). ^{13}C NMR ($CDCl_3$/CD_3OD, 75MHz): δ 207.5, 138.9, 137.2, 136.8, 118.8, 118.2, 104.0, 58.7, 39.6, 38.8, 36.7, 35.1, 28.9, 28.6, 21.2, 17.7, 15.0, 7.6. ESI-MS calcd for $C_{18}H_{25}O_3$ (M^+), 288.17; found, 288.09

4b, 5, 6, 7, 8, 8a-trans-Hexahydro-4b,8,8-trimethylphenanthrene-2,3-diol (25). To a solution of **10** (100 mg, 0.35 mmol) in CH_2Cl_2 (3.0 mL) under N_2 was added BBr_3 (1.0 M in heptane, 0.5 mL, 0.5 mmol). The resulting dark solution was stirred at room

temperature for 2h. The reaction solution was quenched with a solution of brine and extracted with degassed EtOAc. The organic layers were collected, dried with $MgSO_4$, and concentrated. Flash chromatographic separation (25-35% EtOAc in hexanes) under N_2 afforded product **25** as a brown oil (5.4 mg) in 80% yield. ^{1}H NMR ($CDCl_3$, 300MHz): δ 6.71 (s, 1H), 6.58 (s, 1H), 6.39 (d, *J*= 8.7 Hz, 1H), 5.90 (d, *J*= 8.7 Hz, 1H), 5.14 (br s, 1H) 4.94 (br s, 1H), 2.06 (br m, 2H), 1.72-1.49 (m, 3H), 1.27-1.21 (m, 2H), 1.02 (m, 3H), 0.99 (s, 3H), 0.96 (s, 3H). ^{13}C NMR ($CDCl_3$, 75 MHz): δ 142.9, 142.6, 140.9, 128.8, 126.9, 126.7, 113.8, 110.1, 51.3, 41.2, 37.9, 36.3, 33.0, 32.8, 22.7, 20.5, 19.2. ESI-MS calcd for $C_{17}H_{23}O_2$ (M^+), 258.16; found, 258.08.

4b, 5, 6, 7, 8, 8a-trans-Hexahydro-4b,8,8-trimethylphenanthrene-2,3-diol (26). To a solution of **21** (32 mg, 0.11 mmol) in CH_2Cl_2 (2.0 mL) under N_2 was added BBr_3 (1.0 M in heptane, 1 mL). The resulting dark solution was stirred at room temperature for 2h. The reaction solution was quenched with a solution of brine and extracted with degassed EtOAc (100 mL x 2). The organic layers were collected, dried with $MgSO_4$, and concentrated. Flash chromatographic separation (25-35% EtOAc in hexanes) under N_2 afforded product **26** as a brown oil (20 mg) in 68% yield. ^{1}H NMR ($CDCl_3$/CD_3OD, 300 MHz): δ 6.61 (d, *J*= 3.0 Hz, 1H), 6.53 (s, 1H), 5.86 (d, *J*= 2.8 Hz, 1H), 3.51 (s, 2H), 2.18 (s, 3H) 2.00-1.97 (m, 2H), 1.67-1.42 (m, 4H), 1.21-1.15 (m, 2H), 0.98 (s, 3H), 0.93 (s, 3H), 0.90 (s, 3H). ^{13}C NMR ($CDCl_3$/CD_3OD, 75 MHz): δ 143.2, 141.6, 140.3, 127.9, 124.5, 124.2, 120.9, 106.9, 50.9, 41.2, 38.0, 36.5, 32.9, 32.7, 22.5, 20.2, 19.2, 11.3. ESI-MS calcd for $C_{18}H_{25}O_2$ (M^+), 272.17; found, 272.09.

General Synthetic Procedures to cis-analogues 22 and 24. To a solution of geranyl aldehyde **27** (1 g, 6.5 mmol) in THF (25 mL) was added 1,3 propane dithiol (0.9 mL, 1.1 equiv) at -50 ^{o}C was added BF_3Et_2O (2.1 mL, 3 equiv) and the resulting reaction solution was stirred under N_2 for 3 h. The reaction was quenched with a solution of 5% $Na_2S_2O_3$ and extracted with CH_2CL_2 (100 mL x 2). The organic layers were collected, washed with brine, dried with $MgSO_4$, and concentrated. Flash chromatographic separation (10-15% EtOAc in hexanes) afforded product **28** in 71% yield as a colorless oil (1:1 cis/trans mixture). To a solution of thiol-protected citral **28** (1:1 cis/trans mixture) in dry THF (20 mL) at -40 ºC (acetonitrile/dry ice bath) was slowly added a solution of 1.05 equiv n-BuLi (1.6 M in hexanes) under N_2. The resulting reaction solution was stirred at -40 ºC for 1 h, and then a solution of (0.95 equiv) **15a** or **15b** in dry THF (10 mL) was added. After 4h, the reaction flask was transferred into a dessicator and kept in a freezer (-25 ºC) for 48 hours. The reaction solution was quenched with brine (100 mL) and extracted with ether (100 mL x 2). The organic layers were collected, dried with $MgSO_4$, and concentrated. The desired products **29a,b** were purified as cis/trans diastereiomeric mixture by a flash column separation. Further separation of the isomers was not carried out because the subsequent cyclization step afforded diastereoismerically pure *cis*-compounds.

To a solution of **29a,b** in MeOH/H_2O (9:1, 25 mL) was added 1.1 equiv HgO and $HgCl_2$. Prior to this study, we investigated the effect of $CaCO_3$ in the reaction mixture, to neutralize the HCL formed in the reaction, but we found that the reaction worked better with the combination of HgO and $HgCl_2$ in a 1/1 ratio. Therefore, after addition of HgO

and $HgCl_2$, the resulting reaction solution was stirred at room temperature for 12 h. The reaction solution was diluted with CH_2Cl_2, and the precipitation was filtered through Celite. The solution was washed with brine, collected, dried with $MgSO_4$, and concentrated. The desired products **30a,b** were purified as a cis/trans diastereomeric mixture by a flash column separation using (10-15% EtOAc in hexanes).

To a solution of **30a,b** in dry CH_3NO_2 (10 mL) at room temperature was added 10 equiv BF_3OEt_2, and the resulting reaction solution was stirred under N_2 for 2 h. The reaction solution was diluted with saturated $NaHCO_3$ (150 mL) and extracted with CH_2Cl_2 (150 mL x 3). The organic layers were collected, dried with $MgSO_4$, and concentrated. The desired compounds **31a,b** were purified as a diastereoisomeric pure product by a flash column separation (10-25% EtOAc in hexanes). To a solution of **31a,b** in CH_2Cl_2 (2.0 mL) under N_2 was added a solution of BBr_3 (1.0 M in hepatane, 1.0 mL). The resulting solution was stirred at room temperature for 2h. The reaction solution was quenched with brine (100 mL) and extracted with EtOAc (100 mL x 2). The organic layers were collected, dried with $MgSO_4$, and concentrated. The desired products **22** and **24** were purified by a flash column separation (1-5% MeOH in dichloromethane).

2-(3,4-Dimethoxybenzyl)-2-(2,6-dimethylhepta-1,5-dienyl)-1,3-dithiane (29a).

A colorless oil: 1.29 g in 63% yield (10-25% EtOAc in hexanes). ^{1}H NMR ($CDCl_3$, 300 MHz) for the cis/trans diastereomeric mixture: δ 6.80-6.77 (m, 3H), 5.40 (s, 1H), 5.15-5.07 (2 sets of triplet, *J*= 6.7 Hz, 1H), 3.83 (s, 6H), 3.27-3.21 (2 sets of singlet, 2H), 2.92-2.78 (m, 4H), 2.49-2.44 (m, 1H), 2.10-2.05 (m, 5H), 1.80 (2 sets of singlet, 3H), 1.66 (s, 3H), 1.59 (2 sets of singlet, 3H). ^{13}C NMR ($CDCl_3$, 75 MHz) observed: δ 148.2,

142.8, 142.2, 132.0, 131.9, 128.6, 128.4, 128.2, 127.2, 124.4, 124.2, 123.3, 114.4, 110.5, 55.9, 54.8, 54.0, 46.8, 46.5, 41.8, 32.6, 28.1, 27.9, 26.8, 26.3, 25.9, 25.7, 25.6, 24.7, 17.9, 17.2. ESI-MS calcd for $C_{22}H_{33}O_2S_2$ ($M+H^+$), 393.19; found 393.19.

2-(3,4-Dimethoxy-2methylbenzyl)-2-(2,6-dimethylhepta-1,5-dienyl)-1,3-dithiane (29b). A colorless oil: 1.18 g in 54% yield (5-25% EtOAc in hexanes). ^1H NMR ($CDCl_3$, 300 MHz) for the cis/trans diastereomeric mixture: δ 7.05 (d, *J*=8.5 Hz, 1H), 6.67 (d, *J*= 8.5 Hz, 1H), 5.42 (s, 1H), 5.42 (s, 1H), 5.05 (t, *J* =5.4 Hz, 1H), 3.80 (s, 3H), 3.72 (s, 3H), 3.27-3.21 (2 sets of singlet, 2H), 2.97-2.87 (m, 2H), 2.74-2.66 (m, 2H), 2.25 (s, 3H), 2.10-1.96 (m, 6H), 1.66 (s, 3H), 1.62 (s, 3H), 1.58 (s, 3H). ^{13}C NMR ($CDCl_3$, 75 MHz) observed: δ 151.7, 147.2, 142.6, 141.9, 132.4, 131.8, 131.5, 128.5, 127.9, 127.7, 127.6, 127.5, 124.6, 124.4, 108.7, 60.2, 56.0, 55.7, 55.2, 43.7, 43.4, 42.1, 32.0, 28.2, 27.9, 26.6, 26.2, 26.0, 25.9, 25.8, 25.6, 24.9, 17.9, 16.5, 13.4. ESI-MS calcd for $C_{22}H_{33}O_2S_2$ ($M+H^+$), 407.21; found 407.21.

1-(3,4-Dimethoxyphenyl)-4,8-dimethylnona-3,7-dienyl-2-one (30a). A colorless oil: 125 mg in 62% yield (5-20% EtOAc in hexanes). ^1H NMR ($CDCl_3$, 300 MHz) for the cis/trans diastereomeric mixture: δ 6.80-6.71 (m, 3H), 6.07 (s, 1H), 5.10-5.00 (2 sets of multiplet, 1H), 3.84 (s, 6H), 3.62-3.60 (2 sets of multiplet, 2H), 2.57 (t, *J*=7.8 Hz, 1H), 2.12-2.09 (5H), 1.83 (s, 1H), 1.64 (s, 3H), 1.56 (s, 3H). ^{13}C NMR ($CDCl_3$, 75MHz): δ 198.6, 197.9, 160.8, 160.2, 149.1, 148.1, 132.7, 132.3, 127.7, 123.9, 123.1, 122.5, 121.8, 112.7, 111.5, 56.0, 51.3, 41.5, 34.2, 31.8, 26.9, 26.2, 26.0, 25.9, 22.8, 19.7, 17.9, 14.3 ESI-MS calcd for $C_{19}H_{27}O_3$ ($M+H^+$), 303.20; found, 303.08.

1-(3,4-Dimethoxy-2-methylphenyl)-4,8-dimethylnona-3,7-dienyl-2-one (30b).

A colorless oil: 156 mg in 50% yield (25-35% EtOAc in hexanes). ^{1}H NMR ($CDCl_3$, 300 MHz) for the cis/trans diastereomeric mixture: δ 6.84 (d, J=8.3 Hz, 1H), 6.72 (d, *J*= 8.3 Hz, 1H), 6.80-6.71 (m, 3H), 6.07 (s, 1H), 5.10-5.00 (2 sets of multiplet, 1H), 3.82 (s, 3H), 3.76 (s, 3H), 3.64 (s, 2H), 2.60 (t, *J*= 7.4 Hz, 1H), 2.14-2.11 (m, 8H), 1.84 (s, 1H), 1.66 (s, 3H), 1.57 (s, 3H). ^{13}C NMR ($CDCl_3$, 75 MHz) observed; δ 198.6, 197.8, 160.4, 159.7, 151.8, 147.6,132.6, 132.2, 131.4, 127.4, 126.0, 123.9, 123.1, 123.0, 122.5, 109.6, 60.4, 55.8, 49.3, 41.4, 34.1, 26.9, 26.2, 26.0, 25.9, 25.8, 19.7, 17.9, 17.8, 12.5 ESI-MS calcd for $C_{20}H_{29}O_3$ ($M+H^+$), 317.21; found, 317.21.

4b,5,6,7,8,8a-cis-Hexahydro-2,3-dimethoxy-4b,8,8-trimethylphenanthren-9(10H)-one (31a). A colorless oil: 120 mg in 44% yield (25-35% EtOAc in hexanes). ^{1}H NMR ($CDCl_3$, 300 MHz): δ 6.84 (s, 1H), 6.58 (s, 1H), 3.90 (s, 3H), 3.86 (s, 3H), 3.64 (d, *J*= 23.0 Hz, 1H), 3.54 (d, *J*= 23.0 Hz, 1H), 2.47-2.42 (m, 1H), 2.09 (s, 1H), 1.58-1.53 (m, 2H), 1.34-1.31 (m, 3H), 1.05 (s, 3H), 0.94 (s, 3H), 0.36 (s, 3H). ^{13}C NMR ($CDCl_3$, 75 MHz): δ 212.7, 148.1, 147.7, 133.7, 126.3, 111.6, 107.8, 66.7, 56.4, 56.1, 43.9, 42.3, 38.6, 36.6, 34.4, 33.6, 32.3, 22.6, 19.1. ESI-MS calcd for $C_{19}H_{27}O_3$ ($M+H^+$), 303.20; found, 303.21.

4b,5,6,7,8,8a-cis-Hexahydro-2,3-dimethoxy-1,4b,8,8-tetramethylphenanthren-9(10H)-one (31b). A colorless oil: 131mg in 62% yield (5-10% EtOAc in hexanes). ^{1}H NMR ($CDCl_3$, 300 MHz): δ 6.76 (s, 1H), 3.87 (s, 3H), 3.77 (s, 3H), 3.38 (s, 2H), 2.47-2.43 (1H), 2.10 (s, 3H), 2.08 (s, 1H), 1.58-1.52 (m, 2H), 1.34-1.28 (m, 3H), 1.03 (s, 3H), 0.93 (s, 3H), 0.36 (s, 3H). ^{13}C NMR ($CDCl_3$, 75 MHz): δ 212.6, 151.5, 145.8, 137.1, 130.0,

125.5, 106.0, 66.8, 60.7, 56.1, 42.2, 42.0, 39.1, 36.7, 34.2, 33.9, 32.2, 22.6, 19.1, 12.2. ESI-MS calcd for $C_{20}H_{29}O_3$ ($M+H^+$), 317.21; found, 317.21.

4b,5,6,7,8,8a-cis-Hexahydro-2,3-dihydroxy-4b,8,8-trimethylphenanthren-9(10H)-one (22). A colorless oil: 16 mg in 72% yield (5-20% EtOAc in hexanes). ^{1}H NMR ($CDCl_3$ and CD_3OD, 300 MHz): ^{1}H NMR ($CDCl_3$, 300 MHz): δ 6.86 (s, 1H), 6.58 (s, 1H), 5.35 (br, s), 5.33 (br, s), 3.59 (d, *J*= 23.0 Hz, 1H), 3.39 (d, *J*= 23.0 Hz, 1H), 2.39-2.35 (d, *J*= 13.9 Hz, 1H), 2.06 (s, 1H), 1.63-1.48 (m, 2H), 1.33-1.22 (m, 3H), 1.02 (s, 3H), 0.92 (s, 3H), 0.36 (s, 3H). ^{13}C NMR ($CDCl_3$/CD_3OD, 75 MHz): δ 214.1, 143.3, 142.4, 133.8, 125.7, 115.2, 111.3, 66.7, 43.6, 42.3, 38.4, 36.5, 34.4, 33.6, 32.3, 22.6, 18.9. ESI-MS calcd for $C_{17}H_{23}O_3$ ($M+H^+$), 275.16; found, 275.07.

4b,5,6,7,8,8a-cis-Hexahydro-2,3-dihydroxy-1,4b,8,8-tetramethylphenanthren-9(10H)-one (24). A colorless oil: 18 mg in 82% yield (25-35% EtOAc in hexanes). ^{1}H NMR ($CDCl_3$, 300 MHz): δ 6.74 (s, 1H), 5.28 (s, 1H), 5.19 (s, 1H), 3.38 (s, 2H), 2.38-2.34 (d, *J*= 15.0Hz, 1H), 2.09 (s, 3H), 2.08 (s, 1H), 1.60-1.48 (m, 2H), 1.33-1.22 (m, 3H), 0.99 (s, 3H), 0.92 (s, 3H), 0.37 (s, 3H). ^{13}C NMR ($CDCl_3$, 75 MHz): δ 213.1, 142.1, 140.5, 133.7, 125.4, 122.7, 108.6, 66.7, 42.2, 42.0, 38.6, 36.6, 34.1, 32.2, 22.6, 22.5, 19.0, 11.8. ESI-MS calcd for $C_{18}H_{25}O_3$ ($M+H^+$), 289.18; found, 289.09.

Formation of Diterpene QM under Organic Conditions. The oxidation of catechols was achieved using Ag_2O as an oxidant. After vigorous stirring at ambient temperature for 20 min, the solids were removed by filtration with a 0.2μm filter (Acrodisc, 13 CR, PTFE). The resulting yellow solution was confirmed as analytically pure QM or quinonone by ^{1}H and ^{13}C NMR analysis.

Diterpenone QM **32** (5 mg in 0.8 mL $CDCl_3$). ^1H NMR ($CDCl_3$, 300 MHz): δ 6.90 (s, 1H), 6.52 (s, 1H), 6.50 (s, 1H) 6.31 (s, 1H), 2.27 (s, 1H), 1.61-1.44 (m, 2H), 1.35-1.23 (m, 4H), 1.18 (s, 3H), 0.95 (s, 3H), 0.61 (m, 3H). ^{13}C NMR ($CDCl_3$, 75 MHz): δ 201.8, 182.1, 155.6, 149.9, 143.2, 132.3, 122.1, 111.0, 66.9, 41.9, 41.5, 36.3, 35.8, 35.5, 31.0, 24.7, 18.5.

Diterpenone quinone **33** (5 mg in 0.8 mL $CDCl_3$). ^1H NMR ($CDCl_3$, 300 MHz): δ 6.54 (d, *J*= 2.0Hz, 1H), 6.52 (d, *J*= 2.2Hz, 1H), 6.20 (s, 1H) 6.12 (s, 1H), 2.11 (s, 1H), 2.04-1.97 (d, *J*= 12.1Hz, 1H), 1.75-1.72 (m, 2H), 1.58-1.54 (m, 2H), 1.26-1.14 (m, 5H), 1.03 (s, 3H), 1.01 (s, 3H). ^{13}C NMR ($CDCl_3$, 75 MHz): δ 181.4, 180.7, 163.8, 145.0, 143.4, 127.3, 123.2, 121.6, 51.0, 41.5, 40.4, 35.7, 33.5, 32.9, 22.5, 22.5, 18.6.

7-methoxy-2-oxo-2H-chromene-4-carbaldehyde (64). To a solution of **63** (1g, 5.26 mmol) in xylene (25 mL) at 50 ºC was added selenium dioxide (200 mg, 1.8 mmol). The resulting reaction solution was stirred at 50 ºC under for 24 h. The reaction solution was quenched with CH_2Cl_2 and filtered. The organics were collected and concentrated. The residue was dissolved in CH_2Cl_2 and flash chromatography (10%-25% EtOAc in hexanes) afforded product **64** as a yellow solid (0.55 g) in 55% yield. ^1H NMR ($CDCl_3$, 400MHz): δ 10.0 (s, 1H), 8.35 (d, *J*= 8.9 Hz, 1H), 7.06 (d, *J*= 8.35 Hz, 1H), 7.02 (d, 1H), 6.96 (s, 1H), 3.85 (s, 3H). ^{13}C NMR (DMSO, 75 MHz): δ199.3, 168.0, 165.8, 161.3, 148.9, 132.3, 126.7, 118.3, 113.6, 106.5, 61.4.

6a,7,10,10a-tetrahydro-3-methoxy-8-methyl-6-oxo-6H-benzo[c]chromene-10a-carbaldehyde (65). To a solution of **64** (0.5 g, 2.4 mmol) in isoprene (10 mL) was added hydroquinone (25 mg, 0.22 mmol), and the resulting reaction solution was stirred at 50 ºC

in a sealed tube for 24 h. The reaction solution was extracted and concentrated with CH_2Cl_2. Flash chromatographic separation (10-12% EtOAc in hexanes) afforded product **65** as a yellow oil (200 mg) in 31% yield. ^{1}H NMR ($CDCl_3$, 400 MHz): δ 9.50 (s, 1H), 6.90 (s, 1H), 6.68-6.64 (d, 2H), 5.37 (d, 1H), 3.77 (s, 1H), 3.23-3.22 (d, 1H), 2.51-2.43 (m, 2H), 2.33-2.14 (m, 2H), 1.70-1.63 (d, 3H). ^{13}C NMR ($CDCl_3$, 75 MHz): δ198.0, 197.6, 168.8, 168.7, 160.9, 152.4, 132.3, 130.7, 126.7, 126.5, 118.5, 117.3, 114.1, 111.0, 103.6, 55.8, 50.4, 49.5, 38.5, 37.6, 32.2, 28.0, 27.7, 23.6, 23.3.

(4bS,8aS)-1-bromo-4b,5,6,7,8,8a-hexahydro-4-methoxy-4b,8,8-trimethylphenanthren-9(10H)-one. (53). To a solution of **50** (100 mg, 0.28 mmol) in dry CH_3NO_2 (20 mL) at 50 ºC was added BF_3OEt_2 (2.40 mL, 7 equiv), and the resulting solution was stirred under N_2 for 4 h. The reaction solution was diluted with saturated $NaHCO_3$ (150 mL) and extracted with CH_2Cl_2 (150 mL x 3). The organic layers were collected, washed with brine, dried with $MgSO_4$ and concentrated. Flash chromatographic separation (5-10% EtOAc in hexanes) afforded compound **53** as colorless oil (32 mg) in 53-57% yield. ^{1}H NMR ($CDCl_3$, 400 MHz): δ 7.38 (d, *J*= 8.77 Hz, 1H), 6.67 (d, *J*= 8.77 Hz, 1H), 3.78 (s, 3H), 3.68 (s, 1H), 3.29 (s, 1H), 2.61 (s, 1H), 1.73-1.55 (m, 6H), 1.35 (s, 3H), 1.24 (s, 3H), 1.00 (s, 3H). ^{13}CNMR ($CDCl_3$, 75 MHz): δ209.2, 157.4, 138.6, 133.9, 131.0, 115.8, 112.0, 63.2, 55.6, 49.1, 45.9, 42.4, 37.0, 33.0, 22.2, 20.5, 19.4.

2-(2-bromo-5-methoxyphenyl)-1-(1,3,3-trimethyl-7-oxa-bicyclo[4.1.0]heptan-2-yl)ethanone (57). To a solution of **51** (150 mg, 0.42 mmol) in CH_2Cl_2 (15 mL) at 0 ºC was added *m*-chloroperoxybenzoic acid (70-75%, 110 mg). The resulting reaction solution was stirred at 0 ºC under N_2 for 3 h. The reaction solution was quenched with a solution

of Na_2CO_3 and extracted with CH_2Cl_2. Flash chromatography separation (10-20% EtOAc in hexanes) afforded product **57** as a colorless oil (88 mg) in 45% yield. ^{1}H NMR ($CDCl_3$, 400 MHz): δ 7.43 (d, *J*= 8.77 Hz, 1H), 6.76 (s,1H), 6.67 (d, *J*= 8.77 Hz, 1H), 6.14 (s, 1H), 3.82 (s, 2H), 3.75 (s, 3H), 2.67 (m, 1H), 2.31-2.29 (m, 1H), 2.14 (s, 3H), 1.69-1.54 (m, 4H), 1.28 (s, 3H), 1.24 (s, 3H). ^{13}C NMR ($CDCl_3$, 75 MHz): δ196.7, 159.2, 136.3, 133.5, 122.9, 117.3, 114.6, 100.4, 63.7, 58.7, 55.6, 51.6, 38.1, 27.2, 25.0, 19.8, 18.9.

(E)-1-(3-methoxyphenyl)-4-methyl-6-(3,3-dimethyloxirane-2-yl)hex-3-ene-2-one. (54). To a solution of **40** (200 mg, 0.73 mmol) in dry CH_2Cl_2 (15 mL) at 0 ºC was added *m*-chloroperoxybenzoic acid (70-75%, 60 mg). The resulting reaction solution was stirred at 0 ºC under N_2 for 3 h. The reaction solution was quenched with a solution of Na_2CO_3 and extracted with CH_2Cl_2. Flash chromatography separation (15-25% EtOAc in hexanes) afforded product **54** as a colorless oil (120 mg) in 56% yield a cis/trans mixture. ^{1}H NMR ($CDCl_3$, 400 MHz): δ 7.25-7.19 (m, 1H), 6.79-6.73 (m, 3H), 6.11 (s, 1H), 3.77 (s, 3H), 3.65 (s, 2H), 2.63 (t, 1H), 2.67 (m, 1H), 2.28-2.13 (m, 5H), 1.64 (m, 2H), 1.25 (s, 3H), 1.22 (s, 3H). ^{13}CNMR ($CDCl_3$, 75 MHz): δ198.0, 160.0, 158.9, 136.5, 129.8, 122.9, 122.0, 115.2, 112.5, 63.7, 58.7, 55.4, 51.7, 38.2, 27.2, 24.9, 19.7, 18.9.

2-(2-bromo-5-methoxyphenyl)-1-(2,6,6-trimethylcyclohex-2-enyl)ethanone (51). To a solution of **50** (150 mg, 0.42 mmol) in dry CH_3NO_2 (20 mL) at room temp. was added BF_3OEt_2 (2.40 mL, 7eq), and the resulting solution was stirred under N_2 for 4 h. The reaction solution was extracted with CH_2Cl_2 (150 mL x 3). The organic layers were collected, washed with brine, dried with $MgSO_4$ and concentrated. Flash chromatographic separation (5-10% EtOAc in hexanes) afforded compound **51** as colorless oil (32 mg) in

58% yield. ^{1}H NMR ($CDCl_3$, 400 MHz): δ 7.40 (d, *J*= 8.40 Hz, 1H), 6.70 (s,1H), 6.67 (d, *J*= 8.40 Hz, 1H), 5.58 (s, 1H), 4.02-3.90 (q, *J*= 16.0 Hz, 2H), 3.75 (s, 3H), 2.92 (s, 1H), 2.09-2.08 (m, 2H), 1.79-1.77 (m, 2H), 1.55 (s, 3H), 1.17 (s, 1H), 1.00 (s, 3H), 0.96 (s, 3H). ^{13}C NMR ($CDCl_3$, 75 MHz): δ 208.9, 159.0, 135.1, 133.5, 130.1, 124.1, 117.3, 115.9, 114.7, 62.7, 55.6, 53.0, 33.0, 30.7, 28.4, 27.9, 23.7, 22.9.

DNA Oxidative Damage of QMs and Catechol Precursors 1, 22-26 in the presence of $CuCl_2$. The 30 mer oligonucleotide of the DNA target was radiolabeled with 32P-phosphate at the 5'-position by T4 polynucleotide kinase (New England Biolabs, MA) according to the manufacturer's instructions. Hybridization of complementary strands was achieved by heating a solution of oligonucleotides (0.5 μM each, 0.28 μCi/μl) in a 90 ºC water bath and then cooling to room temperature slowly. A series of reaction solutions containing compounds **1**, **22-26** were prepared, and the DNA lesion was initiated by the addition of the catechols. The final reaction solutions (10 μl each) contained 25 μM duplex DNA (0.07 μCi/μl), 10 mM phosphate buffer (pH 7.0), 1 mM $MgCl_2$, $CuCl_2$ (40 μM) compounds **1**, **22-26** (0, 10, 20, 30, and 40 μM, respectively), and 10% acetonitrile. The resulting reaction solutions were incubated at 37 ºC for 12 h. A portion of the reaction solutions (0.1 μCi) was mixed with formaldehyde and directly separated by a 20% denatured PAGE for the investigation of direct DNA cleavage. The piperdine treatment was achieved by mixing the reaction solutions with a 10% piperdine in water (100 μl) and then heating at 90 ºC for 20 min. The resulting solutions were lypholized, and the residues were dissolved in 90% formamide loading buffer. Each reaction solution (0.15 μCi) was separated by 20% denatured PAGE and analyzed by gel image analysis software. The

percentage of DNA damage was calculated based on the amount of the originally radiolabeled DNA band versus the total amount of radioactive DNA using the quantitative analysis software provided by the imager manufacturer.

DNA Oxidative Damage of Diterpenone Catechols 1, 22-26 in the presence of $CuCl_2$ and NADH. A series of reaction solutions containing compounds **1, 22-26** were prepared similarly as described above. The duplex DNA solution was mixed with a solution of $CuCl_2$ and NADH first, and then followed by the addition of catechol solutions. The final reaction solutions (20 μl each) contained 0.25μM duplex DNA (0.07 μCi/μl), 10mM phosphate buffer (pH 7.0), 1 mM $MgCl_2$, 100 μM NADH, $CuCl_2$ (5 μM), compounds **1, 22-26** (0,0.5,1,2, and 5 μM, respectively), and 5% acetonitrile. The resulting reaction solutions were incubated at 37 ºC for 6 h. The piperdine treatment and subsequent PAGE separation were carried out similarly as described above. All the experiments were repeated at least three times independently.

DNA Oxidative Damage by free radicals using Fe^{3+}-EDTA and H_2O_2 The Fenton reactions were carried out according to the published protocol in DNA assays comprehensive volume I and similar to described above. The investigation of the effect by radical scavengers and copper chelators on the DNA damage with terpenone **1** and Cu^{2+} was carried out similarly as described above. The final concentrations for compound **1** were 10-40 μM and $CuCl_2$ 40 μM. The concentrations of radical scavengers and chelators used were 5% for ethanol, 0.1M for mannitol, 0.1M for sodium formate, 5% for DMSO, 1.5 unit/10 μl for catalase, 50 μM for bathocuproine, and 0.1M for methional, respectively.

The piperdine treatment was carried out after incubating the reaction mixtures at 37 ºC for 10 h. All the experiments were repeated at least three times independently.

Spectroscopic Analysis

ROESY NMR was used to confirm the para position of the bromide atom in compound **48** with regard to the methoxy group (Figure 5.3). This experiment is useful because it is used to determine which signals arise from protons that are close to each other in space even if they are not bonded. The ROESY spectrum showed that the proton H_a at 7.45 ppm and proton H_c at 6.85 ppm correlated, which is the chemical shift region for the aromatic hydrogens. Proton H_c also correlated with the methoxy protons H_d located at 3.85 ppm and these hydrogens are correlated with proton H_b at 6.97 ppm which is subsequently correlated to the benzylic protons H_d at 4.32 ppm. The para position with respect to the methoxy group is therefore deduced using the data from the ROESY NMR spectra and ^1H NMR splitting patterns.

List of References

References

1. Sporn, M. B. "Approaches to prevention of epithelial cancer during the preoneoplastic period" *Cancer Res*. **1976**, 36, 2699

2. Sporn, M. B; Suh, N. "Chemoprevention: An Essential Approach to Controlling Cancer" *Nat. Rev. Cancer* **2002**, 7, 537-43

3. Sporn, M. B; Liby, T. K. "Cancer Chemoprevention: scientific promise clinical uncertainty" *Nat.Clin. Pract. Onc.* **2005**, 2, 518-525

4. Lippman, S. M; Hong, W. K. "Cancer prevention by delay" *Clin. Cancer Res*. **2002**, 8, 305-313

5. Stoner, D. G.; Morse, A. M.; Kelloff, J. G. "Perspectives in Cancer Chemoprevention" *Envi. Health Pers.* **1997**, 105, 945-954.

6. Stoner, D. G.; Morse, A. M.; "Cancer chemoprevention: principles and prospects," *Carcinogenesis* **1993**, 14, 1737-1746.

7. Bertram, J. S; Kolonel, L. N; Meyskens, F. L. "Rationale and strategies for chemoprevention of cancer in humans" *Cancer Res*. **1987**, 47, 3012-3031.

8. Greenwald, P."Cancer Chemoprevention: Science, medicine and the future" *British Med. J*. **2002**, 23, 714-718.

9. Balunas, J. M.; Kinghorn, D. A. "Drug discovery from medicinal plants," *Life Sci* **2005**, 78, 431-441.

10. Ravelo, G. A; Braun, E. A; Orellana, C. H; Sacau, P. E; Sivero M. D; "Recent Studies on Natural Products as Anticancer Agents" *Curr. Topics in Med. Chem*. **2004**, 4, 241-265.

11. Dmitrovsky, E; Dragnev, H. K; Freemantle, J. S. "Retinoic Acid in Cancer Chemoprevention" *J. Natl. Cancer Inst.* **2006**, 98, 426-427.

12. Corti, A; Bettuzzi, S; Brausi, M; Arca, D. D; Astancolle, S; Davalli, P; Caporali, A. "The chemopreventive action of catechins in the TRAMP mouse model of prostate carcinogenesis is accompanied by clusterin over-expression" *Carcinogenesis* **2004**, 25, 2217-2234

13. Yang, S.C.; Lee, M.; Chen, L.; Yang, G. "Polyphenols as Inhibitors of Carcinogenesis" *Envi. Health Pers.* **1997**, 105, 4.

14. Massey, E. T; Bedard, L. L. "AflatoxinB1 induced DNA damage and its repair" *Cancer Lett.* **2006**, 1, 1-10.

15. Kelly, J. D; Eaton, D. L; Guengerich, F. P; Coulombe, R.A. Jr. "Aflatoxin B1 activation in human lung" *Toxicol. Appl. Pharmacol*. **1997**, 144, 88-95.

16. Cerutti, P; Hussain, P. S; Aguilar, F. "Aflatoxin B1 induces the transversion of G→T in codon 249 of the p53 tumor suppressor gene in human hepatocytes" *Proc. Natl. Acad Sci USA* **1993**, 90, 8586-8590.

17. Ozturk, M. "p53 mutation in hepatocellular carcinoma after aflatoxin exposure" *Lancet* **1991**, 338, 1356-1369

18. Groopman, J. D; Kensler, T.W. "Role of metabolism and viruses in aflatoxin-induced liver cancer" *Toxicol. Appl. Pharmacol*. **2005**, 206, 131-137.

19. Farmer, B. P; Sharma, A. R."Biological Relevance of Adduct Detection to the Chemoprevention of Cancer" *Clin.Cancer Res.* **2004**, 10, 4901-4912.

20. Verma, A; Judah, J. D; Eaton, L. D; Neal, E. G. "Metabolism and Toxicity of Aflatoxins M1 and B1 in human derived in vitro systems" *Toxic and Appl. Pharm*. **1998,** 151, 152-158

21. Guengerich, P. F; Johnson, W. W; Shimada, T; Ueng, F. Y; Yamazaki, H; Langouet, S. "Activation and detoxification of aflatoxin B1" *Mut. Res*. **1998**, 402, 121-128.

22. Harris, M. T; Guengerich, P. F; Coles, B; Raney, D. K. "The endo-8,9-Epoxide of aflatoxin B1: A new metabolite" *Chem. Res. Toxicol* **1995**, 5, 333-335.

23. Correia, A. M. Wang, H.; Dick, R.; Yin, H.; Licad-Coles, E.; Kroetz, D.; Szklarz, G.; Harlow, G.; Halpert, R. J. "Structure-Function Relationships of Human Liver Cytochromes P450 3A: Alflatoxin B1 Metabolism as a Probe," *Biochem* **1998**, 37, 12536-12545.

24. Essigman M. J; Bailey, A. E; Currier, S. S; Smela, E. M; "The chemistry and biology of aflatoxin B1: from mutational spectrometry to carcinogenesis" *Carcinogenesis* **2001**, 22, 535-545.

25. Harris M. T; Guengerich, P. F; Johnson, W. W; "Kinetics and mechanism of hydrolysis of aflatoxin B1 exo-8,9-oxide and rearrangement of the dihydriol" *J.Am Chem. Soc.* **1996**, 118, 8213-8220.

26. Harris, M. T; Guengrich, P. F; Their, R; Raney, D. K; Coles, B. F; Iyer, S. R: " DNA adduction by the potent carcinogen aflatoxin B1: Mechanistic studies" *J.Am, Chem. Soc.* **1994**, 116, 1603-1609

27. Wogan, N. G; Buchi, G. R; Busby, F. W; Nadzan, M. A; Croy, G. R; Essigman, M. J. "Structural identification of the major DNA adduct formed by aflatoxinB1 in vitro" *Proc. Nat. Acad. Sci*. USA **1977**, 5, 1870-1874

28. Misra,R.P; Muench,K.F; Humayun,M.Z. "Covalent and noncovalent interactions of aflatoxin with defined deoxyribonucleic acid sequences" *Biochemistry* **1983**, 22, 3351–3359

29. Essigman, M. J; Wogan, N. G; Wang, D; Kobertz, R. W; "An intercalator inhibitor altering the target selectivity of DNA damaging agents: Synthesis of site-specific aflatoxin B1 adducts in a p53 mutational hotspot" " *Proc. Natl Acad. Sci. USA* **1997**, 94, 9579-9584

30. Ojha, R.P; Roychoudhury, M; Sanyal, N. K; "Mode of action of intercalators: a theoretical study" *Indian J. Biochem. Biophys*.**1990**, 27, 228-239

31. Raney, K; Gopalkrishnan, S; Byrd, S; Stone, P. M; Harris, M. T; "Alteration of the Aflatoxin Cyclopentenone Ring to a δ-Lactone Reduces Intercalation with DNA and Decreases Formation of Guanine N7 Adducts by Aflatoxin Epoxides" *Chem. Res. Toxicol*. **1990**, 3, 254-261.

32. Raney, K. D; Coles, B; Guengerich, F. B; Harris, M. T. "Comparison of the rates of enzymatic oxidation of aflatoxinB1, G1, and sterigomatocystin and activities of the epoxides in forming guanyl N^7 adducts" *Chem. Res Toxicol* **1989** 2 114-122

33. Guengerich, P. F; Johnson, W. W; Harris, M. T. "Kinetics and mechanism of hydrolysis of aflatoxin B1 exo-8,9-oxide and rearrangement of the dihydriol" *J.Am Chem. Soc.* **1996**, 118, 8213-8220.

34. Guengerich, P. F; Johnson, W. W; Shimada, T; Ueng, F. Y; Yamazaki, H; Langouet, S. "Activation and detoxification of aflatoxin B1" *Mut. Res*. **1998**, 402, 121-128

35. Guengerich, P. F; Johnson, W. W; "Reaction of aflatoxinB1 exo-8,9-epoxide with DNA: Kinetic analysis of covalent binding and DNA induced hydrolysis" *Proc*. *Natl Acad. Sci.* USA **1997**, 94, 6121-6125

36. Lamm G; Pack G: "Acidic Domains around nucleic acids" *Procs. Natl Acad Sci USA* **1990**, 87, 9033-9036.

37. Nafisa B. I, Whalen, L, D; Jerina, M. D; "pH dependence on the mechanism of hydrolysis of benzo[a]pyrene cis-7,8-diol, 9,10-epoxide catalyzed by DNA, poly(G), poly(A)." *Journ Amer. Chem. Soc.* **1987**, 109, 2108-2111.

38. Lasky, T.; Magder, L. "Hepatocelluar Carcinoma *p53* G>T Transversions at Coden 249: The Fingerprint of Aflatoxin Exposure?," *Envir. Health Persp*. **1997**, 105, 392-397

39. Essigman M. J; Bailey, A. E; Currier, S. S; Smela, E. M; "The chemistry and biology of aflatoxin B1: from mutational spectrometry to carcinogenesis" *Carcinogenesis* **2001**, 22, 535-545

40. Cerutti, P; Hussain, P. S; Aguilar, F. "Aflatoxin B1 induces the transversion of G→T in codon 249 of the p53 tumor suppressor gene in human hepatocytes" *Proc. Natl. Acad Sci USA* **1993**, 90, 8586-8590

41. Groopman. J; Lim, S; Puissieux, A.; Oztuk, M, "Selective targeting of P53 gene mutational hotspots in human cancers by etiology defined carcinogens." *Can. Res*. **1991**, 51, 6185-6189

42. McCormick, J; Jang, J, "Kinds of mutations formed when a shuttle vector containing adducts of tetrahydrobenzo[a]pyrene replicates in human cells" *Proc. Natl. Acad. Sci. USA* **1987**, 84, 3787-3791

43. Essigman, M. J; Hamm, L. M; Alekseyev, Y.O, "Aflatoxin B1 formamidopyrimidine adducts are preferentially repaired by the nucleotide excison repair pathway in vivo, *Carcinogenesis*, **2004**, 1045-1051

44. Bueding, E; Dolan, Leroy, J.P: "The antischistosomal activity of oltipraz. *Res. Commun. Chem. Pathol. Phamacol.* **1982**, 37, 293-303.

45. Kensler, W. T; Groopman, D.J; Sutter, R. T; Curphey, J. T; Roebuck, D. B. "Development of Cancer Chemopreventive Agents: Oltipraz as a Paradigm" *Chem. Res. Toxicol*. **1999**, 12, 113-126.

46. Kensler, T; W, Egner; P. A. Trush; M. A. Bueding, " Modification of AFB1 binding to DNA in vivo in rats fed phenolic antioxidants, ethoxyquin and a dithiolthione. *Carcinogenesis*, **1985**, 6, 759-763.

47. Langouet, S; Coles, B. Morel, F; Becquemont, L; Beaune, P; Guengrich, F. P; Ketterer, B; Guillouzo, A; "Inhibition of CYP1A2 and CYP3A4 by oltipraz results in reduction of aflatoxin B1 metabolism in human hepatocytes in primar culture" *Can Res*. **1995**, 55, 5574-5579.

48. Groopman, J. D; Donahue, R. P; Zhu, J; Chen, J; Wogan, N. G. "Aflatoxin metabolites in humans: Detection of metabolites and nucleic acid adducts in urine by affinity chromatography" *Proc. Natl Acad. Sci. USA* **1985**, 19, 6492-6496

49. Groopman, J. D; Donahue, R. P; Zhu, J; Chen, J; Wogan, N. G. "Aflatoxin metabolites in humans: Detection of metabolites and nucleic acid adducts in urine by affinity chromatography" *Proc. Natl Acad. Sci. USA* **1985**, 19, 6492-6496

50. Kensler, W. T; Groopman, D.J; Sutter, R. T; Curphey, J. T; Roebuck, D. B. "Development of Cancer Chemopreventive Agents: Oltipraz as a Paradigm" *Chem. Res. Toxicol*. **1999**, 12, 113-126.

51. Langouet, S; Coles, B; Morel, F; Becquemont. L; Guengrich, F.P; Ketterer, B; Guillouzo, A; "Inhibition of CYP1A2 and CYP3A4 by oltipraz results in reduction of aflatoxin B1 metabolism in human hepatocytes in primary culture. *Cancer Res*. **55**, 5574-5579.

52. Kensler, W. T. "Chemoprevention by Inducers of Carcinogen Detoxifcation Enzymes," *Envir. Health Persp* **1997**, 105, 965-970.

53. Murray, G; W, Melvin; McFadyen, M. "Cytochrome P450 enzymes: Novel options for cancer therapeutics". *Mol. Cancer Ther.* **2004**, 3, 363-371

54. Verma, A; Judah, J. D; Eaton, L. D; Neal, E. G. "Metabolism and Toxicity of Aflatoxins M1 and B1 in human derived in vitro systems" *Toxic and Appl. Pharm*. **1998,** 151, 152-158

55. Guengerich, F. P; Harris T. M; Coles, B; Raney, K.D; Glutathione conjugation of aflatoxin B1 exo and endo by rat and human glutathione S-transferases" *Chem. Res. Toxicol* **1992**, 5, 470-478

56. Kensler, W. T; Groopman, D. J; Helzlsouer, J. K; Munoz, A; Jacobson P. L; Egner, A. P; Zarba, A; Kuang, Y. S; Qian, S. G; Wang, B. J; Zhang, C. B; Zhu, R. Y. Xia, He; Shen, X; Wang, S. J. "Protective Alterations in Phase 1 and 2 Metabolism of AflatoxinB1 by Oltipraz in Residents of Qidong, Peoples Republic of China" *J. of Natl. Cancer Inst.* **1999**, 91, 347-354

57. Kensler, W. T; Groopman, D.J; Sutter, R. T; Curphey, J. T; Roebuck, D. B. "Development of Cancer Chemopreventive Agents: Oltipraz as a Paradigm" *Chem. Res. Toxicol*. **1999**, 12, 113-126.

58. Primiano, T.; Gastel, J. A; Kensler. T. W; Sutter, T. R; "Isolation of cDNAs representing dithiolethione-reponsive genes" *Carcinogenesis*, **1996**, 17, 2297-2303.

59. Velayutham, M.; Villamena, A. F.; Navaman, M.; Fishbein, C. J.; Zweier, L. J. "Glutathione-Mediated Formation of Oxygen Free Radicals by the Major Metabolite of Oltipraz," *Chem. Res. Toxicol*. **2005**, 18, 970-97

60. Breinholt. V; Hendricks, J; Pereira, C; Arbogast, D; Bailey, G; "Dietary Chlorophyllin is a Potent Inhibitor of Aflatoxin B1 hepatocarcinogenesis in rainbow trout" *Can Res*. **1995**, 55, 57-62.

61. Breinholt, V; Schimerlik, M; Dashwood, R; Bailey, G, "Mechanisms of Chlorophyllin Anticarcinogenesis against Aflatoxin B1: Complex formation with the Carcinogen" *Chem. Res. Toxicol*. **1995**, 8, 506-514

62. Kensler, W. Thomas; Groopman, D. J; Bailey, S. G; Helzlsouer, J. K; Jacobson, P. L; Gange, J. S; Kuang, Y. S; Qian, S. G; Zhang, N. Q; Wu, Y; Zhang, C. B; Zhu, R. Y; Wang, B. J; Egner, A. P. "Chlorophyllin intervention reduces aflatoxin-DNA adducts in individuals at high risk for liver cancer" *Proc. Natl. Acad Sci USA* **2001**, 98, 14601-14606

63. Renzulli, C; Guerra, C. M; Galvano, F; Pierdomenico, L; Speroni. "Effects of Rosmarinic Acid against Aflatoxin B1 and Ochratoxin-A-induced Cell Damage in a Human Hepatoma Cell Line (HepG2)" *J. Appl. Toxicol* **2004**, 24, 289-296

64. Galvano, F. Piva, A, Ritieni, A, G; "Dietery strategies to counteract the effects of mycotoxins: a review" *J. Food Protec*. **2001**, 64: 120-131

65. Calvin, C; Mace, K; Offord, A. E; Schilter, B. "Protective effects of coffee diterpenes against aflatoxinB1 induced genotoxicity: mechanisms in rat and human cells" *Food and Chem. Toxicol* **2001**, 39, 549-555

66. Evans, C. D; Watt, P. A; Griffith, N. A; Baillie, A. T. “Drug Protein Adducts: An Industry Perspective on Minimizing the Potential for Drug Bioactivation in Drug Discovery and Development” *Chem. Res. Toxicol* **2004**, 17, 3-16

67. Ravelo, G. A; Braun, E. A; Orellana, C. H; Sacau, P. E; Sivero M. D; “Recent Studies on Natural Products as Anticancer Agents” *Curr. Topics in Med. Chem*. **2004**, 4, 241-265

68. González, A. G.; Alvarenga, N.L.; Bazzocchi, I.L.; Ravelo, A. G.; Moujir, L. “A new bioactive norquinone methide triterpene from Maytenus scutioides” *Planta Medica* **1998**, 64, 769-771.

69. Setzar, W.; Holland, M.; Bozeman, C.A.; Rozmus, G.F.; Setzer, M.C.; Moriarity, D.M.; Reeb, S.; Vogler, B.; Bates, R. B.; Haber, W.A. “Isolation and frontier molecular orbital investigation of bioactive quinone-methide triterpenoids from the bark of Salcia petenensis” *Planta Medica*, **2001**, 67, 65-69.

70. Angle R. S; Arnaiz, O. D; Boyce, P. J; Frutos, P. R; Rainier, D. J; Turnbull D. K; “Formation of Carbon-Carbon Bonds via Quinone Methide-Initiated Cyclization Reactions.” *J. Org. Chem.* **1994**, 59, 6322-6337

71. Wagner, H. U., and Gompper, R, (1974) Quinone methides. In The Chemistry of Quinonoid Compound (Patai, S., Ed) Vol 1, pp 1145-1178, John Wiley & Sons, New York. Kupchan, S. M.; Karim, A.; Marcks, C. “Taxodione and taxodone, two

72. Rokita, S. E.; Yang, J.; Pande, P.; Greenberg, W. A. "Quinone Methide Alkylation of Deoxycytidine," *J. Org. Chem.* **1997**, *62*, 3010-3012.

73. Weinert, E. E.; Dondi, R.; Colloredo-Melz, S.; Frankenfield, K. N.; Mitchell, C. H.; Freccero, M.; Rokita, S. E. "Substituents on quinone methides strongly modulate formation and stability of their nucleophilic adducts," *J. Am. Chem. Soc.* **2006**, *128*, 11940-11947.

74. Tekwani, L. B; Khan, I. S; Sneden, T. A; Thiem, A. D; “Bisnortriterpenes from Salacia madagascariensis” *J. Nat. Prod* **2005**, 68, 251-254

75. Schaller, S., Rahalison, L.; Islam, N.; Potterrat, O.; Hostettmann, K.; Stoeckli-Evans, H.; Marve, S. “ A new potent antifungal quinone methide diterpene with a cassane skeleton from Bobgunnia madagascariensis” *Helv. Chim. Acta.* **2000**, 83, 407-413.

76. Thompson A. J; Malkinson, M. A; Nield, D; Lori, D; Kupfer, R, "Lung Toxicity and Tumor Promotion by Hydroxylated derivatives of 2,6-ditert-Butyl-4-methylphenol (BHT) and 2-tert-Butyl-4-methyl-6-iso-propylphenol: Correlation with Quinone Methide Reactivity" *Chem. Res. Toxicol*. **2002**, 15, 1106-1112

77. Filar, L. J; Winstein, S:"Preparation and behavior of simple quinone methides". *Tet Lett*. **1960**, 25, 9-16

78. Milstein, D; Vigalok, A: "Metal Stabilized Quinone and Thioquinone Methides" *J. Am. Chem. Soc*. **1997**, 119, 7873-7874.

79. Oikawa, S; Hirosawa, I; Hirakawa, K; Kawanishi, S. " Site specificity and mechanism of oxidative DNA damage induced by carcinogenic catechol" *Carcinogenesis* **2001**, 22, 1239-1245

80. Zhou, Q; Zuniga, M. "Quinone Methide Formations in the Cu^{2+}-Induced Oxidation of a Diterpenone Catechol and Concurrent Damage on DNA" *Chem. Res. Toxicol* **2005,** 18, 382-388

81. Bolton, L. J; Vukomanovic, V; Hu, Qing. L; Iverson, L. S:"The influence of the p-Alkyl Substituent on the Isomerization of o-Quinones to p-Quinone Methides: Potential Bioactivation Mechanism of Catechols" *Chem. Res. Toxicol.* **1995**, 8, 537-544.

82. Setzar, W.; Holland, M.; Bozeman, C.A.; Rozmus, G.F.; Setzer, M.C.; Moriarity, D.M.; Reeb, S.; Vogler, B.; Bates, R. B.; Haber, W.A. "Isolation and frontier molecular orbital investigation of bioactive quinone-methide triterpenoids from the bark of Salcia petenensis" *Planta Medica*, **2001**, 67, 65-69.

83. Chavez, H; Estevez-Braum; A. Ravelo, A. G; Gonzalez, A. G: "New phenolic and quinone methide triterpenes from Maytemus amazonia. *J. Nat. Prod*. **1999**, 62, 434-436.

84. M. Tada, Nishiiri, S; Yang, Z; Imai, Y; Tajima, S; Okazaki, N; Kitane, Y; Chiba, K; "Synthesis of (+) and (-) ferruginol via asymmetric cyclization of a polyene" *J. Chem. Soc, Perkin Trans*. 1 **2000**, 2657-2664

85. M. Tada; Arakawa., Y; Doi, H; Kurokawa, N. S; Chiba, K; Kitano, Y; Yang, Z. "Synthesis of various oxidized abietane diterpenes and their antibacterial activities against MRSA and VRE" *Bioorg. Med. Chem*. **2001**, 9, 347-356

86. Vickery, E. H; Phaler, L. F; Eisenbraun, E. J: "Selective O-demethylation of catechol ethers. Comparison of boron tribromide and iodotrimethysilane. *J. Org. Chem*. **1979**, 44, 4444-4446.

87. Ravelo, G. A; Braun, E. A; Orellana, C. H; Sacau, P. E; Sivero M. D; "Recent Studies on Natural Products as Anticancer Agents" *Curr. Topics in Med. Chem*. **2004**, 4, 241-265.

88. Thompson, A. J; Bolton, L. J; Yoerg, G. D; Lewis, A. M: "Alkylation of 2'-Deoxynucleosides and DNA by Quinone Methides Derived from 2,6-Di-tert-butyl-4-methylphenol" *Chem. Res. Toxicol*. **1996**, 9, 1368-1374

89. Wagner, H. U., and Gompper, R, (**1974**) Quinone methides. In The Chemistry of Quinonoid Compound (Patai, S., Ed) Vol 1, pp 1145-1178, John Wiley & Sons, New York.

90. Gardner, D. P; Sarrafizadeh. H; Cavitt, B. S: "Structure of the o-Quinone Methide Trimer" *J. Org. Chem*, **1962**, 27, 1211-1216.

91. Thatcher, J. R. G; Bolton, L. J; McCracken, G. P: "Covalent modification of Proteins and Peptides by the Quinone Methide from 2-tert-butyl-4,6-dimethylphenol: Selectivity and Reactivity with respect to Competitive Hydration" *J. Org. Chem.* **1997**, 62, 1820-1825.

92. Richard, J. P: "Mechanisms for the uncatalyzed and hydrogen ion catalyzed reactions of a simple quinone methide with solvent and halide ions." *J. Am. Chem. Soc*. **113**, 4588-4595.

93. Zhou, Q; Zuniga, M. "Quinone Methide Formations in the Cu^{2+}-Induced Oxidation of a Diterpenone Catechol and Concurrent Damage on DNA" *Chem. Res. Toxicol* **2005,** 18, 382-388

94. Rietjens M. C; Aguilar, S, J; Cenas, Narimantas, C; Tyrakowska, B; Lemanska, K; Symusiak, H; Vervoort, J; Boersma, G. M: "Regioselectivity and reversibility of the Glutathione Conjuation of Quercetin Quinone Methide" *Chem. Res. Toxicol*. **2000**, 13, 185-191

95. Bolton, L. J; Acay, M. N; Vukomanovic, V: "Evidence that 4-Allyl-o-quinones Spontaneously Rearrange to Their More Electrophilic Quinone Methides: Potential Bioactivation Mechanism for the Hepatocarcinogen Safrole." *Chem. Res. Toxicol*. **1994**, 7, 443-450.

96. Marnett, J. L; Dedon, C. P; Plastras, P. J: “Effects of DNA Structure on Oxopropenylation by the Endogenous Mutagens Malondialdehyde and Base Propenal” Biochem. 2002, 41, 5033-5042

97. Oikawa, S; Hirosawa, I; Hirakawa, K; Kawanishi, S. “ Site specificity and mechanism of oxidative DNA damage induced by carcinogenic catechol” *Carcinogenesis* **2001**, 22, 1239-1245

98. Kupchan, S; Karim, M; Marcks, C. “Tumor inhibitors XLVIII. Taxodione and taxodone, two novel diterpenoid quione methide tumor inhibitors from Taxodium Distichium. J. Org. Chem. 34, 3912-3918

99. Zhou, Q; Zuniga, M. “Quinone Methide Formations in the Cu^{2+}-Induced Oxidation of a Diterpenone Catechol and Concurrent Damage on DNA” *Chem. Res. Toxicol* **2005,** 18, 382-388

100. Weinert, E. E.; Dondi, R.; Colloredo-Melz, S.; Frankenfield, K. N.; Mitchell, C. H.; Freccero, M.; Rokita, S. E. "Substituents on quinone methides strongly modulate formation and stability of their nucleophilic adducts," *J. Am. Chem. Soc.* **2006**, *128*, 11940-11947.

101. Angle R. S; Arnaiz, O. D; Boyce, P. J; Frutos, P. R; Rainier, D. J; Turnbull D. K; “Formation of Carbon-Carbon Bonds via Quinone Methide-Initiated Cyclization Reactions.” *J. Org. Chem.* **1994**, 59, 6322-6337

102. Weinert, E. E.; Frankenfield, K. N.; Rokita, S. E. "Time-dependent evolution of adducts formed between deoxynucleosides and a model quinone methide," *Chem. Res. Toxicol.* **2005**, *18*, 1364-1370.

103. Zhou, Q; Zuniga, M. “Quinone Methide Formations in the Cu^{2+}-Induced Oxidation of a Diterpenone Catechol and Concurrent Damage on DNA” *Chem. Res. Toxicol* **2005,** 18, 382-388

104. Livinghouse. T; Harring, R. S:“Polyene Cascade Cyclizations Mediated by BF3CH3NO2 An unusually Efficient Method for the Direct Stereospecific Synthesis of Polyclic Intermediates via Cationic Initiation at Non functionalized 3º Alkenes”. *Tetrahedron*, **1994**, 50, 9229-9254.

105. Corey, E. J; Seebach, D: “Generation and synthetic applications of 2-Lithio-1,3-dithianes” *J. Org. Chem*, **1975**, 40, 231

106. Zuniga, A. M; Wehunt, P. M; Dai, J; Zhou, Q: “DNA Oxidative Damage by Terpene Catechols as Analogues of Natural Terpene Quinone Methide

Precursors in the Presence of Cu(II) and/or NADH" *Chem. Res. Toxicol*, **2006**, 19, 828-836.

107. Penning, M. T. "DNA strand scission by polycyclic hydrocarbon o-quinone: Role of reactive oxygen species Cu(II)/Cu(I) redox cycling and o-semiquinone anion radicals" *Biochemistry* **1997**, 36, 8640-8648

108. Penning, M. T; Harvey, G. R; Troxel, B. A; Szewczuk, M. L; Gopishetty, S; Park, H. J. "Formation of 8-oxo-7,8-dihydro-2'-deoxyguanosine (8-Oxo-dGuo) by PAH o-Quinones: Involvement of Reactive Oxygen Species and Copper II/Copper I Redox Cycling" *Chem. Res. Toxicol*. **2005**, 18, 1026-1037

109. Kawanishi, S; Oikawa, S; "Site Specific DNA damage induced by NADH in the Presence of Copper(II): Role of Active Oxygen Species". *Biochem*, **1996**, 35, 4584-4590.

110. Lloyd, R. V; Hanna, P. M; Mason, R. P. "The origin of the hydroxyl radical oxygen in the Fenton reaction" *Free Rad. Biol. Med* **1997**, 22, 885-888

111. Cronin, D.; Morris, H; Valko, M. "Metals, Toxicity and Oxidative Stress" *Curr. Med. Chem*, **2005**, 12, 1163-1208

112. Zuniga, A. M; Wehunt, P. M; Dai, J; Zhou, Q: "DNA Oxidative Damage by Terpene Catechols as Analogues of Natural Terpene Quinone Methide Precursors in the Presence of Cu(II) and/or NADH" *Chem. Res. Toxicol*, **2006**, 19, 828-836.

113. Murphy A. J; Breen, P. A. "Reactions of oxyl radicals with DNA" *Free Rad. Bio. Med* **1995**, 18, 1033-1077

114. Penning, M. T. "DNA strand scission by polycyclic hydrocarbon o-quinone: Role of reactive oxygen species Cu(II)/Cu(I) redox cycling and o-semiquinone anion radicals" *Biochemistry* **1997**, 36, 8640-8648

115. Hirakawa, K; Oikawa, S. Hirosawa, I; Hirosu, I; Kawanishi, S. "Catechol and hydroquinone have different redox properties responsible for their differential DNA-damaging ability" *Chem. Res. Toxicol*, **2002**, 15, 76-82

116. Penning, M. T; Harvey, G. R; Troxel, B. A; Szewczuk, M. L; Gopishetty, S; Park, H. J. "Formation of 8-oxo-7,8-dihydro-2'-deoxyguanosine (8-Oxo-dGuo) by PAH o-Quinones: Involvement of Reactive Oxygen Species and Copper II/Copper I Redox Cycling" *Chem. Res. Toxicol*. **2005**, 18, 1026-1037

117. Zuniga, A. M; Wehunt, P. M; Dai, J; Zhou, Q: "DNA Oxidative Damage by Terpene Catechols as Analogues of Natural Terpene Quinone Methide Precursors in the Presence of Cu(II) and/or NADH" *Chem. Res. Toxicol*, **2006**, 19, 828-836.

118. Oikawa, S; Hirosawa, I; Hirakawa, K; Kawanishi, S. " Site specificity and mechanism of oxidative DNA damage induced by carcinogenic catechol" *Carcinogenesis* **2001**, 22, 1239-1245

119. Gehm, D. B.; McAndrews, M. J.; Chien, P.; Jameson, L. J. "Resveratrol, a polyphenolic compound found in grapes and wine is an agonist for the estrogen receptor," *Proc. Natl. Acad. Sci.* **1997**, 94, 14138-14143.

120. Bolton, L. J; Geacintov, E. N; Chang, M; Chen, D; Kolbanovskaya, M; Shastry, A; Kuzmin, V; Kolbanovisky, A."Base Selectivity and Effects of Sequence and DNA Secondary Structure on the Formation of Covalent Adducts Derived from the Equine Estrogen Metabolite 4-Hydroxyequilenin" *Chem. Res. Toxicol* **2005**, 18, 1737-1747

121. Cavalieri, E; Rogan, E; Saeed, M; Kohli, E; Zahid, M; "The greater reactivity of Estradiol-3,4-quinone vs Estradiol-2,3-quinone with DNA in the formation of Depurinating Adducts: Implications for Tumor Initiating Activity" *Chem. Res. Toxicol***. 2006**, 19, 164-172

122. Guengrich, F. P; Chun, Y. J; Kim, D; Gilman, E. M. J; Shimada, T: "Cytochrome P4501B1: A target for inhibition in anticarcinogenesis strategies". *Mutat. Res*. **2003**, 523-524, 173-182.

123. Chun, Y. J; Kim, S: "Discovery of cytochrome P450 inhibitors as new promising anti-cancer agents. *Med. Res. Rev*. **2003**, 23, 657-668.

124. Langouet, S; Coles, B; Morel, F; Becquemont. L; Guengrich, F.P; Ketterer, B; Guillouzo, A; "Inhibition of CYP1A2 and CYP3A4 by oltipraz results in reduction of aflatoxin B1 metabolism in human hepatocytes in primary culture. *Cancer Res*. **55**, 5574-5579.

125. Zhou, Q; Hang X; Lin, Z; Stewart K. J; Xing. G, Ryan J. J: "*Cis*-Terpenones as an Effective Chemopreventive Agent against Aflatoxin B1 Induced Cytotoxicity and TCDD-induced P450 1A/B activity in HepG2 Cells." *Chem. Res. Toxicol*. **2006**, *19*, 1415-1419.

126.Tritium www.physics.isu.edu/radin/tritium

127. Hayball J. P; Tan, W. H; Tuck, L. K. “Synthesis of Tritium labeled Hydroxysterol, a Phenolic Compound Found in Olive Oil” J. Agric. Food Chem. **2000**, 48, 4087-4090

128. Newmark, R; Un, S; Williams, G. P; Carson, J. P; Morimoto, H, “^{3}H Nuclear Magnetic Resonance Study of Anaerobic Glycolysis in Packed Erthrocytes” *Proc. Nat. Acad. Sci. USA,* **1990**, 87, 583-587

129. Croteau, R; Coates, M. R; Pyun, J, H; Wagschal, C. K: “Monoterpene Biosynthesis: Isotope Effects Associated with Bicylic Olefin Formation Catalyzed by Pinene Synthases from Sage” *Arch. of Biochem and Biophy*. **1994**, 308, 477-487.

130. Sajiki, H; Mori Y; Tatematsu, K; Hirota, K; Maegawa, T. “Facile and Efficient Postsynthetic Tritium Labeling Method Catalyzed by Pd/C in HTO” *J. Org. Chem.* **2005**, 70, 10581-10583

131. Sajiki, H; Esaki, H.; Ohtaki, R.; Maegawa, T.; Monguchi, Y: “Novel Pd/C-Catalyzed Redox Reactions between Aliphatic Secondary Alcohols and Ketones under Hydrogenation Conditions: Application to H-D Exchange Reaction and the Mechanistic Study,” *J. Org. Chem* **2007**, 72, 2143-2150.

132. Zhou, Q; Hang X; Lin, Z; Stewart K. J; Xing. G, Ryan J. J: "*Cis*-Terpenones as an Effective Chemopreventive Agent against Aflatoxin B1 Induced Cytotoxicity and TCDD-induced P450 1A/B activity in HepG2 Cells." *Chem. Res. Toxicol*. **2006**, *19*, 1415-1419.

133. Sarabia, F. S.; Zhu, B.; Kurosawa, T.; Tohma, M.; Liehr, G. J. “Mechanism of Cytochrome P450-Catalyzed Aromatic Hydroxylation of Estrogens,” *Chem. Res. Toxicol*. **1997**, 10, 767-771

134. Yamamoto H; Ishihara. K; Kumazawa. K: “Tin (IV) Chloride-Chiral Pyrogallol Derivatives as New Lewis Acid-Assisted Chiral Bronstead Acids for Enantioselective Polyene Cyclization” *Org*. *Lett*. **2004**, 6, 2551-2554.

135. Weinhold, F; Topol. A. I; Nemukhin, V. A: “Structure of Magnesium Cluster Grignard Reagent” *Inorg. Chem*, 1995, 34, 2980-2984

136. Pei, T.; Wang, X.; Widenhoefer, A. R. “Palladium-Catalyzed Intramolecular Oxidative Alkylation of Unactivated Olefins,” *J. Am. Chem. Soc*. **2003**, 125, 648-649.

137. Dounay, B. A.; Overman, E. L. “The Asymmetric Intramolecular Heck Reaction in Natural Product Total Synthesis,” *Chem. Rev.* **2003**, 103, 2945-2963.

138. Meyer, E. F; Meijere, A: “Fine Feathers Make Fine Birds: The Heck Reaction in Modern Garb”. *Angew. Chem. Int. Ed. Engl.* **1994**, 33, 2379.

139. Djerrasi. C; Eisenburn. J; Gilbert, V; Finnegan, A. R: “Naturally Occuring Oxygen Heterocycles “Synthesis of some Coumarins related to Mammein” *J. Org. Chem*, **1960**, 25, 2169-2173.

140. Vaccaro, L. Girotti, R.; Marrocchi, A.; Minuti, L.; Piermatti, O.; Pizzo, F: “Diels-Alder Reactions of 3-Substituted Coumarins in Water and under High-Pressure Condition. An Uncatalyzed Route to Tetrahydro-6H-benzo[*c*] chromen-6-ones,” *J.Org. Chem*. **2006**, 71, 70-74.

141. Nakajima, K; Ito, K: “Selenium Dioxide Oxidation of Alkylcoumarins and Related Methyl-Substituted Heteroaromatics” *J. Heterocyclic, Chem*. **1988,** 25, 511-515.

142. Amantini, D.; Fringuelli, F.; Piermatti, O.; Pizzo, F.; Vaccaro, L. “3-Nitrocoumarins as Dienophiles in the Diels-Alder Reaction in Water. An Approach to the Synthesis of Nitrotetrahydrobenzol [*c*] chromenones and Dihydrodibenzol [*b,d*]furans,” *J. Org. Chem*. **2003**, 68, 9263-9268

143. Marocci, A; Baitz. G. E; Tatichi, A; Minuti. L: “High Pressure Diels Alder Reaction of 2-Vinyl-3,4-Dihydronapthalene” *Tetrahedron*, **1995**, 51, 8953-8958.

APPENDIX

^{1}H and ^{13}C NMR spectra.

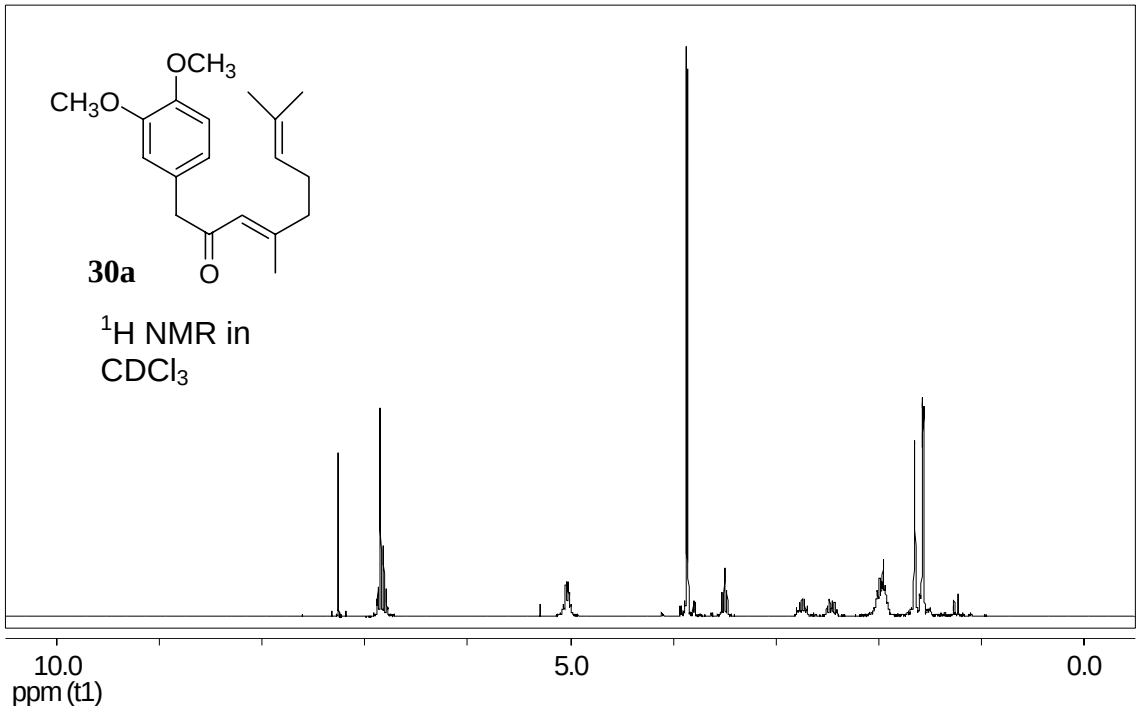
OCH3
CH3O
O
30a
1H NMR in
CDCl3
10.0
ppm (t1)
5.0
0.0

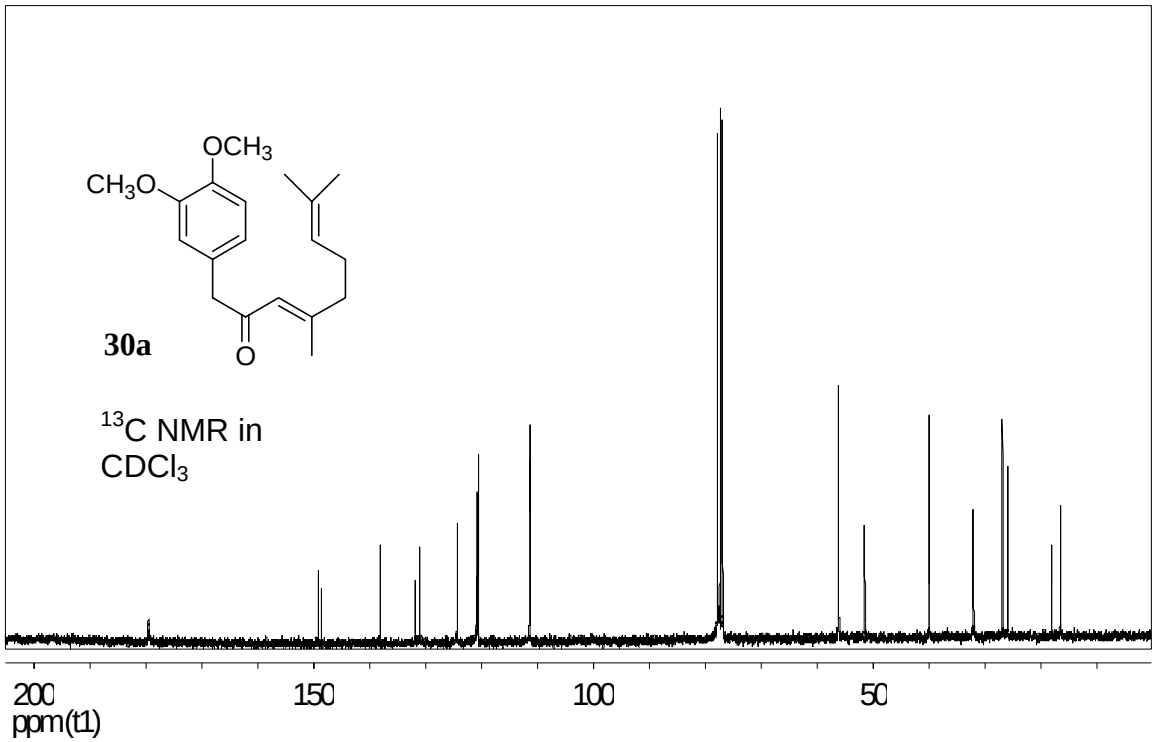
OCH3
CH3O
O
30a
13C NMR in
CDCl3
200
ppm(t1)
150
100
50

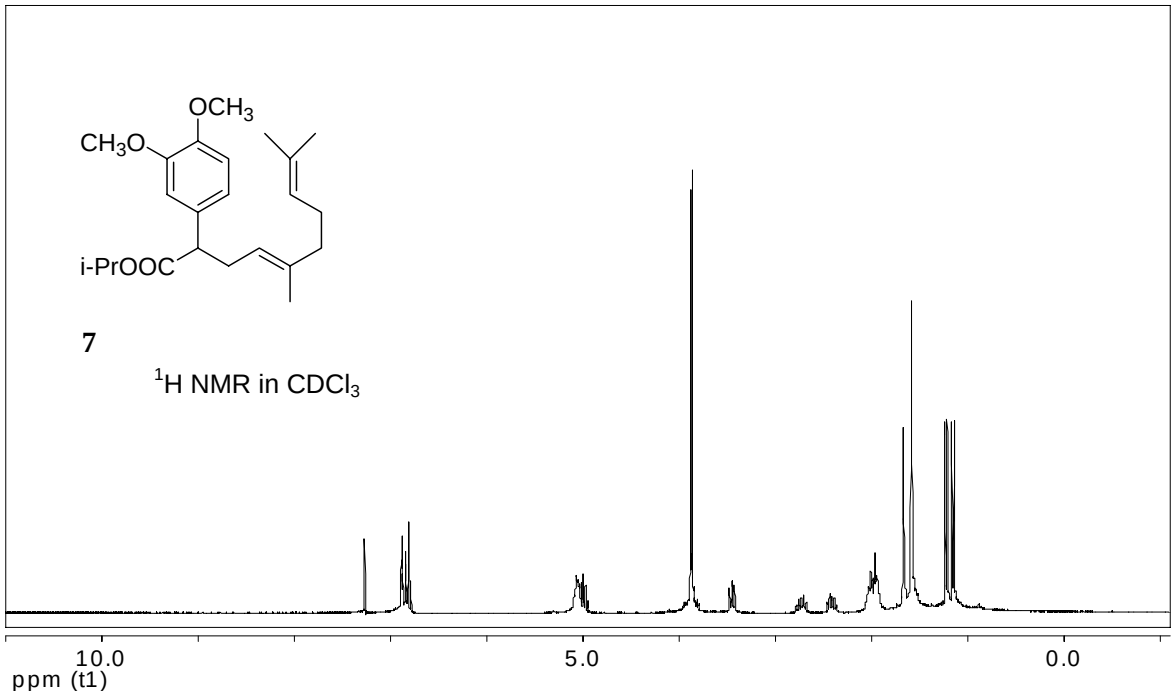
OCH3
CH3O
i-PrOOC
7
1H NMR in CDCl3
10.0
5.0
0.0
ppm (t1)

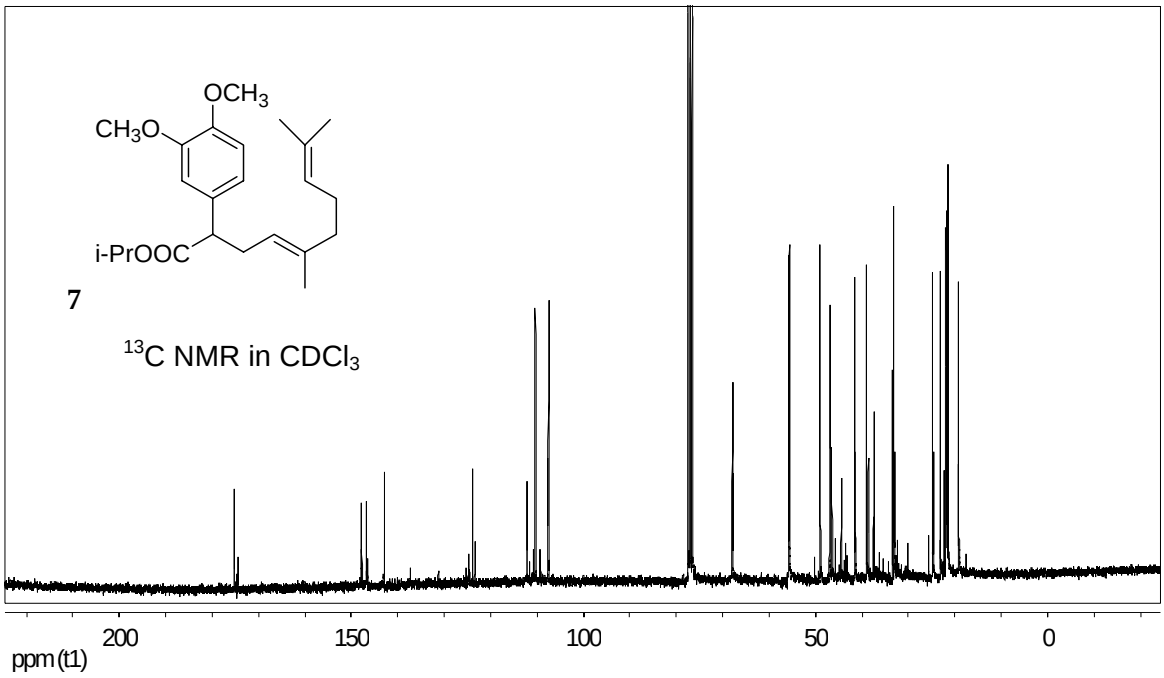
OCH3
CH3O
i-PrOOC
7
13C NMR in CDCl3
200
150
100
50
0
ppm (t1)

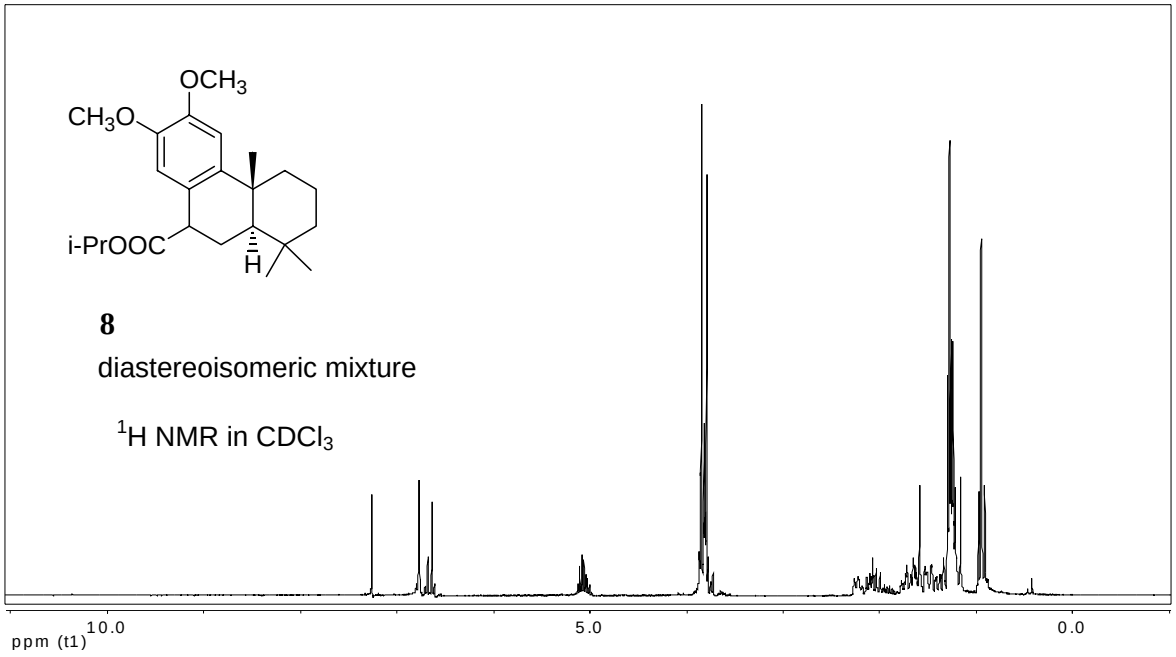
OCH3
CH3O
i-PrOOC
H
8
diastereoisomeric mixture
1H NMR in CDCl3
ppm (t1)
10.0
5.0
0.0

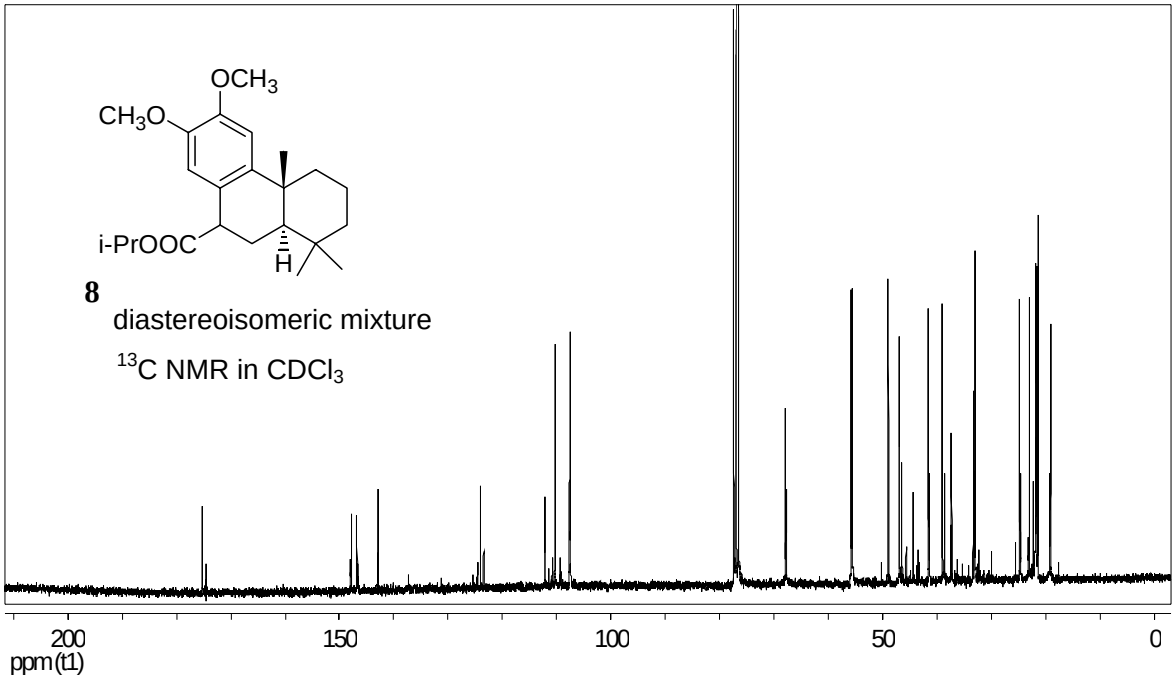
OCH3
CH3O
i-PrOOC
H
8
diastereoisomeric mixture
13C NMR in CDCl3
200
150
100
50
0
ppm (t1)

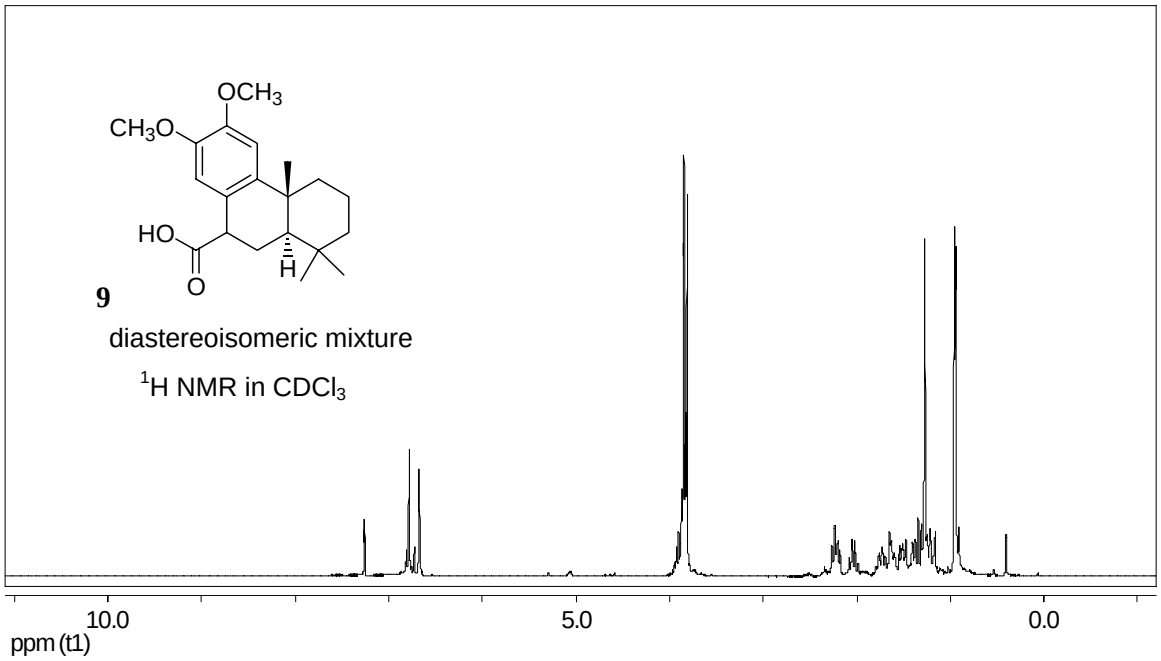
OCH3
CH3O
HO
O
H
9
diastereoisomeric mixture
1H NMR in CDCl3
10.0
5.0
0.0
ppm (t1)

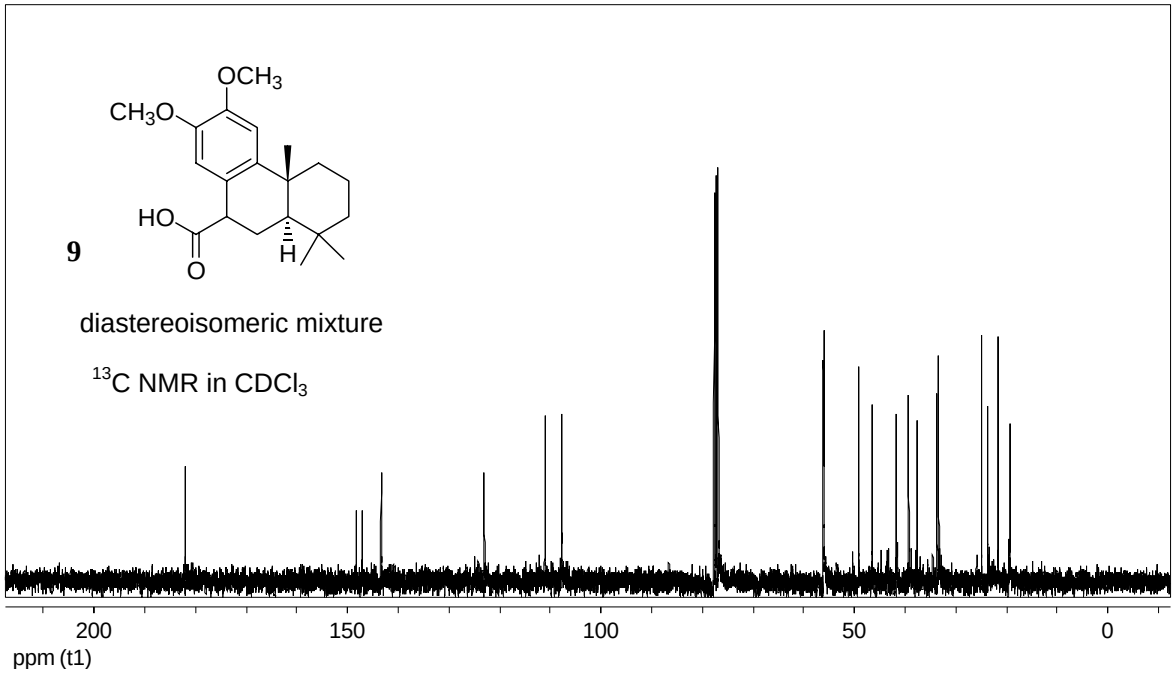
OCH3
CH3O
HO
O
H
9
diastereoisomeric mixture
13C NMR in CDCl3
200
150
100
50
0
ppm (t1)

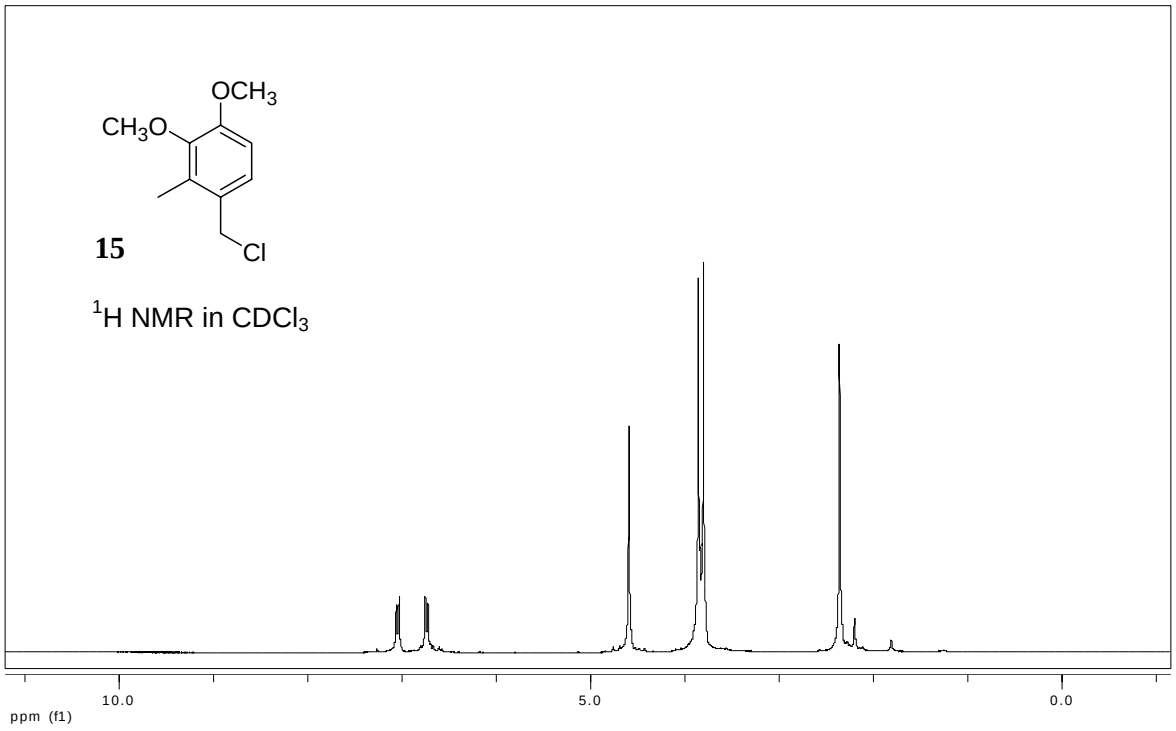
OCH3
CH3O
Cl
15
1H NMR in CDCl3
10.0
5.0
0.0
ppm (f1)

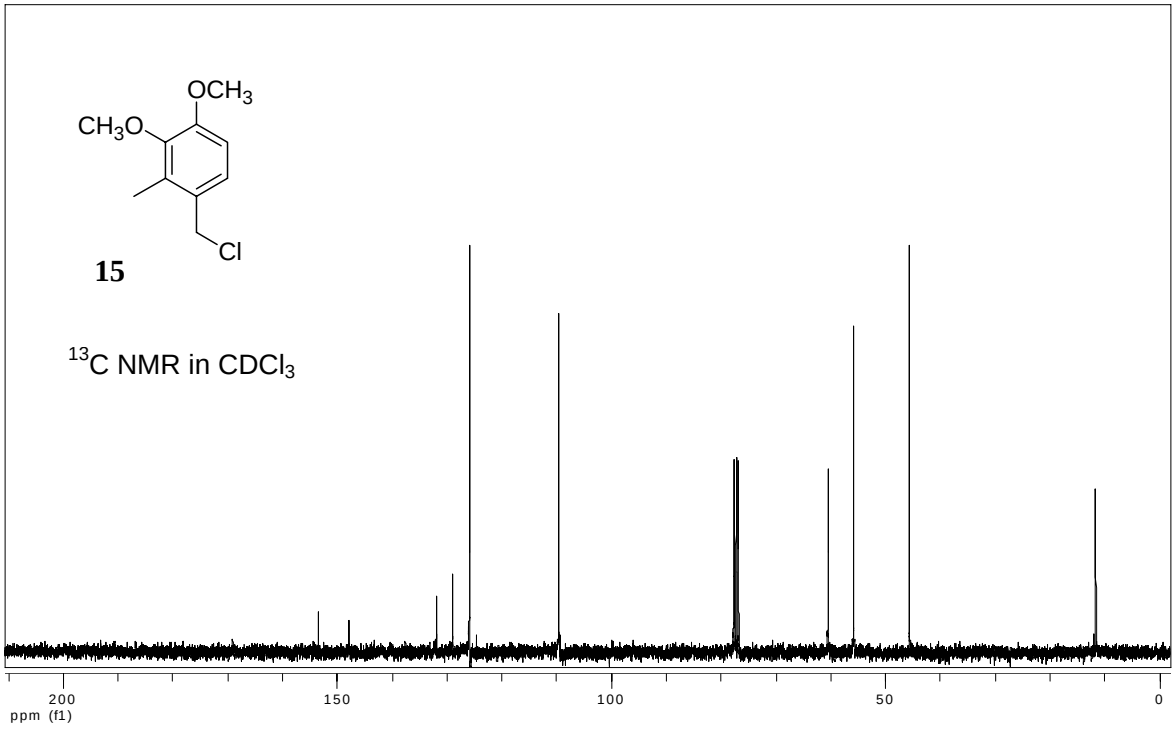
OCH3
CH3O
Cl
15
13C NMR in CDCl3
200
150
100
50
0
ppm (f1)

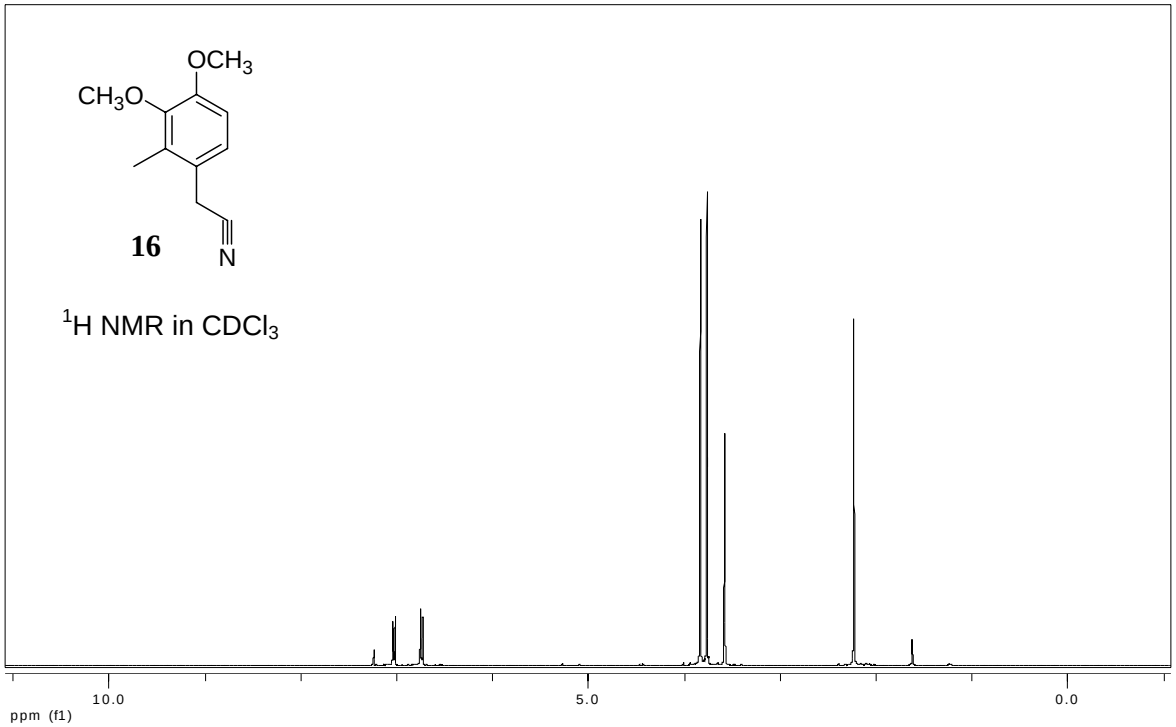
OCH3
CH3O
N
16
1H NMR in CDCl3
10.0
5.0
0.0
ppm (f1)

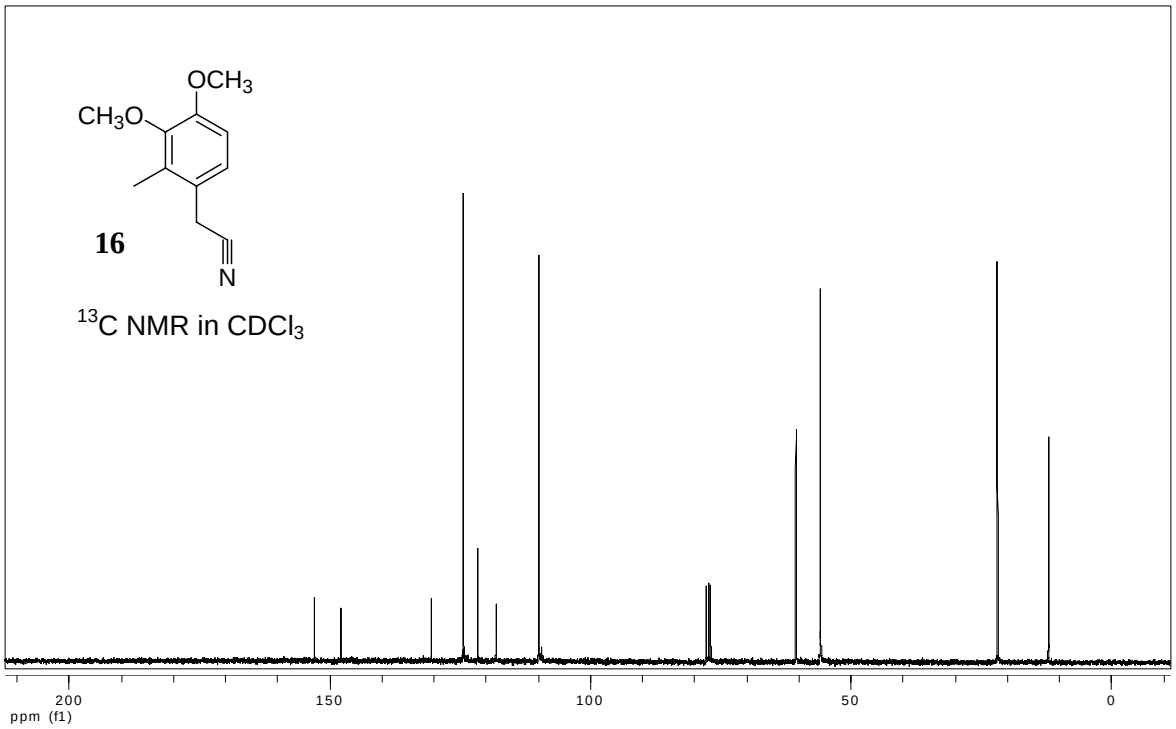
OCH3
CH3O
N
16
13C NMR in CDCl3
200
150
100
50
0
ppm (f1)

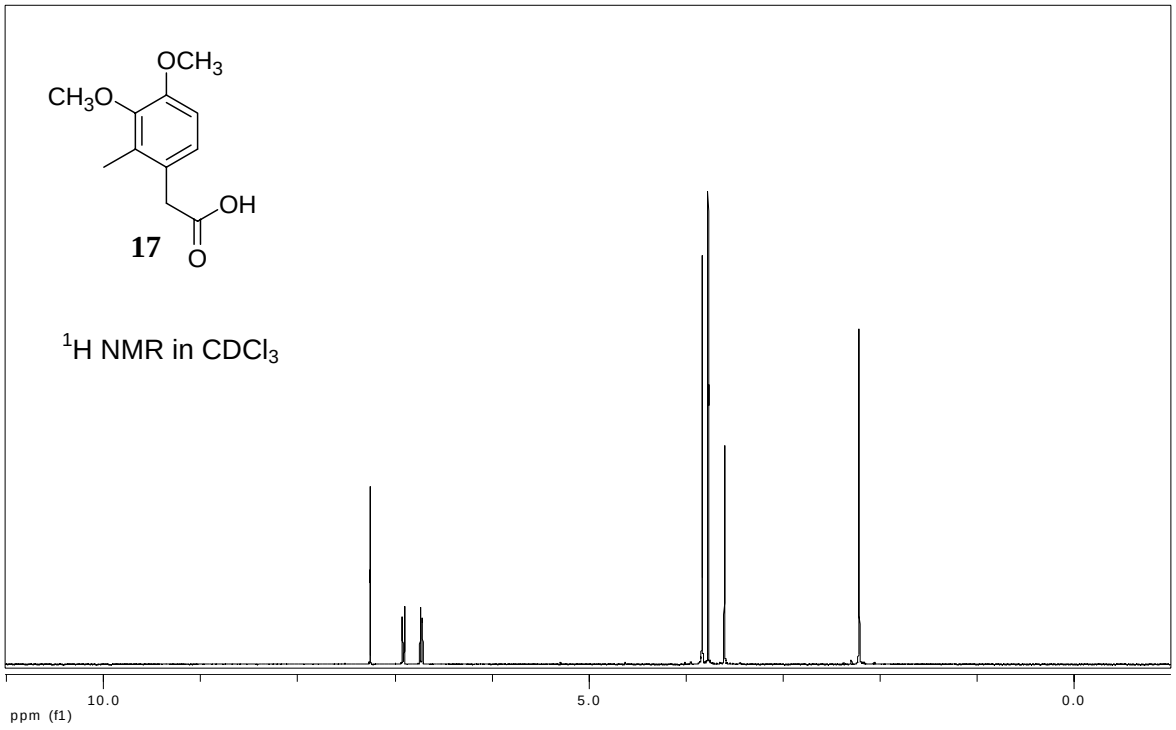
OCH3
CH3O
OH
O
17
1H NMR in CDCl3
10.0
5.0
0.0
ppm (f1)

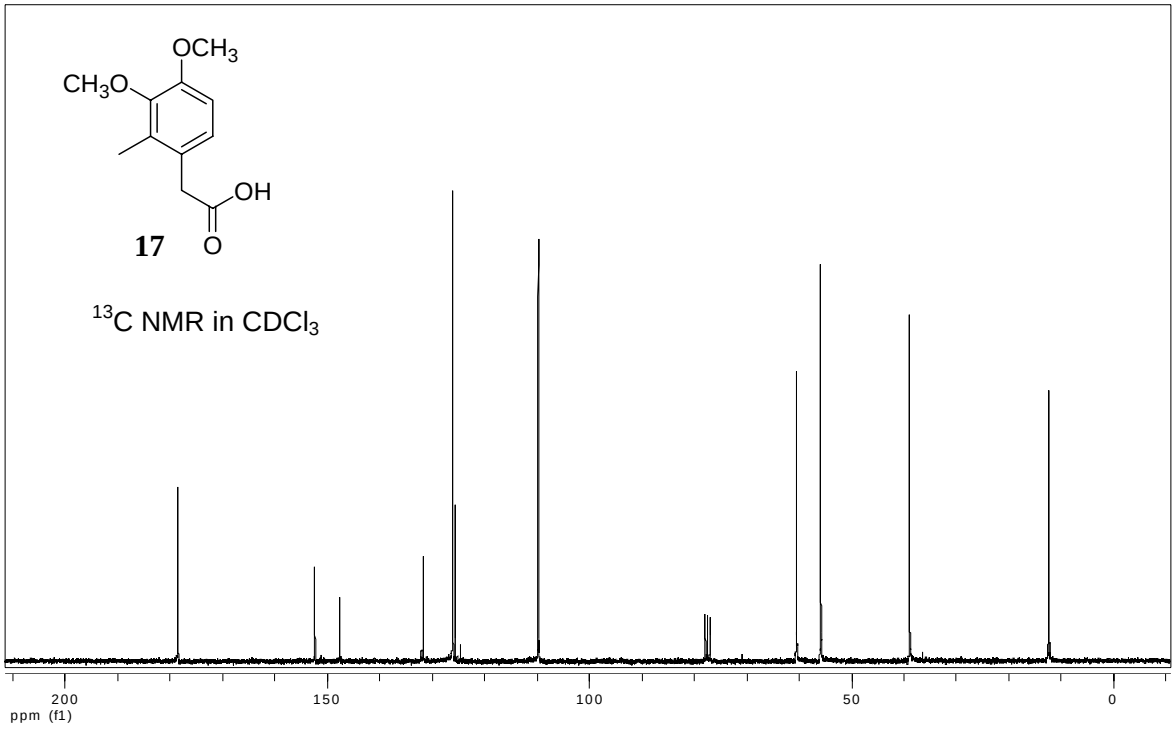
OCH3
CH3O
OH
O
17
13C NMR in CDCl3
200
150
100
50
0
ppm (f1)

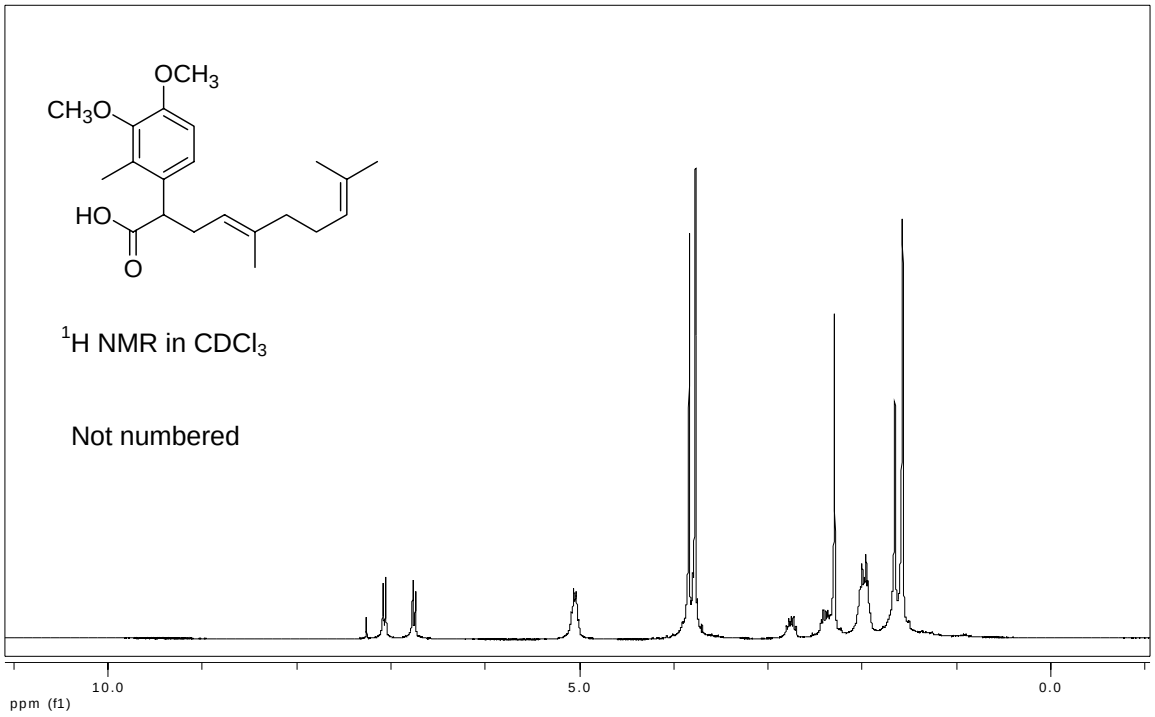
OCH3
CH3O
HO
O
1H NMR in CDCl3
Not numbered
10.0
5.0
0.0
ppm (f1)

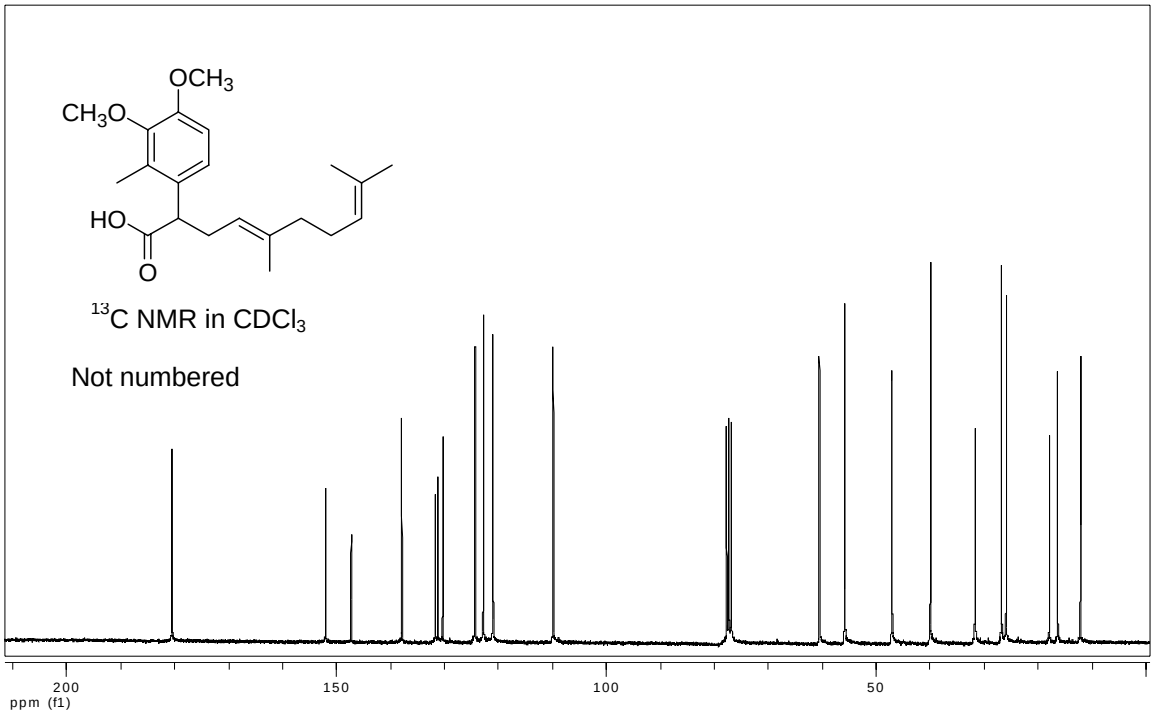
OCH3
CH3O
HO
O
13C NMR in CDCl3
Not numbered
200
150
100
50
ppm (f1)

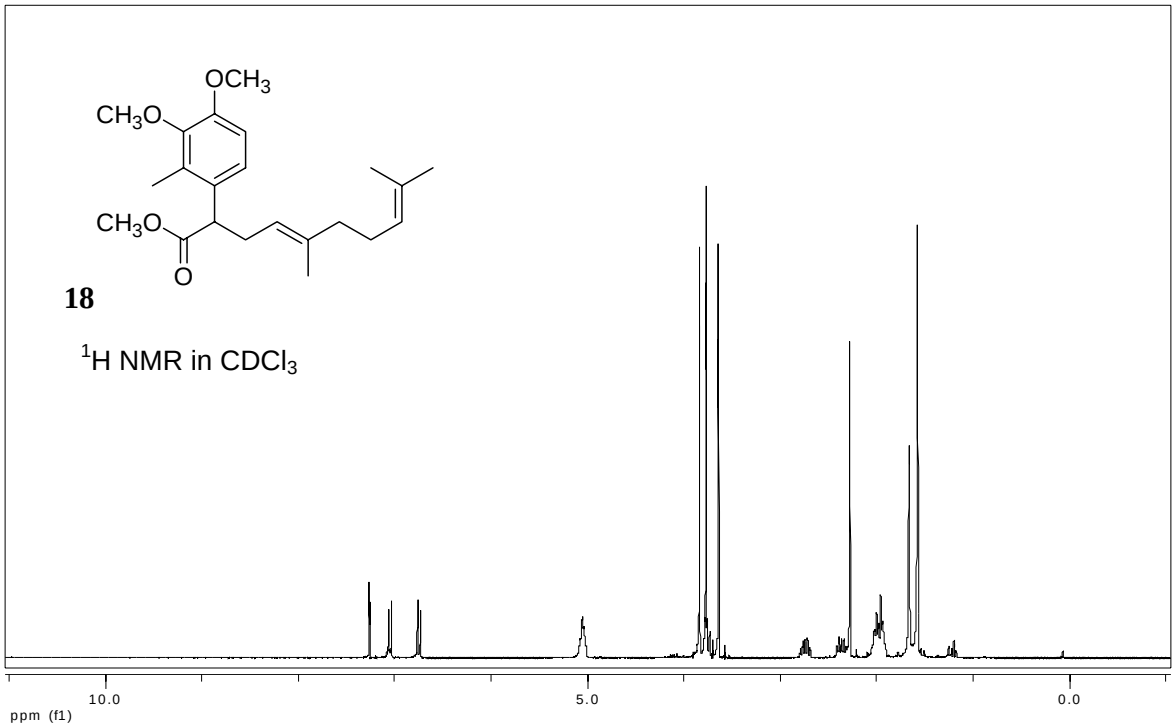

18

^{1}H NMR in $CDCl_3$

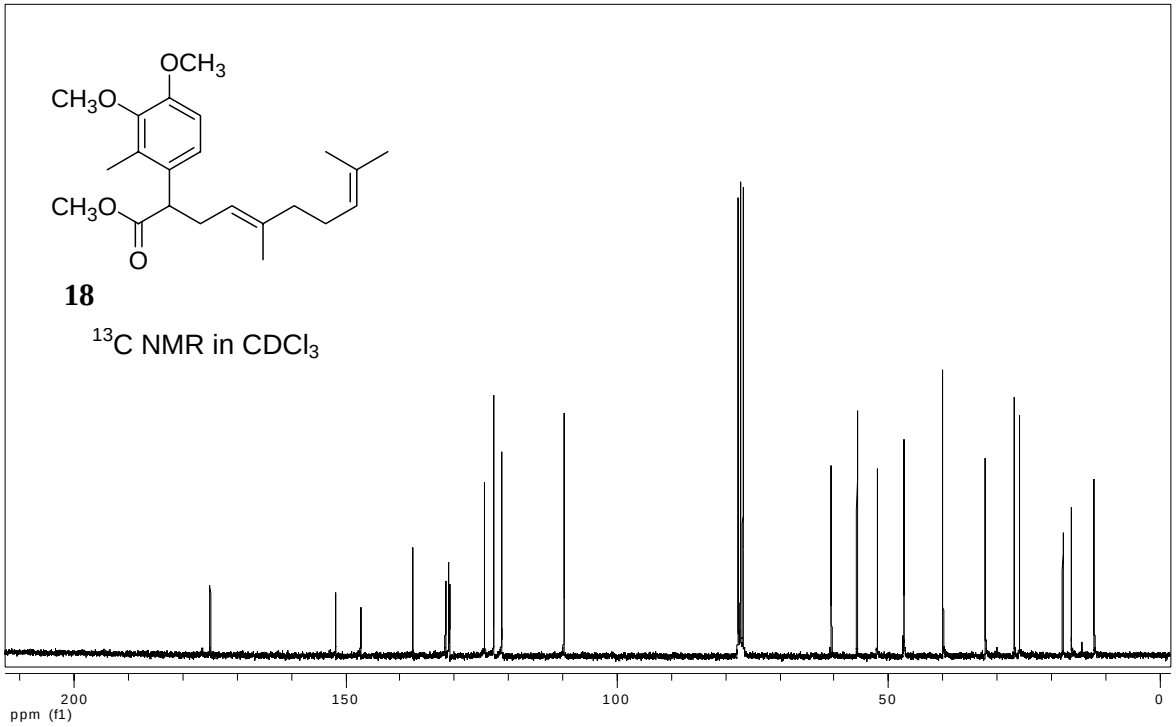

18

^{13}C NMR in $CDCl_3$

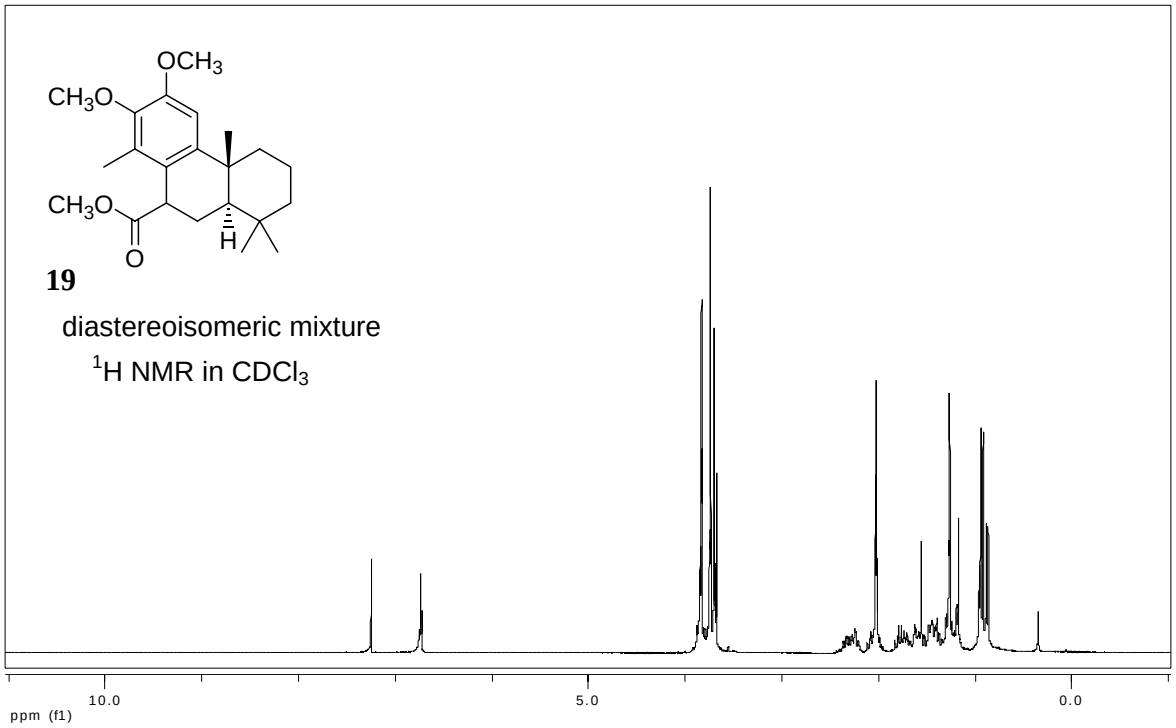
OCH3
CH3O
CH3O
O
H
19
diastereoisomeric mixture
1H NMR in CDCl3
10.0
5.0
0.0
ppm (f1)

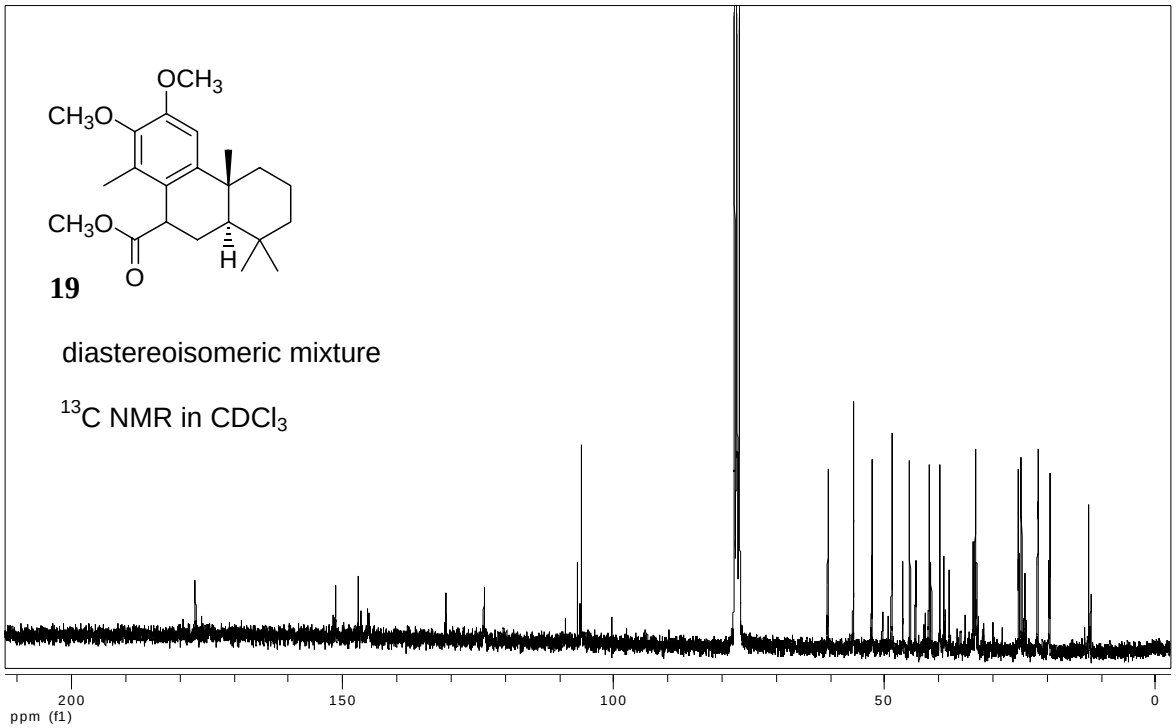
OCH3
CH3O
CH3O
O
H
19
diastereoisomeric mixture
13C NMR in CDCl3
200
150
100
50
0
ppm (f1)

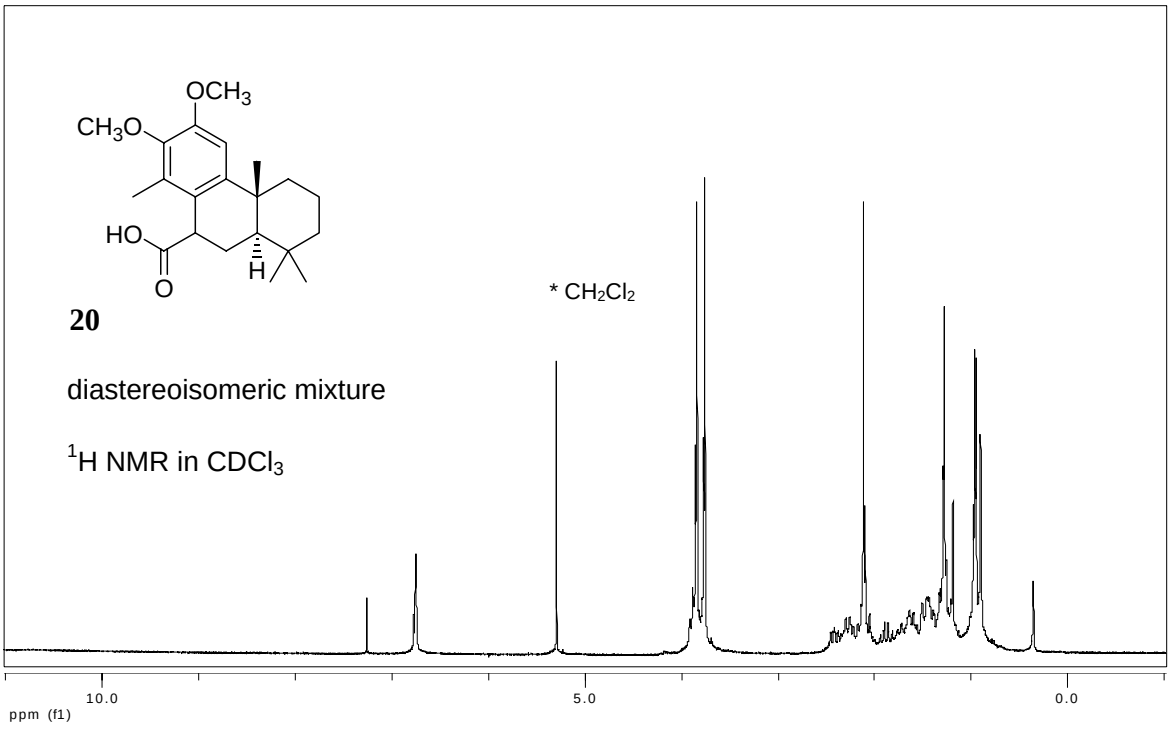

20

diastereoisomeric mixture

^{1}H NMR in $CDCl_3$

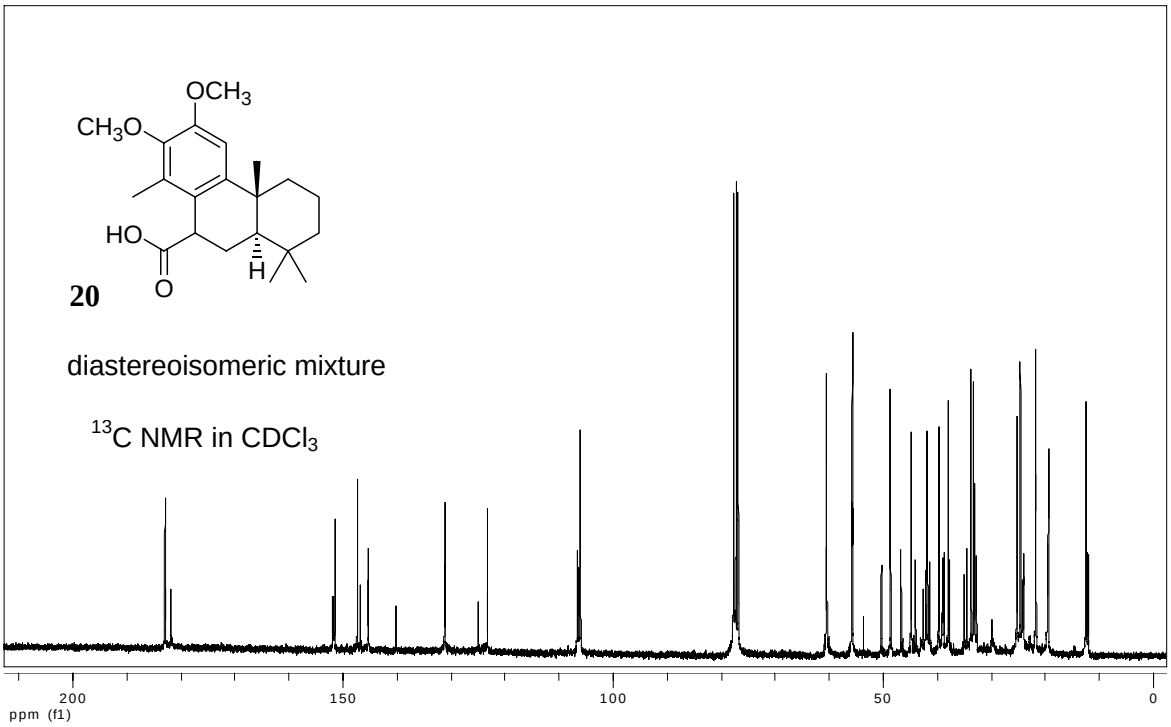

20

diastereoisomeric mixture

^{13}C NMR in $CDCl_3$

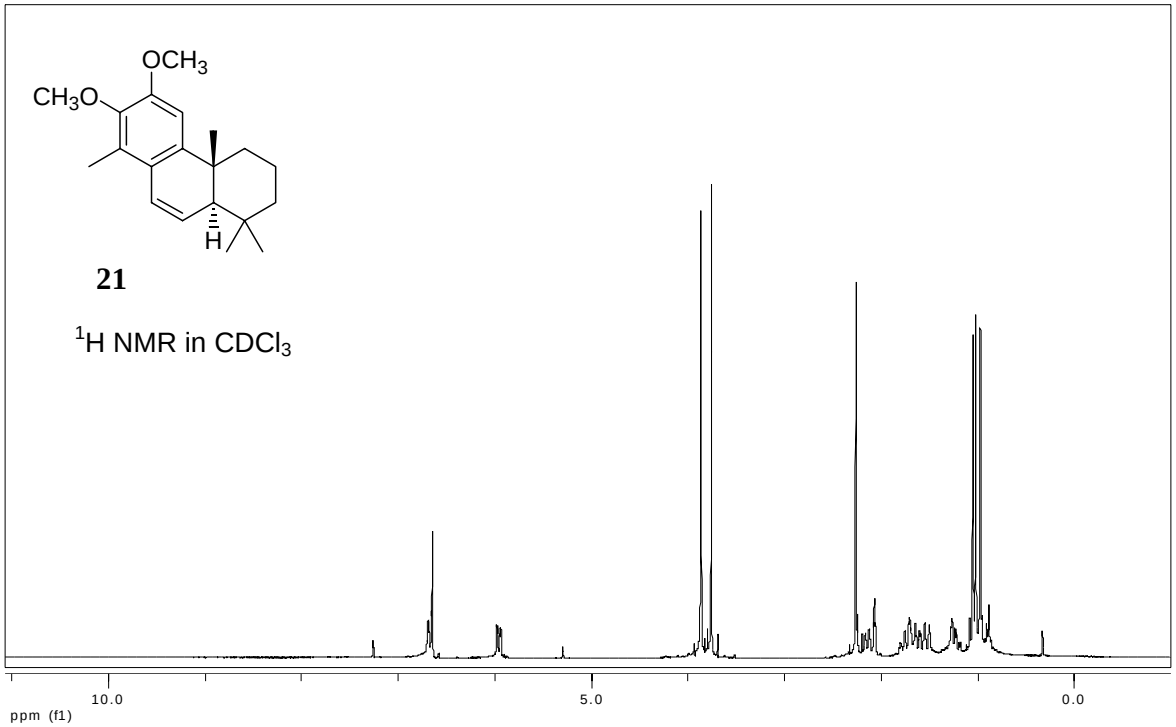

21

^{1}H NMR in $CDCl_3$

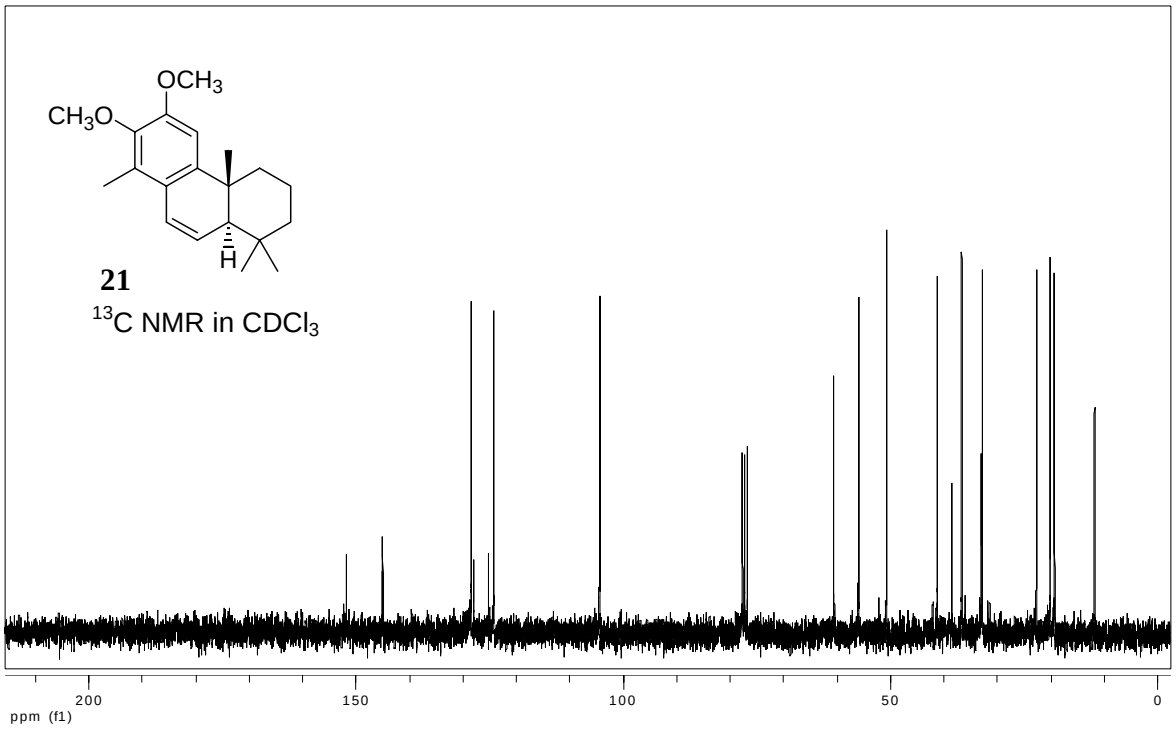

21

^{13}C NMR in $CDCl_3$

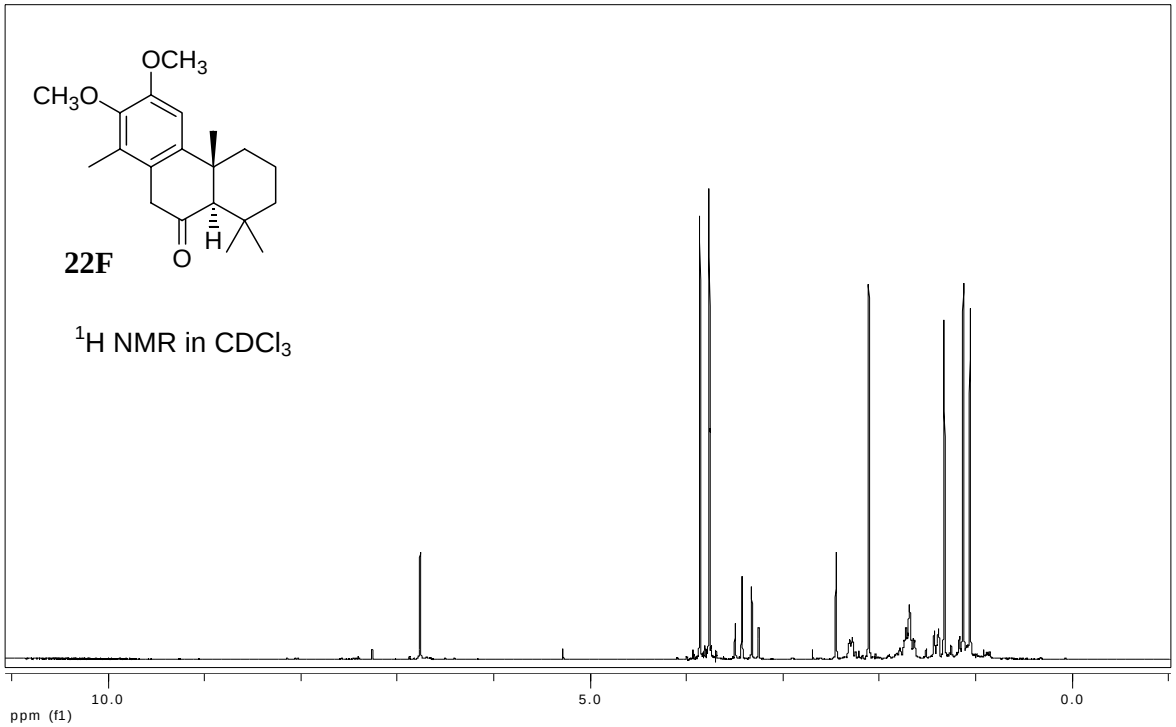
OCH3
CH3O
H
O
22F
1H NMR in CDCl3
10.0
5.0
0.0
ppm (f1)

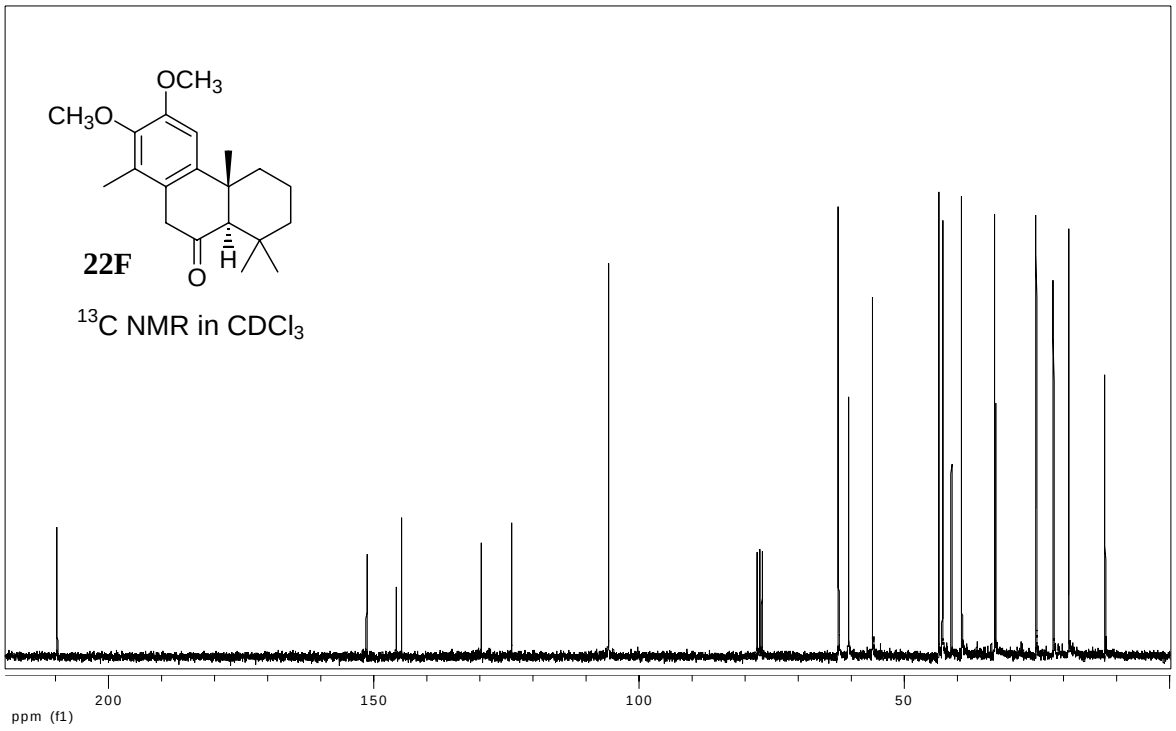
OCH3
CH3O
H
O
22F
13C NMR in CDCl3
200
150
100
50
ppm (f1)

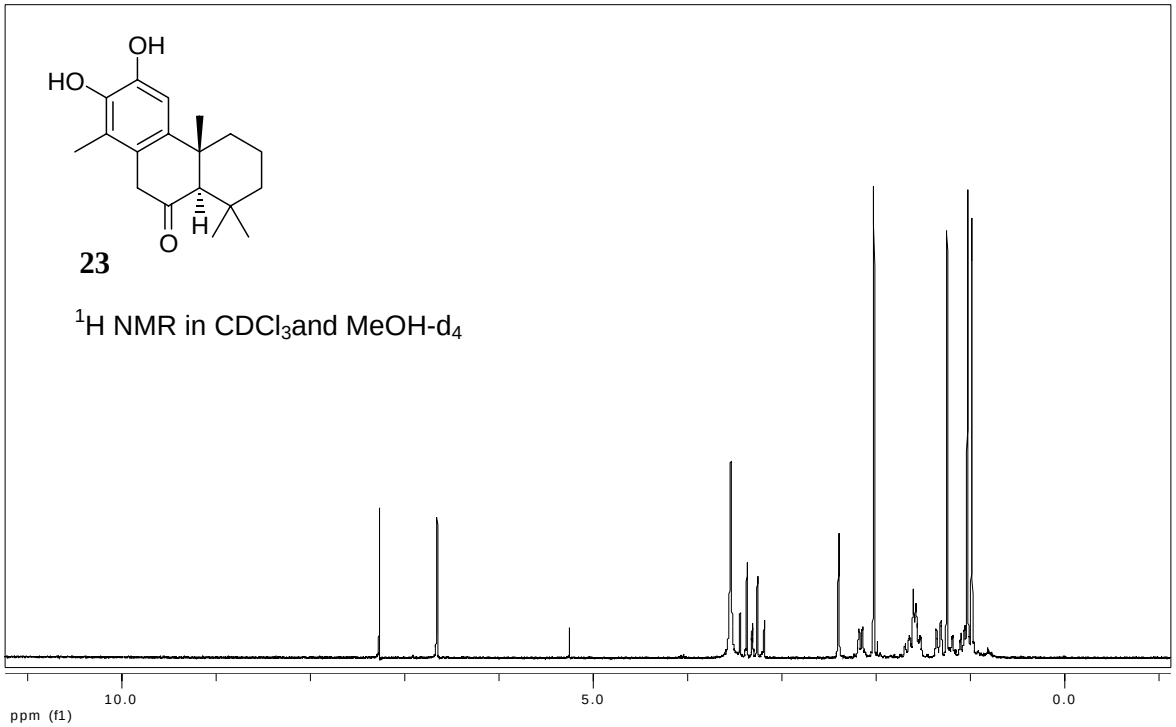

23

^{1}H NMR in $CDCl_3$and MeOH-d_4

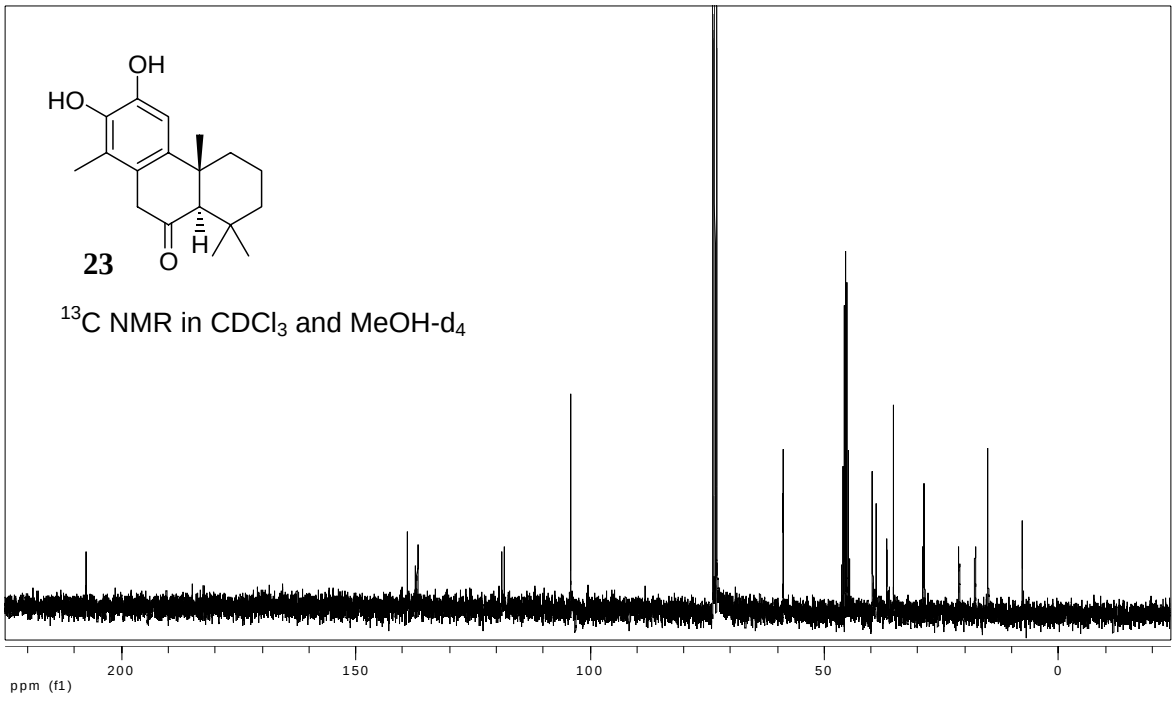

23

^{13}C NMR in $CDCl_3$ and MeOH-d_4

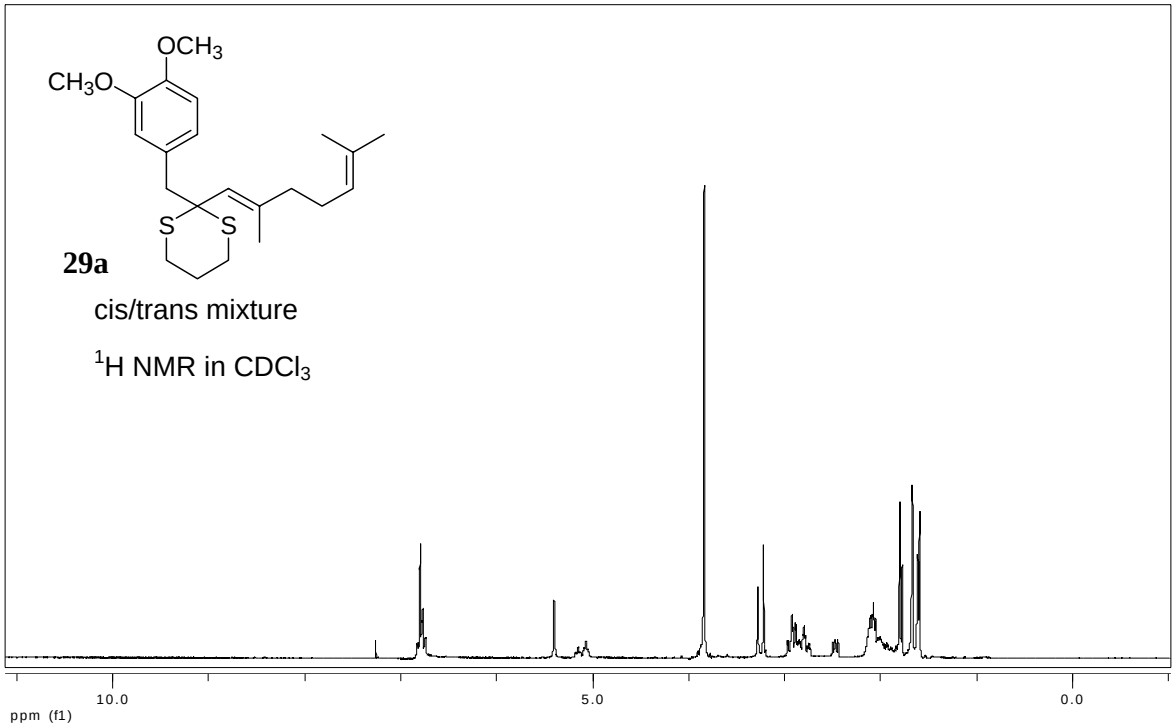
OCH3
CH3O
S
S
29a
cis/trans mixture
1H NMR in CDCl3
10.0
5.0
0.0
ppm (f1)

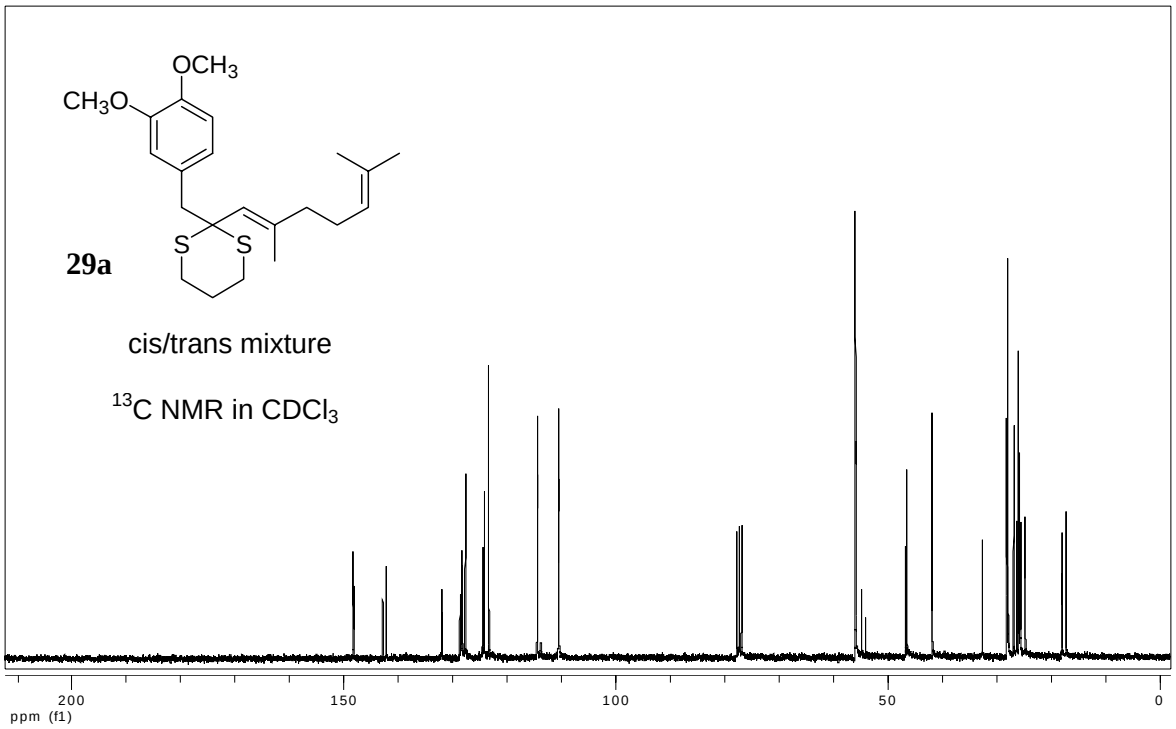
OCH3
CH3O
S
S
29a
cis/trans mixture
13C NMR in CDCl3
200
150
100
50
0
ppm (f1)

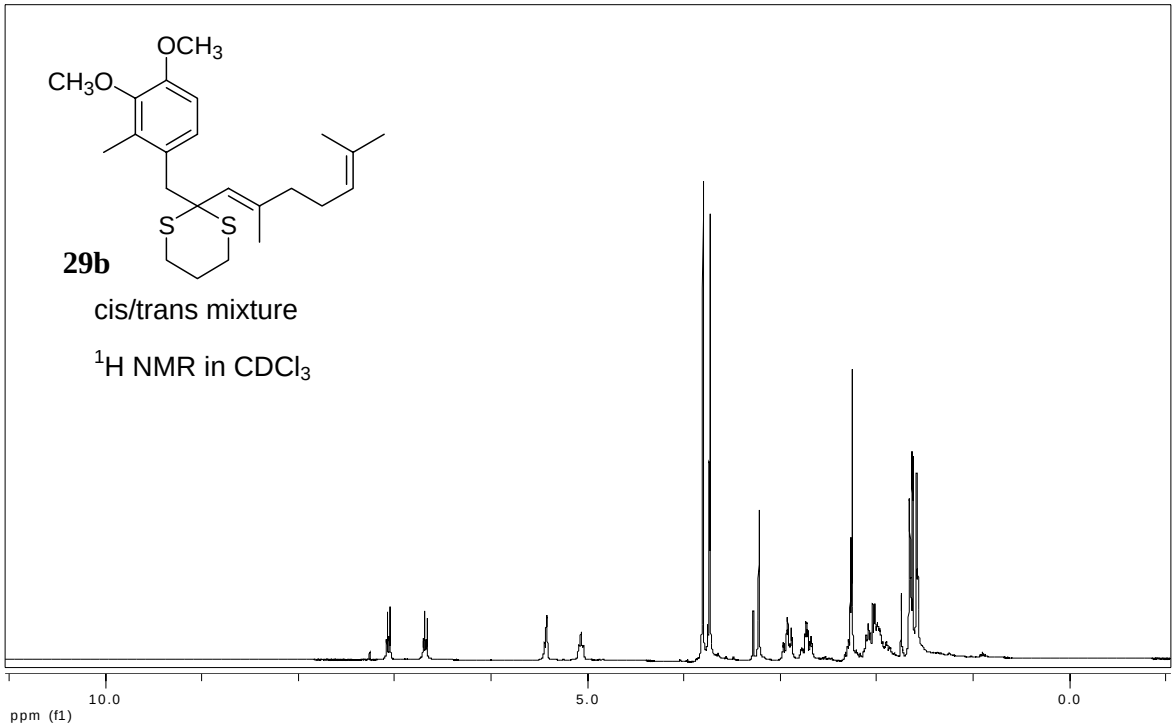
OCH3
CH3O
S
S
29b
cis/trans mixture
1H NMR in CDCl3
10.0
5.0
0.0
ppm (f1)

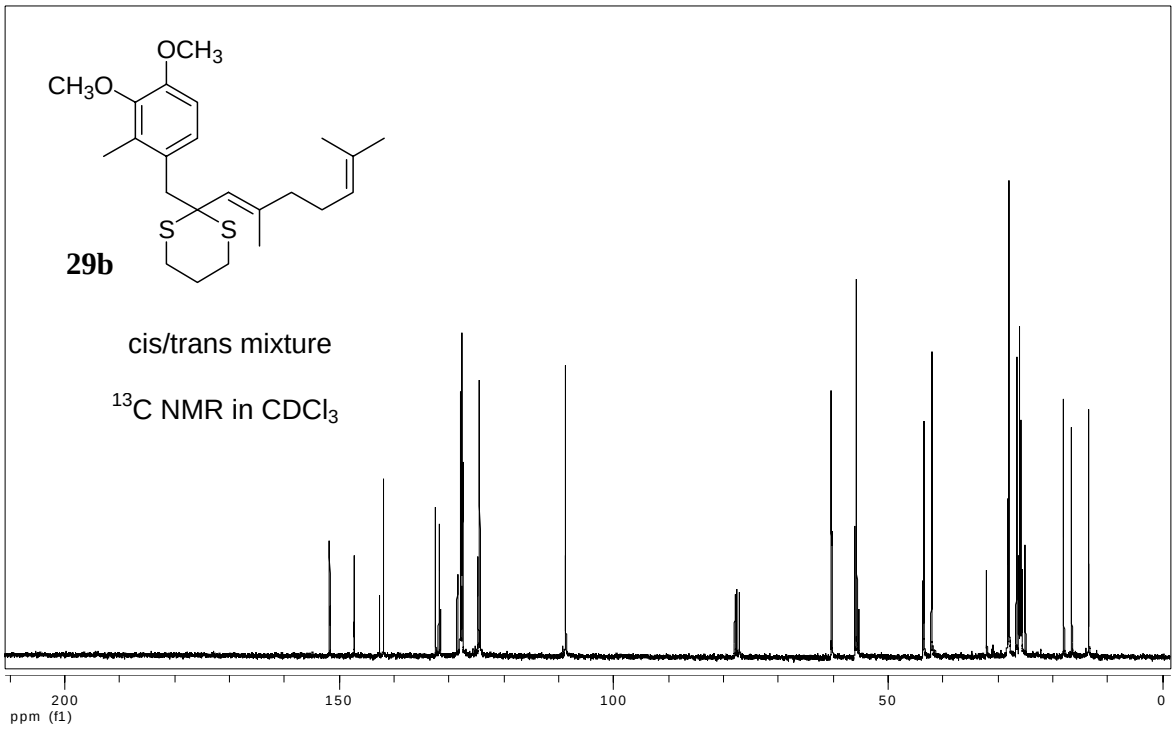
OCH3
CH3O
S
S
29b
cis/trans mixture
13C NMR in CDCl3
200
150
100
50
0
ppm (f1)

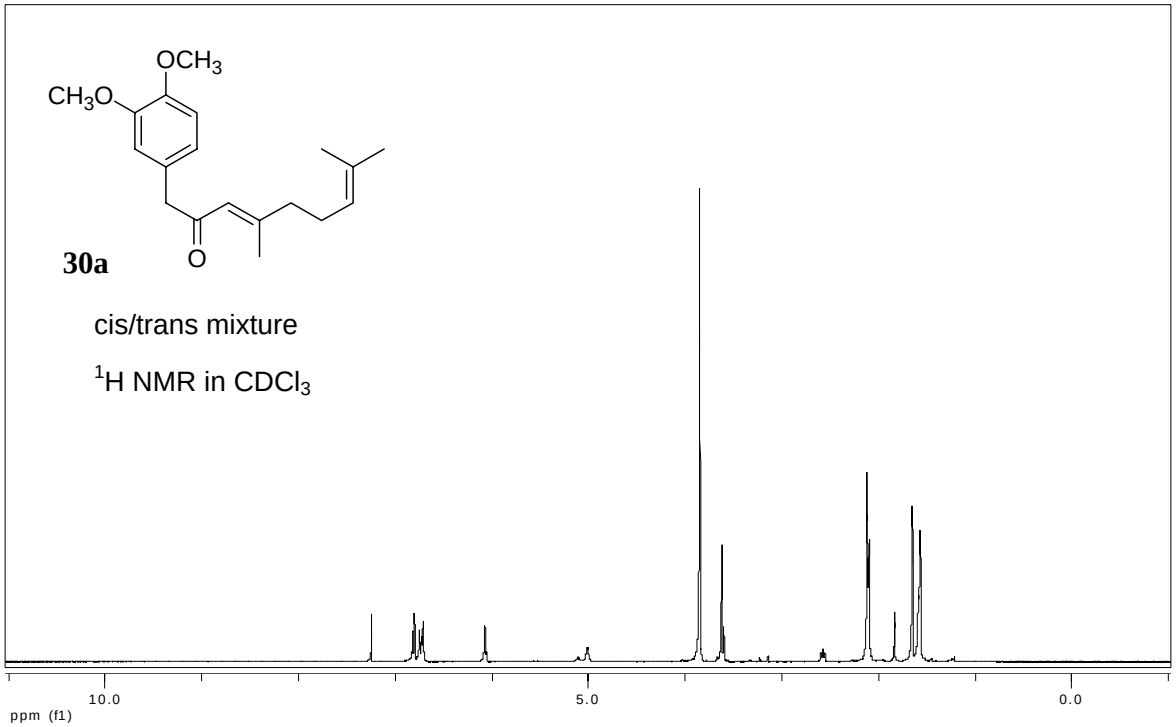
OCH3
CH3O
O
30a
cis/trans mixture
1H NMR in CDCl3
10.0
5.0
0.0
ppm (f1)

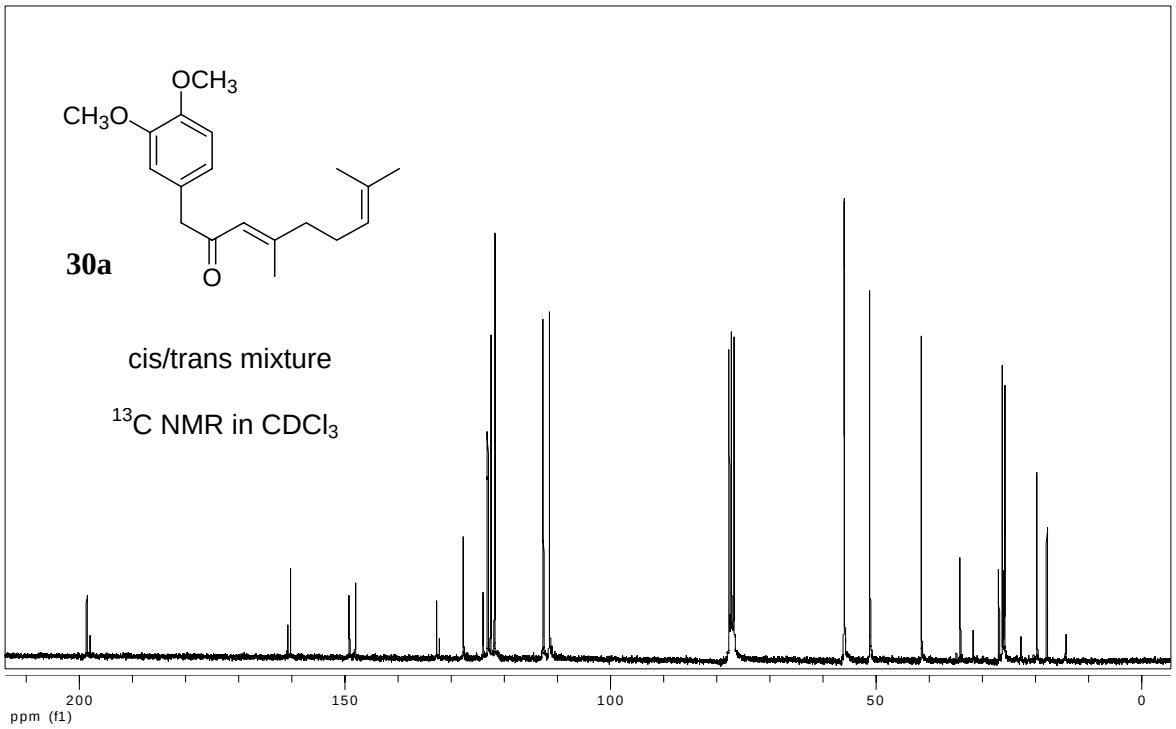
OCH3
CH3O
O
30a
cis/trans mixture
13C NMR in CDCl3
200
150
100
50
0
ppm (f1)

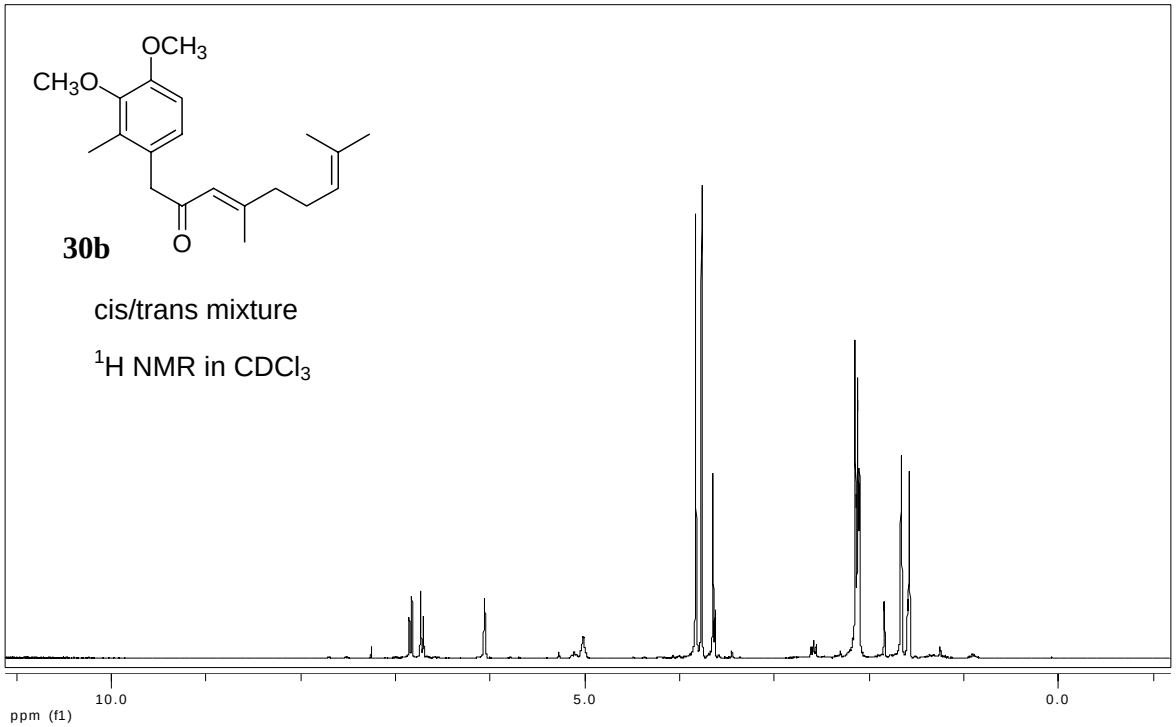
OCH3
CH3O
O
30b
cis/trans mixture
1H NMR in CDCl3
10.0
5.0
0.0
ppm (f1)

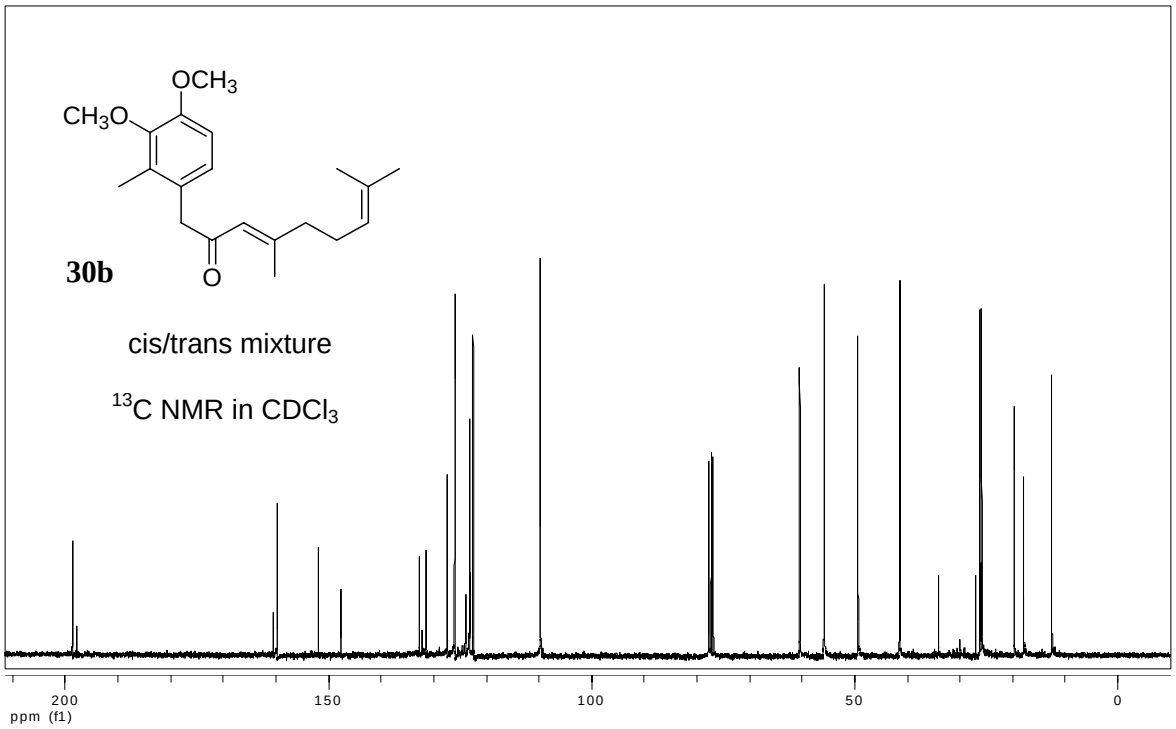
OCH3
CH3O
O
30b
cis/trans mixture
13C NMR in CDCl3
200
150
100
50
0
ppm (f1)

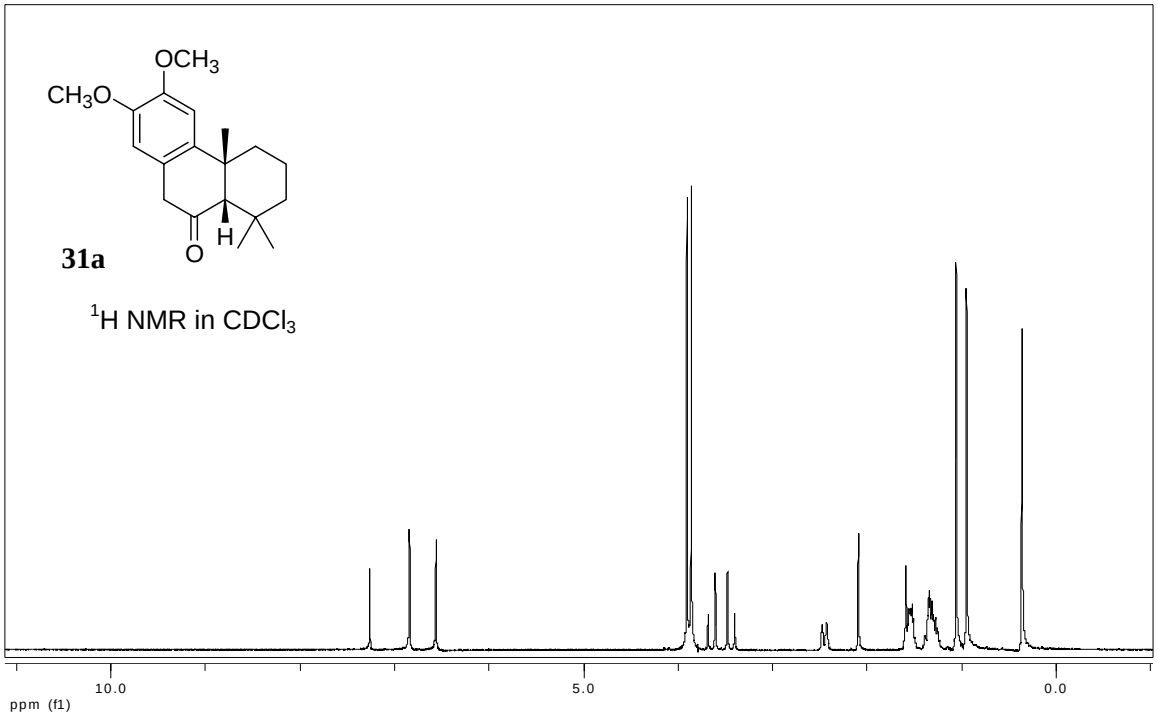
OCH3
CH3O
O
H
31a
1H NMR in CDCl3
10.0
5.0
0.0
ppm (f1)

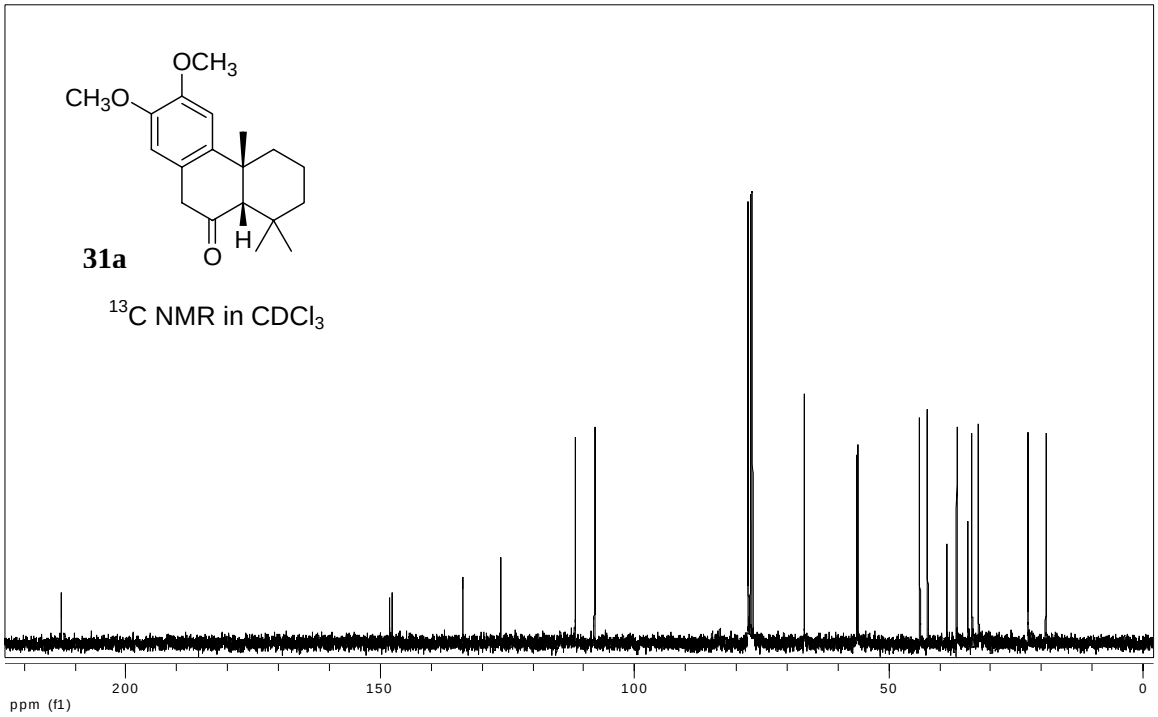
OCH3
CH3O
O
H
31a
13C NMR in CDCl3
200
150
100
50
0
ppm (f1)

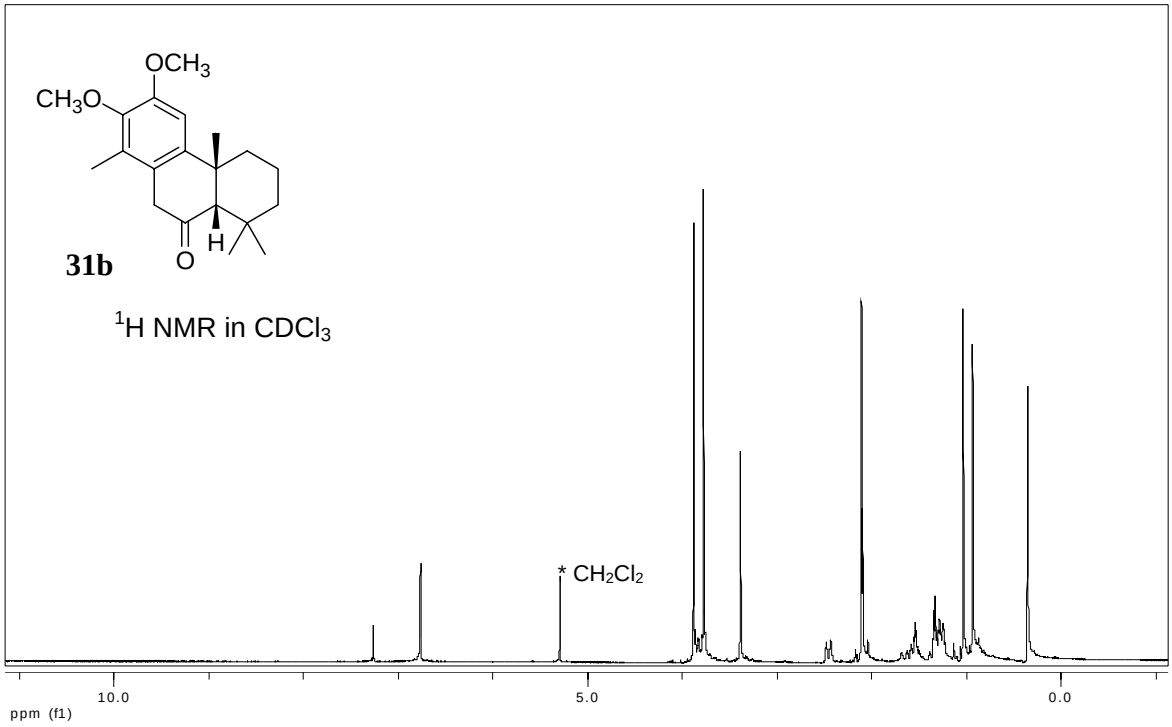
OCH3
CH3O
H
O
31b
1H NMR in CDCl3
* CH2Cl2
10.0
5.0
0.0
ppm (f1)

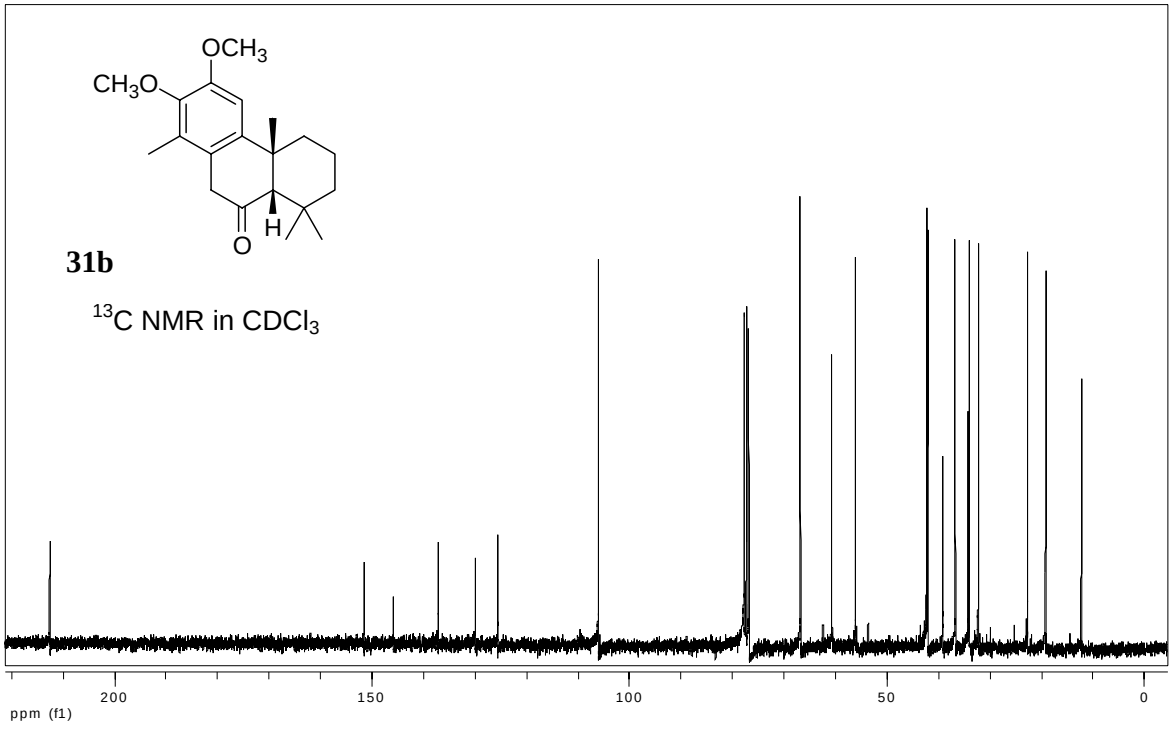
OCH3
CH3O
H
O
31b
13C NMR in CDCl3
200
150
100
50
0
ppm (f1)

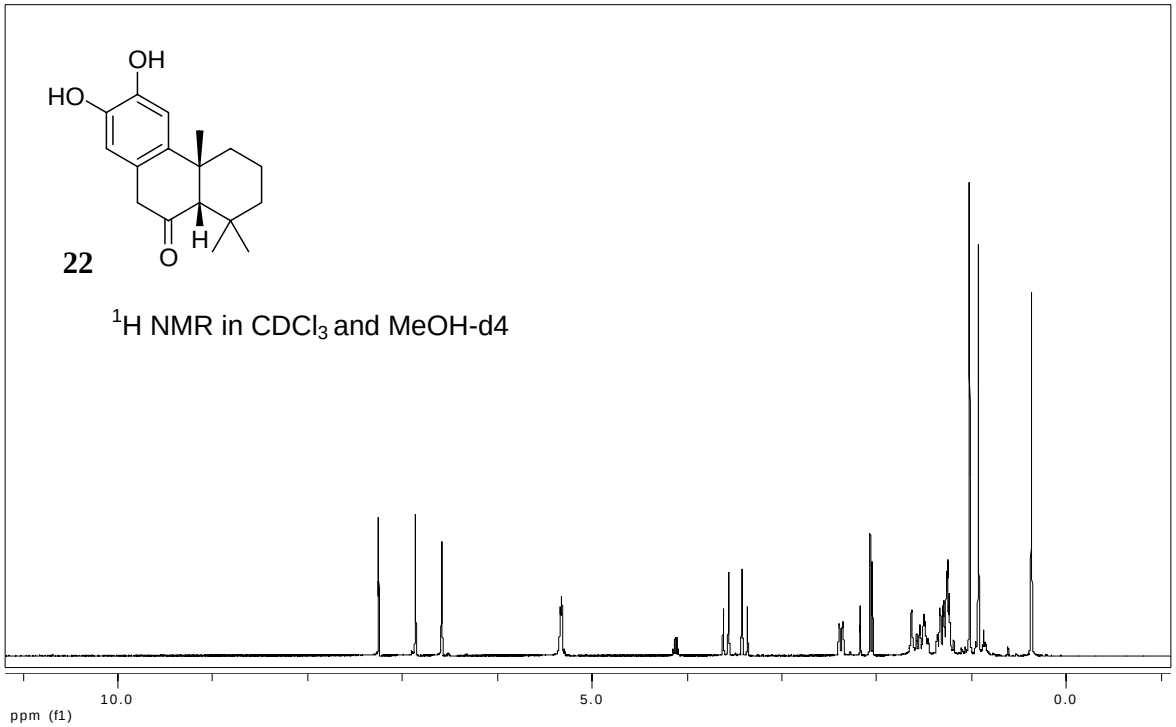

22

^{1}H NMR in $CDCl_3$ and MeOH-d4

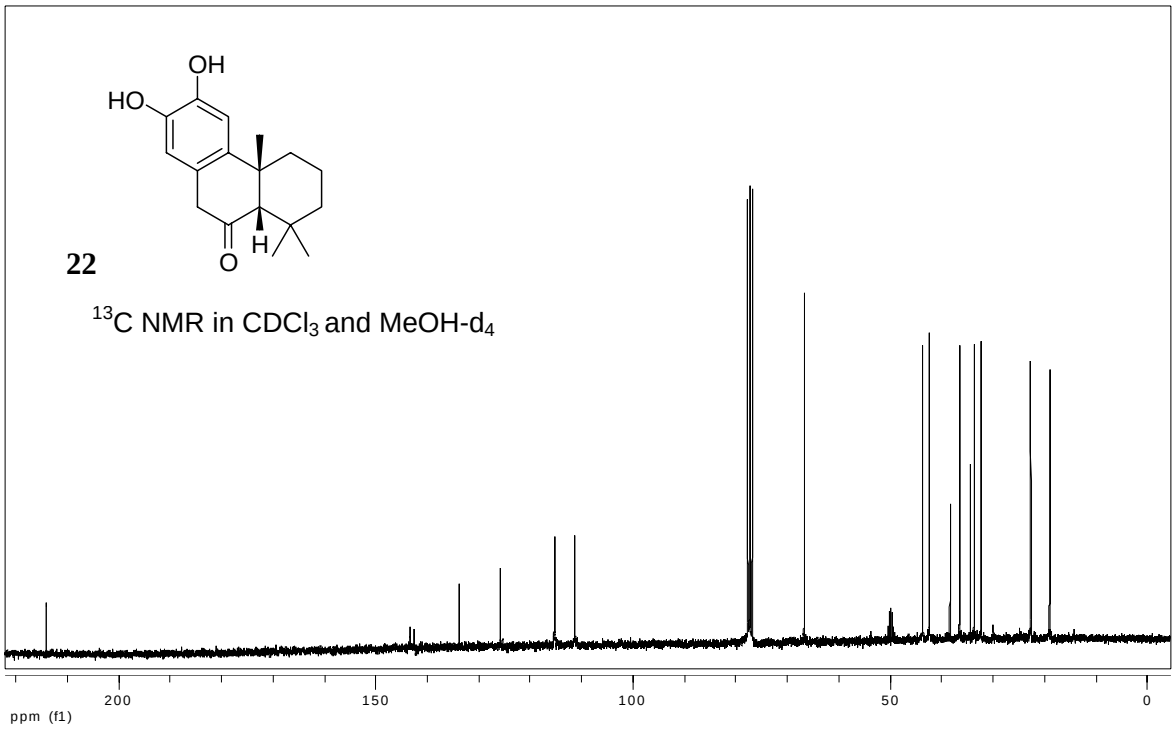

22

^{13}C NMR in $CDCl_3$ and MeOH-d_4

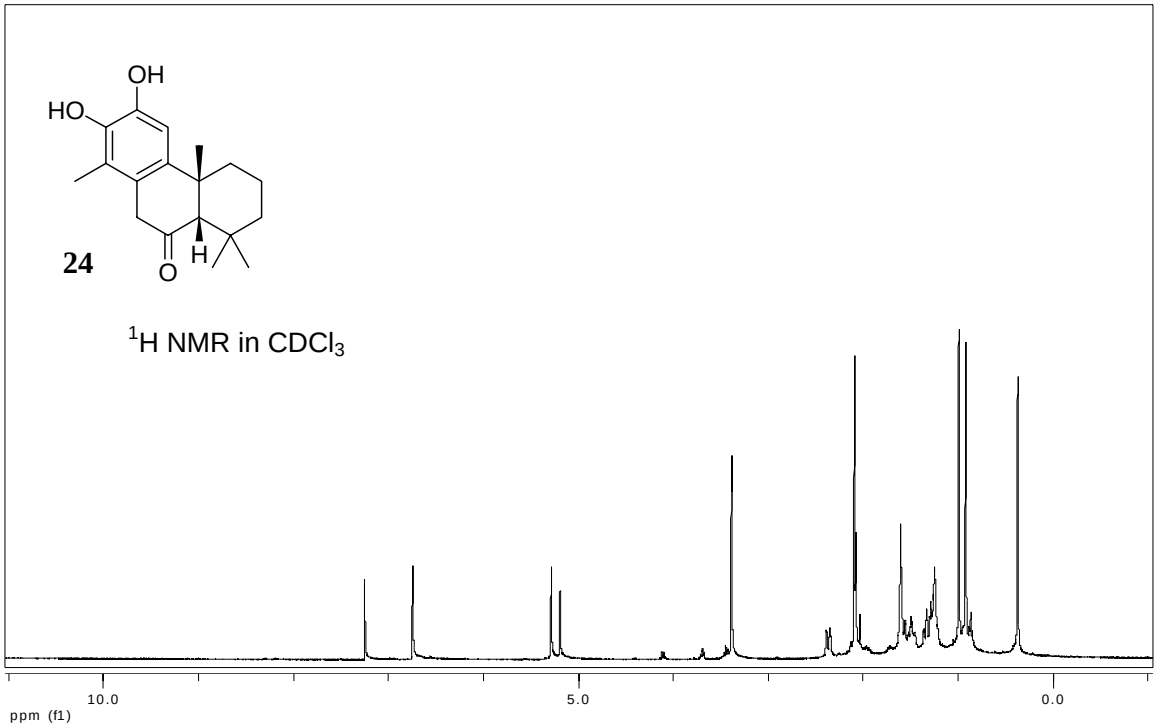

24

^{1}H NMR in $CDCl_3$

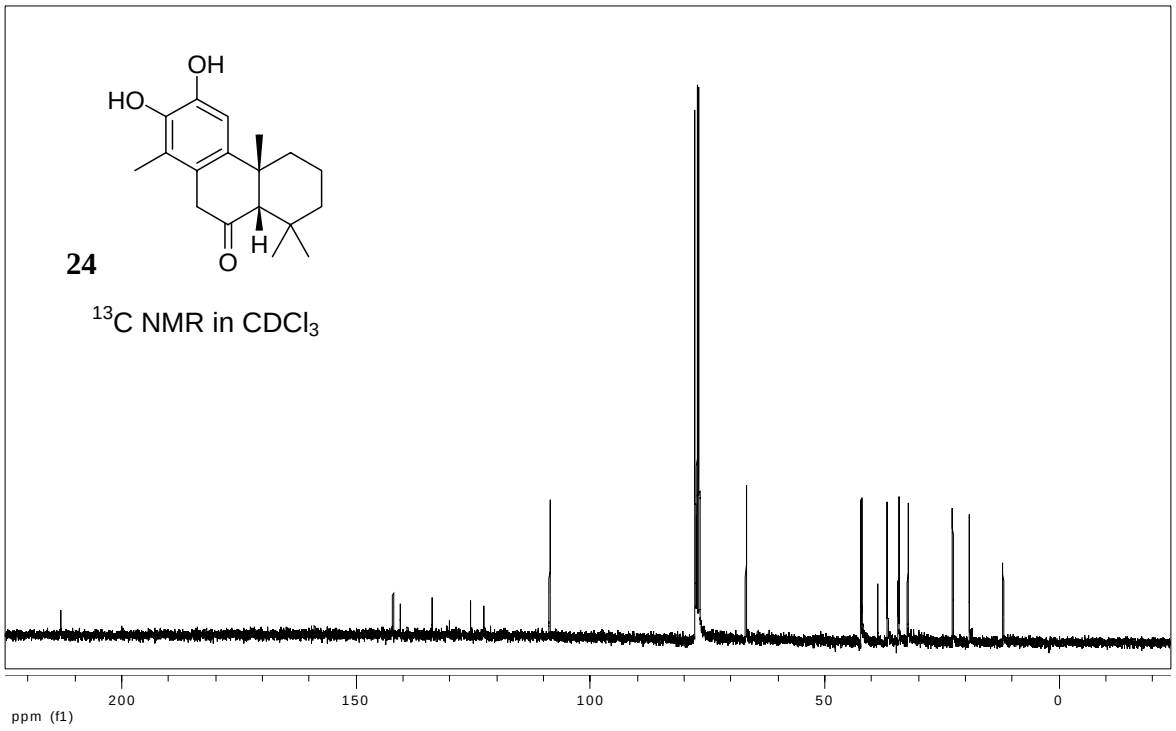

24

^{13}C NMR in $CDCl_3$

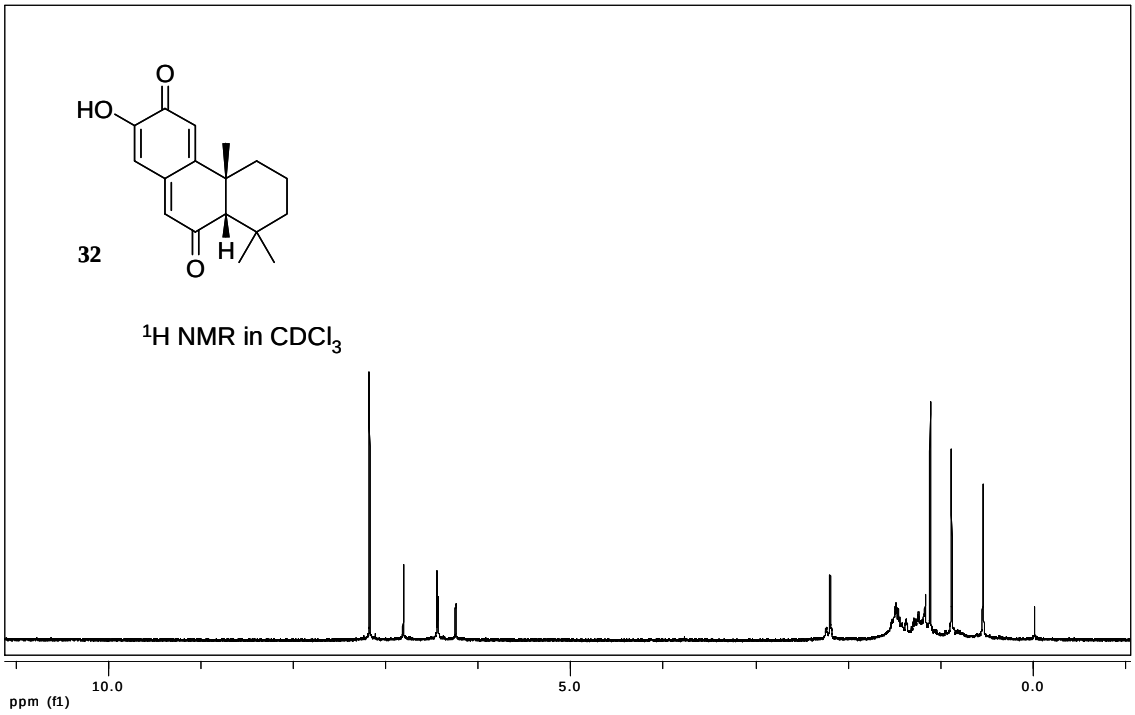
HO
O
O
H
32
^{1}H NMR in $CDCl_3$
10.0
5.0
0.0
ppm (f1)

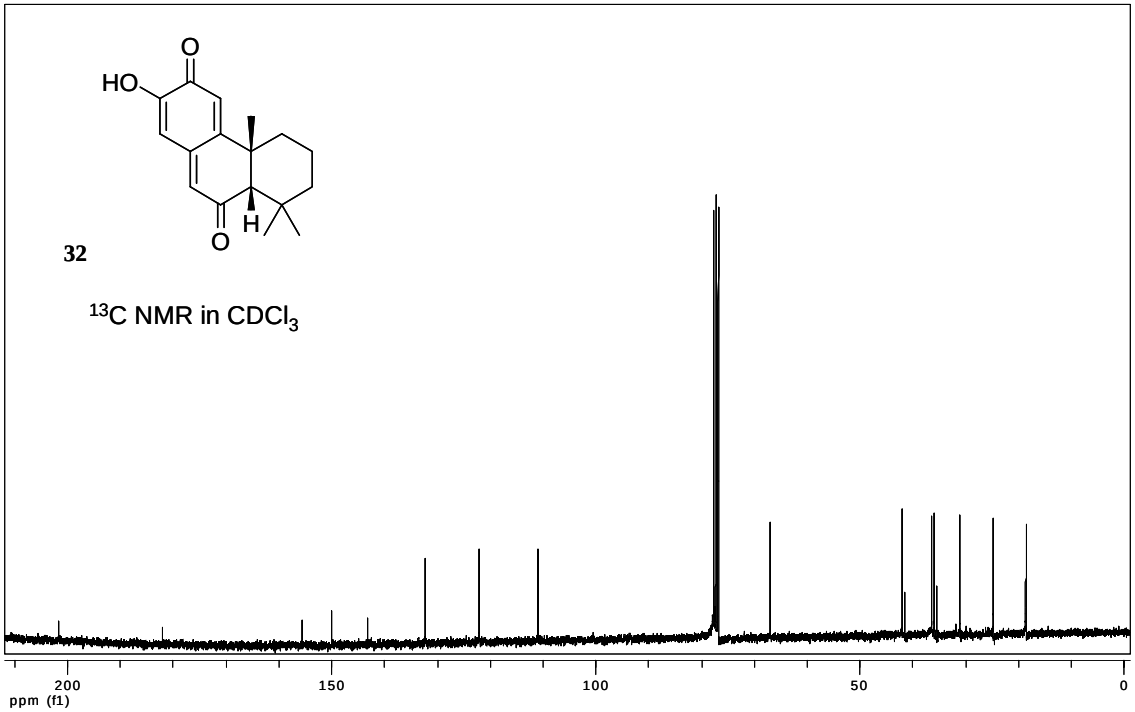
HO
O
O
H
32
^{13}C NMR in $CDCl_3$
200
150
100
50
0
ppm (f1)

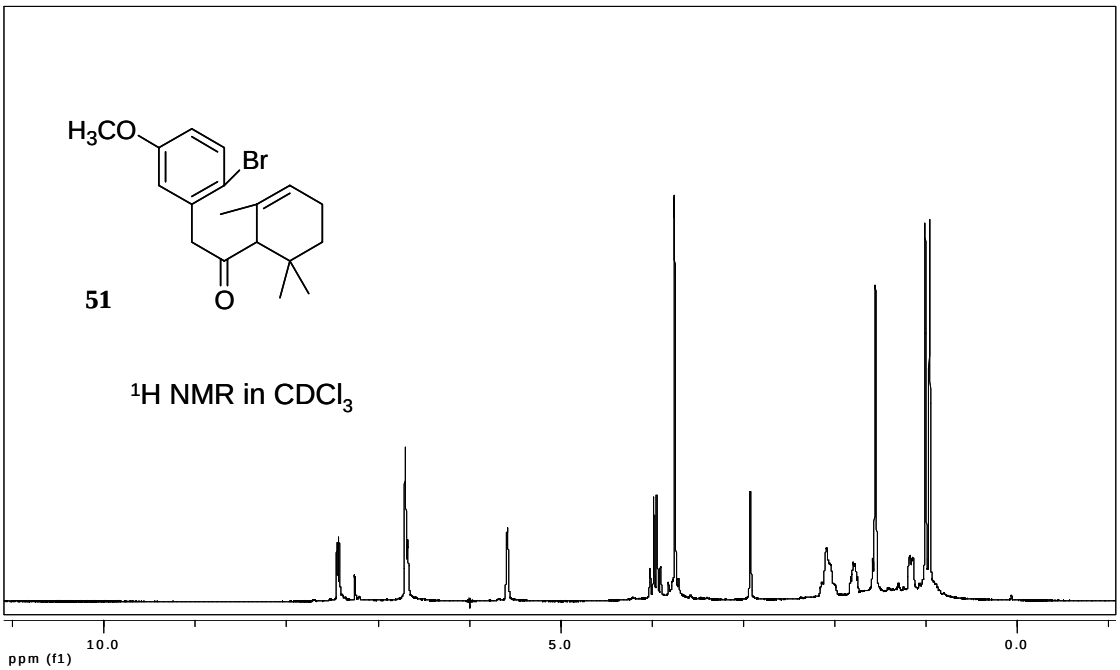
H3CO
Br
O
51
1H NMR in CDCl3
10.0
5.0
0.0
ppm (f1)

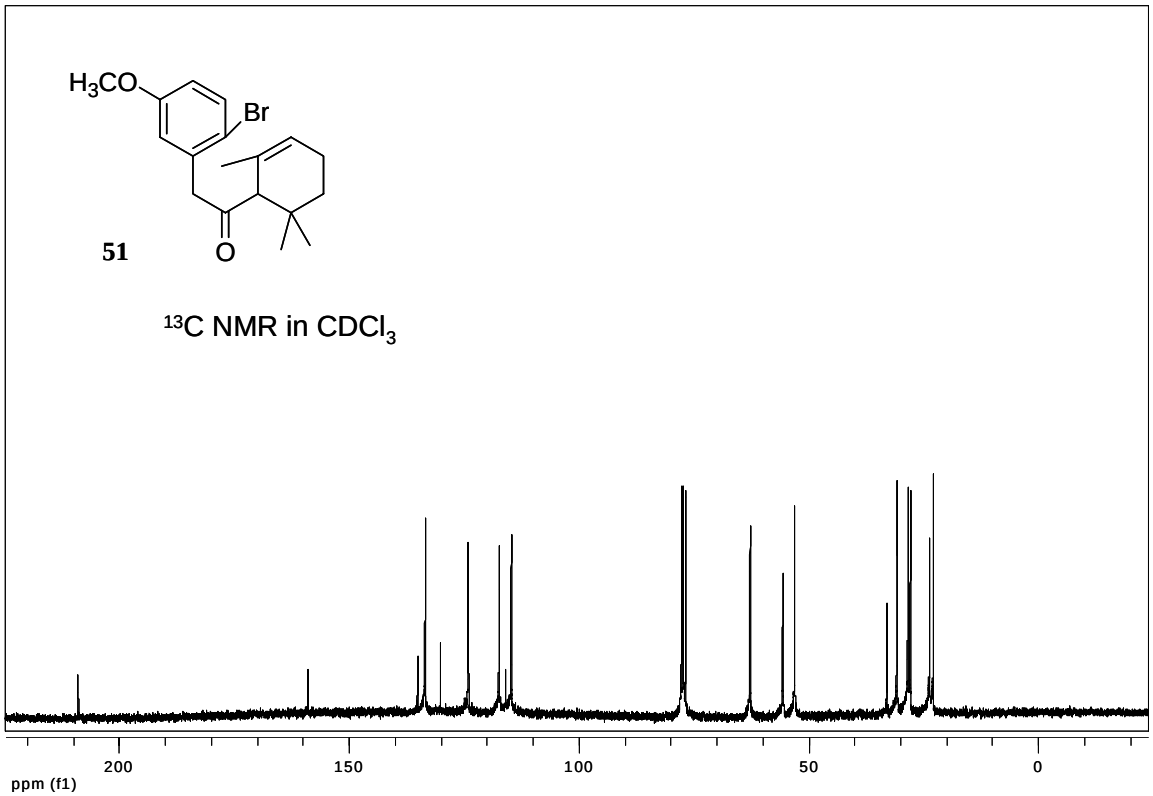
H3CO
Br
O
51
13C NMR in CDCl3
200
150
100
50
0
ppm (f1)

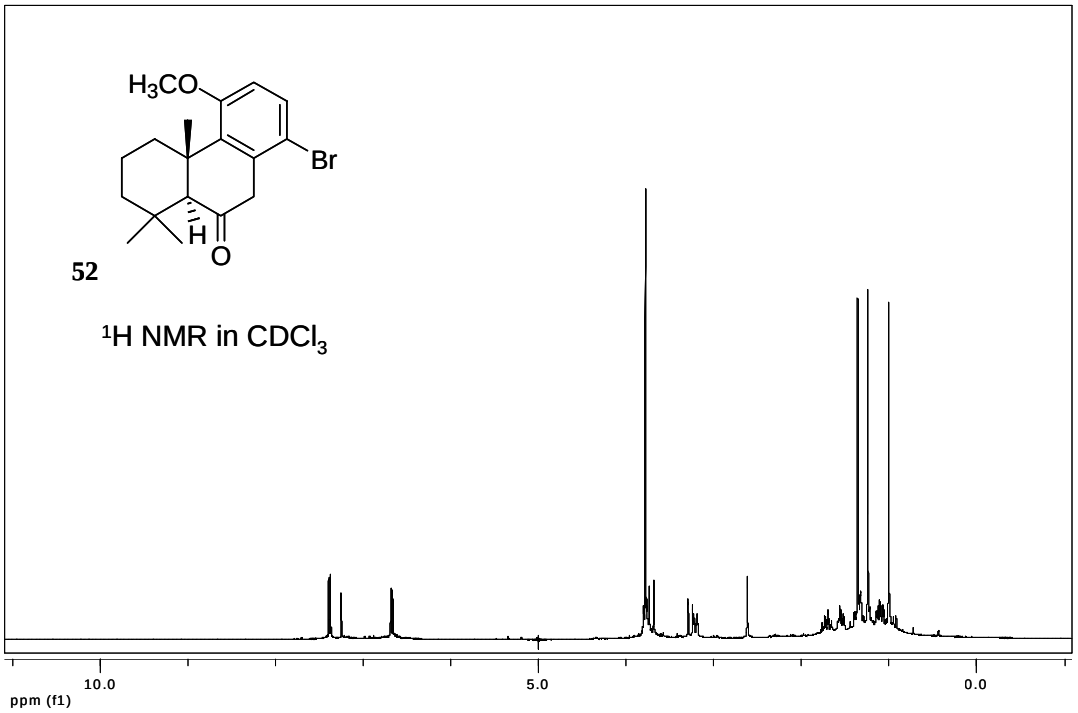
H3CO
Br
H
O
52
1H NMR in CDCl3
10.0
5.0
0.0
ppm (f1)

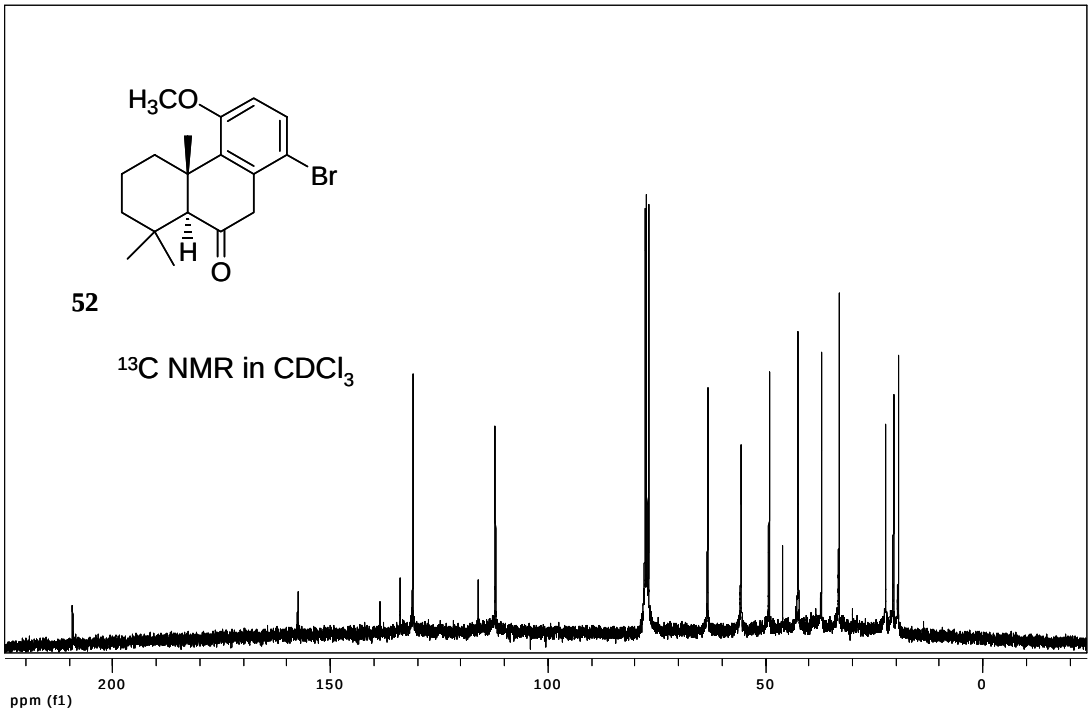
H3CO
Br
H
O
52
13C NMR in CDCl3
200
150
100
50
0
ppm (f1)

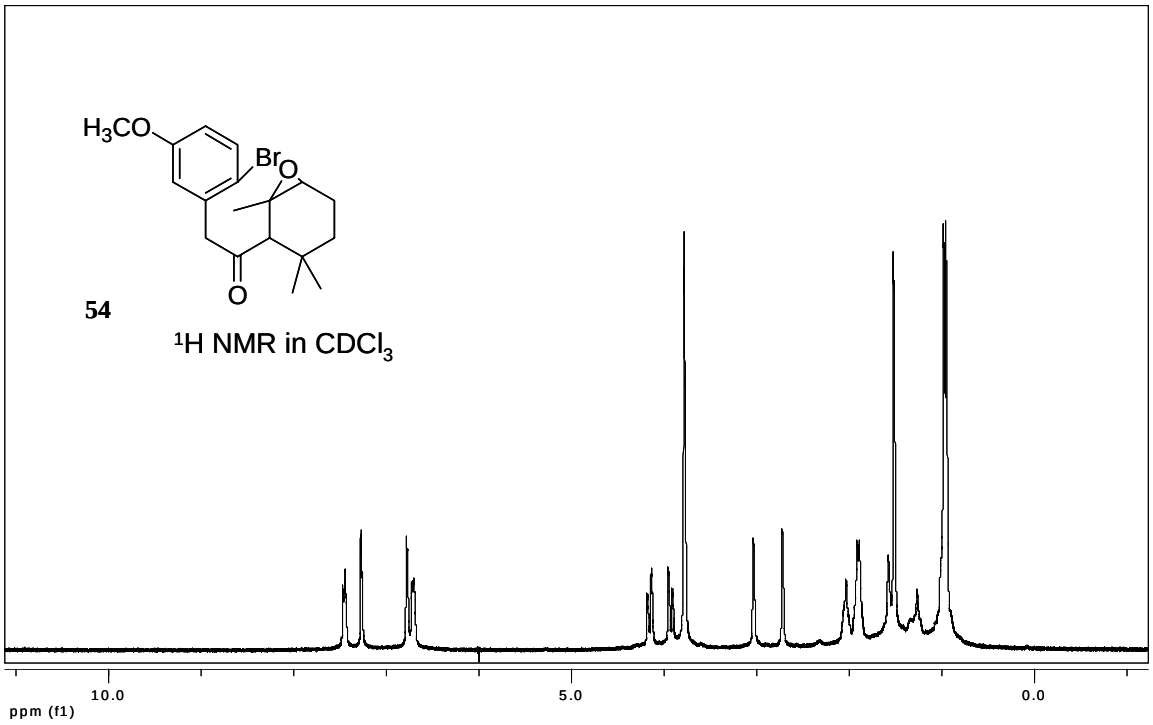

54

^{1}H NMR in $CDCl_3$

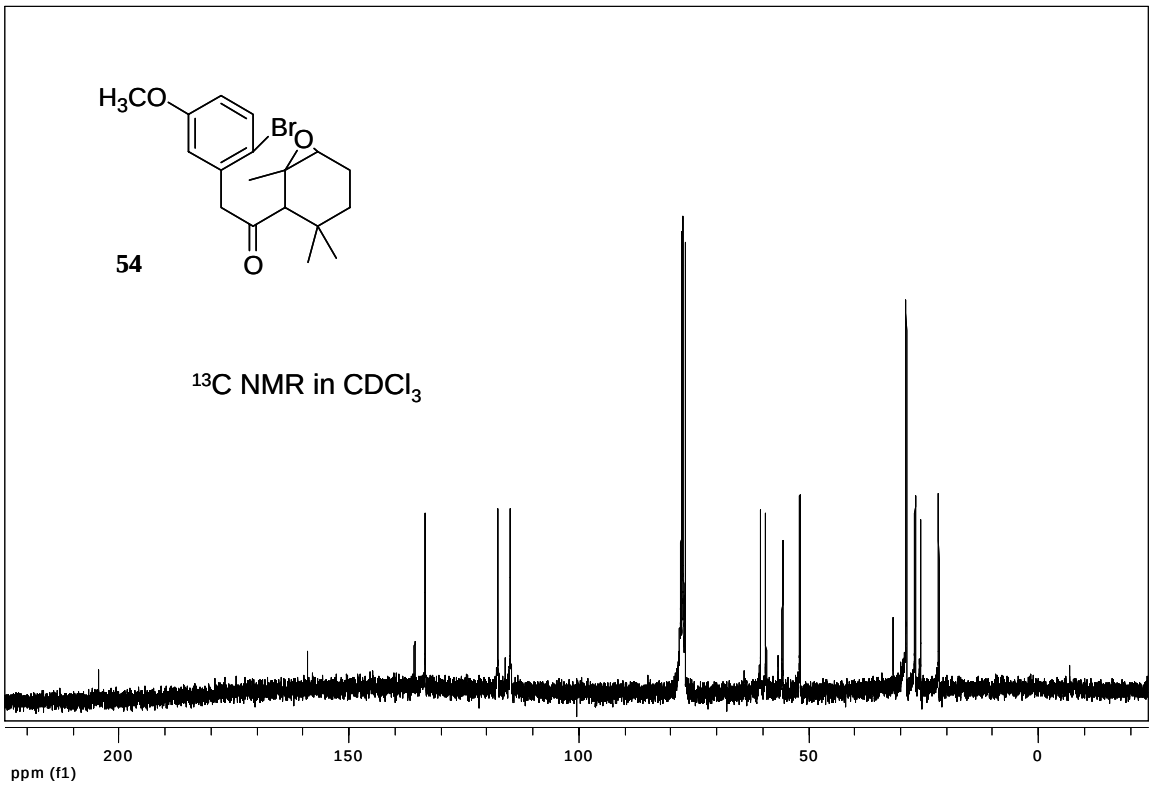

54

^{13}C NMR in $CDCl_3$

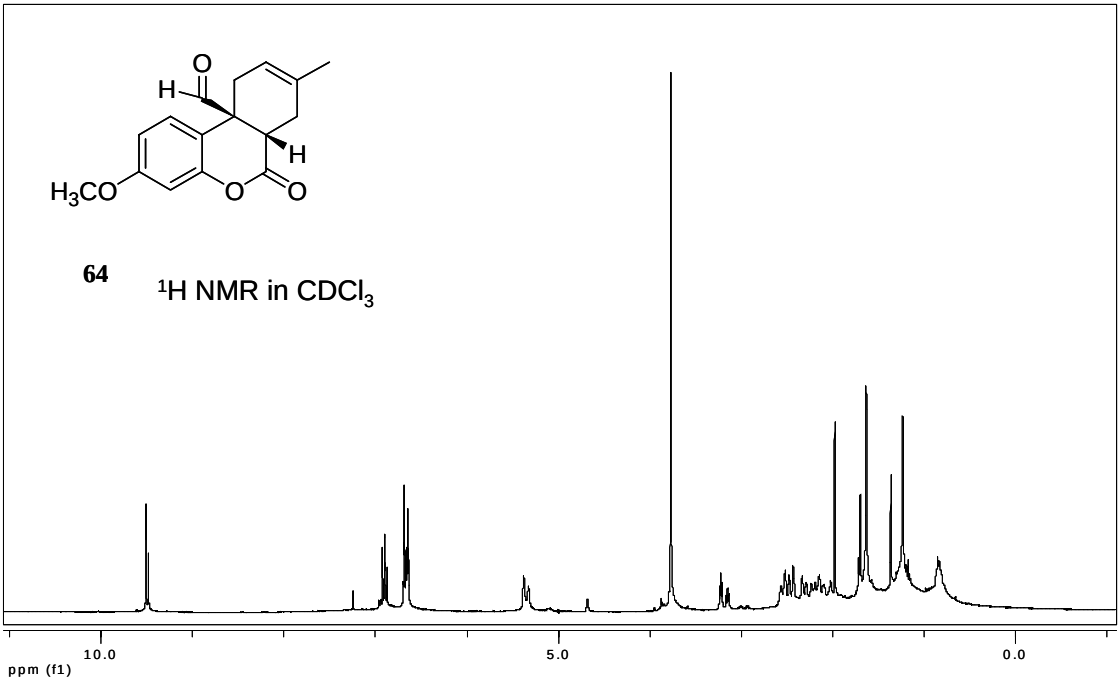

64 ^{1}H NMR in $CDCl_3$

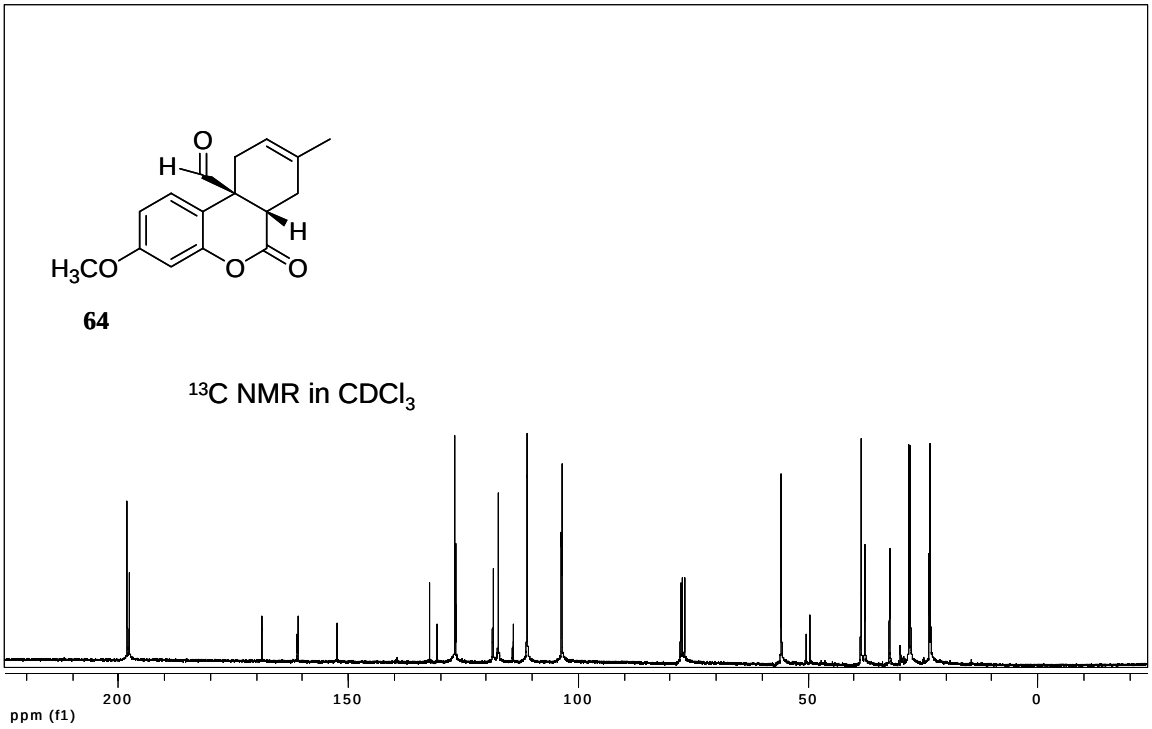

64

^{13}C NMR in $CDCl_3$

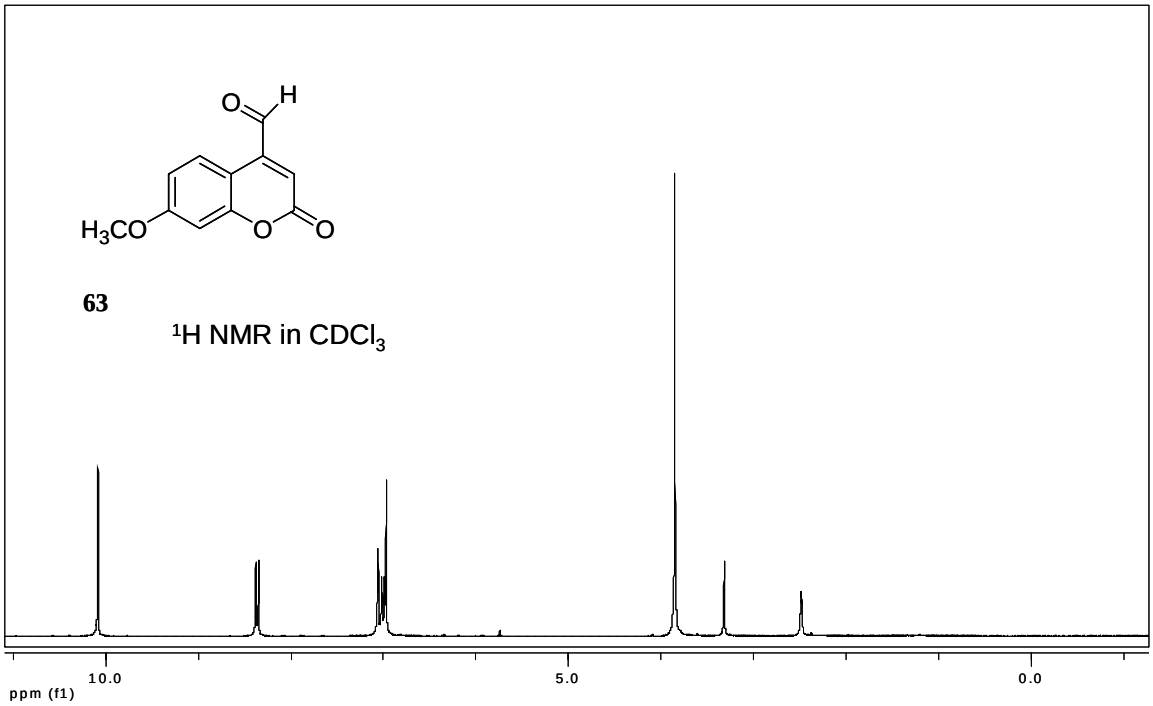
O
H
H3CO
O
O
63
1H NMR in CDCl3
10.0
5.0
0.0
ppm (f1)

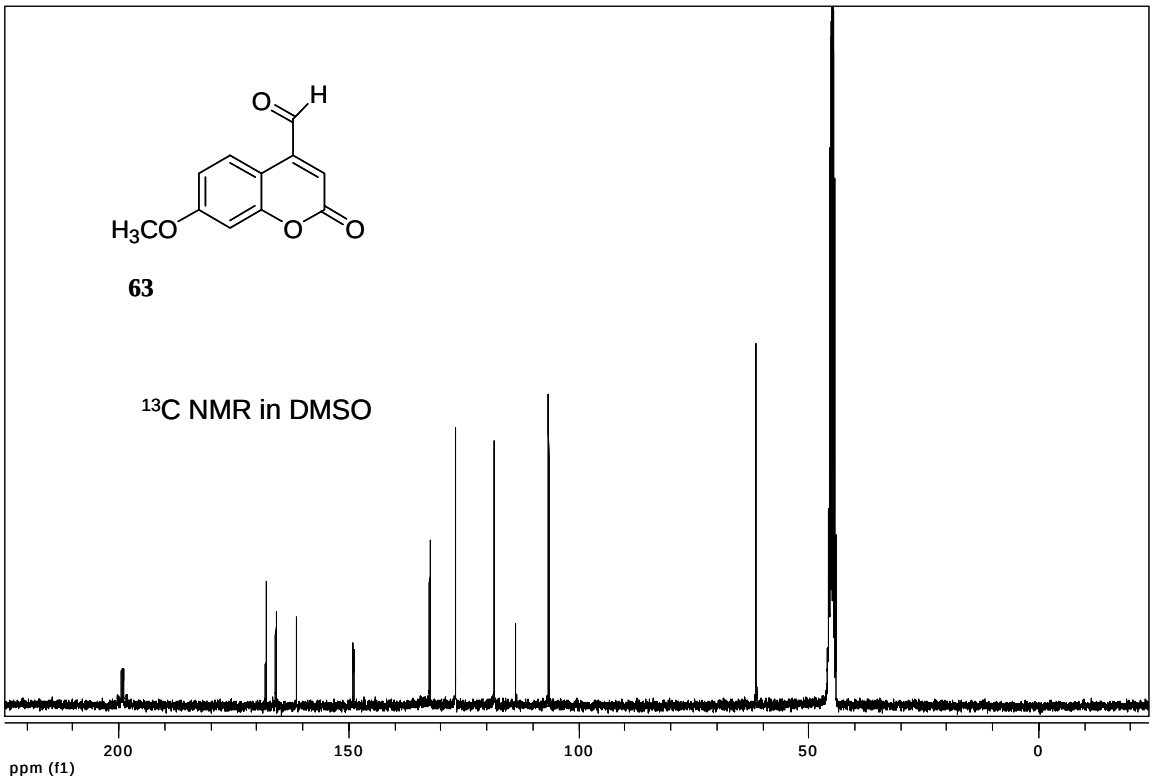
O
H
H3CO
O
O
63
13C NMR in DMSO
200
150
100
50
0
ppm (f1)

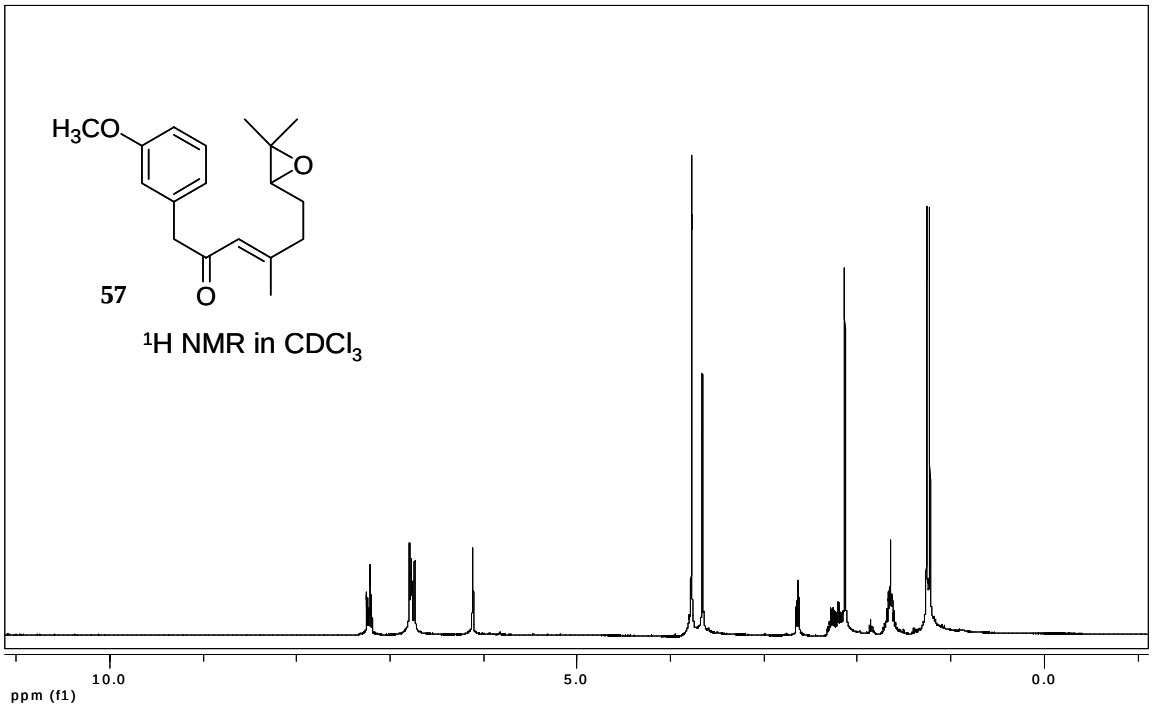

57

^{1}H NMR in $CDCl_3$

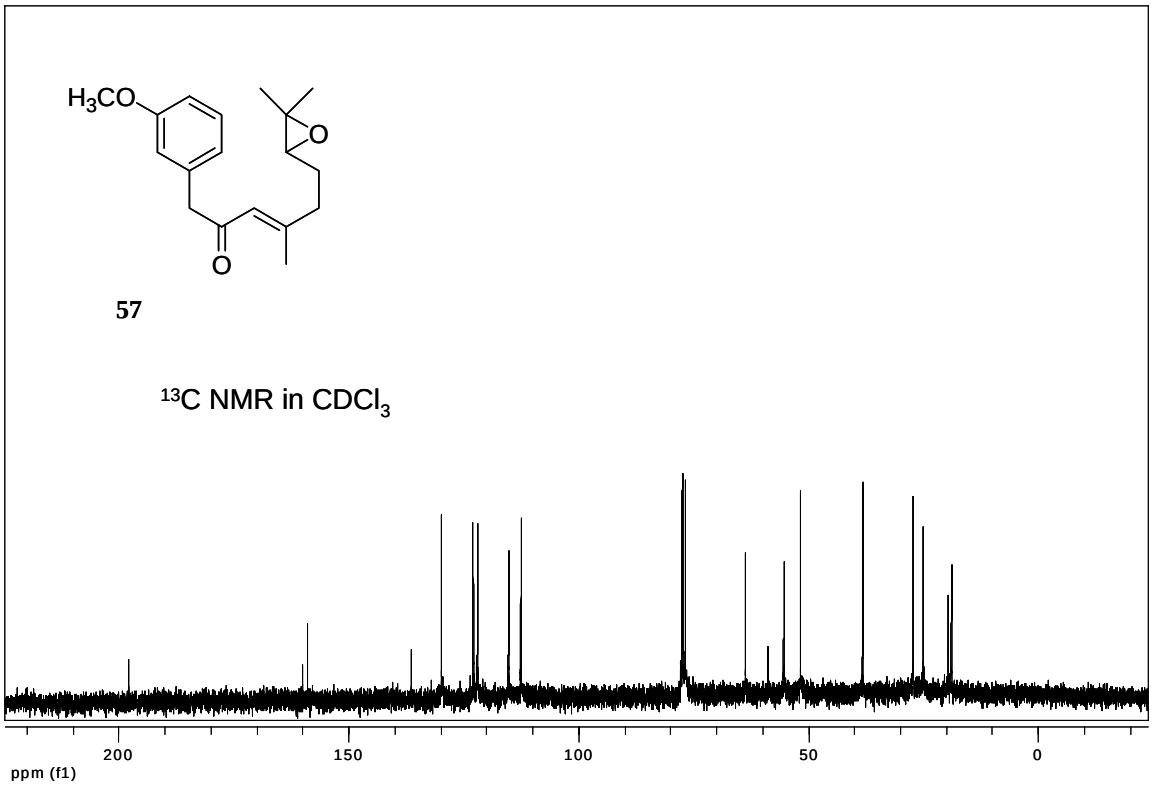

57

^{13}C NMR in $CDCl_3$

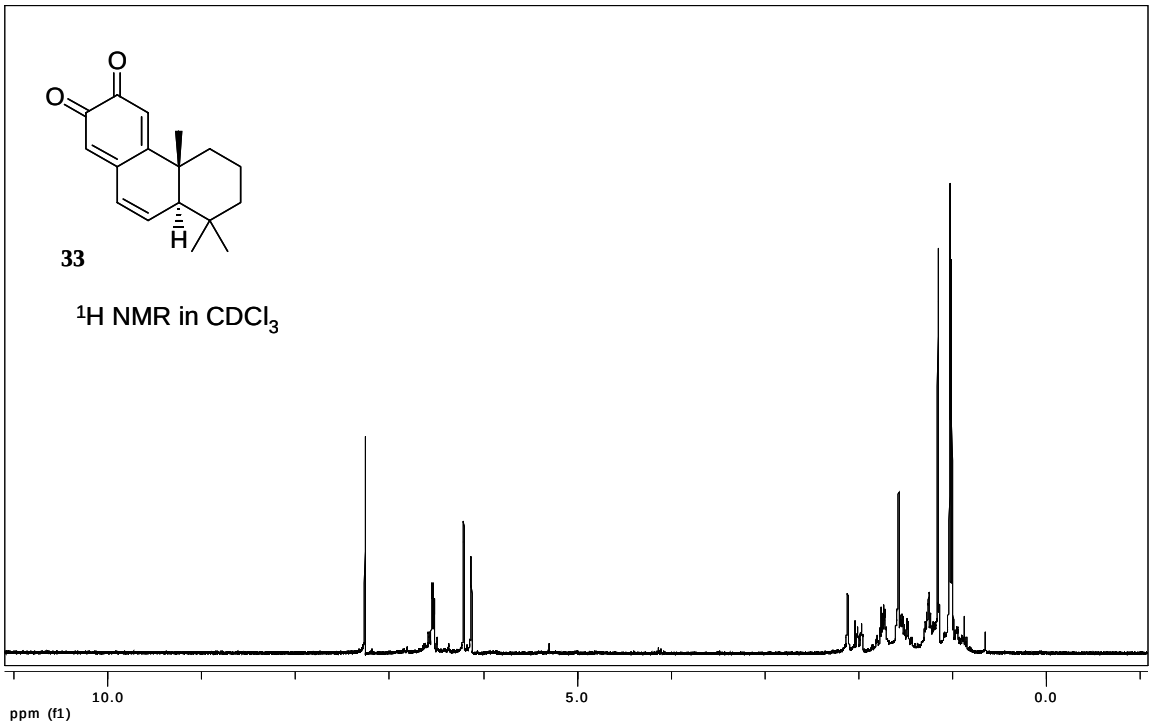

33

^{1}H NMR in $CDCl_3$

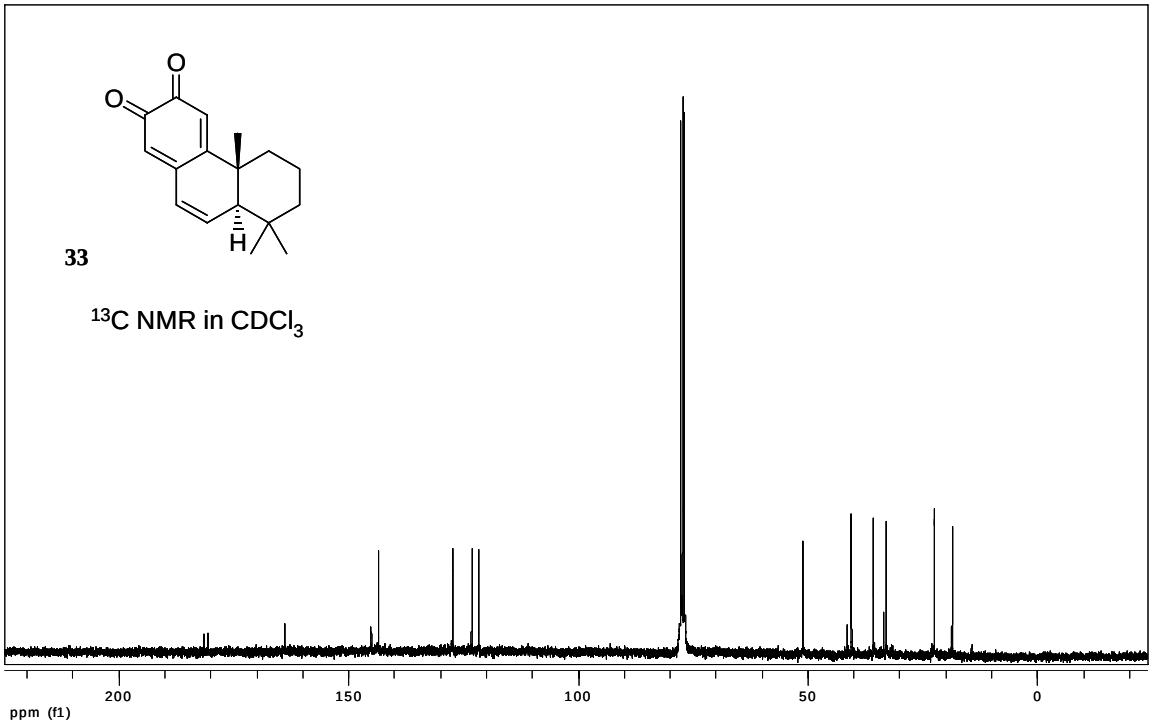

33

^{13}C NMR in $CDCl_3$

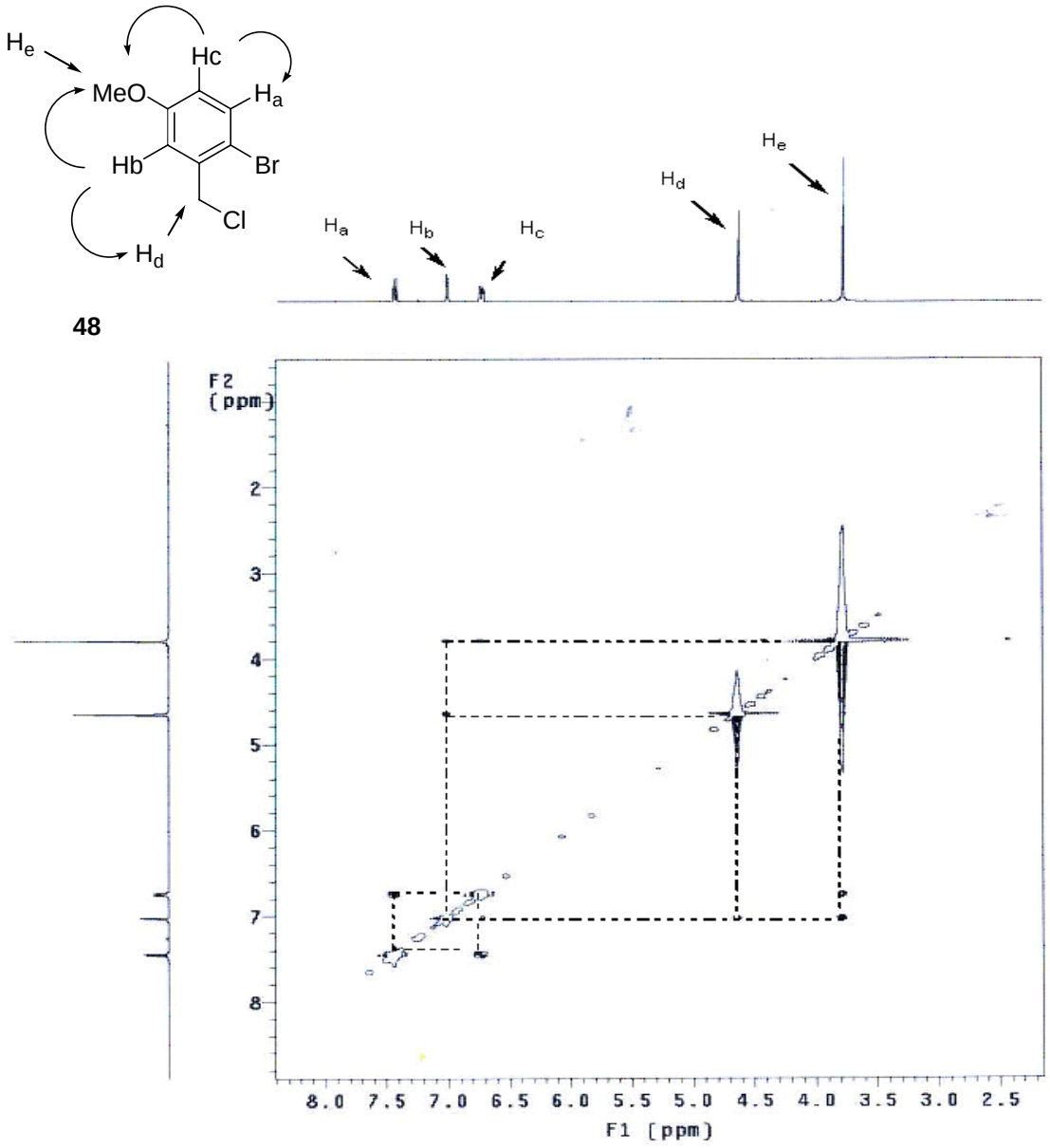

48

ROESY spectrum of compound 48 showing crosspeaks confirming the para position of the bromide

VITA

Miguel A. Zuniga was born on March 14, 1976 in Mier Y Noriega, Nuevo Leon, Mexico and is both a United States and Mexican citizen. He graduated from Jack C. Hays High School in 1995. He received his Bachelor of Science Degree in Chemistry and Mathematics from Southwest Texas State University in 2002. After graduation, he worked for Dupont Dow in Freeport, Texas prior to joining Dr. Zhou's research group at Virginia Commonwealth University. He is the author of two publications and has presented his research at several conferences. He is a member of the American Chemical Society.